

**An evaluation of synergistic interactions between
feruloyl esterases and xylanases during the
hydrolysis of various pre-treated agricultural
residues**

A thesis submitted in fulfilment of the requirements for
the degree of

DOCTOR OF PHILOSOPHY

in

BIOCHEMISTRY

at

RHODES UNIVERSITY

by

LITHALETHU MKABAYI

ORCID ID

<http://orcid.org/0000-0001-7620-5596>

April 2021

Plagiarism declaration

I, Lithalethu Mkabayi, declare that this thesis is my own, original and unaided work. It is being submitted for the degree of Doctor of Philosophy at Rhodes University. It has not been submitted before, for any degree or examination, at any other university.



Signature

Date07 April 2021.....

Abstract

Agricultural residues are readily available and inexpensive renewable resources that can be used as raw materials for the production of value-added chemicals. The application of enzymes to facilitate the degradation of agricultural residues has long been considered the most environmentally friendly strategy for converting this material into good quality value-added chemicals. However, agricultural residues are typically lignocellulosic in composition and recalcitrant to enzymatic hydrolysis. Due to this recalcitrant nature, the complete degradation of biomass residues requires the synergistic action of a broad range of enzymes. The development and optimisation of synergistic enzyme cocktails is an effective approach for achieving high hydrolysis efficiency of lignocellulosic biomass.

The aim of the current study was to evaluate the synergistic interactions between two termite metagenome-derived feruloyl esterases (FAE6 and FAE5) and endo-xylanases for the production of hydroxycinnamic acids and xylo-oligosaccharides (XOS) from model substrates, and untreated and pre-treated agricultural residues. Firstly, the two *fae* genes were heterologously expressed in *Escherichia coli*, and the recombinant enzymes were purified to homogeneity. The biochemical properties of the purified recombinant FAEs and xylanases (XT6 and Xyn11) were then assessed to determine the factors which influenced their activities and to select suitable operating conditions for synergy studies. An optimal protein loading ratio of xylanases to FAEs required to maximise the release of both reducing sugar and ferulic acid (FA) was established using 0.5% (w/v) insoluble wheat arabinoxylan (a model substrate). The enzyme combination of 66% xylanase and 33% FAE (on a protein loading basis) produced the highest amounts of reducing sugars and FA. The enzyme combination of XT6 (GH10 xylanase) and FAE5 or FAE6 liberated the highest amount of FA while a combination of Xyn11 (GH11 xylanase) and FAE5 or FAE6 produced the highest reducing sugar content.

The synergistic interactions which were established between the xylanases and FAEs were further investigated using agricultural residues (corn cobs, rice straw and sugarcane bagasse). The three substrates were subjected to hydrothermal and dilute acid pre-treatment prior to synergy studies. It is generally known that, during pre-treatment, many compounds can be produced which may influence enzymatic hydrolysis. The effects of these by-products were assessed and it was found that lignin and its degradation products were the most inhibitory to the FAEs. The optimised enzyme cocktail was then applied to 1% (w/v) of untreated and pre-treated substrates for the efficient production of XOS and hydroxycinnamic acids. A significant

improvement in xylanase substrate degradation was observed, especially with the combination of 66% Xyn11 and 33% FAE6 which displayed an improvement in reducing sugars of approximately 1.9-fold and 3.4-fold for hydrothermal and acid pre-treated corn cobs (compared to when Xyn11 was used alone), respectively. The study demonstrated that pre-treatment substantially enhanced the enzymatic hydrolysis of corn cobs and rice straw. Analysis of the hydrolysate product profiles revealed that the optimised enzyme cocktail displayed great potential for releasing XOS with a low degree of polymerisation.

In conclusion, this study provided significant insights into the mechanism of synergistic interactions between xylanases and metagenome-derived FAEs during the hydrolysis of various substrates. The study also demonstrated that optimised enzyme cocktails combined with low severity pre-treatment can facilitate the potential use of xylan-rich lignocellulosic biomass for the production of valuable products in the future.

Table of contents

Contents

Plagiarism declaration	ii
Abstract	iii
Table of contents	v
List of figures	x
List of tables	xvi
List of units and abbreviations	xvii
List of research outputs emanating from this study	xix
Publications in peer reviewed journals.....	xix
Book chapter	xix
Conference presentation.....	xix
Acknowledgements	xx
Chapter 1: General introduction and literature review	1
1.1. Introduction	1
1.2. Lignocellulosic biomass: composition and structure	2
1.2.1. Cellulose	3
1.2.2. Hemicellulose	4
1.2.2.1. Xylan	5
1.2.3. Lignin.....	6
1.2.4. Plant cell wall phenolics	6
1.2.4.1. Hydroxycinnamic acids	7
1.2.4.2. Potential applications of hydroxycinnamic acids	8
1.3. Biochemical conversion of lignocellulosic biomass	8
1.3.1. Pre-treatment of lignocellulosic biomass	9
1.3.2. Enzymatic hydrolysis of lignocellulosic biomass	12
1.3.2.1. Xylanolytic enzymes	13
1.4. Xylanases	14
1.4.1. GH10 endo-xylanases.....	15
1.4.2. GH11 endo-xylanases.....	15
1.5. Feruloyl esterases	16
1.5.1. Classification of FAEs.....	16
1.5.2 Biochemical properties and sources of FAEs.....	17
1.5.3. 3D structure and catalytic mechanism of FAEs	17

1.5.4. Release of hydroxycinnamic acids	19
1.6. Synergism between FAEs and xylanases	19
Chapter 2: Motivation, aims and thesis outline	22
2.1. Motivation	22
2.2. Hypothesis.....	23
2.3. Aims and objectives	23
2.4. Thesis outline	23
Chapter 3: Expression and purification of FAE5 and FAE6.....	25
3.1. Introduction	25
3.2. Aims and objectives	26
3.2.1. Aims.....	26
3.2.2. Objectives	26
3.3. Materials and methods	27
3.3.1. Materials	27
3.3.2. Plasmid amplification	27
3.3.3. Plasmid extraction	27
3.3.4. Nucleotide sequencing and sequence verification.....	27
3.3.5. Expression of FAE5 and FAE6	28
3.3.6. Purification of recombinant FAE5 and FAE6	28
3.3.7. SDS-PAGE analysis	29
3.3.8. Protein concentration determination.....	29
3.3.9. FAE activity on <i>p</i> NP-acetate	29
3.4. Results and discussion.....	30
3.4.1. Sequence verification	30
3.4.2. SDS-PAGE analysis of FAE5 and FAE6	31
3.4.3. SDS-PAGE analysis of FAE5 and FAE6 purification	33
3.5. Conclusion.....	37
Chapter 4: Partial characterisation of purified feruloyl esterases and commercial xylanases	38
4.1. Introduction	38
4.2. Aim and objectives.....	39
4.2.1. Aim	39
4.2.2. Objectives	39
4.3. Materials and methods	39
4.3.1. Materials	39

4.3.2. Specific activity determination	39
4.3.2.1 FAE activity on ethyl ferulate	39
4.3.2.2. Xylanase activity	40
4.3.2.2.1. Xylanase activity on insoluble wheat arabinoxylan	40
4.3.2.2.2. Xylanase activity on Azo-Xylan (birchwood).....	40
4.3.3. Reducing sugar quantification	41
4.3.4. Temperature optimum determination	41
4.3.5. Thermo-stability determination	41
4.3.6. pH optimum determination.....	41
4.3.7. Effect of metal ions on the FAE activity	41
4.3.8. Product inhibition studies	42
4.3.9. Statistical analysis.....	42
4.4. Results and discussion.....	42
4.4.1. Specific activity determination	42
4.4.2. Temperature optimum determination	43
4.4.3. Thermo-stability determination	45
4.4.4. pH optimum determination.....	46
4.4.5. Effect of metal ions on the FAE activity	48
4.4.6. Product inhibition studies	50
4.5. Conclusion.....	54
Chapter 5: Pre-treatment of agricultural residues and the impact of their pre-treatment by-products on enzymes	55
5.1. Introduction	55
5.2. Aims and objectives	57
5.2.1. Aims.....	57
5.2.2. Objectives	57
5.3. Materials and methods	58
5.3.1. Materials	58
5.3.2. Pre-treatment of agricultural residues.....	58
5.3.3. Chemical characterisation of agricultural residues.....	58
5.3.4. Microscopic analysis of agricultural residues	59
5.3.4.1. Scanning electron microscopy analysis	59
5.3.4.2. Light microscopy analysis	59
5.3.5. FTIR analysis.....	59
5.3.6. Determination of water retention capacity of agricultural residues	59

5.3.7. The impact of pre-treatment by-products and wash liquors from agricultural residues on enzyme activities	60
5.3.7.1. Pre-treatment by-products	60
5.3.7.2. Pre-treatment by-products inhibition assays.....	60
5.3.7.3. Preparation of wash liquors from pre-treated agricultural residues	60
5.3.7.4. Evaluation of the impact of wash liquors from agricultural residues on enzyme activity	61
5.3.8. Statistical analysis.....	61
5.4. Results and discussion.....	61
5.4.1. Chemical characterisation of agricultural residues.....	61
5.4.2. Microscopic analysis of agricultural residues	63
5.4.2.1. SEM analysis for morphological changes	63
5.4.2.2. Light microscopy analysis	64
5.4.3. FTIR analysis of untreated and pre-treated agricultural residues.....	66
5.4.4. Determination of water retention capacity of agricultural residues	68
5.4.5. Inhibitory effect of pre-treatment by-products on FAEs	69
5.4.6. Determination of inhibition patterns.....	72
5.4.7. Evaluation of the inhibitory effect of wash liquors from pre-treated substrates on enzyme activities	75
5.5. Conclusion.....	79
Chapter 6: Evaluation of synergism between feruloyl esterases and xylanases on model substrates and agricultural residues	80
6.1. Introduction	80
6.2. Aims and objectives	82
6.2.1. Aims.....	82
6.2.2. Objectives	82
6.3. Materials and methods	82
6.3.1 Materials	82
6.3.2. Synergy studies on model substrates	82
6.3.3. Synergy studies on untreated and pre-treated agricultural residues	83
6.3.4. Detection of hydroxycinnamic acids by HPLC-MS/MS.....	83
6.3.5. Determination of xylo-oligosaccharides pattern profiles	84
6.3.6. Quantification of xylo-oligosaccharides.....	84
6.3.7. Statistical analysis.....	84
6.4. Results and discussion.....	84
6.4.1. Evaluation of synergism between FAEs and xylanases on model substrates.....	84

6.4.2. HPLC-MS/MS confirmation of FA released from WAX	90
6.4.3. Release of XOS from model substrates by enzymatic hydrolysis.....	92
6.4.4. Determination of hydrolysate product profiles.....	95
6.4.5 Evaluation of synergism between FAEs and xylanases during the hydrolysis of agricultural residues.....	99
6.4.6. Release of XOS from agricultural residues by enzymatic hydrolysis	99
6.4.7. Determination of hydrolysate product profiles.....	104
6.4.8. Release of hydroxycinnamic acids from agricultural residues by enzymatic hydrolysis.....	111
6.4.9. HPLC-MS/MS confirmation of FA and <i>p</i> -CA released from agricultural residues	115
6.5. Conclusion.....	118
Chapter 7: General discussion, conclusions, and future recommendations.....	119
7.1. General discussion and conclusions.....	119
7.2. Future recommendations	125
References.....	126
Appendices.....	151
Appendix A: Reagents list and suppliers	151
Appendix B: Standard curves.....	153
Appendix C: Chromatograms from HPLC-UV/RID analysis.....	158

List of figures

Figure	Page no.
Figure 1.1: Schematic structures of the main components of lignocellulose.	4
Figure 1.2: Chemical structure of hydroxycinnamic acid.	7
Figure 1.3: Overview of biochemical conversion of lignocellulosic biomass into value added chemicals.	9
Figure 1.4: Schematic representation of untreated and pre-treated lignocellulosic biomass.	10
Figure 1.5: Schematic representation of enzyme sites of the enzymes required for complete degradation of highly branched xylan.	14
Figure 3.1: A Multiple sequence alignment of FAEs performed with Clustal Omega.	31
Figure 3.2: SDS-PAGE analysis of expression of FAE5 and FAE6.	33
Figure 3.3: SDS-PAGE analysis of FAE5 and FAE6 purification with Nickel Affinity chromatography.	34
Figure 3.4: SDS-PAGE analysis of FAE5 and FAE6 purification with a PD-10 desalting column.	36
Figure 4.1: Effects of temperature on the activities of FAEs and xylanases.	44
Figure 4.2: Determination of thermostability of FAEs and xylanases.	46
Figure 4.3: The effect of pH on the activities of FAEs and xylanases.	47
Figure 4.4: The effects of various metal ions on FAE activity.	49

Figure 4.5: The effect of FA on FAE and xylanase activity.	51
Figure 4.6: The effect of xylobiose on FAE and xylanase activity.	53
Figure 5.1: Morphological study of agricultural residues by SEM.	64
Figure 5.2: Histochemical analysis of lignin in untreated and pre- treated agricultural residues using Wiesner's staining.	65
Figure 5.3: FTIR spectra of untreated, hydrothermal treated and acid treated agricultural residues registered in the range of 450-4000 cm^{-1} .	67
Figure 5.4: Inhibitory effects of lignin and its degradation products on FAE5 and FAE6 activity.	70
Figure 5.5: Inhibitory effects of sugar degradation products and acids on FAE5 and FAE6 activity.	71
Figure 5.6: Lineweaver-Burk plot of the inhibition of (A) FAE5 and (B) FAE6 activity by lignin.	73
Figure 5.7: Lineweaver-Burk plot of the inhibition of (A) FAE5 and (B) FAE6 activity by vanillin.	74
Figure 5.8: Determination of the inhibitory effects of soluble pre-treatment by-products in washes of pre-treated agricultural residues.	77
Figure 5.9: Determination of the inhibitory effects of soluble pre-treatment by-products in washes of pre-treated agricultural residues.	78
Figure 6.1: Release of ferulic acid from 0.5% (w/v) WAX at increasing enzyme doses of FAE6 or Xyn11.	86

Figure 6.2: Release of ferulic acid during the degradation of 0.5% (w/v) WAX by individual enzymes or a combination of 66% xylanase: 33% FAE5 or FAE6.	88
Figure 6.3: LC-MS analysis of ferulic acid released during hydrolysis of 0.5% (w/v) WAX by a combination of 66% Xyn11: 33% FAE6.	91
Figure 6.4: Release of reducing sugars during hydrolysis of 0.5% (w/v) oat spelt xylan (OSX) by individual enzymes or a combination of 66% xylanase: 33% FAE5 or FAE6.	93
Figure 6.5: Release of reducing sugars during hydrolysis of 0.5% (w/v) wheat arabinoxylan (WAX) by individual enzymes or a combination of 66% xylanase: 33% FAE5 or FAE6.	94
Figure 6.6: Thin-layer chromatography analysis of hydrolysis of 0.5% (w/v) WAX by (2) xylanase alone, (3) a combination of 66% xylanase: 33% FAE5, and (4) a combination of 66% xylanase: 33% FAE6. Substrate without enzyme was used as a control (1).	96
Figure 6.7: Xylo-oligosaccharide content measured from the hydrolysis of 0.5% (w/v) WAX after incubation with Xyn11 alone or a combination of 66% Xyn11: 33% FAE5 or FAE6.	98
Figure 6.8: Release of reducing sugars during hydrolysis of 1% (w/v) untreated (A), hydrothermally pre-treated (B) and acid pre-treated corn cob (C) by individual enzymes or a combination of 66% Xyn11: 33% FAE5 or FAE6.	101
Figure 6.9: Release of reducing sugars during hydrolysis of 1% (w/v) untreated (A), hydrothermally pre-treated (B) and acid pre-treated rice straw (C) by individual enzymes or a combination of 66% Xyn11: 33% FAE5 or FAE6.	102

Figure 6.10: Release of reducing sugars during hydrolysis of 1% (w/v) untreated (A), hydrothermally pre-treated (B) and acid pre-treated sugarcane bagasse (C) by individual enzymes or a combination of 66% Xyn11: 33% FAE5 or FAE6. 104

Figure 6.11: Thin-layer chromatography analysis of hydrolysis of 1% (w/v) untreated (A), hydrothermal pre-treated (B) and acid pre-treated corn cob (C) by (2) Xyn11 alone, (3) a combination of 66% Xyn11: 33% FAE5, and (4) a combination of 66% Xyn11: 33% FAE6. 105

Figure 6.12: Thin-layer chromatography analysis of hydrolysis of 1% (w/v) untreated (A), hydrothermal pre-treated (B) and acid pre-treated rice straw (C) by (2) Xyn11 alone, (3) a combination of 66% Xyn11: 33% FAE5, and (4) a combination of 66% Xyn11: 33% FAE6. 107

Figure 6.13: Thin-layer chromatography analysis of hydrolysis of 1% (w/v) untreated (A), hydrothermal pre-treated (B) and acid pre-treated sugarcane bagasse (C) by (2) Xyn11 alone, (3) a combination of 66% Xyn11: 33% FAE5, and (4) a combination of 66% Xyn11: 33% FAE6. 108

Figure 6.14: Xylo-oligosaccharide content measured from the hydrolysis of 1% (w/v) untreated (A), hydrothermal pre-treated (B) and acid pre-treated corn cob (C) after incubation with Xyn11 alone or a combination of 66% Xyn11: 33% FAE5 or FAE6. 110

Figure 6.15: Release of *p*-coumaric (*p*-CA) and ferulic acid (FA) during the degradation of 1% (w/v) untreated (A), hydrothermal pre-treated (B) and acid pre-treated corn cobs (C) by individual enzymes or a combination of 66% Xyn11: 33% FAE5 or FAE6. 112

Figure 6.16: Release of *p*-coumaric (*p*-CA) and ferulic acid (FA) during the degradation of 1% (w/v) untreated (A), hydrothermal pre-treated (B) and acid pre-treated rice straw (C) by individual enzymes or a combination of 66% Xyn11: 33% FAE5 or FAE6. 113

Figure 6.17: LC-MS/MS analysis of ferulic acid released during hydrolysis of 1% (w/v) untreated rice straw by a combination of 66% Xyn11: 33% FAE6.	116
Figure 6.18: LC-MS/MS analysis of <i>p</i> -coumaric acid released during hydrolysis of 1% (w/v) untreated rice straw by a combination of 66% Xyn11: 33% FAE6.	117
Figure B. 1.1: Protein standard curve generated using the Bradford protein assay using various concentrations of BSA.	153
Figure B. 2.1: Xylose standard curve generated using the DNS assay.	153
Figure B. 2.2: Glucose standard curve generated using the DNS assay.	154
Figure B. 3.1: <i>p</i> -nitrophenol standard curve.	154
Figure B. 4.1: Glucose standard curve using Megazyme™ kit for glucose determination (K-GLUC).	155
Figure B. 4.2: Arabinose standard curve using Megazyme™ kit for arabinose determination (K-ARGA).	155
Figure B. 4.3: Xylose standard curve using Megazyme™ kit for xylose determination (K-XYLOSE).	156
Figure B. 5.1: Ferulic acid standard curve generated using HPLC- UV analysis.	156
Figure B. 5.2: <i>p</i> -Coumaric acid standard curve generated using HPLC- UV analysis.	157
Figure C. 1.1: HPLC-RID chromatogram of separation of XOS standards (0.4 mg/mL, injected 20 µL).	158

Figure C. 1.2: HPLC-UV chromatogram of ferulic acid standard (0.04 mM, 158 injected 10 μ L).

Figure C. 1.3: HPLC-UV chromatogram of *p*-coumaric acid standard (0.04 mM, 159 injected 10 μ L).

List of tables

Table	Page no.
Table 1.1: Type of lignocellulosic biomasses and their chemical composition (% w/w)	2
Table 1.2: Biochemical properties of microbial FAEs	18
Table 3.1: Purification table for the purification of FAE5 and FAE6 by IMAC	37
Table 4.1: Specific activities of the enzymes assessed in this study (U/mg protein)	43
Table 5.1: Chemical composition of untreated and pre-treated agricultural residues (on a percentage dry mass basis)	63
Table 5.2: Water retention capacity of agricultural residues	68
Table 5.3: Kinetic parameters for FAE5 and FAE6 in the absence/presence of lignin	74
Table 5.4: Kinetic parameters for FAE5 and FAE6 in the absence/presence of vanillin	75

List of units and abbreviations

AA	Auxillary activity
APS	Ammonium persulphate
AX	Arabinoxylan
BSA	Bovine Serum Albumin
°C	Degree(s) Celsius
CAZy	Carbohydrate active enzyme database
CC	Corn Cob
µg	Microgram
µL	Microlitre
µM	Micromolar
µmol	Micromole
DNS	Dinitrosalicylic
DP	Degree of Polymerisation
EC	Enzyme Commission number
<i>E. coli</i>	<i>Escherichia coli</i>
EFA	Ethyl Ferulate
FA	Ferulic Acid
FAE	Feruloyl Esterase
FTIR	Fourier-transform infrared spectroscopy
g	Gram
<i>g</i>	Gravity
GH	Glycoside hydrolase
h	Hour
His	Histidine
HMF	Hydroxymethylfurfural
HPLC	High-performance liquid chromatography
IMAC	Immobilized metal affinity chromatography
IPTG	Isopropylthiogalactoside
kDa	Kilodalton
L	Litre
mg	Milligram
min	Minutes

mL	Millilitre
mM	Millimolar
MS	Mass spectrometry
NCBI	National Centre for Biotechnology Information
NREL	National Renewable Energy Laboratory
OD	Optical density
OSX	Oat spelt xylan
<i>p</i> -CA	<i>p</i> -Coumaric acid
<i>p</i> -NP	<i>p</i> -Nitrophenyl derivative
RS	Rice Straw
SCB	Sugarcane Bagasse
SDS	Sodium dodecyl sulphate
SDS-PAGE	Sodium dodecyl sulphate polyacrylamide gel electrophoresis
SEM	Scanning electron microscopy
TEMED	N, N, N', N'-tetramethylethylenediamine
TLC	Thin layer chromatography
U	Units of enzyme activity
VAPs	Value-added products
w	Weight
WAX	Wheat Arabinoxylan
XOS	Xylo-oligosaccharides
XT6	Xylanase (GH10)
Xyn11	Xylanase (GH11)

List of research outputs emanating from this study

Publications in peer reviewed journals

- i) Malgas, S., Mafa, M. S., **Mkabayi, L.** and Pletschke, B. I. 2019. A mini review of xylanolytic enzymes with regards to their synergistic interactions during hetero-xylan degradation. *World Journal of Microbiology and Biotechnology* 35 (12), 187.
- ii) **Mkabayi, L.**, Malgas, S., Wilhelmi, B.S., Pletschke, B.I.* (2020) Evaluating feruloyl esterase-xylanase synergism for hydroxycinnamic acid and xylo-oligosaccharide production from untreated, hydrothermally pre-treated and dilute-acid pre-treated corn cobs. *Agronomy*, 10 (5), art. no. agronomy10050688
- iii) **Mkabayi, L.**, Malgas, S., Wilhelmi, B.S., Pletschke, B.I.* The inhibitory effects of lignocellulosic pre-treatment by-products on feruloyl esterases. In preparation for submission.

Book chapter

- i) Malgas, S., **Mkabayi, L.**, Mathibe, B.N., Thoresen, M., Mafa, M.S., Le Roes-Hill, M., Van Zyl, W.H. and Pletschke, B.I.* (2020) Enzymatic path to bioconversion of lignocellulosic biomass In: Recent Advances in Bioconversion of Lignocellulose to Biofuels and Value Added Chemicals within the Biorefinery Concept. Edited by Edivaldo Ximenes Ferreira Filho, Leonora Rios de Souza Moreira, Eduardo de Aquino Ximenes, and Cristiane Sanchez Farinas. Elsevier, Amsterdam, Netherlands. ISBN: 978-0-12-818223-9. Pp. 5-32.

Conference presentation

- i) **Mkabayi, L.**, Malgas, S., Wilhelmi, B. S. and Pletschke, B. I. 2019. Synergistic action of two feruloyl esterases and a xylanase for the optimal production of ferulic acid and reducing sugars from plant biomass. The Catalysis Society of South Africa (CATSA) conference, Club Mykonos, Langebaan, South Africa, 10-13 November 2019. (Poster presentation).

Acknowledgements

I would like to take this opportunity to thank the following people, without whom this study would not have been possible:

I would like to give a special thanks to Prof. Brett I. Pletschke and Dr. Brendan S. Wilhelmi, my supervisors at the Department of Microbiology and Biochemistry, Rhodes University. Thank you for allowing me the opportunity to work on this research project, your unwavering encouragement, patience, and support were simply amazing, and it was an honour to work under your guidance.

To Dr. Samkelo Malgas, thank you so much for your valuable contributions towards my work and I can never thank you enough.

I would also like to extend gratitude to my fellow post-graduate students from the Enzyme Science Programme research group for their kindness and assistance.

To the members of the Department of Biochemistry and Microbiology, Rhodes University, for their support.

To my family and friends for their endless love and support throughout this research.

I also wish to acknowledge the South African Department of Science and Technology (Innovation) (DST, now DSI)/Council for Scientific and Industrial Research (CSIR), the National Biocatalysis Initiative, National Research Foundation (NRF) of South Africa and Rhodes University for funding this work. Any opinion, findings and conclusions or recommendations expressed in this material are those of the author(s) and therefore the NRF does not accept liability in regard thereto.

Chapter 1: General introduction and literature review

1.1. Introduction

The abundance of lignocellulosic biomass on earth is of great interest for a wide range of technologies that seek to produce bio-based fuels and value-added products (VAPs). Lignocellulosic biomass is considered a promising alternative to fossil fuels because of its renewable nature. Plant-derived materials, such as agricultural residues (cereal straw and bagasse), forest residues (hardwoods and softwoods), various grasses, and municipal residues (paper wastes) are among renewable biomass resources that are readily available and inexpensive for use in the production of VAPs (Cotana et al., 2014; Yuan et al., 2018). The major advantages of using lignocellulosic biomass as a feedstock for production of VAPs is that it provides environmental benefits and does not compete with food production (Chandel et al., 2018). A vast number of VAPs can be produced from refining lignocellulosic biomass, and this is a demonstration of the enormous potential this source holds for driving society to achieve a sustainable economy (Isikgor and Becer, 2015).

Various methods are available for the generation of products from lignocellulosic biomass, of which thermo-chemical conversion methods such as gasification, pyrolysis combustion, torrefaction and liquefaction have been intensely utilised (Chen et al., 2019). However, some of these methods suffer disadvantages which include consumption of extensive amounts of energy, formation of undesirable by-products and issues related to the environment. In this regard, enzymatic conversion has emerged as a major technological platform as it offers several advantages - such as environmental benefits, lower energy costs and the formation of less undesirable by-products. Due to its structural complexity and heterogeneity, the efficient enzymatic hydrolysis of lignocellulosic biomass requires the synergistic cooperation of several enzymes (Van Dyk and Pletschke, 2012). It is necessary to understand the details of this synergistic cooperation for formulating enzyme cocktails for the optimal production of VAPs. The use of enzymes with novel properties in the development of more efficient and stable enzymatic cocktails is also crucial in reducing the cost of the enzymes via lowering protein loadings or achieving higher product to enzyme ratios for the hydrolysis of lignocellulosic biomass.

1.2. Lignocellulosic biomass: composition and structure

Lignocellulose is a major structural component of plant cell walls and the precise chemical composition of lignocellulosic materials vary greatly depending on the source of the plant biomass. In general, lignocellulosic biomass is mostly composed of three major units, namely, cellulose (40-60%), hemicellulose (20-35%) and lignin (15-40%) (Sharma et al., 2019; Chandel et al., 2018; Ragauskas et al., 2014). Pectins, proteins, extractives and ash make up the remaining fraction. Table 1 shows the typical chemical compositions of all three of these components in various lignocellulosic biomasses from different plant sources. All these components are strongly interconnected, forming an intricately linked network which maintains the structural integrity of the plant cell wall and resist enzymatic attack. Cellulose and hemicellulose are linked through hydrogen bonds, while lignin is covalently linked to hemicellulose forming lignin-carbohydrate complexes (LCCs) (Giummarella et al., 2019). The structure of major components of lignocellulosic biomass is presented in Figure 1.1.

Table 1.1: Type of lignocellulosic biomasses and their chemical composition (% w/w)

	Lignocellulosic biomass	Cellulose	Hemicellulose	Lignin	Reference
Agricultural residues	Corn Cobs	32.56	38.42	15.59	(Aboagye et al., 2017)
	Corn Stalks	40.45	20.66	19.75	(Aboagye et al., 2017)
	Barley Straw	35.40	28.70	13.10	(Liu et al., 2017)
	Rice Straw	40	16	26	(Huang et al., 2016)
	Rice Husks	40	16	26	(Daza Serna et al., 2016)
	Coffee grounds	33.10	30.03	24.52	(Huang et al., 2016)
	Cotton stalk	50.42	15.64	16.32	(Zhang et al., 2018)
	Sorghum Straw	37.74	28.07	21.48	(Dong et al., 2019)

	Sugarcane	42.19	27.60	21.56	(Rocha et al., 2015)
	Bagasse				
	Sugar beet pulp	29.09	25.92	3.91	(Şenol et al., 2019)
	Wheat Straw	33.7	19.1	19.8	(Zheng et al., 2018)
Grasses	Bamboo	47.3	21.8	25.3	(Yuan et al., 2017)
	Switchgrass	31.8	25.0	31.2	(Bonfiglio et al., 2019)
	Miscanthus	45.7	19.6	32.2	(Soares Rodrigues et al., 2016)

1.2.1. Cellulose

Cellulose, the most abundant lignocellulosic biomass polymer, consists of D-glucose units connected to each other by β -1, 4 glycosidic linkages, with the repeating unit of the chain being the disaccharide, cellobiose. The linear cellulose polymers are linked together by parallel intramolecular and intermolecular hydrogen bonds to form microfibrils, which group together to constitute cellulose fibers (Robak and Balcerek, 2018). Cellulose usually consists of both crystalline (highly ordered and difficult to degrade) and amorphous (less ordered) regions. The polymer is further embedded in a lignocellulosic matrix.

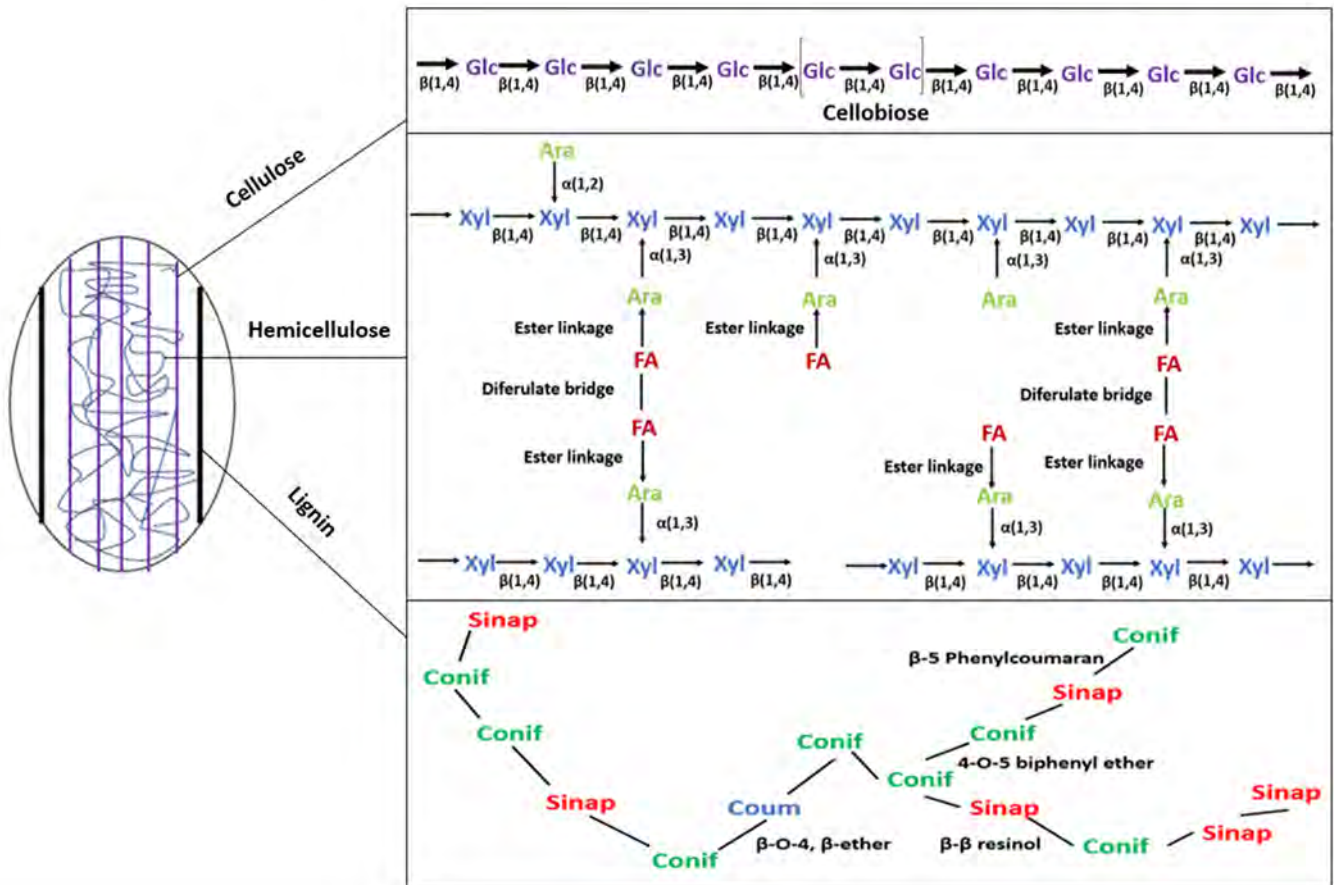


Figure 1.1: Schematic structures of the main components of lignocellulose. For cellulose, Glc (glucose) units linked by β -1, 4 glycosidic linkages are shown. For hemicellulose, a structure of arabinoxylan is shown. The symbols are as follows; Xyl (xylose), Ara (arabinose), FA (ferulic acid), the bonds are β -1, 4 glycosidic linkages, ester linkages and diferulate bridges. For lignin, the building blocks; Sinap (sinapyl alcohol), Conif (coniferyl alcohol), Coum (*p*-coumaryl alcohol), as well as the bonds; (β -O-4 (β -ether), β - β resinol, 4-O-5 biphenyl ether and β -5 phenylcoumaran), are shown (Adapted from Mota et al., 2018).

1.2.2. Hemicellulose

Hemicellulose is the second most abundant terrestrial polysaccharide in nature. It constitutes a type of a heteropolysaccharide with a complex structure that is composed of pentoses (xylose and arabinose), hexoses (mannose, glucose and galactose) and sugar acids (Saha, 2003). The structure is not crystalline, and is, therefore, readily hydrolysed. Unlike cellulose, hemicellulose has a degree of polymerisation (DP) in the range of 100-200 units (Mota et al., 2018), as opposed to 500-1400 glucose units per polymer in cellulose. Hemicelluloses are usually grouped into classes based on the main sugar residues present in the backbone, and

these include xyloglucans, xylans, mannans and glucomannans, and glucans (Scheller and Ulvskov, 2010).

1.2.2.1. Xylan

The distribution of hemicellulose in plants varies greatly; hardwoods and grasses contain xylans as the major hemicellulosic component, whereas mannans are more prevalent in softwoods and some specialised structures such as fruits and seed endosperms. Among hemicelluloses, xylan is the most abundant polysaccharide, its characteristic feature of which is the backbone composed of xylose residues linked by β -1, 4 glycosidic bonds. The main chain carries a variable number of substituents such as D-glucuronic acid, 4-*O*-methyl-D-glucuronic acid, arabinofuranosyl units and *O*-acetyl groups.

Depending on the type of substituents, xylan can be classified into three subfamilies, namely, glucuronoxylan (GX), arabinoglucuronoxylan (AGX) and arabinoxylan (AX). GX is mainly found in hardwoods and is usually composed of a xylan backbone randomly substituted at *O*-2 position of xylose residues by 4-*O*-methyl α -1, 2-D-glucuronic acid or α -D-glucuronic acid (Ebringerova et al., 2005). It may also be found acetylated at *O*-3 and *O*-2 positions of xylose residues (Biely, 2012). In contrast, the AGX main chain is substituted by 4-*O*-methyl α -(1 \rightarrow 2)-D-glucuronic acid and α -L-arabinofuranosyl units (Gatenholm and Tenkanen, 2003). Hydroxycinnamic acids (i.e. ferulic acid and *p*-coumaric acid) can be linked by ester linkages to arabinofuranosyl units (at the *O*-5 position). AX is the major non-starch polysaccharide constituent of many cereal grains such as wheat, sorghum, bamboo, oats, rye, rice and sugarcane (Peng and She, 2014; Revanappa et al., 2015; Stoklosa et al., 2019). The AX backbone is typically substituted by mono- or di- α -L-arabinofuranosyl units which may further be substituted by hydroxycinnamic acids at the *O*-5 position (Lagaert et al., 2014). The main chain may also be substituted by acetyl groups in *O*-2 and *O*-3 positions.

The xylan rich lignocellulosic biomasses (corn cobs, rice straw, sugarcane bagasse, *etc.*) are considered as the potential feedstocks for the production of VAPs. Considerable progress has been made in the development of xylan-based products and their applications in a wide range of industries. Some of the xylan-based chemical products have already found commercial applications, and these include bioactive products (xylo-oligosaccharides), fermentation products (xylitol, ethanol), packaging films and surfactants (Naidu et al., 2018).

Xylo-oligosaccharides (XOS) are the hydrolysis products of xylans with a DP ranging from 2 to 10, and the side groups present and their substitution pattern on the main chain vary greatly

depending on the raw materials used to generate the XOS (Samanta et al., 2015; Belorkar and Gupta, 2016). It has been demonstrated that XOS have prebiotic properties as they selectively enhance the growth of health promoting bacteria (Samanta et al., 2015; Saville and Saville, 2018). Besides prebiotic activity, XOS have been reported to possess several biological benefits such as antioxidant activity, anti-inflammatory properties, prevention of diabetes and neurotoxicity (Bhatia et al., 2019; Amorim et al., 2019). Another widely produced xylan-based product is xylitol. It is used as a natural food sweetener, dental caries reducer, sugar substitute in diabetic products, and ingredient in chewing gum. Xylitol can be produced by chemical and biochemical processes from xylose which is recovered from xylan hydrolysis (Mohamad et al., 2015).

1.2.3. Lignin

Lignin is the most abundant non-polysaccharide fraction of lignocellulosic biomass. It is an extremely complex three-dimensional phenolic polymer composed of *p*-hydroxyphenyl (H), guaiacyl (G) and syringyl (S) monomers which are derived from three *p*-hydroxycinnamyl alcohols (*p*-coumaryl, coniferyl and sinapyl) (Boerjan et al., 2003). The H, G and S monomers are complexed by a variety of inter-unit linkages, namely, β -O-4 (β -ether), β - β resinol, β -5 phenylcoumaran and 4-O-5 biphenyl ether (Boerjan et al., 2003). The distribution of these monomers may vary significantly depending on the plant species (Shigeto et al., 2017). Lignin is responsible for the structural rigidity of the plant cell wall and the plant's chemical resistance against biological attack. Hemicellulose and lignin are believed to be covalently crosslinked forming LCCs. The xylan-lignin complexes in commelinid monocots, such as grasses, are influenced by hydroxycinnamic acids. It has been reported that hydroxycinnamic acids, most especially ferulic acid, can dimerise with other ferulic acid molecules that are esterified in arabinoxylan or can covalently link to the lignin by ether bonds (Terrett and Dupree, 2019; Oliveira et al., 2019). These complexes contribute greatly to the recalcitrance of lignocellulosic biomass and its bio-digestibility.

1.2.4. Plant cell wall phenolics

Plant phenolic compounds are secondary metabolites that can be broadly classified into simple phenols and polyphenols. Their characteristic structural feature is a common aromatic ring with one or more hydroxy groups (Khoddami et al., 2013). They consist of simple phenols, phenolic acids, coumarins, lignins, lignans, tannins and flavonoids. Phenolic acids, characterised by a carboxyl group linked to benzene ring, are one of the main class of phenolic compounds and can be further divided into hydroxybenzoic acids (gallic, syringic and vanillic acids) and

hydroxycinnamic acids (ferulic, *p*-coumaric, caffeic, chlorogenic and sinapic acids) (Durazzo et al., 2019). Hydroxycinnamic acids along with lignins are the two major cell wall phenolics.

1.2.4.1. Hydroxycinnamic acids

Ferulic acid (FA) and *p*-coumaric acid (*p*-CA) are distributed widely throughout most graminaceous plants such as wheat, pineapple, corn, rice, bamboo and oats (Kumar and Pruthi, 2014; Ferreira et al., 2018). FA is the most abundant hydroxycinnamic acid, it is present in particularly high concentrations in numerous biomass sources such as maize bran (3000 mg/100 g), corn bran (2610-3300 mg/100 g), wheat bran (1358-2293 mg/100 g), beets (800 mg/100 mg) as well as in bamboo shoots (243.6 mg/100 g) (Paiva et al., 2013). They are usually found covalently linked to the polysaccharides by ester bonds and with lignin by ether bonds, playing a key role in cross-linking cell wall polymers. The chemical structures of FA and *p*-CA are presented in Figure 1.2.

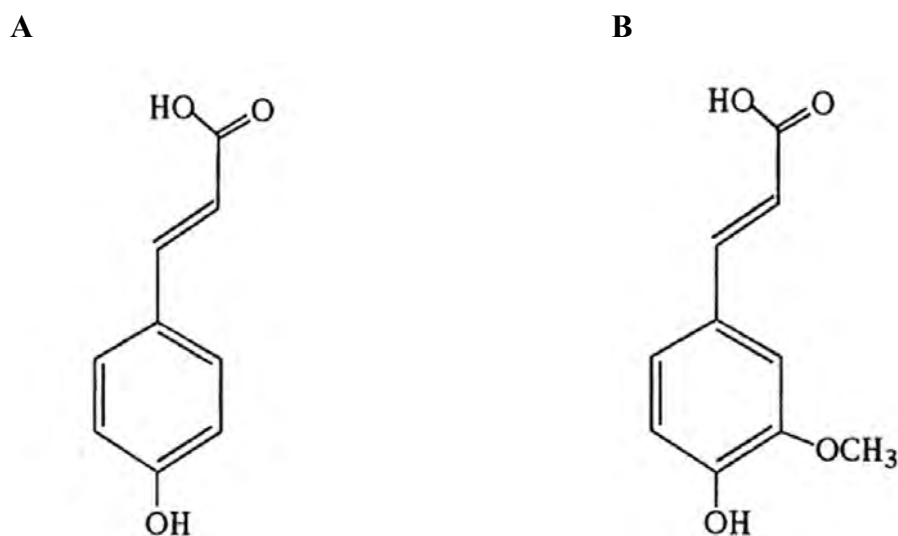


Figure 1.2: Chemical structure of hydroxycinnamic acid. (A) *p*-CA and (B) FA.

One of the most important roles of hydroxycinnamic acids is their ability to stop free radical chain reactions, giving them their effective antioxidant activity. It has been reported that stabilisation of free radicals mainly depends on the number of methoxy and hydroxy groups attached to the phenyl ring (Aguilar-Hernandez et al., 2017).

1.2.4.2. Potential applications of hydroxycinnamic acids

Hydroxycinnamic acids have attracted a growing interest in the chemical, cosmetic, food, health and pharmaceutical industries since they have been shown to be bioactive molecules, possessing excellent biomedical benefits. FA and *p*-CA are well-known for their antioxidant properties; they stabilise free radicals generated by ultraviolet (UV)-light and various metabolic activities, thereby increasing protection against oxidative damage to biomolecules. Several studies have reported that FA exhibited protective effects in organs of rats such as the brain, kidney, intestine and liver, and these effects were attributed to the prevention of oxidative stress (Mhillaj et al., 2018; Kelainy et al., 2019; Mahmoud et al., 2020). Among hydroxycinnamic acids, *p*-CA exhibits lower antioxidant potency in single-component systems compared to when used in complicated systems such as foods and cell lines (Pei et al., 2016). In addition to their antioxidant properties, FA and *p*-CA have other biological activities, including antimicrobial, anti-inflammatory, antiviral, antiplatelet aggregation, anti-arthritis activities, antidiabetic, anticarcinogenic, hepatoprotective and neuroprotective effects (Kumar and Pruthi, 2014; Pei et al., 2016).

1.3. Biochemical conversion of lignocellulosic biomass

The bioconversion of lignocellulosic biomass to bio-based fuels and VAPs normally requires multi-step processing that include pre-treatment, enzymatic hydrolysis and fermentation. The pre-treatment step aims to disrupt the strongly interconnected structure of the holocellulose, a cellulose–hemicellulose–lignin matrix, thereby increasing the surface area, reducing cellulose crystallinity and enhancing bio-digestibility of the biomass (Behera et al., 2014; Rastogi and Shrivastava, 2017). The schematic representation of pre-treatment is shown in Figure 1.4. The pre-treated biomass is then further subjected to enzymatic hydrolysis for the conversion of carbohydrate polymers to fermentable monosaccharides and bioproducts. The fermentation step involves utilisation of monosaccharides (by an appropriate microbial system) produced during the enzymatic hydrolysis to biofuels such as ethanol. Figure 1.3 below summarises the bioconversion of biomass into biofuels and other VAPs.

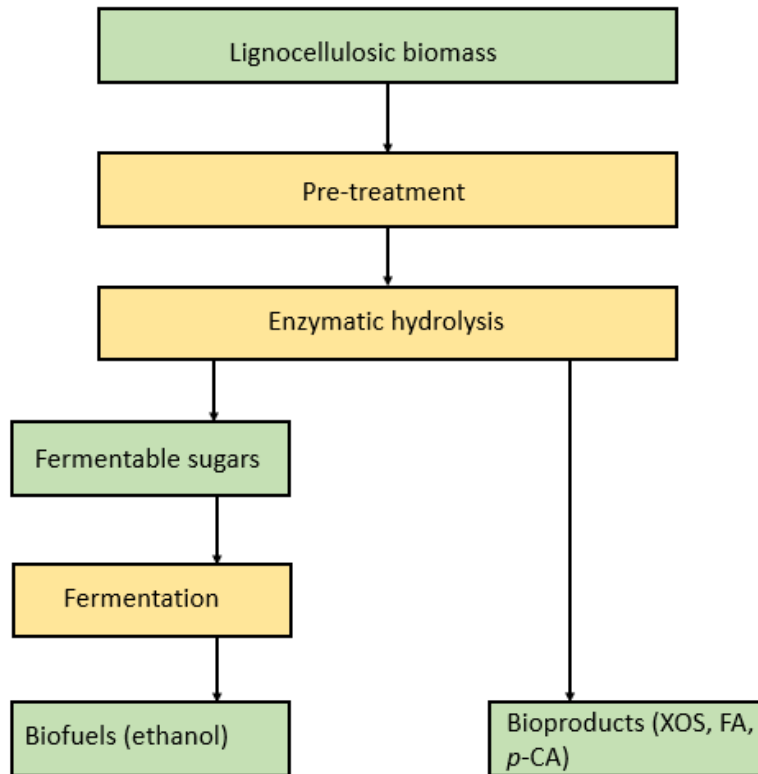


Figure 1.3: Overview of biochemical conversion of lignocellulosic biomass into value added chemicals.

1.3.1. Pre-treatment of lignocellulosic biomass

Despite the huge potential in the valuable utilisation of lignocellulosic biomass via bioconversion, the major challenge encountered is the complex structure and characteristics of different biopolymers in the biomass. In this context, pre-treatment (Figure 1.4) is a significant step for the improvement of bioconversion as it alters the native macromolecular structure of biomass to be more susceptible to enzymatic hydrolysis. The relative chemical compositions of various lignocellulosic biomasses are different, and it is, therefore, necessary to understand the structure in order to select a suitable pre-treatment method. Pre-treatment methods are generally categorised into different groups; physical (milling, grinding and chipping), physico-chemical (hydrothermal, steam explosion, etc.), chemical (alkali, dilute acids and organic solvents) and biological pre-treatments (Kumar and Sharma, 2017). In general, the pre-treatment method selection is based on the following considerations: (a) the selected method should minimise degradation of polysaccharides, (b) minimise the formation of degradation products, (c) increase the production of desirable products and (d) be economically feasible

and environmental friendly (Chen et al., 2017, Kumar and Sharma, 2017; Singh, J. K. et al., 2018).

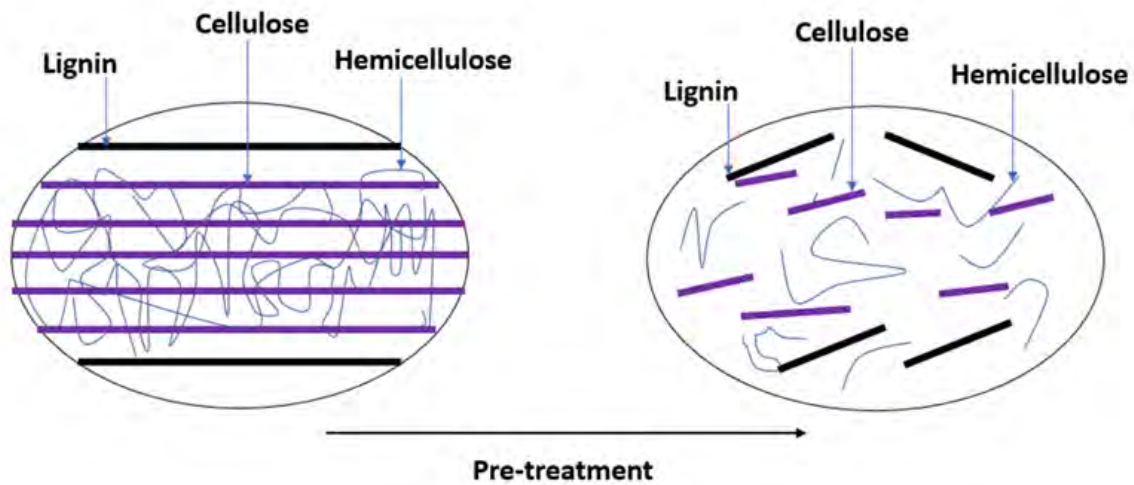


Figure 1.4: Schematic representation of untreated and pre-treated lignocellulosic biomass.

The choice of a pre-treatment strategy is very important and needs to be compatible with the overall process. Generally, the main aim of a physical pre-treatment method is to break down biomass size to increase the surface area, to decrease the DP and the crystallinity of the cellulose, and one of the advantages of this type of pre-treatment is that it does not lead to the generation of toxic side streams (da Silva et al., 2010; Barakat et al., 2014; Zubrowska-Sudol and Walczak, 2014). Commonly used physical methods include milling (colloid milling, vibratory mills, hammer mills and centrifugal mills), grinding, chipping and irradiation. However, many of these methods are unlikely to be economically viable options because of the high-energy requirement. One of the promising pre-treatment methods is biological pre-treatment as it is considered as an efficient, eco-friendly and cheap alternative (Wan and Li, 2012; Wei et al., 2015). Biological pre-treatment is usually performed by employing microorganisms such as bacteria (*Actinomycetes*) and fungi (white-rot fungus) (Rouches et al., 2016; Amin et al., 2017; Chen et al., 2017). However, its disadvantages make it less attractive for industrial purposes, which include long residence times of 10-14 days, necessity to maintain sterile conditions and consumption of some fraction of the carbohydrates by the microorganisms.

Chemical and physico-chemical pre-treatments are widely used because they are more effective and enhance the enzymatic degradation of biomass. The most commonly used chemical methods are concentrated or dilute acid (sulfuric acid, hydrochloric acid and acetic acid) and alkali (sodium hydroxide, potassium hydroxide, lime, aqueous ammonia and hydrogen peroxide) (Behera et al., 2014; Kim et al., 2016; Solarte-Toro et al., 2019). The category of physico-chemical methods includes steam explosion, liquid hot water, wet oxidation, organosolv, ammonia fibre explosion and carbon dioxide explosion (Kumari and Singh, 2018; Kumar et al., 2020). These varied processes have different impacts on the structure of the biomass after processing. Acid pre-treatments usually alter the structure of lignin by solubilising acid soluble lignin and the hemicellulosic fraction of the biomass. Unlike acid treatment, alkali treatments remove lignin by breaking acetyl groups and various ester linkages between lignin and hemicellulose, improving access of the enzyme for hydrolysis in the subsequent steps. The physico-chemical methods combine high temperature, pressure and some chemicals for the efficient disruption of the recalcitrant structure of biomass to facilitate the access of enzymes in the subsequent biomass processing step.

Despite the effect of the pre-treatment combating lignocellulose recalcitrance and increasing the rate and extent of enzymatic hydrolysis of the raw material, different methods have different advantages and disadvantages. Alkaline treatments are comparatively more effective in applications that require highly efficient removal of lignin and a variety of uronic acid substitutions on hemicellulose (Shahabazuddin et al., 2018). A significant disadvantage of alkaline pre-treatment is the introduction of large amounts of salts into biomass and the high cost of the chemicals. Acid treatment is responsible for exposing cellulose to enzymatic hydrolysis via solubilisation of the hemicellulose component. Several studies have demonstrated that the use of dilute acid can greatly enhance the production of reducing sugars from pre-treated biomass (Tao et al., 2017; Sahoo et al., 2018). However, harsh operating acid conditions can lead to the production of undesirable compounds, namely, furfural and 5-hydroxymethyl furfural, which have a negative impact on enzymatic hydrolysis (Kucharska et al., 2018) and fermentation of sugars.

Steam explosion and liquid hot water (hydrothermal) are physico-chemical methods, which are most widely employed for treating the biomass. During steam explosion, lignocellulosic materials are treated by pressurised steam in a temperature range of 160-270°C for a few seconds to few minutes. Various lignocellulosic materials such as wheat straw, sugarcane bagasse and *Miscanthus* have been treated using this method (Bruno et al., 2016; Ivo et al.,

2016; Carvalho et al., 2018). In contrast to steam explosion, liquid hot water employs high temperature and pressure to keep the water in a liquid state which leads to disruption of the structure of biomass. Different reports suggest that it can be an effective pre-treatment technique for a variety of agricultural residues (Chandra et al., 2012; Kumari and Singh, 2018). Steam explosion and liquid hot water are advantageous because they are usually performed in the absence of any chemical or catalyst, which makes them an eco-friendly and cost-effective method.

To overcome some of the limitations mentioned above, a combination of two or more methods for improving the pre-treatment process is usually utilised. For example, Wen et al. (2011) investigated the application of dilute acid in combination with steam explosion pre-treatment of rice straw for maximizing xylose yield and reducing the production of inhibitors. In another study, dilute acid and alkaline wet oxidation of corn stover was investigated by An et al. (2018). The method showed significant improvements in sugar recovery and lignin removal. Several combinations have been studied and the results obtained from these experiments display an increased efficiency of production and shorter processing time (Kumari and Singh, 2018).

1.3.2. Enzymatic hydrolysis of lignocellulosic biomass

The complete enzymatic hydrolysis of lignocellulosic biomass requires a variety of enzymes, including cellulases, hemicellulases and oxidative enzymes (of which most of them are involved in the degradation of lignin). Enzymes involved in complex polysaccharide deconstruction and modification are collectively known as Carbohydrate-Active EnZymes (CAZymes) and are classified into several enzyme classes, namely, glycoside hydrolases (GHs), glycosyl transferases (GTs), polysaccharide lyases (PL), carbohydrate esterases (CE), and auxiliary activities (AA) (Lombard et al., 2014).

Cellulose, the major polysaccharide within plant cell walls, is degraded by cellulases; endoglucanases (EG, EC 3.2.1.4), exoglucanases, including both cellobiohydrolases (CBH) I and II (CBHs, EC 3.2.1.91 and EC 3.2.1.176), and (3) β -glucosidases (EC 3.2.1.21). EGs internally cleave glycosidic bonds in the amorphous regions of cellulose thereby creating new ends for CBHs to bind to. CBHs act processively along the crystalline portion of cellulose releasing cellobiose as a major product from the reducing (CBHI) or nonreducing ends (CBHII), whereas β -glucosidases ultimately hydrolyse cellobiose to release glucose, completing the hydrolysis of cellulose (Kubicek and Kubicek, 2016; Srivastava et al., 2018). It has been reported that a group of enzymes under the AA families, namely, lytic polysaccharide

monooxygenases (LPMOs) are able to facilitate the cleavage of glycosidic bonds of cellulose chains through an oxidative mechanism (Ezeilo et al., 2017).

The hemicellulosic component of plant cell walls is much more heterogenous and, therefore, its degradation demands the action of several types of enzymes. Depending on the main sugar residues present in the backbone, the enzymatic machinery required might be xylanolytic or mannanolytic as well as accessory enzymes. Hemicellulose degradation requires two different groups of enzymes: depolymerising enzymes which are responsible for hydrolysing glycosidic linkages in the main chain and debranching enzymes that remove substituent from the main chain (Van Dyk and Pletschke 2012; Malgas et al., 2019). Lignin degradation is mainly accomplished by enzymes belonging to AA families which include manganese-dependent peroxidases (MnP, EC 1.11.1.13), lignin peroxidases (LiP, EC 1.11.1.14), versatile peroxidases (VPs, EC 1.11.1.16) and laccases (EC 1.10.3.2) (Brown and Chang, 2014; Andlar et al., 2018; Chio et al., 2019). These laccases and peroxidases take part in redox processes, where phenolic compounds are transformed into free-radicals. They are also involved in the production of redox mediators which facilitate lignin depolymerization.

1.3.2.1. Xylanolytic enzymes

Xylan rich lignocellulosic biomass is readily available in nature and there is a need for degradation of this complex polymer for its efficient utilisation for various applications in industrial processes. The complete depolymerisation of xylan into simple monosaccharides and XOS is accomplished by a group of xylanolytic enzymes which act synergistically (Biely et al., 2016; Malgas et al., 2019). Among these, endo-xylanase (EC 3.2.1.8) is the key enzyme which initiates degradation by randomly cleaving the glycosidic bonds in the xylan backbone releasing XOS (Mendis and Simsek, 2015; Bhardwaj et al., 2019). β -Xylosidases (EC 3.2.1.37) catalyses the hydrolysis of xylobiose and the non-reducing ends of short XOS produced by endo-xylanase into xylose. α -L-Arabinofuranosidases (E.C. 3.2.1.55) remove the arabinofuranose residues substituted at position O-2 or O-3 of mono- or di-substituted xylose residues present in the xylan backbone. α -Glucuronidases (EC 3.2.1.139) are required for the cleavage of the α -1, 2-glycosidic linkages between xylose and D-glucuronic acid. Feruloyl esterases (EC 3.1.1.73) are primarily involved in the hydrolysis of ester bonds between a hydroxycinnamate and xylan, releasing a phenolic acid such FA or *p*-CA (Wong et al., 2013), while acetyl xylan esterases (EC 3.1.1.72) are responsible for the hydrolysis of ester bonds to liberate acetic acid from acetylated xylan (Zhang et al., 2011). The schematic representation of the xylan structure showing bonds which are hydrolysed by key xylanolytic enzymes for

complete hydrolysis of xylan to its constituent monomeric units is presented in Figure 1.5. Here, in this study, the focus will be on the biochemical aspects and synergistic action of endo-xylanases (EC 3.2.1.8) and feruloyl esterases (EC 3.1.1.73).

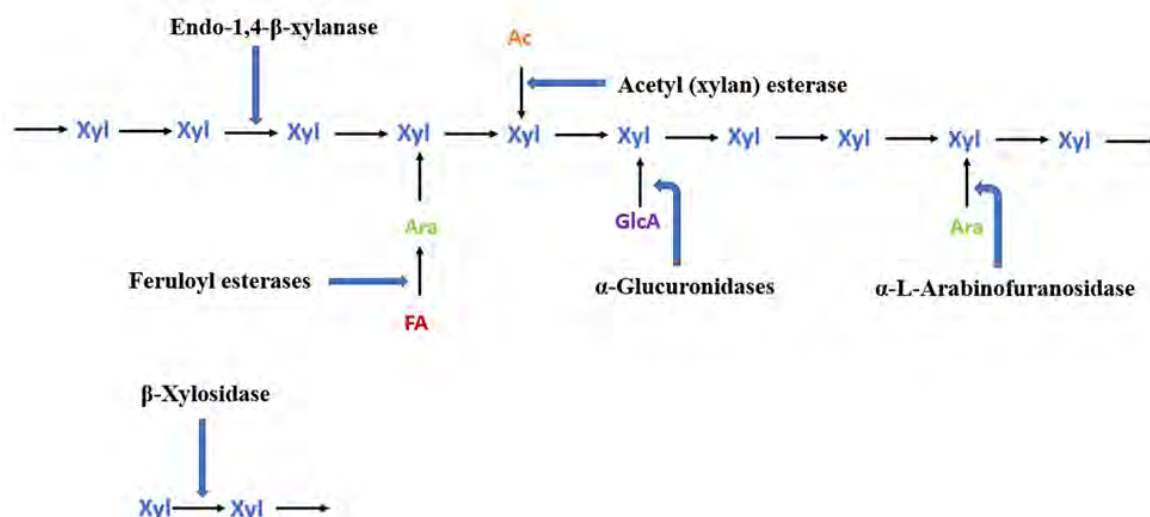


Figure 1.5: Schematic representation of enzyme sites of the enzymes required for complete degradation of heteroxylan. The symbols are as follows; Xyl (xylose), Ara (arabinose), GlcA (glucuronic acid), Ac (acetic acid) and FA (ferulic acid) (Adapted from Malgas et al., 2019).

1.4. Xylanases

The presence of xylanases is observed in a wide range of microorganisms such as bacteria, actinomycetes, yeasts and fungi (Azeri et al., 2010; Driss et al., 2012; Walia et al., 2013). Among those, the major sources are bacteria and filamentous fungi, the latter being the dominant source of commercial xylanases. According to the CAZy database (<http://www.cazy.org>), xylanases are classified under several GH families, namely, family 5, 8, 9, 10, 11, 16, 30, 43, 51, 62 and 98. These enzymes vary in terms of their mechanisms of action, substrate specificities, physico-chemical characteristics and structural features (Bhardwa et al., 2019). Members of families 16, 51 and 62 are generally bi-functional enzymes as they appear to contain two catalytic domains while enzymes grouped under families 5, 8, 10, 11, and 43 possess single distinct catalytic domains (Collins et al., 2005). Xylanases in GH families 10 and 11 have been thoroughly explored. The catalytic mechanism of xylanases may occur by two different mechanisms, namely, retention or inversion. Briefly, the xylanase catalysed xylan hydrolysis may result either in the retention or inversion of the anomeric centre

of the reducing sugar monomer of the carbohydrate (Motta et al., 2013; Lombard et al., 2014). The inversion of the configuration at the anomeric centre is a single displacement mechanism while retention is the double displacement mechanism. Members of families 5, 7, 10 and 11 catalyse the xylan hydrolysis with the retention of the anomeric configuration (Motta et al., 2013).

1.4.1. GH10 endo-xylanases

Xylanases from the GH10 family are known to have high molecular weights (more than 30 kDa) and low isoelectric points (pI), and according to structural studies, members of this family exhibit the TIM barrel (α/β)₈ fold as a catalytic domain (Teplitsky et al., 2000). Their active sites can have between four to five substrate-binding sites. The binding sites for xylose residues in xylanases are called subsites, and glycosidic bond cleavage takes place between the monomeric residues at the -1 (non-reducing) and the +1 (reducing) ends of xylan. Studies on arabinoxylan hydrolysis reveal that products generated by GH10 xylanase have arabinose residues substituted on xylose at the +1 subsite (Maslen et al., 2007). This suggests that GH10 members are less hampered by the presence of substituents along the xylan backbone and, therefore, are able to cleave regions closer to the side-chain residues (Motta et al., 2013). Furthermore, decorated XOS generated by GH10 xylanases have two unsubstituted xylose residues at the reducing end and the side groups at the non-reducing end (Mathew et al., 2018). It has been reported that GH10 xylanases require two consecutive unsubstituted xylose monomers to cleave the xylan backbone (Karlsson et al., 2018). They have low substrate specificity and exhibit high catalytic versatility as they can catalyse the hydrolysis of aryl β -D-cellobiosides. However, their ability to hydrolyse insoluble xylan substrates is low and they usually require a pre-treatment step for efficient hydrolysis of insoluble biomass (Falck et al., 2014).

1.4.2. GH11 endo-xylanases

Family GH11 enzymes are generally characterised by a low molecular weight (less than 30 kDa), a high pI and a β -jelly roll fold structure. The three-dimensional (3D) structure consists of two large β -pleated sheets and a single α -helix, forming a structure that resembles the shape of a partially closed right-hand (Torrönen and Rouvinen, 1997). This family consists solely of xylanases and they are exclusively active on D-xylose containing substrates (Collins et al., 2005). They also display high substrate selectivity and high catalytic efficiency. Like GH family 10 xylanases, GH 11 can act on the aryl β -glycosides of xylobiose and xylotriose at the aglyconic bond, but these enzymes are incapable of catalysing hydrolysis of aryl β -D-

cellobiosides (Motta et al., 2013). Xylanases from family 11 require three consecutive unsubstituted xylose monomers to cleave the xylan main chain, and they preferentially cleave the unsubstituted regions. GH11 enzymes are more likely to be hampered by the presence of xylan side-chain decorations due to a narrow binding cleft with no acceptance on the -1 and +1 subsites (Paes et al., 2012; Wan et al., 2014). In contrast to the family 10 xylanases, these enzymes are most active on long chain substrates, generating XOS which can be further hydrolysed by GH10 xylanases as these are highly active on short XOS. Furthermore, members of GH11 family are more efficient in hydrolysing insoluble xylan substrates as they are able to penetrate the cell wall matrix because of their small size (Karlsson et al., 2018).

1.5. Feruloyl esterases

Feruloyl esterases (E.C. 3.1.1.73), also known as ferulic acid esterases (FAEs), cinnamoyl esterases and cinnamoyl ester hydrolases, represent a diverse group of carbohydrate esterases that specifically catalyse the hydrolysis of ester bonds between hydroxycinnamic acids and plant cell wall polysaccharides. FAEs are usually employed as accessory enzymes as they remove hydroxycinnamic acids which would have hindered the action of xylanases, this leads to improvement in lignocellulosic biomass conversion (Oliveira et al., 2019; Malgas et al., 2019). The hydroxycinnamic acids released from complex plant cell walls have been shown to have positive health benefits, such as antioxidant, anti-microbial and anti-inflammatory activities. Therefore, these abilities make FAEs potential biocatalysts in a wide variety of applications such as in the food and feed, cosmetics and pharmaceutical industries.

1.5.1. Classification of FAEs

According to the CAZy database (CAZy; www.cazy.org), FAEs are members of Carbohydrate Esterase Family 1 (CE1), on the basis of their similarities in amino acid sequences and mode of action (Lombard et al., 2014). For the classification of these enzymes, different systems have been proposed. Crepin et al. (2004) proposed a broad classification based on their substrate specificity towards four model substrates (methyl ferulate-MFA, methyl sinapate-MSA, methyl caffeate-MCA and methyl *p*-coumarate-MpCA), FAEs are classified into A, B, C and D types. Type A FAEs are active on MFA, MpCA and MSA, and are capable of releasing diferulic acid. Type B FAEs are able to hydrolyse MFA, MpCA and MCA, but not MSA and cannot release diferulic acid from plant cell walls. Type C and D FAEs are active on all four substrates, but only type D has the ability to release diferulic acid. This classification system was useful, but it was based on a limited number of confirmed FAEs and amino acid sequences. A refined classification system which grouped FAEs into seven subfamilies was proposed

based on phylogenetic analysis of fungal FAEs by Benoit et al. (2008). A further refinement which grouped (for the first time) FAEs from fungi, bacteria and plant into 12 distinct families was proposed by Udatha et al. (2011). A major drawback of this system is that FAEs share high amino acid sequence identities with other proteins such as proteases, acetyl esterases and lipases, and it is, therefore, difficult to classify FAEs based on only amino acid sequences without biochemical data. More recently, Dilokpimol et al. (2016) proposed a classification system based on both amino acid sequences and substrate specificity. According to this system, FAEs can be divided into 13 sub families and an unclassified group.

1.5.2 Biochemical properties and sources of FAEs

FAEs have been identified in various plant cell wall degrading microorganisms and exhibit broad enzymatic properties (see Table 1.2). The biochemical characteristics of FAEs, such as reported molecular weights (18.5-210 kDa), optimum pH and temperature values ranging from pH 3.0 to 10.0 and 25°C to 75°C, respectively, vary greatly (Dilokpimol et al., 2016; Oliveira et al., 2019). There are also few studies that have reported on the impact of metal ions and inhibitors on FAE activities. The major sources of these FAEs are several fungal and bacterial microorganisms. Among these microorganisms, fungi are still the principal sources of FAEs used in industry (Topakas et al., 2007). Many FAEs have been produced from culturable microorganisms, but these represent a small fraction of microbial diversity which limit the search for possible novel enzymes. Recently, several novel FAEs have been discovered from various environmental niches using a metagenomic approach (Yao et al., 2013; Rashamuse et al., 2014; Li et al., 2018; Wong et al., 2019).

1.5.3. 3D structure and catalytic mechanism of FAEs

Structural information for FAEs is based on very few crystal structures that have been resolved. Structurally, FAEs exhibit the canonical common α/β -hydrolase fold of an esterase (Hermoso et al., 2004; Goldstone et al., 2010). The α/β -hydrolase fold consists of a nine β -sheet core that is surrounded by five α -helices and two additional β -strands. Other structural features include the classical catalytic triad, Ser-His-Asp, found at the core of active side. It has been reported that lipase crystal structures have been used to construct many FAE models based on sequence identities (Oliveira et al., 2019). The substrate specificity is usually determined by amino acid residues found within domains positioned in close proximity to the substrate binding sites and the catalytic triad (Hermoso et al., 2004; Suzuki et al., 2014). Generally, the catalytic mechanism of FAEs involves a covalent acyl-enzyme intermediate. This mechanism is similar to that of other esterases, serine proteases and lipases. The first step is acylation of the

nucleophilic serine residue which leads to formation of the intermediate. The second step involves deacylation which is initiated by the nucleophilic attack of water and the subsequent breakdown of the intermediate causing the release of the product, mostly FA (Dilokpimol et al., 2016).

Table 1.2: Biochemical properties of microbial FAEs

Microorganism	Enzyme	MW (kDa)	pH opt	T opt (°C)	T sta (°C)	Reference
-	rXyn10A/F ae1A	114.3	7.0	50	40	Wang et al., 2020
<i>Eupenicillium parvum</i>	EpFAE1	37	5.5	50	50	Long et al., 2020
-	BDS4	38.8	8.0	37	-	Wu et al., 2019
-	FAE-C1	38.9	≥ 7	35-40	-	Wong et al., 2019
<i>Xanthomonas campestris</i>	FAE-C2	25.7	≥ 7	35-40	-	Wong et al., 2019
<i>Lactobacillus johnsonii</i>	FAE-C3	38.9	≥ 7	35-40	-	Wong et al., 2019
<i>Clostridium thermocellum</i>	FAE-C4	35.5	≥ 7	35-40	-	Wong et al., 2019
<i>Thermogutta terrifontis</i>	FAE-C5	43.7	≥ 7	35-40	-	Wong et al., 2019
<i>Bacillus coagulans</i>	FAE-C6	43.7	≥ 7	35-40	-	Wong et al., 2019
-	FAE-C7	30.2	≥ 7	35-40	-	Wong et al., 2019
<i>Aspergillus terreus</i>	AtFaeD	43	7.0	50	37	Mäkelä et al., 2018
<i>Aspergillus niger BE-2</i>	AnFaeA	40	5.0	45	< 55	Wu et al., 2017
<i>Actynomyces sp.</i>	ActOFaeI	32	6.5	30	40	Hunt et al., 2016
<i>Lactarius hatsudake</i>	LhFae	55	4.0	30	-	Wang et al., 2016
<i>Schizophyllum commune</i>	ScFaeD1	63	7.5	45	45	Nieter et al., 2016
<i>Aspergillus terreus</i>	AtFaeA	35	5.0	50	-	Zhang et al., 2015
<i>Panus giganteus</i>	PgFae	61	4.0	40	40	Wang et al., 2014
<i>Aspergillus oryzae</i>	AoFaeA	37	5.0	50	50	Zeng et al., 2014

Where pH opt represents pH optimum, T opt represents temperature optimum and T sta represents thermostability.

1.5.4. Release of hydroxycinnamic acids

Hydroxycinnamic acids, particularly FA and *p*-CA, are key components of plant cell walls, and they are mainly cross-linked to hemicellulosic carbohydrate moieties and to lignin. FA, the most dominant hydroxycinnamic acid, is distributed widely throughout cereal grains. Agricultural residues resulting from cereal grain processing are a cheap alternative source for the extraction of FA as they usually contain about 0.5% to 3.0% (w/w) FA content (Long et al., 2018). Extraction of FA from agricultural residues is generally facilitated by alkaline hydrolysis. However, this method is not preferred because of the generation of unwanted by-products. Various attempts have been made in the enzymatic extraction of FA from different agricultural substrates using FAEs, as this method is more environmentally friendly and leads to the release of specific products. A study by Zhang et al. (2013) reported that FAE from *Aspergillus flavus* (AfFaeA) was capable of releasing FA from steam exploded corn stalk. The AcFAE from *Aspergillus clavatus* was applied to the release of both FA and *p*-CA from sugarcane bagasse (Damasio et al., 2013). FAEs from different microorganisms have also been used to release FA from wheat bran (Uraji et al., 2014; Cao et al., 2015). However, some of these reports showed that FAEs only released a low level of FA. Many studies have demonstrated that other hemicellulose degrading enzymes, most especially endo-xylanases are important for enhancing FAE activity during the release of hydroxycinnamic acids from various agricultural residues.

1.6. Synergism between FAEs and xylanases

The structure and composition of xylan in lignocellulosic biomass is heterogeneous and complex and not easily accessible to enzymes. Therefore, the efficient production of XOS and other useful compounds from xylan requires the cooperation of many xylanolytic enzymes (Malgas et al., 2019). Enzyme synergy refers to the cooperation between enzymes where the combined enzyme activities greatly improve the efficiency of substrate hydrolysis (Jalak et al., 2012). FAEs exhibit a strong synergistic relationship with endo-xylanases for the efficient production of XOS and hydroxycinnamic acids from various xylan rich lignocellulosic biomass (Mkabayi et al., 2020). The synergistic interactions between these two groups of enzymes take place in two ways. Firstly, xylanases act on parts of the xylan polymer generating short feruloylated XOS. This action enhances the activity of FAEs since short feruloylated XOS are preferred FAE substrates compared to the xylan polymer. In turn, the cleavage of FA decorations increases the accessibility of xylanases to short-chain XOS for further hydrolysis (Oliveira et al., 2019). It has been suggested that the synergistic effect of endo-xylanases is

dependent on several factors which include (a) the type and the degree of side group substituents present on the xylan polymer, (b) physical properties of the substrate such as solubility/insolubility and particle size, and (c) enzyme's capability to accommodate variability and hydrolyse the heteroxylan substrate (Wong et al., 2013).

Several studies have shown that FAEs could efficiently release FA from lignocellulosic biomass only in the presence of endo-xylanases. A study by Long et al. (2020) evaluated the synergistic interactions between a new FAE from *Eupenicillium parvum* (EpFAE1) and GH10 endo-xylanase (EpXYN1), and it was shown that addition of EpXYN1 significantly increased the release of FA from de-starched wheat bran (DSWB). FAE from a rumen microbial metagenome (RuFae2) has been employed in release of FA from various natural substrates in synergism with GH10 xylanase of *Cellvibrio mixtus* (Wong et al., 2013). It was reported that RuFae2 alone was capable of releasing FA, but the addition of GH10 xylanase significantly increased the amount of FA released, wheat bran being the highest with a 6.73-fold increase, followed by wheat-insoluble arabinoxylan (2.76-fold increase). Mäkelä et al. (2018) showed the significance of sequential and simultaneous synergistic interactions between a commercial xylanase and FAE from *Aspergillus terreus* (AtFaeD). The study indicated that the release of FA from wheat-insoluble arabinoxylan was improved by 11-fold when AtFaeD acted sequentially with the xylanase, than when the enzymes were co-incubated. More recently, Wang et al. (2020) evaluated the inter-domain synergism of multi-modular bifunctional recombinant enzymes (rXyn10A/Fae1A) for the co-production of XOS and FA from agricultural residues such as DSWB, ultrafine grinding corn stover and steam-exploded corn cobs.

It has been suggested that hydrolysis of FA ester linkages by FAEs improves the enzymatic degradation of xylan in lignocellulosic biomass to XOS. Wu et al. (2017) evaluated synergism between FAE (AnFaeA) and GH11 xylanase (AnXyn11A) from *Aspergillus niger* BE-2 in hydrolysing wheat bran to produce FA and XOS. The study demonstrated that co-incubation of the enzymes improved the release FA from 16.8% to 70%, while the XOS yield was double when compared to single enzyme action. A study on the synergistic effect of cFae from *Aspergillus clavatus* and a commercial xylanase reported a 1.97-fold improvement in reducing sugar release from sugarcane bagasse hydrolysis (Oliveira et al., 2016). In another study, the synergistic activities of the FAEs of *Bacteroides intestinalis* (BiFae1A and BiFae1B) and a bifunctional endo-xylanase/ α -arabinofuranosidase on wheat-insoluble arabinoxylan resulted in an increased production of reducing sugars (Wefers et al., 2017). A study by Kmezik et al.

(2020) showed that multi-modular fused acetyl–feruloyl esterases were capable of substantially improving the performance of a commercial xylanase (Xyn11A). The experiments showed that the enzymatic hydrolysis of corn cob and Japanese beechwood biomass were improved by close to 2-fold and up to 20-fold, respectively. The difference in synergistic effects likely reflected the complexity and variations in the xylan structure of these two substrates.

The products generated from the degradation of xylan polymer, including FA, *p*-CA and XOS, are known to have potential health benefits arising from their antioxidant and prebiotic properties. The use of enzyme-based technology for their production presents an environmentally friendly method for the utilisation of agricultural residues. Evidence from recent scientific reports suggests that the synergistic action of FAEs and endo-xylanases is crucial to obtain significant hydrolysis yields from these agricultural residues. Recent developments have focused on employing a genome mining strategy to discover novel FAEs with novel properties, and it was, therefore, important to evaluate the synergistic effects of these newly discovered FAEs for the formulation of enzyme cocktails which can be used for the efficient production of high value-added chemicals.

Chapter 2: Motivation, aims and thesis outline

2.1. Motivation

Agricultural residues are widely considered as an ideal renewable feedstock for the production of VAPs. Several primary drivers underpin the increasing interest in the utilisation of agricultural residues as raw materials for VAPs production. These include availability and low-cost and output: input energy ratio (Isikgor and Becer, 2015; Arevalo-Gallegos et al., 2017). A number of conversion technologies can be used with agricultural residues, but enzymatic conversion is generally considered the most sustainable technology for the production of value-added chemicals (Lopes et al., 2018). However, the conversion of these resources is hindered by their structural complexity and heterogeneity which can prevent enzymatic hydrolysis. The efficient enzymatic hydrolysis of agricultural residues requires the synergistic cooperation of several enzymes. FAEs, working synergistically with xylanases, are responsible for the release of hydroxycinnamic acids, whilst also reducing lignocellulosic biomass recalcitrance for the production of fermentable sugars. Various FAEs have been isolated and characterised from fungi and bacteria, but only few have been applied on an industrial level due to their low levels of expression and low catalytic activities. Therefore, discovery and application of novel FAEs still remains important.

Recent developments have highlighted that metagenomic technologies offer promising new strategies for discovering novel FAEs with unique properties. Rashamuse et al. (2014) employed a metagenomic mining strategy and functionally screened novel FAEs from the hindgut prokaryotic symbionts of *Trinervitermes trinervoides* termite species. However, the application of these enzymes in degrading agricultural residues has not yet been explored. Exploration of these novel enzymes in the formulation of FAE-xylanase cocktails is important, as it can lead to an improvement in efficient lignocellulosic biomass degradation. This, in turn, could lead to an improvement in the economic viability of the bioconversion of high xylan-containing lignocellulosic biomass into hydroxycinnamic acids and XOS, which hold great potential for industrial application.

2.2. Hypothesis

Highly efficient co-production of hydroxycinnamic acids and XOS from agricultural residues can be achieved through the synergistic action of termite metagenome-derived FAEs and commercially available xylanases.

2.3. Aims and objectives

The main aim of this study was to evaluate synergism between two termite metagenome-derived feruloyl esterases (FAE5 and FAE6) and endo-xylanases from *Thermomyces lanuginosus* (Xyn11) and *Bacillus stearothermophilus* T6 (XT6) for the production of hydroxycinnamic acids and XOS from various feedstocks; model substrates (oat spelt xylan and insoluble wheat arabinoxylan), and untreated and pre-treated agricultural residues (corn cob, rice straw and sugarcane bagasse).

The following objectives were set at the onset of the study, to address the aim above:

- To over-express and purify FAE5 and FAE6;
- To biochemically characterise the purified FAEs and commercial xylanases (Xyn11 and XT6);
- To conduct pre-treatment of the selected agricultural residues;
- To conduct compositional, morphological, and chemical analysis of untreated and pre-treated agricultural residues.
- To evaluate the impact of pre-treatment by-products and wash liquors on enzyme activities;
- To evaluate synergistic interactions between purified FAEs and xylanases on model substrates and agricultural residues.

2.4. Thesis outline

This thesis is presented as follows:

- **Chapter 1** provides a general overview of the fundamental concepts of lignocellulosic biomass bioconversion with a focus on the structure and chemical composition of biomass, potential applications of VAPs extracted from lignocellulosic biomass, pre-treatment methods, enzymatic hydrolysis, and the nature, and function of xylanases and FAEs. The synergistic interactions between FAEs and xylanases during degradation of agricultural residues were also discussed.

- The amplification of plasmids harbouring *fae5* and *fae6* genes, confirmation of sequences, over-expression as well as enzyme purification are described in **Chapter 3**.
- **Chapter 4** reports on partial biochemical characterisation of purified FAEs (FAE5 and FAE6) and commercial xylanases (Xyn11 and XT6).
- **Chapter 5** describes the pre-treatment of the selected agricultural residues by hydrothermal and dilute acid methods. The chapter also describes chemical composition and characterisation of untreated and pre-treated substrates as well as the potential impact of various pre-treatment by-products on the activity of FAEs.
- **Chapter 6** reports on evaluation of synergistic interactions between FAEs and xylanases during biomass degradation with a focus on the production of hydroxycinnamic acids and XOS. The co-operation of these enzymes was first tested on oat-spelt xylan and wheat arabinoxylan (model substrates) and protein loading ratios were also optimised. The optimised FAE-xylanase cocktails were then applied to untreated and treated agricultural residues for the production of hydroxycinnamic acids and XOS.
- A general discussion, research highlights, conclusions and future work of this study are provided in **Chapter 7**.

Chapter 3: Expression and purification of FAE5 and FAE6

3.1. Introduction

Although numerous studies have examined the isolation and purification of FAEs from various sources such as bacteria and fungi, some of these enzymes suffer from low expression levels and weak catalytic activities for industrial applications. Therefore, it is important to develop new methods for improving the production of FAEs because of their potential for industrial applications. Application of heterologous expression systems may be useful for obtaining increased amounts of FAEs. Heterologous protein expression can be achieved by using a number of expression systems such as bacterial, fungal and yeast (Juturu and Wu, 2018; Kaur et al., 2018). The application of *Komagataella phaffii* (*K. phaffii*) (previously known as *Pichia pastoris*) as a yeast expression system is highly attractive due to a lot of advantages such as its ability to perform eukaryotic post-translational modifications, its capacity to grow at high cell densities and its ability to secrete reasonable amounts of protein into the fermentation media (Daly and Hearn, 2005; Varnai et al., 2014).

With bacterial expression, *Escherichia coli* (*E. coli*) is the preferred and most widely used expression host because of several advantages. These include the requirement of only simple transformation techniques, rapid growth on inexpensive growth conditions, high level of protein accumulation in the cell cytoplasm, easy isolation, and purification of expressed proteins (Jhamb and Sahoo, 2012). The *E. coli* T7 RNA polymerase-based protein production is the most widely used approach (Makino et al., 2011; Studier, 2014). In this system, the strain BL21 (DE3) is used in combination with a T7 promoter-based expression vector containing the gene of interest. The gene encoding the recombinant protein is transcribed by the chromosomally encoded T7 RNA polymerase, which is induced by the addition of isopropyl- β -D-1-thiogalactopyranoside (IPTG). For the purification of recombinant proteins, immobilized metal affinity chromatography (IMAC) is one of the most simple and reliable purification techniques. The best-known application of IMAC is the purification of histidine-tagged (His-tagged) proteins (Cheung et al., 2012). The IMAC consists of a supporting material (agarose), a linker, a chelating compound (nitrilotriacetic acid) and a divalent transition metal ion (Ni(II) or Co(II)) (Yang et al., 2013). The purification is based on the affinity of divalent transition metal ions towards a His-tag (usually six consecutive histidine residues) fused to either the N or C terminus of the target protein (Block et al., 2009; Cheung et al., 2012). Generally, the presence of the 6 \times His-tag does not affect the functional activity and structure of purified recombinant protein, because of its small size.

Most well studied FAEs have been cloned and expressed in heterologous expression systems. These recombinant FAEs have been used to investigate several aspects of enzyme studies, including structure-function relationships, increasing production, engineering them to be suitable for industrial use by manipulating their thermal and pH stability, investigating the role of particular amino acid residues, and purification of enzymes in a single step with high yield (Oliveira et al., 2019). In the present study, two novel metagenome derived FAEs (FAE5 and FAE6) were expressed in an *E. coli* BL21 (DE3) expression system and their subsequent purification was achieved by IMAC. These FAEs were produced for use in the enzymatic degradation of agricultural residues.

3.2. Aims and objectives

3.2.1. Aims

To produce recombinant FAE5 and FAE6 in an *E. coli* BL21 (DE3) expression system and purify these enzymes by IMAC for use in activity assays.

3.2.2. Objectives

To achieve this aim, the following objectives were set:

- To amplify plasmid harbouring *fae5* and *fae6* genes;
- To verify the coding sequences of *fae55* and *fae6* by sequencing;
- To express functional FAEs in *E. coli* BL21 cells;
- To purify FAEs using Ni-NTA Superflow Cartridges;
- To assess the purification procedure by constructing a purification table.

3.3. Materials and methods

3.3.1. Materials

The pET28a expression plasmids harbouring the *fae5* and *fae6* genes were kindly provided by Dr K. Rashamuse (Council for Scientific and Industrial Research (CSIR), Biosciences, Pretoria, South Africa). *E. coli* JM109 and BL21 (DE3) cells were purchased from Invitrogen (Carlsbad, USA). Reagents for preparation of Luria agar (LA) and Luria broth (LB) media were purchased from Merck (Darmstadt, Germany). The plasmid DNA extraction kit was purchased from BioFlux (Bioer Technology Co., Ltd, Hangzhou, China). The 5 mL Ni-NTA Superflow Cartridge was purchased from QIAGEN (Hilden, Germany). PageRuler™ pre-stained protein ladder was purchased from Thermo Scientific (Waltham, USA). Bradford reagent was purchased from Sigma-Aldrich (St. Louis, USA).

3.3.2. Plasmid amplification

Competent *E. coli* JM109 cells were transformed with one of the recombinant plasmids pET28a-*fae5* or pET28a-*fae6* using the heat-shock transformation method (Froger and Hall, 2007). Briefly, a stock of competent *E. coli* JM109 cells (50 µL) was thawed on ice. The plasmid (2 µL) was mixed with competent cells and the mixture kept on ice for 30 minutes, followed by heat shocking at 42°C for 30 seconds and cooling on ice for 2 minutes. Super optimal broth with catabolite repression (SOC) media (20 g/L tryptone, 5 g/L yeast extract, 0.584 g/L NaCl, 0.186 g/L KCl, 2.034 g/L MgCl₂, 2.464 g/L MgSO₄) was added and the mixture was incubated while shaking at 37°C for 1 hour. Positive transformants were obtained by plating the transformation mixture onto LB agar plates containing 50 µg/mL kanamycin and incubated overnight at 37°C. Single colonies were inoculated into 5 mL LB broth containing 50 µg/mL kanamycin and grown overnight at 37°C.

3.3.3. Plasmid extraction

The plasmids were extracted from the overnight cultures using the BioFlux BioSpin plasmid DNA extraction kit according to the manufacturer's instructions (Bioer Technology Co., Ltd.) and plasmid DNA was quantified using a Nanodrop 2000 spectrophotometer.

3.3.4. Nucleotide sequencing and sequence verification

The plasmids with the *fae5* and *fae6* genes were sent to Inqaba Biotech™ (Pretoria, South Africa) for sequencing to confirm the nucleotide composition of the desired genes. The DNA sequences were analysed and edited using Geospiza's FinchTV software. The sequences of the *fae5* and *fae6* genes were then analysed using a BLASTx search engine (Altschul et al., 1997).

The theoretical molecular weights of FAE5 and FAE6 were predicted using the EXPASY proteomics server (Gasteiger et al., 2005). Multiple sequence alignment was carried out with Clustal Omega (Sievers et al., 2011).

3.3.5. Expression of FAE5 and FAE6

Two cultures of the *E. coli* BL21 (DE3) cells that had been transformed with one of the recombinant plasmids; pET28a-*fae5* or pET28a-*fae6*, were grown in tubes containing 5 mL LB media for 16 hours at 37°C, shaking in a Labcon bench shaker at 180 rpm. The overnight cultures were used to inoculate 100 mL of LB containing 50 µg/mL of kanamycin and incubated in a Labcon shaker (180 rpm) at 37°C until an OD600 of between 0.6 and 0.8 was reached. The expression of the recombinant FAEs was induced by the addition of 1 mM IPTG, and cultures were incubated at 18°C with shaking (150 rpm) for 7 hours. For the determination of optimum induction time, 1 mL samples were collected at 1 hour intervals over 7 hours and stored at -20°C for SDS-PAGE analysis. The remaining culture was then used for subsequent purification.

3.3.6. Purification of recombinant FAE5 and FAE6

The *E. coli* BL21 (DE3) cells from induction studies were chilled on ice for 30 minutes, harvested by centrifugation at $6\ 000 \times g$ for 15 minutes at 4°C using an Avanti® J-E centrifuge and a JA-14 rotor (Beckman Coulter). Upon centrifugation, the pellets were resuspended in lysis buffer (50 mM NaH₂PO₄, 300 mM NaCl, 1 mg/mL lysozyme, pH 8). The solution was incubated on ice for 1 hour and frozen at -80°C for a minimum of 4 hours. The solution was then thawed and centrifuged at $10\ 000 \times g$ for 20 minutes at 4°C and the supernatant (cleared lysate) was filtered using 0.22 µm sterile filters. Purification was conducted using nickel affinity chromatography. The 5 mL Ni-NTA Superflow Cartridge (QIAGEN®) was first equilibrated with 10 column volumes of binding buffer NPI-10 (50 mM NaH₂PO₄, 300 mM NaCl, 10 mM imidazole, pH 8). The cleared lysate was applied to the cartridge using a flow rate of 5 mL/minute and the flow-through was collected. The unbound proteins were removed with a washing step using 10 column volumes of washing buffer NPI-20 (50 mM NaH₂PO₄, 300 mM NaCl, 20 mM imidazole, pH 8). His-tagged FAEs were eluted into 5 mL fractions with elution buffer NPI-250 (50 mM NaH₂PO₄, 300 mM NaCl, 250 mM imidazole, pH 8). The purified FAEs were desalted with PD-10 desalting columns (Sephadex G-25) (GE Healthcare) and concentrated by centrifugation at $3\ 000 \times g$ for 20 minutes at 4°C using Amicon® Ultra -

15 Centrifugal filters (10 kDa). The samples were then stored for SDS-PAGE analysis, protein concentration determination and enzyme activity assays.

3.3.7. SDS-PAGE analysis

Sodium dodecyl sulphate polyacrylamide gel electrophoresis (SDS-PAGE) was performed using a mini PROTEAN® tetra system (BIO-RAD). The protein samples were analysed with a 10% resolving gel and 4% stacking gel using the procedure described by Laemmli (1970). Protein samples were mixed 4:1 with SDS loading buffer (50 mM Tris HCl, pH 6.8; 40% (w/v) glycerol; 3% (w/v) SDS; 0.14% (w/v) bromophenol blue; 5% (w/v) β -mercaptoethanol) and incubated at 100°C for 10 minutes on a Labnet AccuBlock™ digital dry bath before loading. Sample aliquots of 15 μ L were loaded onto the gel. PageRuler™ prestained protein ladder (size range, 10-180 kDa) was used as a molecular weight marker for protein size estimation. Electrophoresis was performed in SDS running buffer (25 mM Tris base; 192 mM glycine; 1% (w/v) SDS) at a constant voltage of 100 V using BioRad PowerPac™ power supply. The SDS-PAGE was stained with a staining solution (0.1% (w/v) Coomassie Brilliant Blue G250; 20% (w/v) methanol and 15% (w/v) glacial acetic acid) for 20 minutes on a rocker platform (Bellco technology) and destained with a destaining solution (45% (w/v) methanol and 10% glacial acetic acid). The bands were finally visualized using the BIO-RAD ChemiDoc™ XRS+ imaging system.

3.3.8. Protein concentration determination

For protein quantification, the Bradford assay was used (Bradford, 1976). A standard curve was constructed using bovine serum albumin (BSA) (see Appendix Figure B.1.1). An amount of 25 μ L of the BSA standard or unknown sample was mixed with 230 μ L of Bradford's reagent and incubated at room temperature shaking on a rocker platform for 10 minutes. The absorbance values were measured at 595 nm using a SynergyMx microplate reader (BioTek®).

3.3.9. FAE activity on *p*NP-acetate

The enzyme activity was determined by measuring the amount of released *p*-nitrophenol product from *p*NP-acetate (dissolved in 90% acetonitrile). All reactions were carried out in triplicate using standard 96-well microplates. The standard assay mixture (200 μ L) contained 0.8 mM *p*NP-acetate, a sodium phosphate buffer (50 mM, pH 7.4) and the reaction was started by the addition of 5 μ L diluted enzyme solution. The release of *p*-nitrophenyl product was monitored at 40°C every 1 minute for over a period of 10 minutes at 405 nm using a SynergyMx microplate reader (BioTek®). A *p*-nitrophenol standard was constructed for the estimation of

concentration (see Appendix Figure B.3.1). One unit of enzyme activity was defined as the amount of activity required to release 1 μmol of *p*-nitrophenol per minute from *p*NP-acetate under the standard assay conditions.

3.4. Results and discussion

3.4.1. Sequence verification

The recombinant plasmids, pET28a-*fae5* or pET28a-*fae6*, were used to transform competent *E. coli* JM109 cells. The transformed cells were grown overnight at 37°C in order to amplify the recombinant plasmids. Amplified plasmids were then extracted as described in section 3.3.3 and sent to Inqaba Biotech™ for sequencing. The nucleotide sequences were analysed as described in section 3.3.4 and the result indicated the presence of the desired genes in the correct orientation. As expected, translational analysis (BLASTx) revealed a 100% sequence identity for FAE5 (accession no. AGJ83838.1). Contrary to the results seen for FAE5, the analysis for FAE6 revealed a high sequence identity (84.31%) with a carboxylesterase family protein (accession no. NLV31826.1). The slight changes for FAE6 might be due to sequence refinements after its first deposition into the National Centre for Biotechnology Information (NCBI) database. For further analysis, the sequences obtained from BLASTx were used to predict the molecular masses for FAE5 and FAE6, and were found to be 30.1 kDa and 57.7 kDa, respectively. Translated FAE5 and FAE6 sequences were then aligned with two termite metagenome derived FAEs to confirm the presence of conserved regions corresponding to the common functional features of esterases (Figure 3.1). The amino acid sequences of FAE5 and FAE6 exhibited the typical esterase G-x-S-x-G motif which is found in the catalytic triad. Multiple sequence alignment also revealed numerous fully conserved amino acid residues across FAE sequences. Overall, the results indicated that recombinant plasmids, pET28a-*fae5* or pET28a-*fae6*, were amplified successfully and contained the desired genes in the correct orientation. Amino acid sequence analysis revealed that the two sequences have highly conserved residues corresponding to functional features of typical esterases.

```

NLV31826.1  GALRWKAPQAVPMDGVKRAFRFAPGPMQDTAFGALLGGPQET----- 103
AGJ83835.1  -----MAVLTCNFMSQLGRVCPIFVLLPVPAAAGS-----LFDSRIEPYKE 41
AGJ83838.1  -----MSNIRVEFFSNLSLRPVSFEMY-----IPNDFRADVPRQPNYY 39
AGJ83834.1  -----MSVFKVRYYSALRRQVCFNAVLPLDEIIIPENMRPDIPK---YEK 43
          .          :          :          :
          :          :          :          :

NLV31826.1  SEDCLYLNWVTGARTTDEKRPVMVWIYGGGFGIGMTSSPAYDGTSLAKKGVVLSVAYRV 163
AGJ83835.1  NPPFKTLYLLHGVSIGN-----YTGWIYDSRVAQY-----A-ESKGIADV---MPS 82
AGJ83838.1  ERNCKTVFILHGYTGW-----GKGMD---NIYEL-----A-EKYNFALV---FPS 77
AGJ83834.1  KRDFKTVYLLHGYGGN-----DDDHLHGSMIDFL-----S-LKYNLAFV---MPS 84
          .          :          :          :          :
          :          :          :          :          :
          :          :          :          :          :

NLV31826.1  GPMGFLAHPELSAESGGGSGAYGIQQQIAGLRWVKENIARFGG-----DPANVTLFGE 216
AGJ83835.1  GDNSFYTDND-----PANRYGE-----FIGSELVQATRAMFPLSRREDTYIGGL 127
AGJ83838.1  GENSFYLDSE-----ATAGKYGT-----FVGSELVEYIRKTFNLCRTKDDTYISGL 123
AGJ83834.1  VENSFYLDLP-----ARQAFYSR-----FLCEEIIDFTRKAFSLSHKREDTAICGL 130
          *          .          :          :          :          :
          :          :          :          :          :
          :          :          :          :          :

NLV31826.1  SAGGISVA---M-LAGSPGAAGLFQRAISQSGGSMAPPRMTRAAAEAQKAYLAALGAGD 272
AGJ83835.1  SMGGYGALRNGMKYSGTFSVIAAFSSAIIQEG----- 159
AGJ83838.1  SMGGYGALHTGFAYPDTFGKIVALSSALIVHG----- 155
AGJ83834.1  SMGGYGALRNGLLRPDVFGAIVAFSSALITDE----- 162
          * **          .          :          :          :          :
          :          :          :          :          :
          :          :          :          :          :

NLV31826.1  IRAARALGAEIQRNTRGMGSFWPVPDGETIVADQYERYLAGRFNDTPILVGTNSNEGGL 332
AGJ83835.1  -----IENSTED-----APIFFMRRS--YERVFGDLSRFKGSMDMDLYAL 197
AGJ83838.1  -----ISGMKPG-----ENHKVANY--YYRNCFGDLENLIQSDNNPETL 193
AGJ83834.1  -----ISELPPG-----VGNEVASYE--YYRHIFGPLDALKGSDKDPKAL 200
          .          .          *          *          :          :          :          *
          :          :          :          :          :          :          :          :

NLV31826.1  FVTQPVTRDGFERMVRGQYPEG-ADVLLAAYPHATDEEASRSARDIM--RDSTFAWPTWA 389
AGJ83835.1  ANE---KARDLR---FYITCGTEDPLLAANRGFAGHLKGLGADLIYEESPGGHSDSDFWE 250
AGJ83838.1  VKKLIQQGKIPR---IFMACGTEDFLLEENRRFYNFLAEHNVNVEYFESSGSHDMKFWH 250
AGJ83834.1  AKRLKESGAELPR---IYMACGTEDFLDRNRDMHRCLQALNIPHDYHESPGTHVWSFWD 257
          *          *          *          *          .          .          .          *

```

Figure 3.1: A Multiple sequence alignment of FAEs performed with Clustal Omega. FAE5 and FAE6 were aligned with two other termite metagenome derived FAEs. The common esterase GxSxG motif is identified with a box. The degree to which an amino acid position is conserved is indicated by symbols. Key: *(fully conserved residue); :-(conservation of residues with strongly similar properties); .-(conservation of residues with strongly similar properties).

3.4.2. SDS-PAGE analysis of FAE5 and FAE6

The expression of the recombinant FAE5 and FAE6 enzymes was confirmed the *E. coli* BL21 (DE3) cells by following IPTG-induced expression. Figure 3.2 shows SDS-PAGE analysis of IPTG-induced expression of FAE5 and FAE6. For FAE5, upon induction of *E. coli* BL21 (DE3) containing pET28a-*fae5* with IPTG, a band representing a protein of molecular weight of approximately 30 kDa was produced (Figure 3.2A). The relative quantity of recombinant FAE5 appeared to increase up to 4 hours after induction. There was no band corresponding to FAE5 found in the uninduced sample (negative control, lane 1). The expression of FAE6 shows a very similar pattern to that seen with the recombinant FAE5 (Figure 3.2B). The recombinant FAE6 displayed a molecular weight of approximately 60 kDa and was consistent with the findings obtained from the EXPAsy proteomics server (protein size prediction). As expected,

the uninduced sample did not show a FAE6 band (negative control, lane1). The figures clearly show the over-expression of both FAE5 and FAE6 as evidenced by the prominent protein bands. Both FAE5 and FAE6 were recombinantly produced in the soluble cytoplasmic fraction of *E. coli* BL21 (DE3) cells.

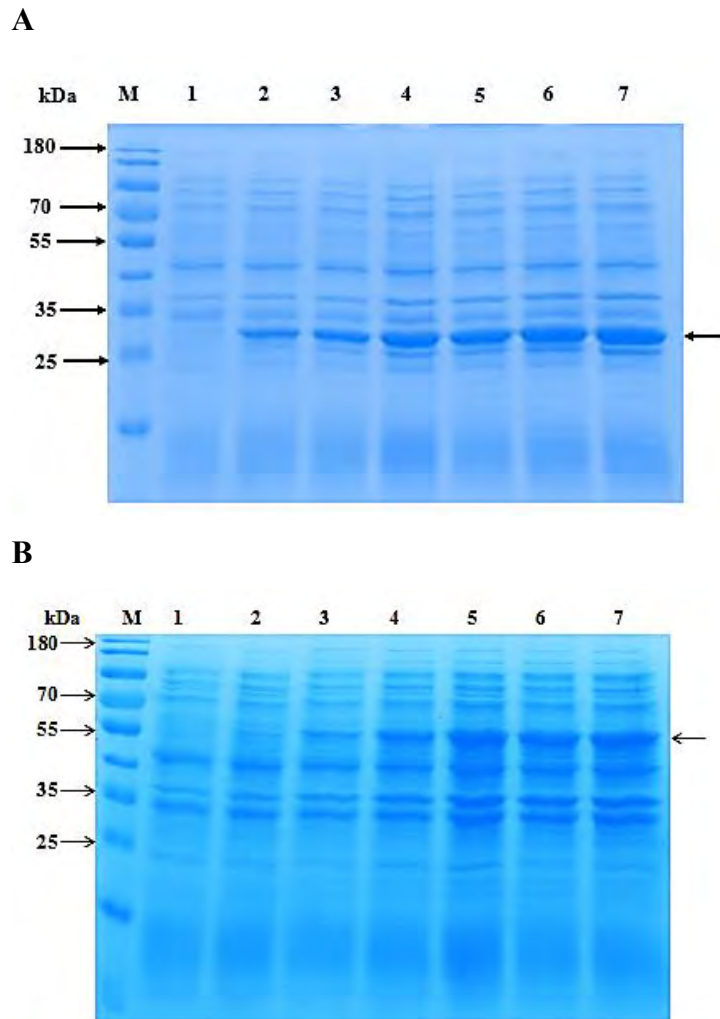


Figure 3.2: SDS-PAGE analysis of expression of FAE5 and FAE6. (A) SDS-PAGE gel of IPTG induced expression of FAE5. Lane M: Protein molecular marker. Lane 1: uninduced sample. Lane 2-7: Samples collected at 1 hour interval after IPTG addition. **(B)** SDS-PAGE gel of IPTG induced expression of FAE6. Lane M: Protein molecular marker. Lane 1: uninduced sample. Lane 2-7: Samples collected at 1 hour intervals after IPTG addition.

3.4.3. SDS-PAGE analysis of FAE5 and FAE6 purification

To efficiently purify the expressed FAE5 and FAE6 enzymes from *E. coli* BL21 (DE3), a His-tag purification procedure was employed. The soluble FAE5 and FAE6 enzymes extracted from *E. coli* BL21 (DE3) cells were purified under non-denaturing conditions with nickel affinity chromatography and the relative protein contents and molecular weights were determined by SDS-PAGE analysis (Figure 3.3). The molecular weights were consistent with those observed during protein expression. The efficacy of purification procedure is shown in Figure 3.3A and Figure 3.3B for FAE5 and FAE6, respectively. It can be seen that the selected purification procedure was successful as both FAE5 and FAE6 appeared only in the crude and elution fractions. Furthermore, bands representing FAE5 and FAE6 were not observed in the flow-through and wash fractions. This observation suggests that the procedure resulted in efficient binding of the tagged proteins.

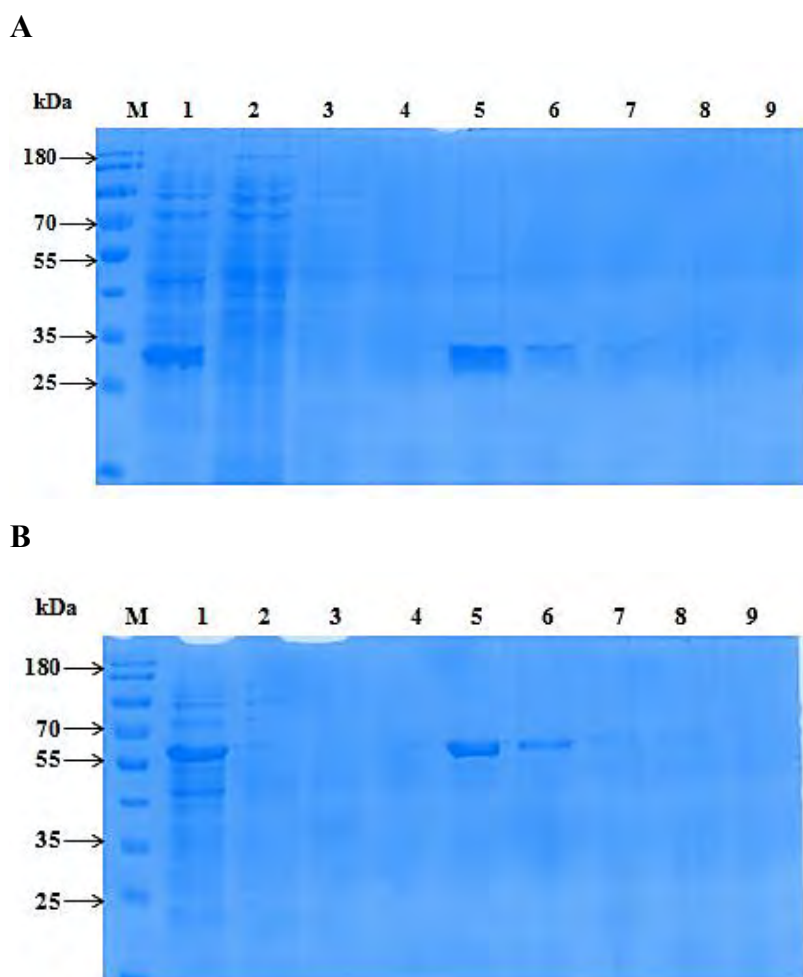


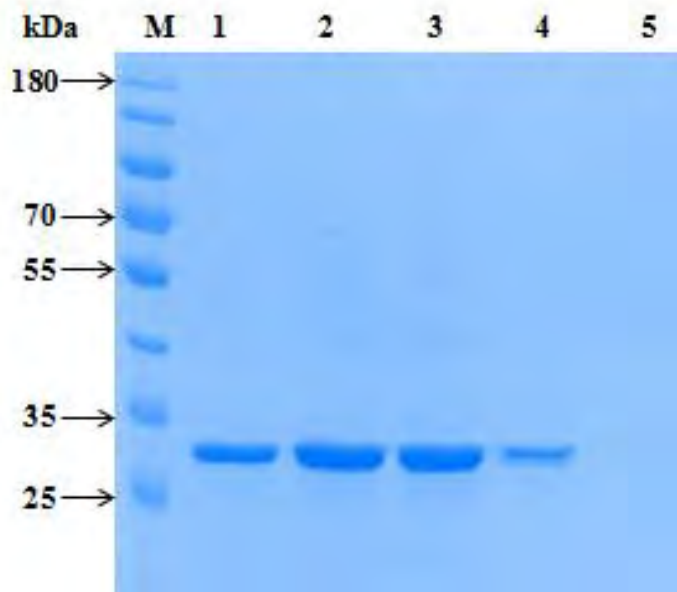
Figure 3.3: SDS-PAGE analysis of FAE5 and FAE6 purification with Nickel Affinity chromatography. (A) Purification of FAE5. Lane M: Protein molecular marker. Lane 1: cleared lysate. Lane 2: Flow-through sample from cleared lysate. Lane 3: Wash sample. Lanes 4 -9: elution samples with a band at approximately 30 kDa. **(B) Purification of FAE6.** Lane M: Protein molecular marker. Lane 1: cleared lysate. Lane 2: Flow-through protein. Lane 3: Wash sample. Lanes 4 - 9: elution samples showing a band at approximately 60 kDa.

In addition to nickel affinity chromatography, FAE5 and FAE6 were subjected to PD-10 desalting columns (containing Sephadex G-25). Desalting was performed mainly to remove the imidazole which was used during the elution step in nickel affinity chromatography (described in section 3.3.6). The results showing fractions collected during desalting are presented in Figures 3.4A and B for FAE5 and FAE6, respectively. The SDS-PAGE analysis in Figure 3.4 demonstrated that recombinant FAE5 and FAE6 eluted in high quantities within

4 fractions as evidenced by the prominent protein bands at approximately 30 kDa (FAE5) and 60 kDa (FAE6). The results revealed the presence of minor impurities at approximately 40 and 70 kDa. These are usually histidine-rich *E. coli* proteins, the two most common being ArnA, a bifunctional enzyme with several non-consecutive histidine residues, and SlyD, a peptidyl-prolyl cis/trans-isomerase containing 15 histidines (Andersen et al., 2013). Because of the relatively high specificity and affinity of the His-tag, this method presents an efficient purification providing a reasonably high purity of the target protein preparation, which is sufficient for activity assays.

The current investigation demonstrated that metagenome-derived FAEs can be overexpressed in an *E. coli* expression system and purified in sufficient yields for enzyme activity assays. Several FAEs from different sources have been successfully overexpressed in an *E. coli* expression system and tested for their ability to hydrolyse ester bonds in the complex substrates. For example, Wong and colleagues applied a metagenomics strategy to discover seven FAEs, which were then expressed in *E. coli* BL21(DE3) and purified in active form (Wong et al., 2019). The enzymes were able to facilitate the release of FA from complex and model substrates (Wong et al., 2019). In another study, a metagenome-derived FAE was expressed in *E. coli* BL21(DE3) and applied in the release of FA from de-starched wheat bran (Wu et al., 2019). These studies clearly indicate that recombinant FAEs that are expressed in *E. coli* BL21 (DE3) can be applied to the enzymatic hydrolysis of complex and model substrates. Overall, the expression system selected for this study enabled the production of the recombinant FAE5 and FAE6 and allowed for a two-step purification by IMAC and size exclusive chromatography. These enzymes are suitable for application in the enzymatic hydrolysis of complex substrates.

A



B

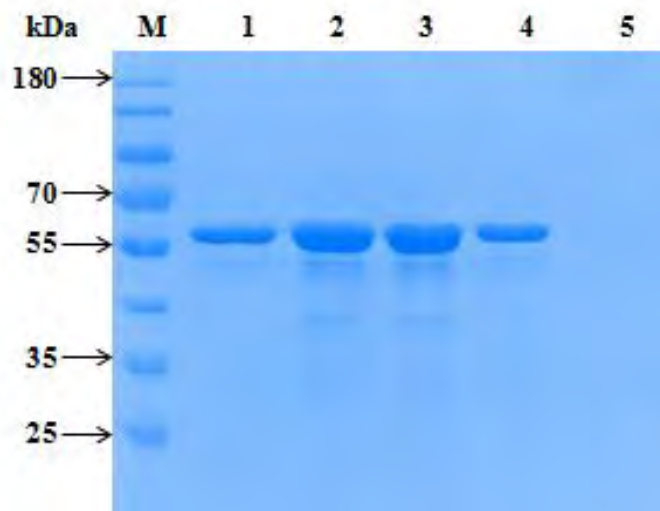


Figure 3.4: SDS-PAGE analysis of FAE5 and FAE6 purification with a PD-10 desalting column. (A) SDS-PAGE gel for the purification of FAE5. Lane M: Protein molecular marker. Lanes 1-5 contain elution samples with the protein of interest. (B) SDS-PAGE gel for the purification of FAE6. Lane M: Protein molecular marker. Lanes 1-5 contain elution samples with FAE6.

A summary of nickel affinity chromatography purification for FAE5 and FAE6 is provided in table 3.1. The activity was determined under standard enzyme assay conditions as described in section 3.3.9 and the concentration was determined (as described in section 3.3.8). For FAE5 purification, the yield and purification fold were estimated to be 97.04% and 2.57, respectively. The FAE6 was purified with a yield of 91.11% and purification fold of 2.83. The data summarized in Table 3.1 confirmed that both enzymes were purified in sufficient yields for use in subsequent enzyme assay experiments.

Table 3.1: Purification table for the purification of FAE5 and FAE6 by IMAC

Purification step	Total protein (mg)	Total activity (U)	Specific activity (U/mg)	Yield (%)	Purification fold
FAE5 Crude	41.12	2.70	0.066	100	1
FAE6 Crude	47.04	3.15	0.067	100	1
FAE5 Ni-NTA	15.69	2.62	0.17	97.04	2.57
FAE6 Ni-NTA	14.65	2.87	0.19	91.11	2.83

3.5. Conclusion

Sequence analysis confirmed that the expression vector, pET28a, contained the desired genes. IPTG-induced expression in *E. coli* BL21 (DE3) cells led to high levels of expression for both recombinant FAEs. SDS-PAGE analysis results after induction studies revealed that sufficient yields of soluble proteins were obtained within 6 hours. SDS-PAGE analysis after nickel affinity chromatography purification indicated that both recombinant enzymes were purified to homogeneity with high recovery yields and folds of purification. The recombinant FAEs were therefore produced and purified in sufficient yields for subsequent use in the following characterisation and application studies.

Chapter 4: Partial characterisation of purified feruloyl esterases and commercial xylanases

4.1. Introduction

Xylan is a major hemicellulose component of many non-woody materials (agricultural crops) such as grasses and cereals. It is a heterogeneous polysaccharide with a backbone made up of β -1,4-linked xylose units. The enzymatic hydrolysis of xylan requires various xylanolytic enzymes (Malgas et al., 2019). Among these enzymes, xylanases are primarily responsible for catalysing the depolymerisation of the xylan backbone into short-chained XOS. In addition, FAEs are also key in the enzymatic hydrolysis of xylan as they catalyse the removal of side decorations (hydroxycinnamic acids) which may pose steric hindrance to the xylanases. The biochemical properties of these enzymes have important implications in the biodegradation of xylan, and their characterisation is an important prerequisite for their successful application in industry. In recent years, xylanolytic enzymes have received a great deal of attention because of their diverse application in the pharmaceutical, food, and feed industries and for sustainable production of fuels and fine chemicals (Juturu and Wu, 2012; Silva et al., 2015).

Xylanases have been purified from several sources including bacteria and fungi, and these show significant variations in biochemical properties such as isoelectric point, molecular weight, and optimal hydrolytic reaction conditions (Malhotra and Chapadgaonkar, 2018; Bhardwaj et al., 2019). Among the commercially available xylanases, GH11 xylanase (Xyn11) from *Thermomyces lanuginosus* and GH10 xylanase (XT6) from *Bacillus stearothermophilus* T6, are commonly used. Khucharoenphaisan and Sinma (2011) expressed a *T. lanuginosus* xylanase in *E. coli* in order to investigate the effect of its signal sequence on its biochemical properties. The study showed an optimum pH value of 7.0 and an optimum temperature of 70°C, which were similar to those of the original enzyme expressed by the host. For the xylanase from *B. stearothermophilus*, the pH and temperature optima have been reported to be approximately 6.5 and 70°C, respectively (Mangan et al., 2017). In terms of FAEs, it has been reported that the majority of well characterised FAEs show a broad range of biochemical properties, including an optimum pH of between 3.0 and 10.0 and a temperature range of 20-75°C (Oliveira et al., 2019). The optimum hydrolytic reaction conditions for these two xylanases seem to be within the range reported for most characterised FAEs, making them suitable candidates for the formulation of xylanolytic enzyme cocktails for the efficient degradation of xylan-rich lignocellulosic biomass.

In the present study, purified recombinant FAEs (FAE5 and FAE6) and commercially available xylanases (Xyn11 and XT6) were partially characterised for their biochemical properties including product inhibition profiling.

4.2. Aim and objectives

4.2.1. Aim

To perform partial characterisation of purified recombinant FAE5 and FAE6, and the commercial xylanases.

4.2.2. Objectives

To achieve this aim, the following objectives were set:

- To determine the specific activity of enzymes on model substrates;
- To determine the temperature optimum of the enzymes;
- To determine the thermo-stability of the enzymes;
- To determine the pH optimum of the enzymes;
- To determine the effect of metal ions on FAE activity;
- To conduct product inhibition studies on the enzymes.

4.3. Materials and methods

4.3.1. Materials

The recombinant enzymes, FAE5 and FAE6, were expressed and purified in Chapter 3. Xylanase (Xyn11, GH11) from *Thermomyces lanuginosus*, ferulic acid, Remazol Brilliant Blue R-D-xylan and ethyl ferulate were purchased from Sigma-Aldrich (St Louis, USA). Xylanase (XT6, GH10) from *Bacillus stearothermophilus* T6 and insoluble wheat arabinoxylan were purchased from MegazymeTM (Bray, Ireland).

4.3.2. Specific activity determination

4.3.2.1 FAE activity on ethyl ferulate

FAE activity was determined by measuring the amount of FA released from ethyl ferulate (EFA). In a 1.5 mL Eppendorf tube, the reaction (1 mL) was carried out in sodium phosphate buffer (50 mM, pH 7.4) that contained 1 mM EFA. The reaction was started by the addition of an appropriately diluted enzyme solution. The reaction was conducted for 15 minutes at 40°C,

followed by incubation at 100°C for 5 minutes to terminate the enzymatic activity. The concentration of FA was quantified using a Shimadzu HPLC system (Shimadzu Corp, Japan) equipped with a diode array detector (DAD), where chromatographic separation was achieved on a Phenomenex® C18 5 µm (150 × 4.6 mm) LC column (Torrance, US A). Ambient conditions were used for analysis. The mobile phase A was 0.01 M phosphoric acid and the mobile phase B was HPLC grade acetonitrile. The isocratic mobile phase consisted of A: 70% and B: 30% and ran for 10 minutes at a flow rate of 0.8 mL/min. The injected sample volume was 10 µL and the UV absorption of the effluent was monitored at 320 nm. One unit of enzyme activity was defined as the amount of enzyme that released 1 µmol of FA per minute under standard conditions. A FA standard curve was constructed for the estimation of enzyme released FA (see Appendix Figures B.5.1 and C.1.2).

4.3.2.2. Xylanase activity

4.3.2.2.1. Xylanase activity on insoluble wheat arabinoxylan

For xylanase activity assay, 10 mg/mL of insoluble wheat arabinoxylan (WAX) was used as a substrate. The reaction mixture consisted of 300 µL of 1.33% (w/v) substrate dissolved in 50 mM sodium phosphate buffer (pH 7.4) and 100 µL of properly diluted enzyme. After 15 minutes of incubation at 40°C, the enzymatic activity was terminated by incubation at 100°C for 5 minutes, followed by centrifugation at $16\ 060 \times g$ for 5 minutes. The xylanase activity was determined by measuring the amount of reducing sugars produced (see section 4.3.3. below). One unit of enzyme activity was defined as the amount of enzyme that released 1 µmol of reducing sugars per minute under the assay conditions specified.

4.3.2.2.2. Xylanase activity on Azo-Xylan (birchwood)

For reactions containing compounds that interfere with the DNS assay, xylanase activity assay was performed using Azo-Xylan (birchwood) as a substrate. The reaction mixture consisted of 200 µL of 1% (w/v) of substrate solution and 200 µL buffered enzyme solution (50 mM sodium phosphate buffer, pH 7.4). After 15 minutes incubation at 40°C, the enzymatic activity was terminated by the addition of 1 mL 95% (v/v) ethanol, followed by vigorous stirring on a vortex mixer and incubation at room temperature for 5 minutes. Non-hydrolysed substrate precipitated by ethanol was removed by centrifugation at $1000 \times g$ for 10 minutes. A 200 µL of solution supernatant was transferred into a 96 well plate and the absorbance was measured at 590 nm. For preparation of the control, 200 µL of 50 mM sodium phosphate buffer, (pH 7.4) was used

in place of a buffered enzyme solution. A Remazol brilliant Blue R standard curve was used to calculate the quantity of product produced.

4.3.3. Reducing sugar quantification

The concentrations of reducing sugars were measured using 3,5-dinitrosalicylic acid (DNS) method described by Miller, (1959). Briefly, a 150 μ L of sample was mixed with 300 μ L of DNS reagent followed by boiling for 5 minutes. Reducing sugars were estimated using a xylose standard curve (see Appendix Figures B.2.1 and B.2.2).

4.3.4. Temperature optimum determination

To determine the temperature optimum, the enzyme reactions were carried out at temperatures ranging from 30°C to 70°C in 50 mM sodium phosphate buffer (pH, 7.4). Enzyme activity was determined by standard activity assay as described in section 3.3.9 for FAE activity and 4.3.2.2.1 for xylanase activity.

4.3.5. Thermo-stability determination

Thermo-stability of the enzymes was investigated by incubating the enzyme without substrate at two temperatures; 40°C and 50°C, in 50 mM sodium phosphate buffer (pH 7.4). The residual enzyme activity was determined at various time intervals (from 1 to 24 hours) using the standard activity assays described in section 3.3.9 for FAE activity and 4.3.2.2.1 for xylanase activity. Enzyme activity without any incubation period (i.e. time interval of 0 min) was considered as 100%.

4.3.6. pH optimum determination

To evaluate the pH optimum, the enzyme activity was measured over a pH range from 3.0 to 11.0 in universal buffer (Britton and Robinson, 1931). Incubation was carried out at a constant temperature of 40°C and enzyme activity was determined using standard activity assays as described in section 3.3.9 for FAE activity and 4.3.2.2.1 for xylanase activity.

4.3.7. Effect of metal ions on the FAE activity

To evaluate the effect of divalent metal ions on FAE activity, the enzyme was incubated with 1 mM and 10 mM of salt solutions (MgSO_4 , CoSO_4 , FeSO_4 , MnSO_4 , CaCl_2 , ZnSO_4 , CuSO_4) in 50 mM sodium phosphate buffer (pH, 7.4). The enzyme activity was determined using standard activity assay as described in section 3.3.9. The enzyme activity without any addition of metal ions was considered as 100%.

4.3.8. Product inhibition studies

To evaluate the effect of hydrolysis products on FAE activity, the enzyme was incubated with 5 mM to 50 mM of FA and xylobiose in 50 mM sodium phosphate buffer (pH, 7.4). The enzyme activity was determined using standard activity assay as described in section 3.3.9. The enzyme activity without any addition of metal ions was considered as 100%. For the determination of xylobiose and FA inhibition effects on xylanase activity, the standard activity assay described in section 4.3.2.2.2 was used. The enzyme activity without addition of xylobiose or FA was considered as 100%.

4.3.9. Statistical analysis

All statistical analyses were performed by GraphPad Prism 6.0 software using the t test. A *p* value less than 0.05 was considered to illustrate statistical significance between compared data sets.

4.4. Results and discussion

4.4.1. Specific activity determination

FAEs and xylanases are able to act on a variety of substrates, including agricultural residues, releasing valuable compounds (e.g. FA, *p*-CA and XOS). These enzymes are widely used in the food, feed, pulp and paper, and pharmaceutical industries, as well as in biofuel production. These broad applications often require various types of enzymes to fit specific operating conditions such as temperature and pH. In this section, physico-chemical properties and product inhibition profiles of recombinant FAEs (FAE5 and FAE6) and commercially available xylanases (Xyn11 and XT6) were investigated. The enzymes were tested for their specific activities on EFA and WAX at 40°C using sodium phosphate buffer (50 mM, pH 7.4) (Table 4.1). As expected, both Xyn11 and XT6 were only active on WAX, while FAE5 and FAE6 showed activity only on EFA. FAE5 and FAE6 demonstrated relatively similar feruloyl esterase activities of 28.36 U/mg and 27.34 U/mg, respectively. These specific activities were less than those reported by Rashamuse et al. (2014). Their study reported that FAE5 showed a specific activity of 53.2 U/mg and FAE6 showed 39.94 U/mg using EFA as a substrate. It is possible that the differences observed in specific activities are associated with different recombinant production and purification approaches. For xylanase, XT6 displayed a specific activity of 10.25 U/mg, this value was quite close to the specific activity (12 U/mg) reported on the data booklet for this enzyme (Megazyme™, Ireland) and Xyn11 displayed a specific

activity of 15.08 U/mg. All the tested enzymes displayed expected results and this specific activity data is very useful in the subsequent formulation of xylanases-FAEs cocktails for the degradation of complex substrates.

Table 4.1: Specific activities of the enzymes assessed in this study (U/mg protein).

Substrate	Enzyme tested			
	Xyn11	XT6	FAE5	FAE6
WAX ^a	15.08 ± 0.30	10.25 ± 0.46	Nd	Nd
EFA ^b	Nd	Nd	28.36 ± 0.56	27.34 ± 0.76

^a-Analysed by DNS method for xylanase activity and ^b-analysed by HPLC DAD for feruloyl esterase activity. The data presented are averages of triplicate values. “Nd” = Not detected.

4.4.2. Temperature optimum determination

The profiles of enzyme activities as a function of temperature are presented in Figure 4.1. The optimum temperature of each enzyme was measured by incubating the reaction mixture over a temperature range from 30°C to 70°C. According to the data presented in Figure 4.1A, FAE5 showed maximal activity around 40°C and retained more than 80% activity at 45°C. However, the activity decreased dramatically from 50°C to 70°C, retaining about 40% and 16% of the maximum activity, respectively. The optimum temperature of FAE6 was found to be 40°C as well and about 83% and 67% of the maximum activity were retained at 45°C and 50°C, respectively (Figure 4.1B). These findings coincided well with the optimum temperature reported for FAE5 and FAE6 by Rashamuse et al. (2014).

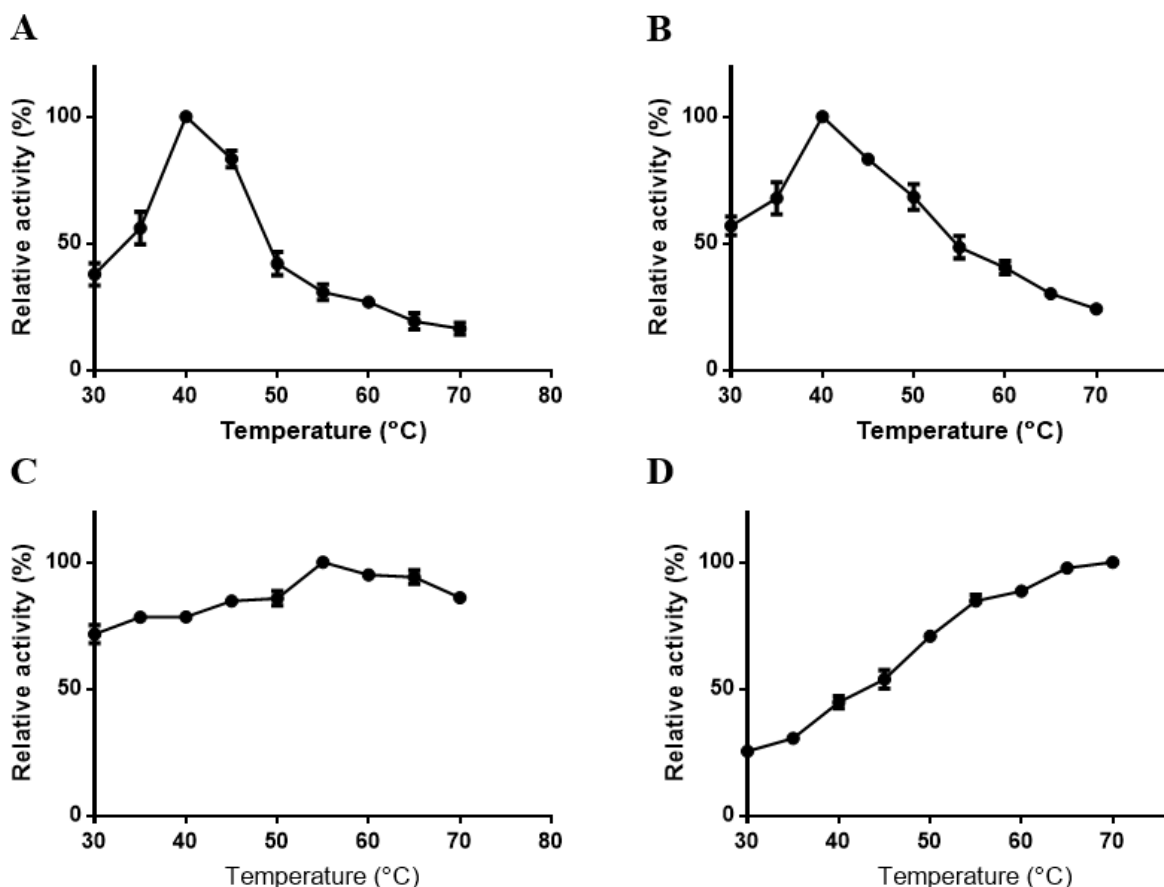


Figure 4.1: Effects of temperature on the activities of FAEs and xylanases. (A) FAE5, (B) FAE6, (C) Xyn11 and (D) XT6. Enzyme activities were expressed as percentages of the maximal activities at the optimum temperatures. Each point presented is the average \pm standard deviations of triplicate values.

A few studies have reported the optimum temperature for metagenome derived FAEs be around 40°C (Wu et al., 2019; Wong et al., 2019). Contrary to the findings for FAE5 and FAE6, Xyn11 (Figure 4.1C) remained active over a wide range of temperatures, retaining about 78% to 84% activity between 40°C and 70°C, respectively. The maximum activity for this enzyme appeared to be around 55°C. This optimum temperature was comparable to other *Thermomyces* derived xylanases (Shrivastava et al., 2013; Kumar and Shukla, 2018). This remarkable tolerance over a wide range of temperatures is a very useful property, especially for synergistic interaction studies. The maximum activity for XT6 was observed at 70°C but the enzyme retained more than 45% activity at 40°C (Figure 4.1D). The findings were expected since this is a thermophilic enzyme (Hegazy et al., 2019). Except for XT6, all the enzymes tested showed

substantially high hydrolytic activities around 40°C, and this temperature was therefore selected as the temperature at which to perform the synergy studies.

4.4.3. Thermo-stability determination

The thermostability of the enzymes was examined by measuring the enzymatic activity after incubation at 40°C and 50°C (Figure 4.2). As shown in Figure 4.2A, after 1 hour incubation, FAE5 lost about 50% activity within an hour of incubation at 40°C and 50°C. The enzyme was able to maintain about 50% activity throughout the 24 hour incubation period. As for FAE6, the enzyme could retain more than 90% activity at 40°C after 1 hour incubation and around 80% after 24 hour incubation period (Figure 4.2B). However, the activity dramatically decreased at 50°C - the enzyme could only retain about 45% activity after 1 hour incubation and around 30% activity after 24 hour incubation. Interestingly, Xyn11 and XT6 displayed activation at both 40°C and 50°C. Xyn11 displayed a slight activation of about 20% at 40°C and 10% at 50°C after 24 hour incubation (Figure 4.2C). This trend was much more pronounced for XT6 (Figure 4.2D) as the activity was almost triple at 40°C and double at 50°C after 6 hour incubation. The activity observed remained relatively high even after 24 hour incubation at both temperatures. The activation of these two enzymes might be due to the fact that their thermostability was conducted at temperatures lower than their optimum temperature, which was 55°C and 70°C for Xyn11 and XT6, respectively. Overall, the thermostability data indicated that these enzymes have satisfactory catalytic capabilities at 40°C for a period of 24 hour which is sufficient for bioconversion processes.

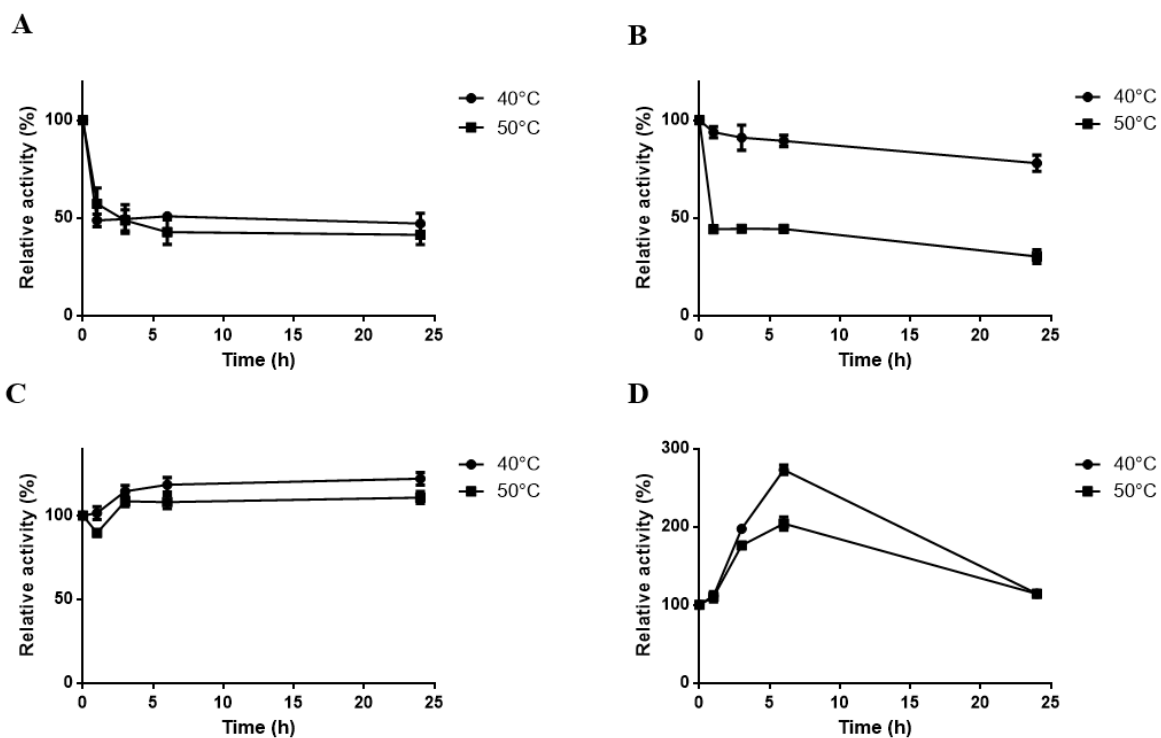


Figure 4.2: Determination of the thermostability of FAEs and xylanases. (A) FAE5, (B) FAE6, (C) Xyn11 and (D) XT6. Thermo-stability was measured by incubating the enzyme at different temperatures (40°C and 50°C). The residual activity was measured by collecting samples at 1 hour, 3 hour, 6 hour and 24 hour. Enzyme activities without incubation (i.e. time = 0) were defined as 100%. Each dat point represents the average \pm standard deviations of triplicate assays.

4.4.4. pH optimum determination

The enzyme activity profiles as a function of pH were also determined and the data is presented in Figure 4.3. This study was conducted to determine the pH range at which the highest activity profiles of the enzymes selected for this study overlap. FAE5 was active at neutral pH, with more than 85% of its activity observed between pH 7.0 and 8.0 (Figure 4.3A). The maximum activity was observed at pH 7.0. A similar trend was observed for FAE6, the enzyme retained more than 80% of its activity at a very narrow range of pH 7.0 and 8.0 (Figure 4.3B). The pH for the optimum activity of FAE6 was determined to be 7.5, which is relatively similar to the optimum pH of FAE5. The activity profiles of FAEs reported in this study are consistent with other recombinant FAEs derived from rumen microbial metagenome (Wong et al., 2013; Wu

et al., 2019). Xyn11 displayed a broad pH range, retaining more than 80% of its activity between pH 6.0 and 10 (Figure 4.3C). XT6 showed a similar broad pH range to Xyn11, although their overall pH activity profiles appeared quite different (Figure 4.3D). This enzyme retained more than 70% of its activity between 5.0 and 9.0, showing optimum activity at pH 7.0. The pH optimum trend observed for XT6 was similar to the trend reported by Anand and co-workers (2013), where a *Geobacillus* derived xylanase was active in a broad range of pH (5.0 -10.0). All the enzymes evaluated in this study displayed appreciable activities at neutral pH.

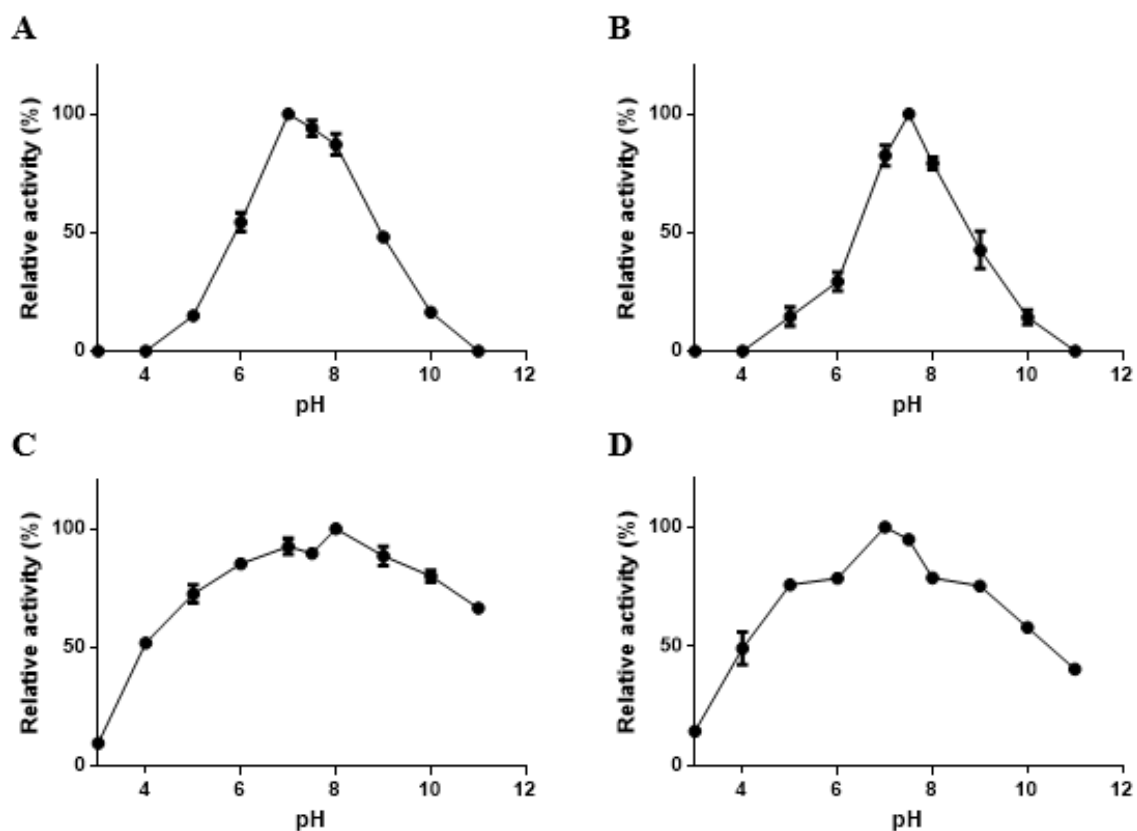


Figure 4.3: Effect of pH on the activities of FAEs and xylanases. (A) FAE5, (B) FAE6, (C) Xyn11 and (D) XT6. Enzyme activities were expressed as percentages of the maximal activities observed at the optimal pH. Each data point represents the average \pm standard deviations of triplicate assays.

4.4.5. Effect of metal ions on the FAE activity

The effect of several metal ions on the activities of FAE5 and FAE6 was evaluated. This was conducted in order to identify metal ions that could potentially enhance the activity of these two enzymes. There is considerable evidence that bivalent metal ions can have an activating effect on FAE activity. A recombinant FAE from *Aspergillus niger* (AnFaeA) showed a 2.1-fold increase in activity when Fe^{2+} was added in the reaction mixture (Zhou et al., 2015). Li et al. (2018) reported that the activity of novel FAE-Xuan was enhanced by addition of K^+ , Na^+ and Mg^{2+} to 120, 131, and 116% of its maximum activity, respectively. However, the mechanism by which these metal ions activate FAEs is not well elucidated. As indicated in Figure 4.4, there were no metal ions capable of activating both FAE5 and FAE6. There was no significant loss of FAE5 activity observed in the presence of Co^{2+} (at low concentration. 1 mM), Ca^{2+} , Fe^{2+} , Mg^{2+} and Mn^{2+} (Figure 4.4A). However, high concentrations (10 mM) of Zn^{2+} , Co^{2+} and Cu^{2+} significantly reduced the enzyme activity. A relatively similar pattern was also observed for FAE6 activity (Figure 4.4B), except for Zn^{2+} where the enzyme could only retain less than 20% activity for both low and high concentrations. The strong inhibition showed by Zn^{2+} was expected, because Zn^{2+} ions are known to bind strongly to proteins (Maret, 2013). It has been reported that Zn^{2+} ions have high binding affinity for enzymes which have active sites that contain catalytic triads with glutamate (aspartate), histidine and cysteine residues, which are all known to be zinc-binding ligands (Maret, 2013). FAEs are known to contain the classical catalytic triad at the core of the active site which is composed of serine, histidine, and asparagine residues (Ser-His-Asp) (Uraji et al., 2018). Overall, the data indicated that there was no metal ion that could enhance the activities of FAE5 and FAE6.

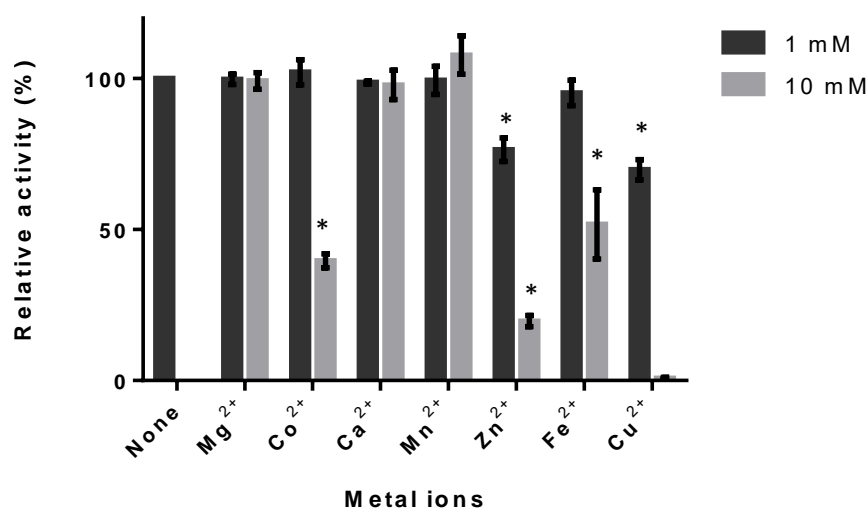
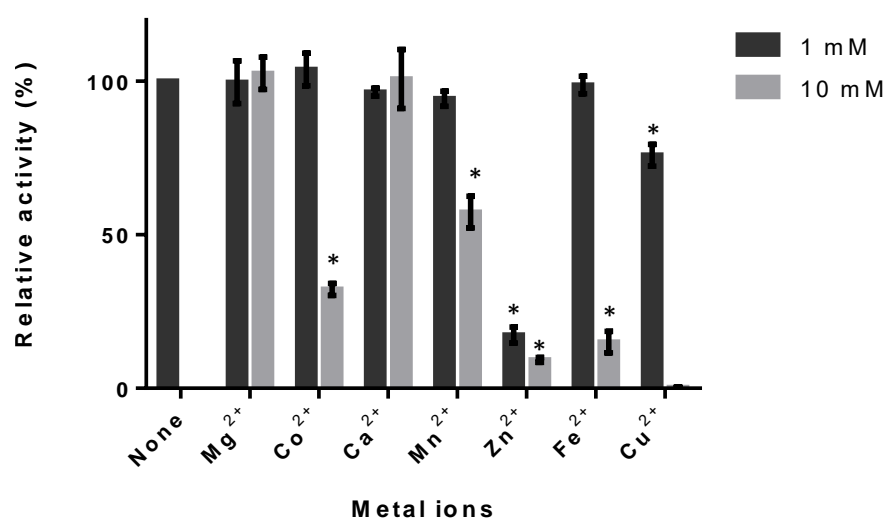
A**B**

Figure 4.4: The effects of various metal ions on FAE activity. (A) FAE5 and (B) FAE6. Metal ions were added into the reaction mixture to a final concentration of 1 mM or 10 mM. Averages and standard deviations from three replicate experiments are presented. Statistical analysis was conducted using t-test for inhibition or activation of FAE activity by metal ions compared to the activity in the absence of metal ions, key: * (p value < 0.05).

4.4.6. Product inhibition studies

Factors limiting the efficient enzymatic release of FA and reducing sugars from various lignocellulosic materials have been well described. Some of these factors are based on the structural features of the substrate and are greatly influenced by the interactions between substituents present on the polysaccharides and other cell wall components (Wong et al., 2013). The inhibitory effects of end-products on enzymatic hydrolysis appear to be one of the major limiting factors to biomass conversion (Andric et al., 2010). The inhibitory effect of FA on FAE activity and its impact on FA release from lignocellulosic substrates has been investigated (Xiros et al., 2009). As shown in Figure 4.5, enzymatic reactions were performed in the presence of various FA concentrations (5-100 mM). A significant decrease (56%) in FAE5 activity was observed for a FA concentration of 5 mM, while higher FA concentrations completely abolished enzyme activity (Figure 4.5A). FAE6 could tolerate a FA concentration of 5 mM as the enzyme retained 87.5% of its maximum activity, but no activity was observed in the presence of higher FA concentrations (Figure 4.5B). An earlier study evaluated the inhibitory effect of FA with a concentration range of 0 - 0.75 mM and reported a decrease in end-product release of about 87% (Xiros et al., 2009). The FA inhibition findings from this study demonstrated that FAE5 and FAE6 could still maintain appreciable activity levels in the presence of 5 mM FA. The amount of FA released during hydrolysis of complex substrates is unlikely to reach extremely high concentrations as the total hydroxycinnamic acid contents of various complex substrates range between 0.08 mg/g and 33 mg/g (Gopalan et al., 2015).

Furthermore, the effect of the presence of FA on xylanases activity was also investigated. The influence of FA on xylanase activity during degradation of biomass has been reported previously. Monclaro et al. (2019) showed that FA is able to cause a conformational change in AtXyl1 (GH11 xylanase from *Aspergillus niger*), which could influence fitting of the substrate into the active site. It has been reported that phenolic compounds are likely to inhibit glycoside hydrolases non-competitively, because these compounds do not share structural similarities with the substrates of these enzymes (Surendran et al., 2018). In the present study, Xyn11 was not significantly inhibited by FA at all the concentrations evaluated (Figure 4.5C). The inhibitory effect of FA on the activity of XT6 was only observed at a concentration of 50 mM (Figure 4.5D). Other studies have demonstrated that xylanase activity is stimulated by the addition of FA. For example, da Silva et al. (2019) reported that the endo-xylanase activity from *Aspergillus japonicus* was stimulated by FA (residual activity of 177.26%). The effect of FA on xylanase activity appears to be influenced by the type of substrate used (Monclaro et al.,

2019). In summary, no significance impact of FA on xylanase activity was observed, except for the activity of XT6 in the presence of a high concentration of FA (50 mM). This characteristic tolerance of xylanases to hydroxycinnamic acid during hydrolysis indicates that these enzymes could be used in synergy studies with FAEs for the efficient release of FA from agricultural residues.

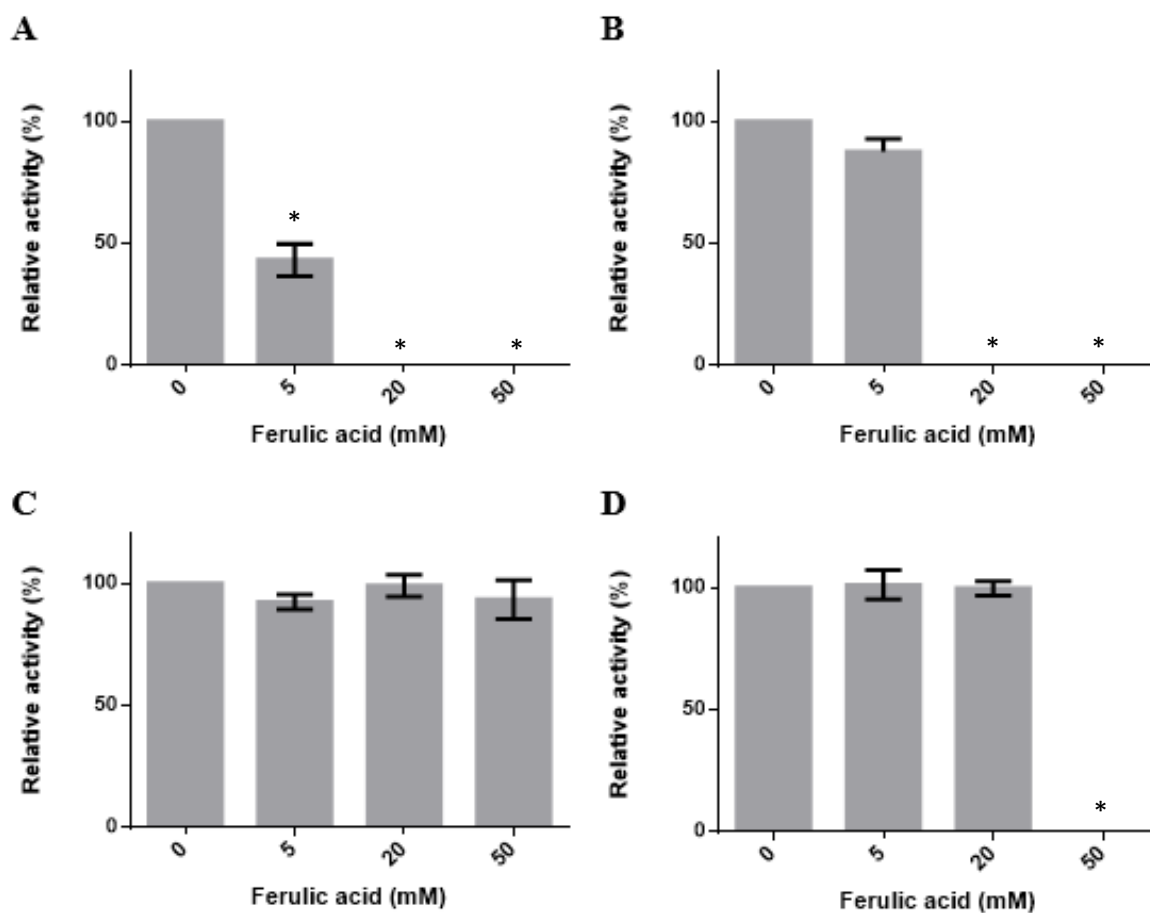


Figure 4.5: The effect of FA on FAE and xylanase activity. (A) FAE5, (B) FAE6, (C) Xyn11 and (D) XT6. FA was added into the reaction mixture to a final concentration of between 5 mM and 50 mM. Averages and standard deviations from three replicate experiments are presented. Statistical analysis was conducted using a t-test for inhibition of enzyme activity by FA compared to the activity in the absence of FA, key: * (p value < 0.05).

The inhibitory effects of the end products produced during xylanase hydrolysis on the enzyme activities were also investigated. Several studies have shown that the main hydrolysis products released from various xylan-rich materials by some xylanases consists mainly of xylobiose (Bragatto et al., 2013; Khandeparker et al., 2017; Singh, R. D. et al., 2018). However, xylobiose is also known to potentially inhibit xylanases, which could further limit the production of XOS by the enzymes (Jommuengbout et al., 2009). Therefore, it was important to evaluate the inhibitory effect of xylobiose on enzyme activities. FAE and xylanase activities were measured in the presence of xylobiose at a concentration of 0 – 50 mM (Figure 4.6). There was no significant effect of xylobiose on the activities of FAE5 (Figure 4.6A) and FAE6 (Figure 4.6B). It was also found that the xylanase activities of Xyn11 and XT6 (Figures 4.6C and D) were reasonably constant, even in the presence of 50 mM xylobiose. Information on the effect of XOS on FAE activity in the literature is very limited. The results obtained in this study show that xylobiose (at a concentration range of 0 – 50 mM) had no effect on the activities of the enzymes. Therefore, the enzymes selected for this study could be used in studies that involve the efficient enzymatic production of hydroxycinnamic acids and XOS from various substrates.

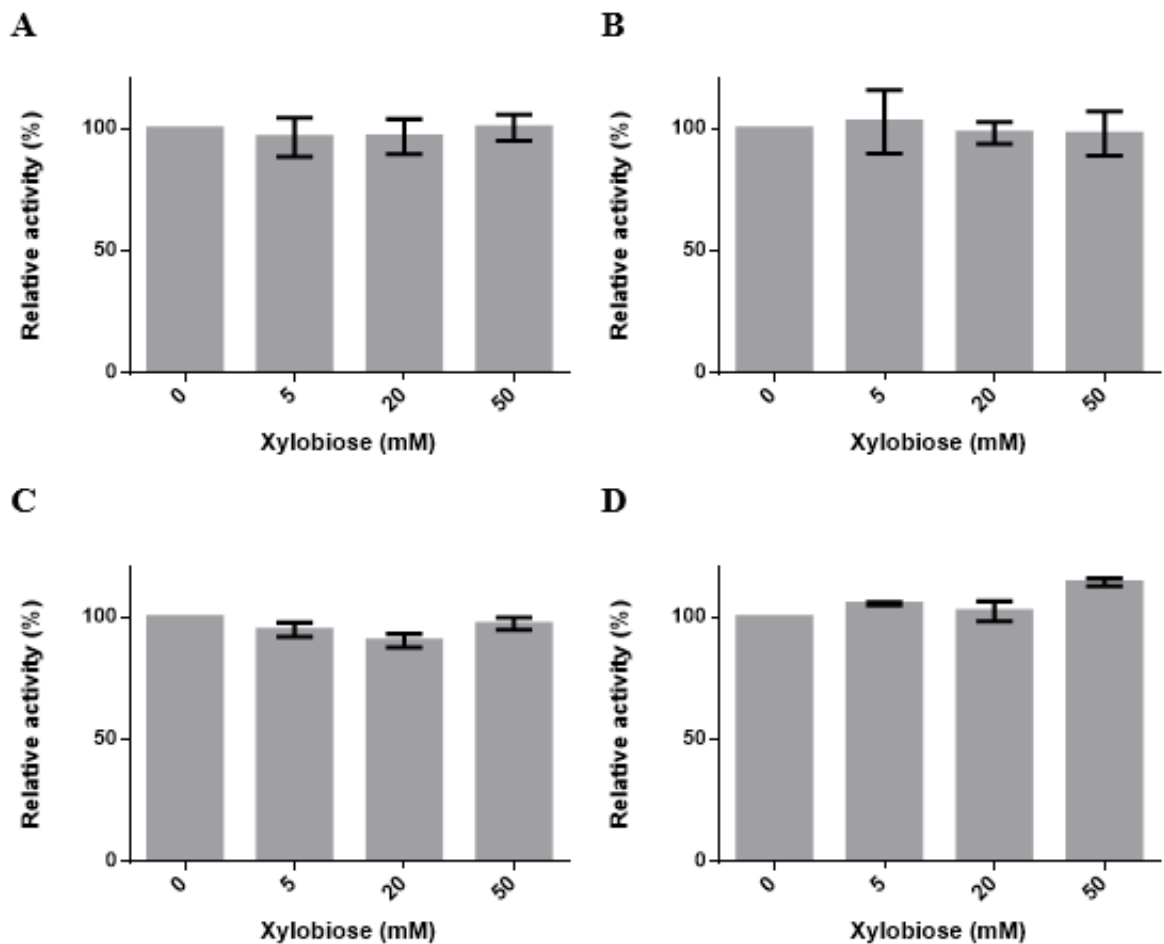


Figure 4.6: The effect of xylobiose on FAE and xylanase activity. (A) FAE5, (B) FAE6, (C) Xyn11 and (D) XT6. Xylobiose was added into the reaction mixture to a final concentration of 5 mM, 20 mM or 50 mM. Averages and standard deviations from triplicate experiments are presented. Statistical analysis was conducted using a t-test for inhibition of enzyme activity by xylobiose compared to the activity in the absence of xylobiose, key: * (p value < 0.05).

4.5. Conclusion

In the present study, two novel metagenome-derived FAEs (FAE6 and FAE6) and commercial xylanases (Xyn11 and XT6) were partially characterised with respect to their physico-chemical properties. The enzymes exhibited acceptable specific activities and the data revealed that there was no cross reactivity between the enzymes on the substrates tested. This indicates that there is a reduced chance of substrate competition occurring when the enzymes are applied in synergy studies. The pH and temperature optima for both FAEs were 7.0 and 40°C, respectively. Xyn11 and XT6 retained high activities over a broad pH range, and the pH optima of FAEs were within this range. All the enzymes exhibited reasonable thermostability over an incubation time of 24 h, except for FAE5 which could only retain about 50% of its maximum activity. The metal ions tested did not show any activation of FAE activities – instead, some of them showed an inhibitory effect. Both Xyn11 and XT6 showed high tolerance to the major end products, FA and xylobiose. The data from this study indicated that the physico-chemical properties of FAEs overlapped nicely with the operating conditions of Xyn11 and XT6. Therefore, these enzymes could be used in the formulation of synergistic enzyme cocktails for the efficient release of hydroxycinnamic acids and XOS from various agricultural residues.

Chapter 5: Pre-treatment of agricultural residues and the impact of their pre-treatment by-products on enzymes

5.1. Introduction

The enzymatic degradation of lignocellulosic biomass is considered a safe and environmentally friendly method for the production of VAPs. However, a few challenges are associated with the valuable utilisation of lignocellulosic biomass. Some of the major factors impeding its use include the degree of lignification, crystalline nature of cellulose, and the structural heterogeneity and complexity of plant cell wall components (Guerriero et al., 2016). In this regard, the pre-treatment process is a significant step for achieving success in the biochemical conversion method. The main goal of pre-treatment is to decrease the recalcitrance of lignocellulosic biomass to enzymatic hydrolysis by partially breaking down the close inter-component association between lignin and carbohydrates (Jönsson and Martín, 2016). The proportions and composition of cellulose, hemicelluloses and lignin differ between various types of biomasses and these should be considered when selecting a pre-treatment method (Dahadha et al., 2017).

Some of the commonly used pre-treatment strategies include hydrothermal and dilute acid methods. Hydrothermal pre-treatment utilises water in liquid phase or in vapour phase at elevated temperatures (160-240°C), and wide range of pressures (Hu and Ragauskas, 2012). Dilute acid pre-treatment is considered to be a promising procedure for decreasing the recalcitrance of lignocellulosic biomass. This pre-treatment has been extensively studied using several agricultural residues such as rice straw (Kapoor et al., 2017), corn stover (Liu, Q. et al., 2016), wheat straw (Ji et al., 2015) and sugar beet pulp (Zheng et al., 2013). Requirements for this method include relatively high temperatures (120 to 215°C), pressure (2 to 10 atm), low acid concentrations (0 to 5%, w/w) and residence times ranging from 10 to 120 minutes (Solarte-Toro et al., 2019). In general, higher-severity pre-treatment conditions are associated with solubilisation of parts of the hemicellulose fraction and undesirable cellulose degradation leading to the generation of inhibitory compounds such as furfural, hydroxymethylfurfural (HMF), formic acid, and levulinic acid (Kim, 2018). It has been demonstrated that the solubilisation of hemicellulose can be minimised when pre-treatment is performed at low to mild severity (Nitsos et al., 2013). Therefore, the operating conditions for pre-treatment methods should be in line with the aims of the overall enzymatic conversion process.

Several analytical techniques have been developed to study the effects of pre-treatment methods on lignocellulosic biomass. These techniques are mainly used to gain deeper insights into the structural aspects of biomass which include composition, crystallinity, pore size, surface properties and degree of polymerisation (Karimi and Taherzadeh, 2016). To determine the overall efficiency of the pre-treatment process, it is necessary to examine the composition of lignocellulosic biomass before and after pre-treatment. Different methods have been developed for the compositional analysis of untreated and pre-treated biomass, and these are mainly based on estimation of the carbohydrate and lignin content. One of the most extensively used methods is that developed by Sluiter et al. (2008), provided by the National Renewable Energy Laboratory (NREL). This method uses a two-step acid hydrolysis approach where polymeric carbohydrates are converted into their monomeric sugars. The acid hydrolysis leads to fractionation of lignin into acid insoluble material and acid soluble material. The monomeric sugars, acid soluble material and acetyl content can be measured using a couple of techniques such as HPLC and UV-Vis spectroscopy.

To achieve reasonable conclusions about the effects of the pre-treatment process, it is necessary to assess surface, chemical and morphological characteristics of biomass. Scanning electron microscopy (SEM) and Fourier transform infrared spectroscopy (FTIR) are among the powerful tools used to examine physico-chemical characteristics of biomass. FTIR has been applied in qualitative and quantitative analysis of biomass as is time-efficient and requires very small amounts of sample material (Xu et al., 2013). This technique is based on information about molecular bond vibrations induced by infrared radiation, and it can be used to assess variations in functional groups and other structural features. Another important technique to investigate the impact of pre-treatments on disrupting biomass is imaging analysis, and SEM is one of the tools widely used for evaluation of surface characteristics (Amiri and Karimi, 2015). Because of its relatively high resolution, SEM can provide information about surface erosion, and re-localisation of cell wall constituents (Donohoe et al., 2011). All these analysis techniques help in providing information about the mechanisms by which pre-treatment improves the enzymatic degradation of biomass.

In this chapter, hydrothermal and dilute sulfuric acid pre-treatment methods were applied to agricultural residues (rice straw, sugarcane bagasse and corn cob). The effect of pre-treatment on these residues was investigated by conducting compositional and morphological analysis of the untreated and pre-treated agricultural residues.

5.2. Aims and objectives

5.2.1. Aims

To perform pre-treatment on and chemical characterisation of agricultural residues and to the impact of pre-treatment by-products on FAE activity.

5.2.2. Objectives

To achieve these aims the following objectives were set:

- To pre-treat agricultural residues using the dilute acid and hydrothermal pre-treatment methods
- To conduct compositional analysis of the untreated and pre-treated agricultural residues;
- To study morphological changes on untreated and pre-treated agricultural residues using microscopic techniques;
- To assess chemical changes on untreated and pre-treated agricultural residues using FTIR;
- To evaluate the impact of model pre-treatment by-products on enzyme activity; and
- To evaluate the impact of wash liquors prepared from pre-treated agricultural residues on enzyme activity.

5.3. Materials and methods

5.3.1. Materials

The agricultural residues selected for pre-treatment were rice straw (RS), sugarcane bagasse (SCB) and corn cob (CC). SCB used was obtained from Ushukela Milling (Pty) Ltd., Durban, South Africa. CC was obtained from a local supermarket, Grahamstown, in the Eastern Cape Province of South Africa and RS was obtained from the School of Bioresources and Technology, King Mongkut's University of Technology Thonburi, Bangkok, Thailand.

5.3.2. Pre-treatment of agricultural residues

All substrates were milled using a Platinum coffee grinder and the fractions passing through a wire sieve mesh was used for subsequent pre-treatment. Substrates were treated using either a hydrothermal pre-treatment or a dilute acid pre-treatment. A total of 10 g of substrate was suspended in Milli-Q water (for hydrothermal treatment) or in a 0.5% (w/w) sulphuric acid solution (for dilute acid treatment) (solid: liquid ratio of 1:10) and autoclaved for 20 minutes at 121°C. The pre-treated substrate solution was filtered, followed by washing the solids repeatedly with Milli-Q water and then oven drying to constant weight at 50°C for 48 hours.

5.3.3. Chemical characterisation of agricultural residues

The total carbohydrates of untreated and pre-treated substrates were determined using a modified sulphuric acid method described by Sluiter et al. (2010). A total of 300 mg of each substrate was hydrolysed with 72% (v/v) sulphuric acid at 30°C for 1 hour with intermittent stirring using glass rods. The solution was then diluted to 3% (v/v) sulphuric acid with Milli-Q water and autoclaved for 1 hour to solubilise the carbohydrate fraction. Following the hydrolysis, fractions were filtered to remove the insoluble lignin from the solution, the carbohydrate content, including, glucan, xylan and arabinan, was estimated using Megazyme sugar kits (K-GLUC, K-XYLOSE and K-ARGA, see Appendix Figures B.4.1, B.4.2 and B.4.3), and total reducing sugars were determined using the DNS method as described in section 4.3.3.

Determination of hydroxycinnamic acid content was carried out by performing alkaline hydrolysis. The experiments were performed as follows: 10 mg of untreated or pre-treated substrate was treated with 1 M NaOH solution for 24 hours at room temperature in the dark. The liquors obtained from alkaline treatment were separated from the solid fractions by centrifugation at $16\,000 \times g$ for 5 minutes. The liquors were neutralised by 2 volume

equivalents of 1 M HCl and analysed by HPLC as described in section 4.3.2.1. All the hydrolysis experiments were conducted in triplicate.

5.3.4. Microscopic analysis of agricultural residues

5.3.4.1. Scanning electron microscopy analysis

A scanning electron microscope (SEM), JOEL JSM 840, was used to study the morphological structure of untreated and pre-treated substrates. Substrates were mounted on a metal stub with adhesive tape and coated with a thin layer of gold using a sputter coater prior to SEM analysis.

5.3.4.2. Light microscopy analysis

The Wiesner test was used for the detection of lignin in untreated and pre-treated substrates as described by Abbott et al. (2002), with slight modifications. Phloroglucinol staining was performed as follows: samples were soaked in phloroglucinol staining solution (two parts of 5% (w/v) phloroglucinol in 95% (v/v) ethanol with one part concentrated hydrochloric acid) and left at room temperature for 5 minutes. The images showing colour changes in substrates were recorded using an Olympus DP72 digital camera on an Olympus BX40 light microscope.

5.3.5. FTIR analysis

In order to obtain information on the chemical changes that occur during pre-treatment, FTIR analysis of untreated and pre-treated substrates was conducted using a Spectrum 100 FTIR spectrometer system (Perkin Elmer, Wellesley, MA). FTIR spectra were recorded in quadruplicate at a range of 650-4000 cm^{-1} with a resolution of 4 cm^{-1} . The data obtained was edited using the Spectrum One software.

5.3.6. Determination of water retention capacity of agricultural residues

Water retention capacity (WRC) of agricultural residues was measured using a modified method by Brachet et al. (2015). Briefly, 1.5 mL of milli-Q water was added to 30 mg of substrate material in an Eppendorf tube. After 1 hour incubation on a rotor (25 rpm) at room temperature, the mixture was centrifuged (16 000 x g for 10 minutes at room temperature). The supernatant was then removed using a pipette before WRC measurement. The hydrated material was then placed in a fume hood for 10 minutes to evaporate excess water before weighing. WRC was expressed as mL of water retained per g of biomass.

5.3.7. The impact of pre-treatment by-products and wash liquors from agricultural residues on enzyme activities

5.3.7.1. Pre-treatment by-products

To evaluate the impact of pre-treatment by-products on FAEs, a broad spectrum of compounds known for their inhibitory properties were selected. These compounds included lignin, gallic acid, vanillin, vanillic acid, *p*-coumaric acid, furfural, HMF and levulinic acid. The compounds were evaluated individually in order to identify which compounds play a major role in impacting on the activity of FAEs. All compounds were dissolved in milli-Q water and stored at 4°C until use.

5.3.7.2. Pre-treatment by-products inhibition assays

The impact of various compounds generally during biomass pre-treatment was quantified by measuring the residual enzyme activity after exposing FAE5 and FAE6 to each compound. The standard assay described in section 3.3.9 was performed in the presence of each compound at a concentration range of 0.1 to 2 mg/mL. A reaction mixture without any compound was used as a positive control. The pH of each concentration (in 50 mM phosphate buffer, pH 7.4) for all compounds was monitored using a pH Test Strip (Languettes pH Test) to determine if the effect observed was induced by changes in pH. The enzyme kinetics were also investigated, and kinetic parameters were calculated using non-linear regression (GraphPad Prism 6.0) and the inhibition patterns displayed by some of the compounds were determined using Lineweaver-Burk (double-reciprocal) plots.

5.3.7.3. Preparation of wash liquors from pre-treated agricultural residues

The wash liquors of the dilute sulphuric acid and hydrothermal pre-treated RS, SCB and CC samples were prepared as follows: a 10 mg/mL load of each pre-treated substrate was prepared in 50 mM sodium phosphate buffer (pH 7.4) in a total volume of 20 mL. The suspensions were shaken at 40°C for 24 hours, and the solids were then separated from the wash liquors by centrifugation at $10\,000 \times g$ for 15 min at 4°C in an Avanti® J-E centrifuge and a JA-20 rotor (Beckman Coulter). The pH was recorded with a BANTE INSTRUMENTS PHS-3BW Bench TOP PH/MV/°C Meter. Wash liquors were stored at 4°C until use.

5.3.7.4. Evaluation of the impact of wash liquors from agricultural residues on enzyme activity

In order to evaluate the impact of wash liquors on enzyme activity, the standard assays described in sections 3.3.9 and 4.3.2.2 were used. The 50 mM sodium phosphate buffer (pH 7.4) was replaced by wash liquors and all other substrates, enzyme solution and incubation conditions remained the same. A reaction where wash liquors were substituted with a buffer was included as a positive control.

5.3.8. Statistical analysis

All statistical analyses were performed by GraphPad Prism 6.0 software using the t test. A *p* value less than 0.05 was considered to illustrate statistical significance between compared data sets.

5.4. Results and discussion

5.4.1. Chemical characterisation of agricultural residues

Utilisation of lignocellulosic biomass for bioconversion requires a pre-treatment step, this is due to the biomass recalcitrance caused by the structural heterogeneity and complexity of cell-wall constituents. The main goal of pre-treatment is to enhance the enzymatic hydrolysis of biomass for the production of value-added chemicals. However, some of the pre-treatment methods can easily solubilise some parts of the carbohydrate fraction, mostly hemicellulose (Rabemanolontsoa and Saka, 2016). To overcome this drawback, pre-treatment parameters should be adjusted in a manner that will lead to high recovery of the biomass components while retaining the ability to improve enzymatic digestibility. In this study, various agricultural residues (CC, RS and SCB) were subjected to hydrothermal or dilute sulphuric acid pre-treatment methods. To ensure that the hemicellulosic and hydroxycinnamic contents were preserved in the solid fraction, an extremely low pre-treatment severity was applied for both hydrothermal and dilute sulphuric acid pre-treatment methods. It has been shown that hydrothermal pre-treatment conducted at higher severities (165-175°C and 20-40 minutes) results in the solubilisation of xylan, arabinan and ferulic acid, but this effect is minimised at moderate severities (155°C and 20 minutes) (Jiang et al., 2018).

The chemical characterisation of CC, RS and SCB was conducted to determine the recoverable sugars and hydroxycinnamic acids after pre-treatment (Table 5.1). The quantification of other plant cell-wall constituents such as lignin was omitted and the study focused solely on the

analysis of glucan, xylan, arabinan, and hydroxycinnamic acids. As depicted in Table 5.1, the percentage of xylan and arabinan for CC and SCB was higher in pre-treated samples than in untreated samples. In contrast to the above observations, hydrothermal and dilute acid pre-treatment methods resulted in slight decreases in xylan and arabinan contents for RS samples. These differences in the contents may be partially attributed variations to structural features which include the amount of hydroxycinnamic acids esterified to polysaccharides. In terms of hydroxycinnamic acid content, the results suggest that the ester linkage survived the pre-treatment conditions and that FA and *p*-CA remained linked to polysaccharides in the solid fraction. The total hydroxycinnamic acid contents were approximately 1.35%, 1.08% and 2.11% for CC, RS and SCB, respectively. These values were within the range (0.5% to 2%, extractable amount) reported for the majority of hydroxycinnamic acid-rich agricultural residues (Kumar and Pruthi, 2014). The results presented in Table 5.1 shown that with low pre-treatment severity, high amounts of polysaccharide and hydroxycinnamic acid could be retained in the solid fraction.

Table 5.1: Chemical composition of untreated and pre-treated agricultural residues (on a percentage dry mass basis)

	Glucan ^a	Xylan ^a	Arabinan ^a	Total reducing sugars ^b	Ferulic acid ^c	<i>p</i> -coumaric acid ^c
Untreated						
CC	30.86	11.46	7.79	53.00	0.61	0.63
RS	24.80	10.0	7.51	49.29	0.75	0.34
SCB	15.40	4.73	3.81	31.33	0.45	1.66
Hydrothermally treated						
CC	36.03	13.47	11.24	62.38	0.68	0.61
RS	23.73	7.43	6.06	40.33	0.74	0.34
SCB	19.57	6.01	4.10	34.90	0.41	1.66
Acid treated						
CC	32.58	12.22	8.52	59.20	0.68	0.67
RS	24.10	9.33	7.37	48.10	0.81	0.37
SCB	19.71	7.03	3.84	35.83	0.39	1.62

^aMegazyme sugar kits, ^bDNS method, ^cHPLC. The data represent the averages of triplicate values. Corn cob (CC), rice straw (RS) and sugarcane bagasse (SCB).

5.4.2. Microscopic analysis of agricultural residues

5.4.2.1. SEM analysis for morphological changes

In order to determine the effect of pre-treatment, changes on the surfaces were studied for untreated and pre-treated agricultural residues through SEM examination. SEM micrographs of untreated and pre-treated samples are shown in Figure 5.1. The untreated samples (Figure 5.1A, D and G) appear to possess a compact and rigid structure constituted by parallel stripes for RS (Figure 5.1D) and CC (Figure 5.1G). The intact surfaces showed little debris for RS and SCB, while the surfaces of CC seem to be smooth. The effect of pre-treatment methods was similar for all samples. The micrographs of pre-treated samples display collapsed and disrupted surfaces with large amounts of hollow areas, as well as fibrous debris. The destruction of the biomass fibres may result in increased enzyme-accessible surface area. The structural changes induced by pre-treatment are known to decrease biomass recalcitrance which can lead to an enhanced enzymatic hydrolysis of pre-treated biomass (Zheng et al., 2013).

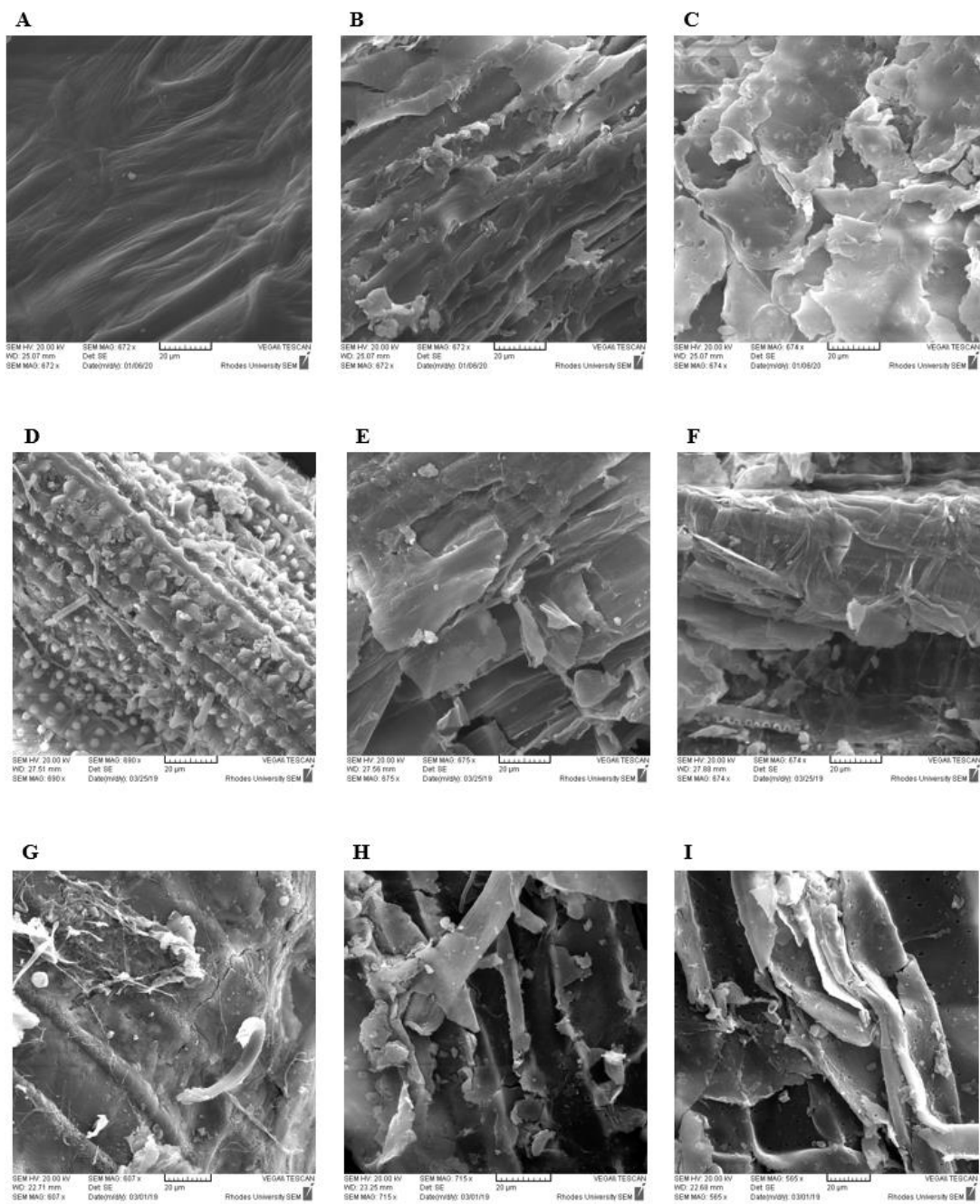


Figure 5.1: Morphological study of agricultural residues by SEM. SEM micrographs of (A) untreated, (B) hydrothermal treated, (C) and acid treated CC; (D) untreated, (E) hydrothermal treated, (F) and acid treated RS; (G) untreated, (H) hydrothermal treated, (I) and acid treated SCB at 2kx magnification.

5.4.2.2. Light microscopy analysis

Morphological observations provided evidence of changes in the agricultural residues during their pre-treatment. To gain a better understanding of these changes that occurred due to the pre-treatment procedures, histochemical analysis of lignin distribution in untreated and pre-

treated samples was conducted and the results are presented in Figure 5.2. Lignin has been known to be a major hindrance to enzymatic hydrolysis as it forms a physical barrier that restricts the access of enzymes to the substrate. Lignin modification increases cell wall porosity which could potentially enhance enzymatic hydrolysis.

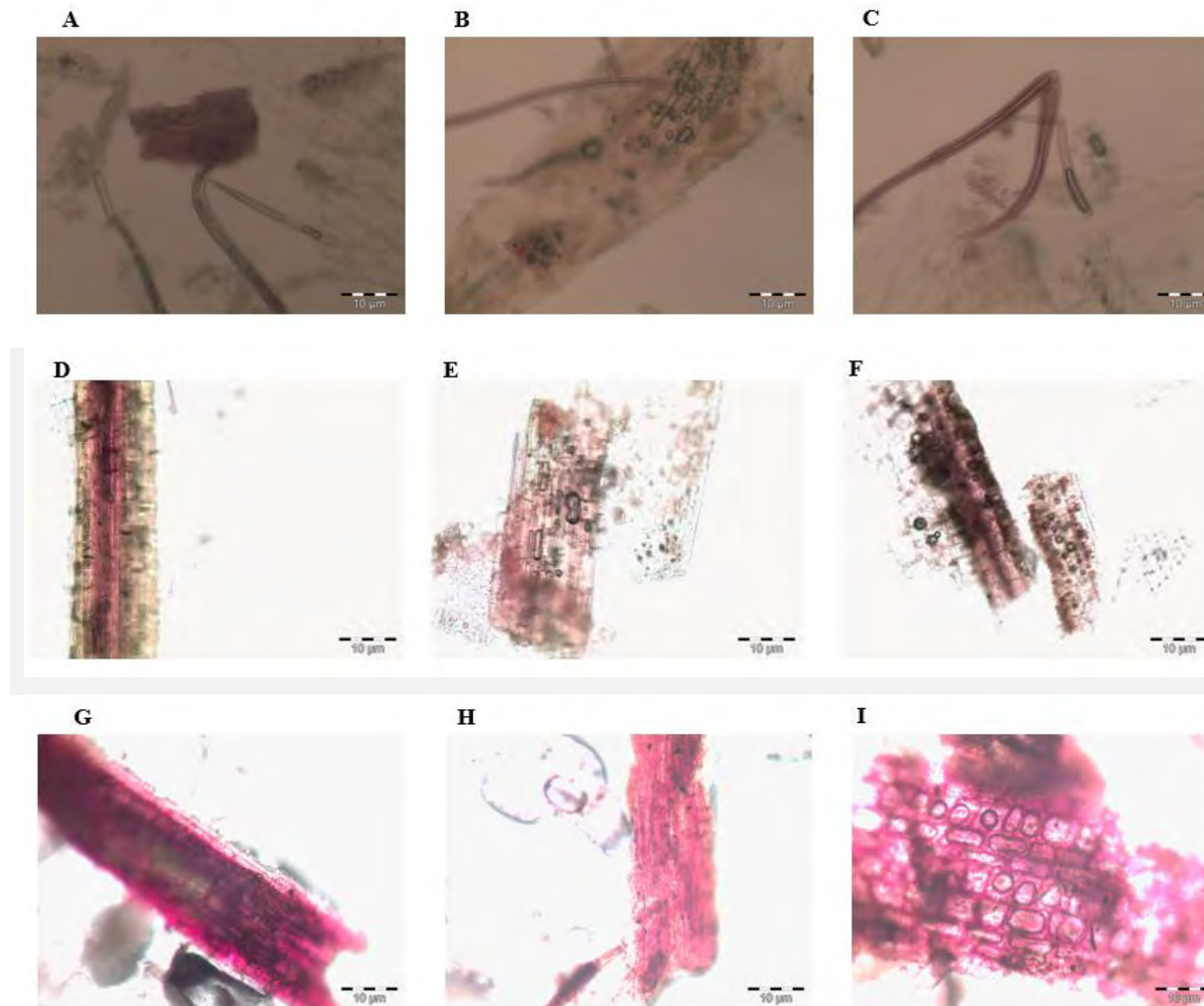


Figure 5.2: Histochemical analysis of lignin in untreated and pre-treated agricultural residues using Wiesner's staining. (A) Untreated, (B) hydrothermal treated, and (C) acid treated CC; (D) untreated, (E) hydrothermal treated, and (F) acid treated RS; (G) untreated, (H) hydrothermal treated, and (I) acid treated SCB.

Figure 5.2 shows Wiesner's staining images of CC, RS and SCB, before and after pre-treatment. All three substrates followed a similar trend, there were no substantial changes in lignin distribution after applying hydrothermal and dilute sulphuric acid pre-treatment methods. This was expected, because when dilute acid and hydrothermal pre-treatments are applied under

mild conditions, they generally lead to partial disruption and structural modifications of lignin but not substantial removal (Cao et al., 2012; Kellock et al., 2019). It has been reported that modification of lignin structure by pre-treatment can enhance enzymatic hydrolysis of biomass even without substantial lignin removal (Yoo et al., 2016).

5.4.3. FTIR analysis of untreated and pre-treated agricultural residues

FTIR spectroscopy is generally used to investigate the chemical changes and the structure of constituents in lignocellulosic biomass after pre-treatment. In this study, FTIR analysis was conducted to get an overall view of chemical modifications after subjecting agricultural residues to two pre-treatment strategies. The FTIR spectra of the untreated agricultural residues, as well as the dilute sulphuric acid and hydrothermally treated solids are displayed in Figure 5.3. The absorption peaks at around the 1730 cm^{-1} region are predominantly attributed to the C=O stretching vibration of the ester linkage of the carboxylic group of FA and *p*-CA of lignin and/or hemicellulose (Gabhane et al., 2015). The FTIR spectra of untreated and pre-treated CC (Figure 5.3A), and SCB (Figure 5.3C) show relatively similar intensities of these peaks around this region, suggesting that changes due to pre-treatment did not solubilise hemicellulose and hydroxycinnamic acids. A slight decrease in the intensity of peaks around the 1730 cm^{-1} region of pre-treated RS samples (Figure 5.3B) was observed. The hydrothermal pre-treated CC sample (Figure 5.3A) displayed strong absorption bands around 1000 cm^{-1} and in the $3500\text{-}3200\text{ cm}^{-1}$ region mainly attributed to β -glycosidic linkages and OH groups of glucose units, respectively (Chandra et al., 2016). These peaks which are associated with the carbohydrate abundance were distinct in all the samples. The FTIR data is in agreement with composition analysis data (Table 5.1), confirming that changes due to pre-treatment (observed in SEM micrographs) did not lead to the removal of hemicellulose and hydroxycinnamic acids. Overall, these results demonstrated that dilute acid and hydrothermal pre-treatment methods modified the structure of these selected agricultural residues and led to the recovery of hemicellulose in the solid fraction.

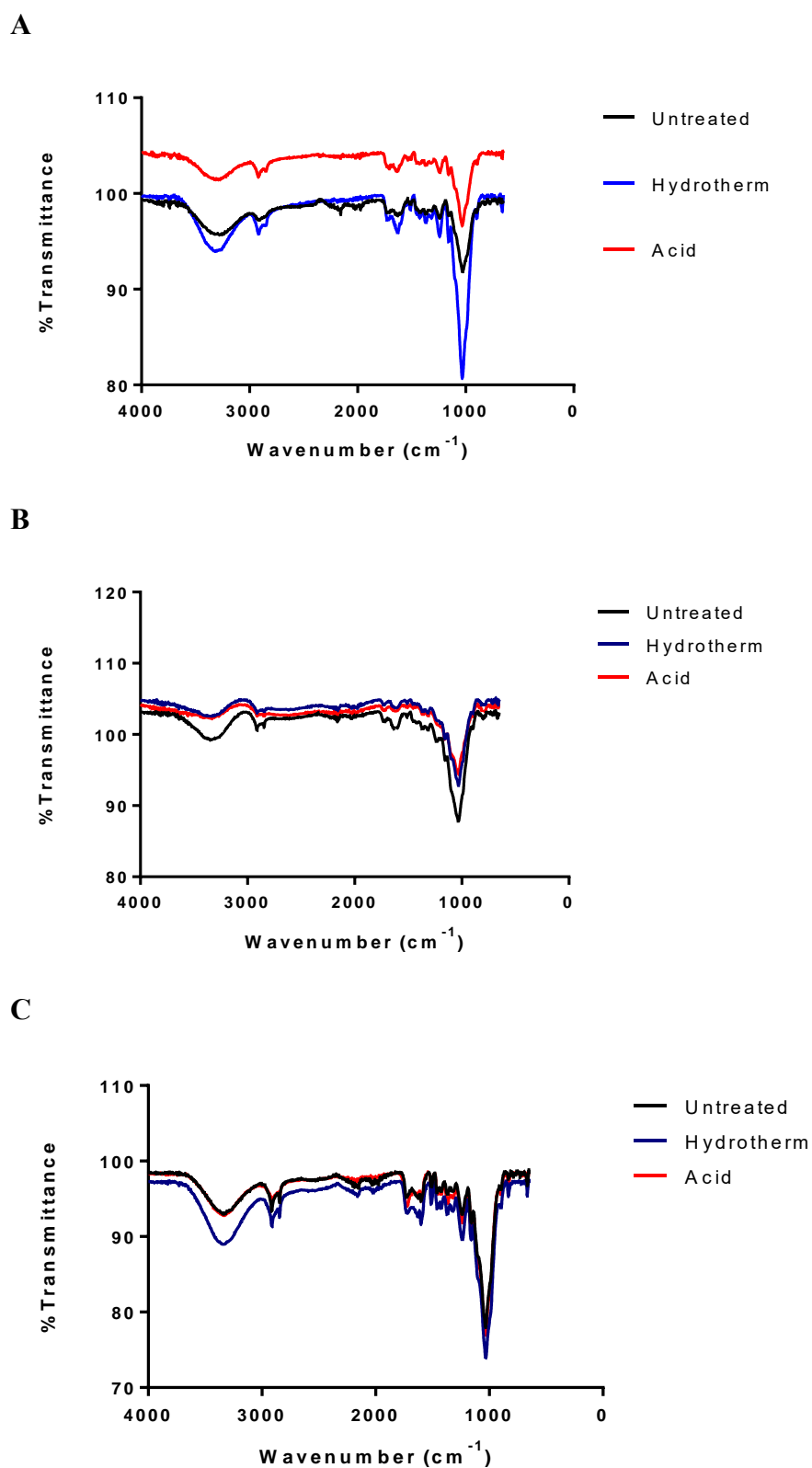


Figure 5.3: FTIR spectra of untreated, hydrothermal treated and acid treated agricultural residues registered in the range of 450-4000 cm⁻¹. (A) CC, (B) RS and (C) SCB.

5.4.4. Determination of water retention capacity of agricultural residues

Biomass-water interactions have been used as an indirect measurement to evaluate biomass recalcitrance. One such techniques is WRC which is defined as a measurement of the amount of water that is retained by the lignocellulosic biomass after the application of centrifugation or negative pressure (Sanchez et al., 2019). An increase in the amount of water retained by biomass has been found to positively correlate with the improved biomass enzymatic digestibility, and therefore suggests reduced biomass recalcitrance (Weiss et al., 2018). In this study, WRC was used as a measure of the effectiveness of the selected pre-treatment methods in increasing enzymatic digestibility of the agricultural residues. The results showing the WRC of untreated and pre-treated agricultural residues are presented in Table 5.2. An increase of about 15% in WRC was observed for hydrothermal and dilute acid pre-treated CC when compared to untreated CC. For RS, the highest WRC measurements were obtained for pre-treated samples when compared to the untreated sample. Hydrothermal and dilute acid pre-treated RS samples resulted in an increase of 23.37% and 43.76%, respectively. On the other hand, hydrothermal pre-treated SCB showed no substantial increase in WRC while a decrease was observed for dilute acid pre-treated SCB. This was quite unexpected because SEM analysis of pre-treated SCB was relatively similar to that of RS and CC (Figure 5.1), and SEM micrographs also showed morphological changes which are usually associated with an increased surface area of biomass. One likely explanation could be that the extremely low pre-treatment severity applied in this study was not as effective for SCB when compared to RS and CC. This might be due to the fact that SCB is known to contain a higher lignin content than RS and CC (Sahare et al., 2012; Sakdaronnarong et al., 2014).

Table 5.2: Water retention capacity (WRC) of agricultural residues

Biomass	WRC (mL/g)		
	Untreated	Hydrothermal	Dilute acid
CC	4.26 ± 0.33	4.88 ± 0.59	4.9 ± 0.38
RS	5.69 ± 0.13	7.02 ± 0.60	8.18 ± 0.13
SCB	7.22 ± 0.79	7.23 ± 0.72	6.34 ± 0.48

The data represent the averages of triplicate determinations ± standard deviations. Corn cob (CC), rice straw (RS) and sugarcane bagasse (SCB).

5.4.5. Inhibitory effect of pre-treatment by-products on FAEs

Dilute acid and hydrothermal pre-treatments represent important methods that can significantly improve the enzymatic digestibility of various pre-treated lignocellulose feedstocks. However, these methods can potentially generate inhibitors which hamper enzymatic hydrolysis of biomass. The concentrations of these inhibitors vary depending on the type and severity of the pre-treatment (Michelin et al., 2016). These inhibitory compounds include multiple phenolics produced by the degradation of lignin, furan derivative degradation products of pentoses and hexoses (furfural and HMF) and weak organic acids (acetic, formic and levulinic acids) (Kim, 2018). The purpose of this section was to evaluate the inhibitory effect of various pre-treatment by-products on FAE5 and FAE6 activities. This was necessary because the FAEs used in this study have never been applied to the bioconversion of lignocellulose biomass.

This study followed two different approaches: firstly, various compounds were selected and the inhibitory effects of each individual model pre-treatment by-product on FAEs was evaluated. The second approach involved generation of wash liquors from pre-treated agricultural residues and evaluating their effects on enzyme activities. The pre-treatment by-products selected for this study were evaluated in the range of expected concentrations resulting from the aqueous pre-treatment of lignocellulosic biomass (Ximenes et al., 2011). The results for inhibitory effects of lignin and its degradation products on the activities of FAEs are presented in Figure 5.4. Lignin and vanillin (Figure 5.4A and B) exhibited a concentration dependent inhibition for both FAE5 and FAE6 - inhibition of activities of FAEs by lignin was observed in the concentration range of 0.5 to 2 mg/mL. In the presence of lignin at a concentration of 0.5 mg/mL, the level of residual activities of FAE5 and FAE6 were 75.2% and 52.5%, respectively. At a higher concentration of lignin, FAE5 and FAE6 could retain about 65.6% and 38.4% of their maximum activities, respectively. Vanillin resulted in a strong inhibitory effect which was more profound at higher concentrations. Unlike lignin, the presence of the lowest concentration of vanillin resulted in decrease in activity of about 33% for FAE5 and 26% for FAE6. The level of inhibition elicited by the highest concentration of vanillin on activities of FAE5 and FAE6 was 95% and 88.4%. There were no significant changes observed in the pH of the reaction (no more than ± 0.5 pH unit variation) - this is an indication that the inhibition was due to the physical interaction between FAEs and the two compounds, rather than due to differences in pH. On the other hand, high concentrations (0.5 to 2 mg/mL) of gallic acid (Figure 5.4C) and vanillic acid (Figure 5.4D) resulted in substantial changes in the pH of the reaction medium, and a complete loss of enzyme activity at concentrations of 1 and 2

mg/mL for gallic acid and 2 mg/mL for vanillic acid, respectively. There is a lack of information on the inhibitory mechanisms of FAEs by lignin degradation products. The non-productive binding of enzymes on lignin is known as the main mechanism involved in lignin-enzyme interactions (Kim et al., 2016; dos Santos et al., 2019). It is likely that this mechanism is also the major route by which FAE5 and FAE6 are inhibited.

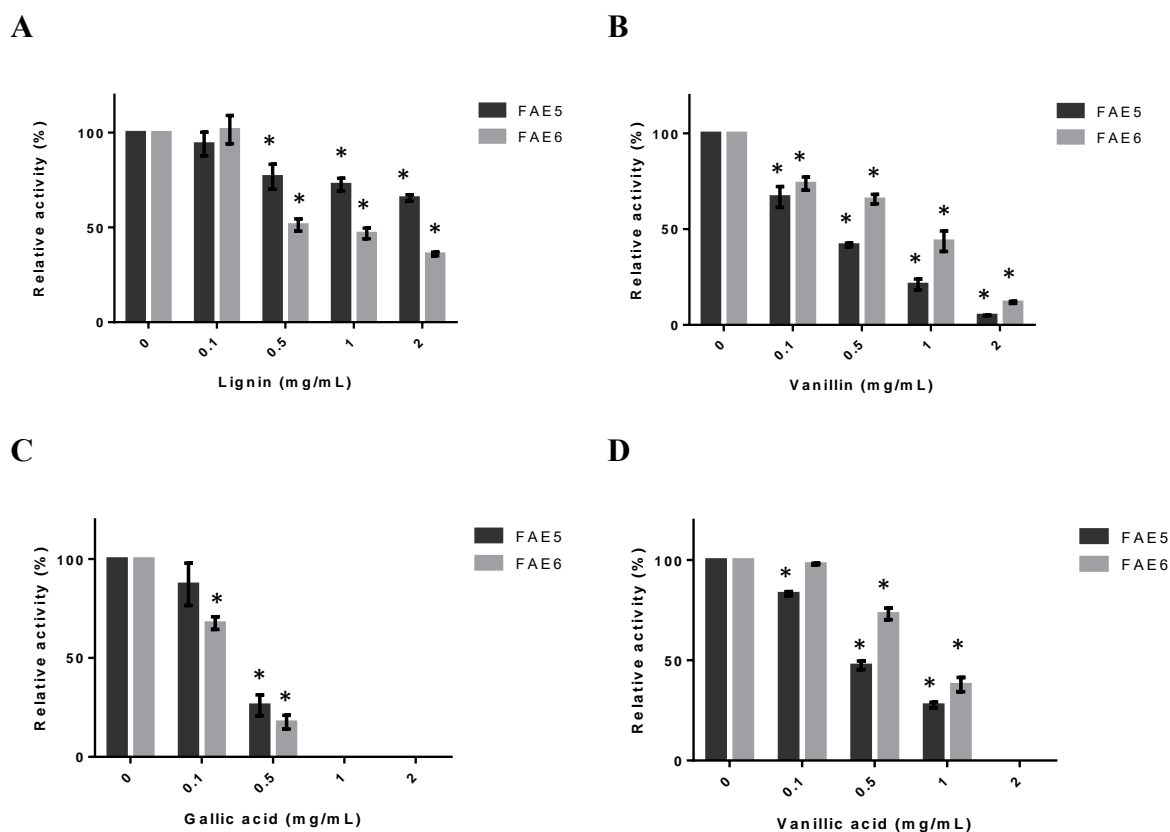


Figure 5.4: Inhibitory effects of lignin and its degradation products on FAE5 and FAE6 activity. (A) Lignin, (B) Vanillin, (C) Gallic acid and (D) Vanillic acid. The concentration of inhibitors varied between 0 and 2 mg/mL. A reaction mixture without inhibitor was assigned as 100% FAE activity. Data points represent the mean values of triplicates and error bars indicate standard deviations. Statistical analysis was conducted using a t-test for inhibition of enzyme activity by lignin degradation products compared to the activity in the absence of degradation products, key: * (p value < 0.05).

Literature with respect to the inhibitory effects of lignin degradation products is mostly available for cellulases and xylanases (Tian et al., 2013; de Souza Moreira et al., 2013; Mhlongo et al., 2015). In terms of the inhibition mechanism, the structural composition of lignin derivatives has been described as a major contributing factor in increasing the level of

inhibition. For example, Boukari et al. (2011) demonstrated that the hydroxyl group was the key structural feature causing inhibition of xylanase from *Thermobacillus xylanilyticus* by phenolics. There was no clear correlation between the number of hydroxyl groups on a compound and the level of enzyme inhibition. Structural insights could be constructive in understanding the interaction between lignin derivatives and FAEs. Next, the inhibitory effect of sugar degradation products on the activities of FAE5 and FAE6 was assessed (Figure 5.5). These studies showed that FAEs were not significantly affected by the presence of furfural (Figure 5.5A) and HMF (Figure 5.5B), even at the highest concentration tested (2 mg/mL).

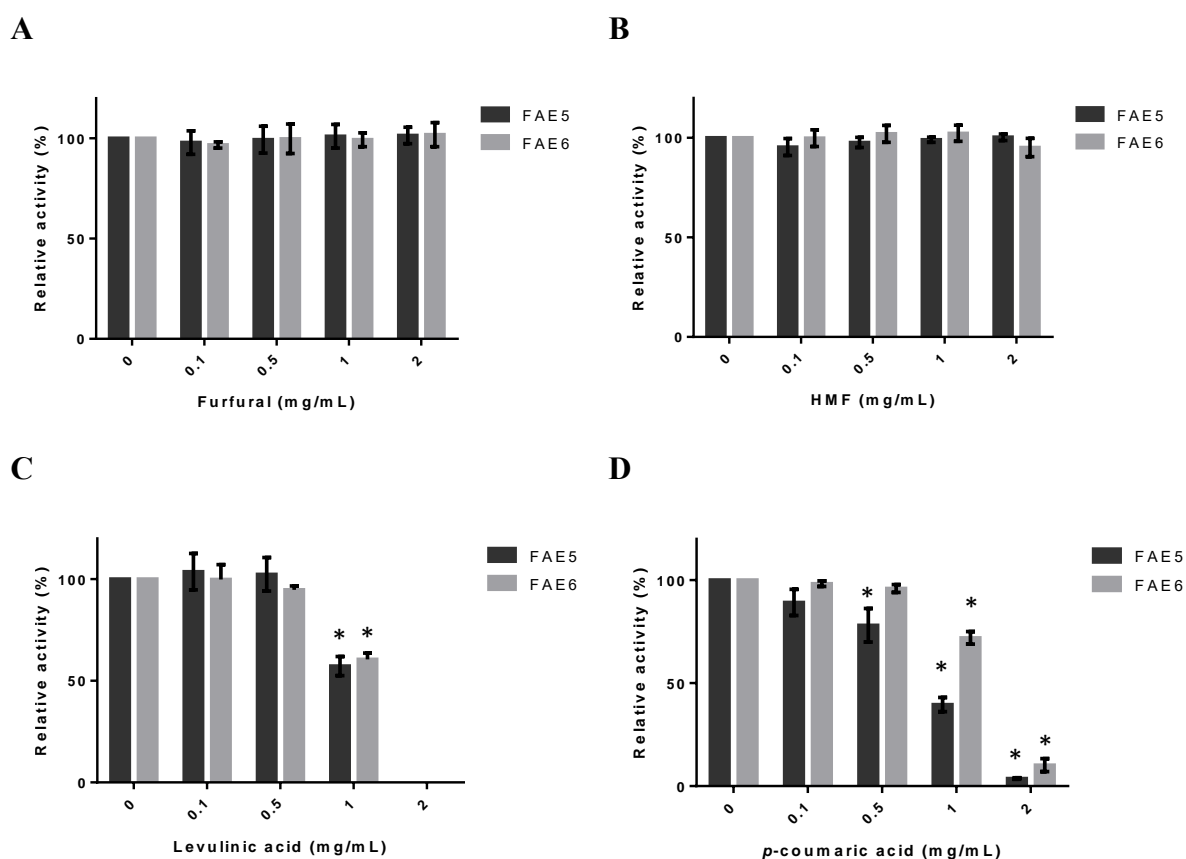


Figure 5.5: Inhibitory effects of sugar degradation products and acids on FAE5 and FAE6 activity. (A) Furfural, (B) HMF, (C) Levulinic acid and (D) *p*-coumaric acid. The concentration of inhibitors ranged between 0 and 2 mg/mL. A reaction mixture without inhibitor was assigned as 100% FAE activity. The results represent the mean value of triplicates and error bars indicate standard deviations. Statistical analysis was conducted using a t-test for the inhibition of enzyme activity by sugar degradation products or acids compared to the activity without addition of degradation products or acids, key: * (p value < 0.05).

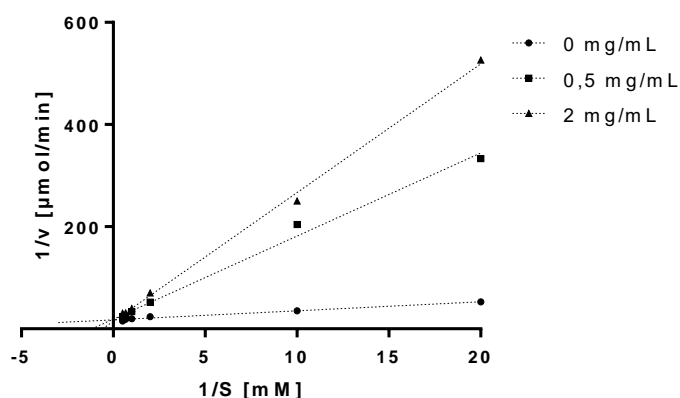
The enzymes also tolerated the presence of levulinic acid in the concentration range of 0.1 to 0.5 mg/mL (Figure 5.5C). Higher concentrations of levulinic acid caused substantial changes in the pH of the reaction medium. Therefore, it is possible that the observed reduction in activity may not be due to compound and enzyme interactions, but rather due to a change in pH. Overall, the results revealed that FAE5 and FAE6 may be susceptible to inhibition by lignin and its degradation products. This inhibition seems to be largely concentration dependent. This implies that pre-treatment methods should be conducted in such a manner that the accumulation of lignin degradation products are limited. It has been reported that non-catalytic proteins, such as bovine serum albumin (BSA), have the potential to minimise the non-specific adsorption of enzymes on lignin (Florescio et al., 2016; Siqueira et al., 2017). The addition of lignin-blocking agents may be a potential strategy to address the adsorption of enzymes onto lignin (Ying et al., 2018). This would enable a more effective use of FAE5 and FAE6 in the degradation of the complex substrate.

5.4.6. Determination of inhibition patterns

Since lignin and vanillin inhibited FAE5 and FAE6 without causing changes in pH - at all concentrations tested, further experiments were conducted to determine the type of inhibition exhibited on FAEs in the presence of these two compounds. The data generated from activity assays were used to prepare Lineweaver-Burk plots in order to determine the type of inhibition exerted by lignin and vanillin; the kinetic parameters calculated from non-linear regression are shown in Tables 5.3 and 5.4. Lignin and vanillin did not inhibit the FAEs competitively - this was expected because of structural differences between these compounds and the substrates of FAEs. Competitive inhibition occurs when the presence of an inhibitor increases the K_M value while the V_{max} remains relatively constant (Maulana Hidayatullah et al., 2020). The effect of competitive inhibition can be completely overcome by increasing the substrate concentration, while other forms of inhibition cannot be overcome in this way. The results presented in Figures 5.6 and 5.7 show that the mode of inhibition displayed by lignin and vanillin is mixed inhibition. This form of inhibition is characterised by a decreasing V_{max} and a fluctuating K_M value (Maulana Hidayatullah et al., 2020). The presence of lignin and vanillin decreased both the V_{max} and K_M values of the FAEs (Tables 5.3 and 5.4). Mixed inhibitors are reported to bind to both the free enzyme and the enzyme-substrate complex with different affinity. In the case of lignin (Table 5.3), the K_M values of FAE5 and FAE6 appeared to be increasing with concentration suggesting that the inhibitor may favour the free enzyme. For vanillin (Table 5.4), the K_M values of FAEs were also higher compared to the reaction without inhibitor,

suggesting that lignin may also favour free enzyme. The presence of both inhibitors drastically decreased the catalytic efficiencies (k_{cat}/K_M) of the FAEs (Tables 5.3 and 5.4). As mentioned previously, studies on the inhibitory effects of lignin and its degradation products (in the literature) are mostly available for cellulases and xylanases. The mechanisms of inhibition by these compounds on FAEs are not fully elucidated. The data obtained from this study demonstrated that lignin and vanillin both inhibited FAEs in a mixed competitive manner, suggesting that these compounds were able to bind to both free enzyme and the enzyme-substrate complex - but with higher affinity for the free enzyme. An understanding of the enzyme kinetics involved will allow the development of improved strategies to reduce the impact of these inhibitors.

A



B

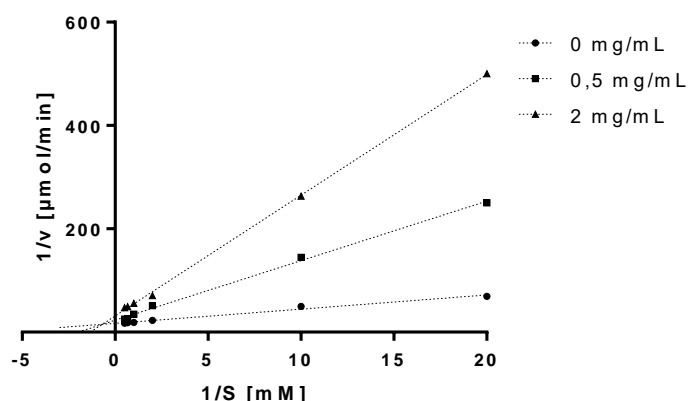
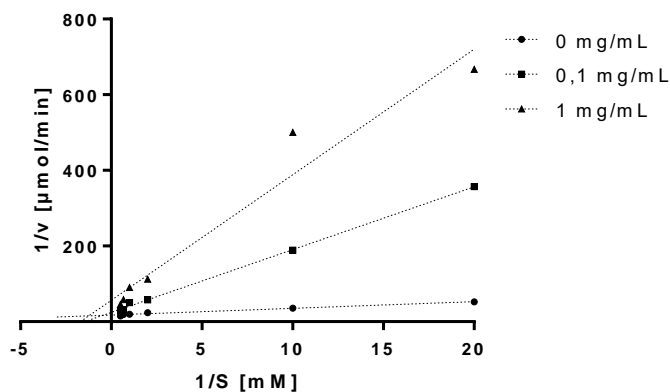


Figure 5.6: Lineweaver-Burk plot of the inhibition of (A) FAE5 and (B) FAE6 activity by lignin. Averages and standard deviations from triplicate experiments are presented.

Table 5.3: Kinetic parameters for FAE5 and FAE6 in the absence/presence of lignin

	Inhibitor (mg/mL)	V_{max} ($\mu\text{mol}/\text{min}$)	K_M (mM)	k_{cat} (s^{-1})	k_{cat}/K_M (mM/s)
FAE5	No inhibitor	0.0603	0.131	2.41	18.41
	Lignin (0.5)	0.0817	1.59	3.27	2.06
	Lignin (2)	0.0565	1.32	2.26	1,71
FAE6	No inhibitor	0.0634	0.205	5.07	24.74
	Lignin (0.5)	0.0616	1.03	4.93	4.78
	Lignin (2)	0.0269	0.496	2.15	4.34

A



B

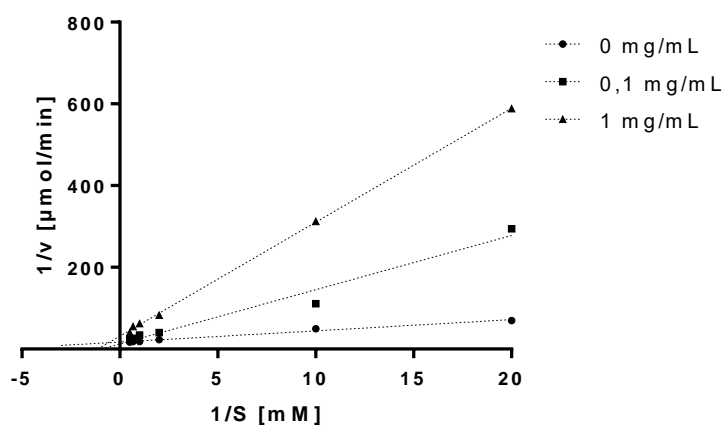


Figure 5.7: Lineweaver-Burk plot of the inhibition of (A) FAE5 and (B) FAE6 activity by vanillin. Averages and standard deviations from triplicate experiments are presented.

Table 5.4: Kinetic parameters for FAE5 and FAE6 in the absence/presence of vanillin

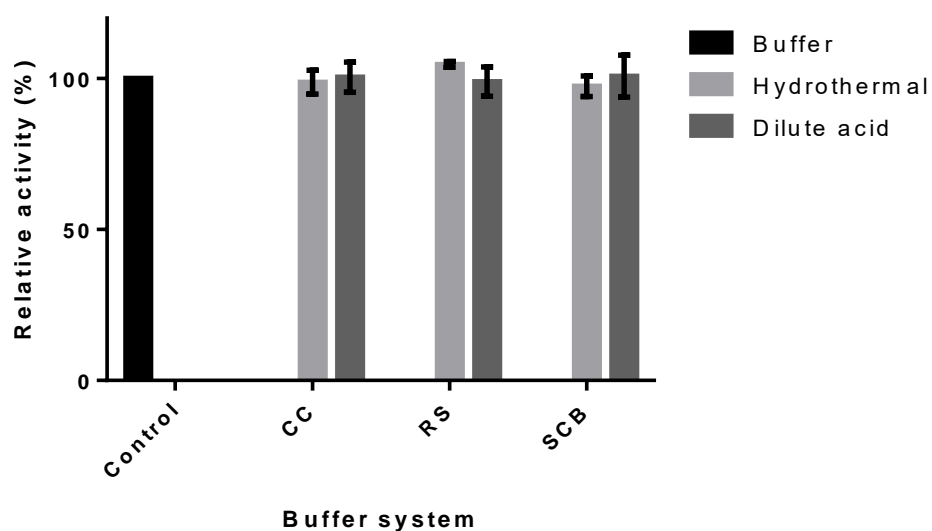
	Inhibitor (mg/mL)	V_{max} ($\mu\text{mol}/\text{min}$)	K_M (mM)	k_{cat} (s^{-1})	k_{cat}/K_M (mM/s)
FAE5	No inhibitor	0.0604	0.131	2.42	18.44
	Vanillin (0.1)	0.0559	1.29	2.27	1.73
	Vanillin (1)	0.0431	2.34	1.72	0.74
FAE6	No inhibitor	0.0653	0.205	5.22	25.48
	Vanillin (0.1)	0.0591	0.790	4.73	5.98
	Vanillin (1)	0.0367	1.29	2.94	2.27

5.4.7. Evaluation of the inhibitory effect of wash liquors from pre-treated substrates on enzyme activities

The results from the pre-treatment by-product inhibition studies demonstrated that lignin and its degradation products have the potential to inhibit the activities of FAE5 and FAE6. This part of the study evaluated the effect of potential pre-treatment by-products (which may have been formed and remained in the solid fraction during pre-treatment step of CC, RS and SCB in section 5.3.2). Wash liquors were generated from substrates that were pre-treated using dilute sulphuric acid and hydrothermal pre-treatment methods (section 5.3.6.3). Wash liquors were used as the buffering medium in the reaction and enzyme activities were compared to when pure phosphate buffer was used. The results are presented in Figures 5.8 and 5.9 for FAEs and xylanases, respectively. The activities of FAE5 (Figure 5.8A) and FAE6 (Figure 5.8B) were not affected by liquors from all pre-treated agricultural residues. On the other hand, a slight increase in the activity was observed for Xyn11 (Figure 5.9A) and XT6 (Figure 5.9B). This trend was more pronounced for XT6 when liquors from CC were used. It is more likely that this is the reflection of long chain XOS (from the pre-treated substrate) hydrolysis rather than an increase in the activities of Xyn11 and XT6 because activity was determined by measuring reducing sugars. In summary, the obtained data indicated that liquors from all pre-treated agricultural residues did not inhibit the activities of the enzymes selected for this study.

These findings suggest that there were no inhibitory pre-treatment by-products generated. It has been reported that the concentrations of inhibitors produced are dependent on the type and severity of pre-treatment (Michelin et al., 2016). An extremely low pre-treatment severity was applied for all substrates in this study; the formation of inhibitory compounds was therefore unlikely. Furthermore, it is well established that some of the inhibitory pre-treatment by-products are water soluble (Kim et al., 2011). Washing the pre-treated solids with water is a well-known strategy that minimises inhibition of enzymes. In this study, all the pre-treated solids were repeatedly washed with water, this may have removed the water-soluble inhibitors if they had been formed. These findings suggest that all the tested enzymes can be applied in the enzymatic hydrolysis of pre-treated agricultural residues selected for this study.

A



B

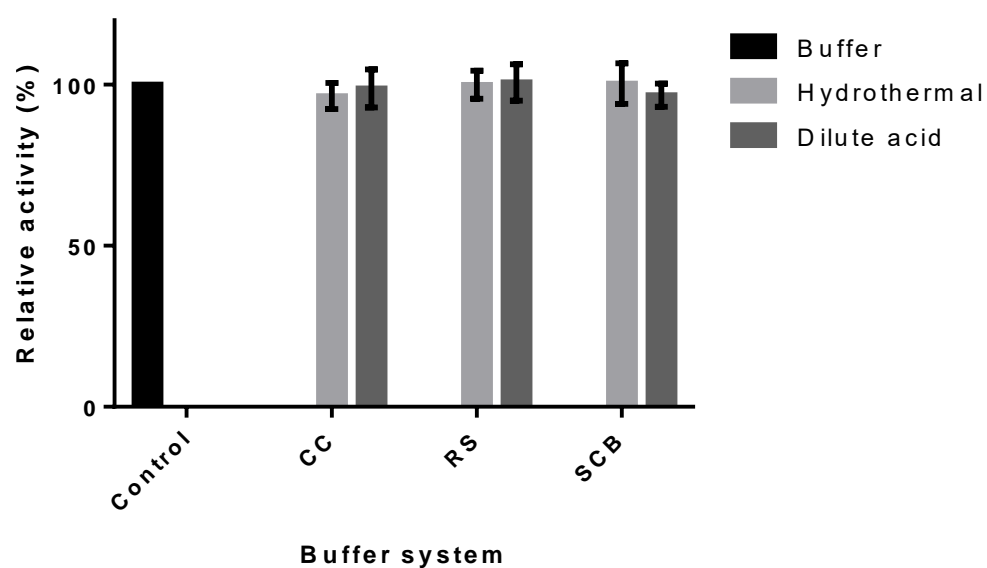
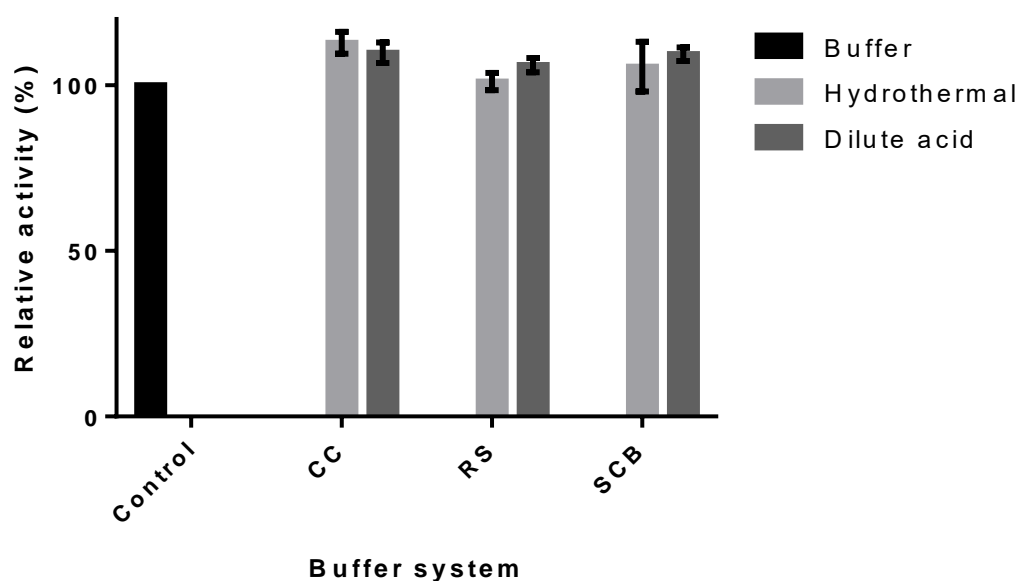


Figure 5.8: Determination of the inhibitory effects of soluble pre-treatment by-products in washes of pre-treated agricultural residues. Enzyme activity assays were conducted for (A) FAE5 and (B) FAE6. Averages and standard deviations from triplicate experiments are presented. Statistical analysis was conducted using a t-test for the inhibition of FAEs in a buffer system of pre-treated substrate wash compared to activity in phosphate buffer, key: * (p value < 0.05).

A



B

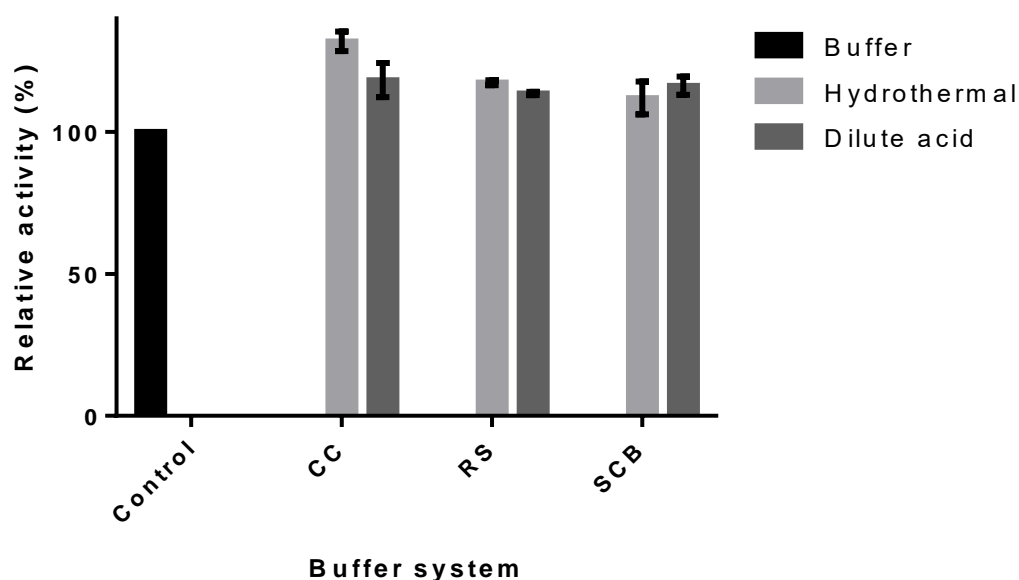


Figure 5.9: Determination of the inhibitory effects of soluble pre-treatment by-products in washes of pre-treated agricultural residues. Enzyme activity assays were conducted for (A) Xyn11 and (B) XT6. Averages and standard deviations from triplicate experiments are presented. Statistical analysis was conducted using a t-test for the inhibition of xylanases in a buffer system of pre-treated substrate wash compared to the activity in phosphate buffer, key: * (p value < 0.05).

5.5. Conclusion

This section of the study focused on the pre-treatment of agricultural residues using dilute sulphuric acid and hydrothermal pre-treatment methods. The inhibitory effect of various pre-treatment by-products on enzyme activities was also explored. In terms of pre-treatment, an extremely low severity method was used to preserve the hemicellulose in the solid fraction, while increasing the accessible area for enzymes. A number of analyses were conducted to investigate the effects of the pre-treatment on the substrates. The results obtained for composition analysis indicated that there was no change in recoverable sugars and that the hydroxycinnamic acid content was maintained in all pre-treated samples. In addition, FTIR data indicated that the presence of bands which are mainly attributed to the hemicellulose component and the intensity of the bands was relatively similar between untreated and pre-treated samples. The morphology of the untreated and pre-treated samples was also investigated. SEM analysis revealed that pre-treated samples had a more disorganised morphology characterised by surface erosion and deconstruction. This impact is directly correlated to the increased surface area and can potentially lead to enhanced enzymatic hydrolysis of the pre-treated substrates. Furthermore, the inhibitory effects of individual pre-treatment by-products on FAEs were investigated. The results indicated that only lignin and its degradation products had a significant impact on FAEs. However, wash liquors generated from the pre-treated samples did not show any inhibitory effect on all the enzymes selected for this study, suggesting that no inhibitory compounds were generated during pre-treatment step. Overall, the findings from this section demonstrated that the selected pre-treatment methods were highly effective, and that the enzymes were suitable for use in the hydrolysis of the pre-treated substrates.

Chapter 6: Evaluation of synergism between feruloyl esterases and xylanases on model substrates and agricultural residues

6.1. Introduction

Lignocellulosic biomass is known to be a significant source of components that can be converted into industrially relevant bio-products. Agricultural residues such as corn cob, wheat bran, rice straw, wheat straw and sugarcane bagasse, are considered cheaper raw materials which can be used to produce VAPs. These high VAPs include hydroxycinnamic acids (*p*-CA and FA) which are generally present in the primary cell walls of commelinid monocots in high concentrations (> 3.5 mg/g biomass) (Oliveira et al., 2019). FA, the most abundant hydroxycinnamic acid, is usually esterified at the C-5 hydroxy group of the arabinofuranosyl units of arabinoxylan. FA and *p*-CA have several commercial applications in the food and pharmaceutical industries. For instance, FA can be used in the food industry as a precursor for vanillin (flavouring agent), *p*-hydroxybenzoic acid and 4-vinylphenol production, and as a food preservative because of its antimicrobial properties (Furuya et al., 2017; Shirai et al., 2017). FA and *p*-CA can be used as therapeutic agents because of their anti-inflammatory, antibacterial, antidiabetic and antioxidant properties (Kumar and Pruthi, 2014; Pei et al., 2016). Agricultural residues have another valuable fraction, namely xylan, which can be transformed through partial degradation to xylooligosaccharides (XOS). Studies have shown that XOS generated from agricultural residues have prebiotic potential and antioxidant activity, making them suitable for applications in the food, feed and pharmaceutical industries (Aachary and Prapulla, 2010; Samanta et al., 2015).

Traditional methods for obtaining these biomass constituents often require a chemical process where an acidic or basic catalyst is used. For example, hydroxycinnamic acid extraction can be facilitated by alkaline hydrolysis, but this treatment may also release other phenolics, proteins and sugars which necessitate further purification steps (Liu, L. Y. et al., 2016). It has been reported that use of harsh conditions for the chemical preparation of XOS can lead to increased depolymerisation of XOS to xylose (Samanta et al., 2015). This is a major disadvantage of chemical treatment because, for prebiotic function, XOS with 2-4 xylose units are preferred. In general, enzymatic conversion is considered more environmentally friendly than chemical methods and is also more specific, as it releases only certain compounds without affecting other valuable chemicals. An integrated process where a mild pre-treatment method is combined

with enzymatic hydrolysis is also an attractive strategy for XOS production, and much progress has been made in this regard using agricultural residues (Poletto et al., 2020).

The major obstacle to the efficient enzymatic release of hydroxycinnamic acids and XOS from agricultural residues is the complex structure of hemicellulose. Studies have shown that the efficient release of these valuable biomass constituents requires enzymatic cocktails composed of several enzymes that synergistically deconstruct the complex biomass (Van Dyk and Pletschke, 2012). Xylanases and FAEs are key enzymes for the degradation of xylan, the most abundant hemicellulose. Xylanases facilitate the endo-catalytic hydrolysis of β -1,4 glycosidic bonds from the xylan backbone chain, releasing XOS of varying DP (Paës et al., 2012). FAEs catalyse the cleavage of ester-linkages between the polysaccharides and hydroxycinnamic acids (Faulds, 2010).

The majority of studies have demonstrated strong synergistic interactions between xylanases and FAEs, which result in the efficient co-production of hydroxycinnamic acids and XOS (Malgas et al., 2019). It is suggested that xylanases cleave the xylan main-chain and generate short feruloylated XOS which are the preferred substrates of FAEs for the release of FA or *p*-CA. On the other hand, the action of FAEs makes short XOS to be more accessible for further hydrolysis by xylanases through the removal of sterically hindering side-chains (Oliveira et al., 2019). Several studies have investigated the cooperation of FAEs and xylanases for the production of FA and XOS from a variety of agricultural residues, such as wheat bran, corn stalks, corn cobs and sugarcane bagasse (Wu et al., 2017; Long et al., 2018; Zhang et al., 2015; Oliveira et al., 2016). However, some of the studies have reported limited hydrolysis efficiency due to low enzymatic activities. Therefore, identifying and characterising novel FAEs with appealing biotechnological characteristics and using them for the formulation of efficient enzymatic cocktails remains an attractive field of research.

In this study, synergistic interactions between two novel termite metagenome-derived FAEs (FAE5 and FAE6) and commercially available xylanases (Xyn11 and XT6) for the co-production of hydroxycinnamic acids and XOS was investigated. These enzyme cocktails were optimised on insoluble wheat arabinoxylan (a model substrate) and then applied to untreated and pre-treated corn cobs, rice straw and sugarcane bagasse (complex substrates).

6.2. Aims and objectives

6.2.1. Aims

To investigate the synergistic associations between the recombinant FAEs and commercial xylanases during their action on model substrates, untreated and pre-treated agricultural residues for the optimal production of XOS and hydroxycinnamic acids.

6.2.2. Objectives

To achieve this aim, the following objectives were set:

- To evaluate the synergistic interactions between xylanases and FAEs during their activity on model substrates in order to establish an optimal xylanase to FAE protein loading ratio for efficient XOS and hydroxycinnamic acid release;
- To evaluate the performance of the optimised xylanase-FAE cocktails on untreated and pre-treated agricultural residues;
- To determine the mode of interaction between xylanases and FAEs through mapping of the hydrolysis product patterns on substrates.

6.3. Materials and methods

6.3.1 Materials

Xylobiose, xylotriose, xylotetraose, xylopentaose and xylohexaose were all purchased from Megazyme™ (Bray, Ireland).

6.3.2. Synergy studies on model substrates

To evaluate synergism between FAEs and xylanases, enzyme combinations were tested on 0.5% (w/v) oat-spelt xylan (OSX) and insoluble wheat arabinoxylan (WAX) for their ability to release FA and reducing sugars. Enzymes were first used in different combinations to determine the optimal xylanase to FAE protein loading ratio. This was carried out using two strategies. In the first strategy, FAE supplementation, varying amounts of FAE (0 to 0.0125 mg) were supplemented to a fixed amount of xylanase (0.0125 mg). In the second strategy, xylanase supplementation, varying amounts of xylanase (0 to 0.0125 mg) were supplemented to a fixed amount of FAE (0.0125 mg). Finally, the ratios that resulted in the highest product release were used to formulate a fixed total protein loading. Once the optimal enzyme combination was established, the total protein loading was adjusted to 4 mg per g of substrate. The optimum xylanase to FAE protein loading ratio was then used for all subsequent synergy

studies. All hydrolysis experiments were carried out in triplicate in 50 mM sodium phosphate buffer (pH 7.4) in a 400 μ L total volume at 40°C, agitating at 25 rpm for 24 hours. Substrate and enzyme controls were run at the same time by incubating the substrates without enzymes and by incubating the enzymes without substrates (replacing the removed enzyme/substrate with buffer). The amount of FA released was determined using the HPLC method described in section 4.3.2.1 and the amount of reducing sugars released was determined as described in section 4.3.3.

6.3.3. Synergy studies on untreated and pre-treated agricultural residues

The protein loadings for all single enzymes and combinations were kept at a total protein loading of 8 mg per g of substrate. For combination experiments, an enzyme mixture consisting of xylanase and FAE at 66:33% protein ratio was used. The enzymatic hydrolysis was performed at 1% (w/v) substrate loading in 50 mM phosphate buffer (pH 7.4) in a 400 μ L total volume. The reaction buffer contained 1 mg/mL of BSA to prevent non-specific adsorption of enzymes to lignin. The reaction mixture was incubated at 40°C with agitation at 25 rpm for 24 hours and the reaction was terminated by boiling at 100°C for 5 minutes. Hydrolysis controls included reactions without the addition of either enzyme or substrate (replacing the removed component with an equal amount of buffer). All the experiments were performed in triplicate. The amount of FA and *p*-CA released was determined using the HPLC method described in section 4.3.2.1 and the HPLC-MS/MS method described in section 6.3.4, reducing sugars were measured using a DNS method (section 4.3.3) and XOS were quantified using the HPLC-RID method described in section 6.3.6.

6.3.4. Detection of hydroxycinnamic acids by HPLC-MS/MS

For the detection of hydroxycinnamic acids, analysis was carried out using a HPLC-MS/MS system with a Dionex UHPLC (Thermo Fisher Scientific, Sunnyvale, USA). Chromatographic separation was performed on a Kinetex polar C-18 column (3.0 \times 100 mm, 2.6 μ m; Phenomenex, Torrance, USA). The flow rate was 0.3 mL/min, and the following gradient composed of (A) water with 0.1% formic acid and (B) acetonitrile with 0.1% formic acid was used: 0-12 minutes 80% of A and 20% B; 12-18 minutes 60% of A and 40% of B. The injection volume was 5 μ L. The MS/MS analysis was conducted on a Bruker Compact QToF mass spectrometer using an electrospray ionization probe (Bruker, Bremen, Germany). Negative mode MS was used, and precursor ions were selected for the acquisition of m/z spectra at collision energies of 20 eV in data-dependent acquisition mode. The data files were converted

to mzXML format using Bruker Compass software (Bruker, Bremen, Germany). Further data analysis was carried out in MZmine 2 (ver. 2.34).

6.3.5. Determination of xylo-oligosaccharides pattern profiles

The hydrolysis product profiles from synergy studies were determined by analysing XOS on thin-layer chromatography (TLC). A volume of 5 μ L of hydrolysate sample and a mixture of XOS standards were applied onto a silica gel plate (MERCK, Darmstadt, Germany). The migration was repeated twice using a mobile phase consisting of 1-butanol, acetic acid and water in a 2:1:1 ratio. The plate was then submerged in Molisch's Reagent (0.3% (w/v) α -naphthol dissolved in methanol and sulphuric acid in a 95:5 ratio (v/v) respectively). The spots corresponding to the different XOS were visualized by heating the plate in an oven at 110°C for 10 minutes.

6.3.6. Quantification of xylo-oligosaccharides

Quantification of XOS was performed on a Shimadzu HPLC system (Shimadzu Corp, Kyoto, Japan) equipped with a refractive index detector (RID) using a CarboSep CHO 411 column (Concise Separations, San Jose, USA) with water as the mobile phase in isocratic mode. The column oven was set at 80°C and separation was performed within 35 minutes at a flow rate of 0.3 mL per minute. An injection volume of 20 μ L was used for all samples and XOS standards (xylohexaose, xylopentaose, xylotetraose, xylotriose and xylobiose) (see Appendix Figure C.1.1).

6.3.7. Statistical analysis

All comparisons on product release due to single enzyme versus enzyme combination were performed on GraphPad Prism 6.0 software using the t test. A *p* value less than 0.05 was considered to illustrate statistical significance between compared data sets.

6.4. Results and discussion

6.4.1. Evaluation of synergism between FAEs and xylanases on model substrates

Effective enzymatic hydrolysis of the hemicellulose fraction of lignocellulosic biomass into VAPs has been shown to require a combination of various enzymes, including glycoside hydrolases and auxiliary activity enzymes such as FAEs (Andlar et al., 2018). These enzymes usually act synergistically during the degradation of their substrates and their combined action is believed to be greater than the sum of the actions of the individual enzymes (Visser et al.,

2013). Furthermore, the synergistic enzyme interactions lead to relatively low enzyme loadings which make the enzymatic hydrolysis process more cost effective. Several studies have reported that xylanases exhibit strong synergistic relationship with FAEs for the degradation of various agricultural residues. This cooperation is demonstrated by improved yields in the production of value-added chemicals such as XOS and hydroxycinnamic acids (Malgas et al., 2019). The present study was designed to evaluate the synergism between novel metagenome-derived FAEs and commercially available xylanases during the degradation of untreated and pre-treated agricultural residues.

In order to evaluate the synergism between FAEs and xylanases on agricultural (complex substrates), the enzymes were tested on WAX and OSX (model substrates) for their ability to release FA and XOS. Firstly, the total amount of FA in the model substrates was determined by alkaline extraction. This is a well-known method used to recover hydroxycinnamic acids from lignocellulosic biomass. The FA content of the liquor from WAX alkaline hydrolysis was found to be $81.16 \pm 3.22 \mu\text{g/mL}$. On the other hand, the presence of FA was not detected in the liquor of OSX. It is likely that these differences in FA content are due to the methods utilised to extract and purify WAX and OSX. WAX is usually extracted in such a way that the FA cross-links in native arabinoxylan are maintained. The alkaline hydrolysis results suggest that WAX is a better substrate than OSX for FA release. The subsequent optimisation study was therefore carried out using only WAX.

The first batch of assays were performed in order to identify potential synergistic interactions between the purified recombinant FAEs and commercial xylanases. The initial approach was to determine if the individual enzymes were capable of releasing FA on their own. It was observed that FAEs or xylanases alone could not release FA from WAX. The data indicated that both FAEs could release FA only in the presence of xylanases. This was the first hint of a significant synergistic effect occurring between recombinant FAEs and xylanases in generating FA from WAX. The optimal xylanase to FAE protein loading ratio was then determined and this was performed by using FAE6 and Xyn11. The data presented in Figure 6.1 demonstrates the maximal amount of FA was released from 0.5 % (w/v) WAX with increasing dosage of Xyn11 or FAE6. It appeared as if, when the amount of Xyn11 was fixed at 0.0125 mg, the amount of FAE6 required to achieve 100% FA release was 0.00625 mg, and a further increase in FAE6 loading beyond this point did not result in a significant improvement in product release. This observation was an indication of strong synergistic interactions occurring between FAE6 and Xyn11, rather than an additive effect. When the FAE6 loading was fixed at 0.0125

mg, the amount of FA released increased with increasing Xyn11 loading and reached a plateau at a protein loading of 0.0125 mg. This was expected as FAEs were shown to release FA from WAX only in the presence of xylanases. It appears as if xylanases may generate feruloylated short chained XOS but not free FA. FAEs appeared to act on these feruloylated short chain XOS leading to the generation of FA. Overall, the maximum amount of FA was released with an enzyme combination consisting of Xyn11 and FAE6 in a 66:33% protein mass ratio. This optimised protein loading ratio was then used in all subsequent synergy studies.

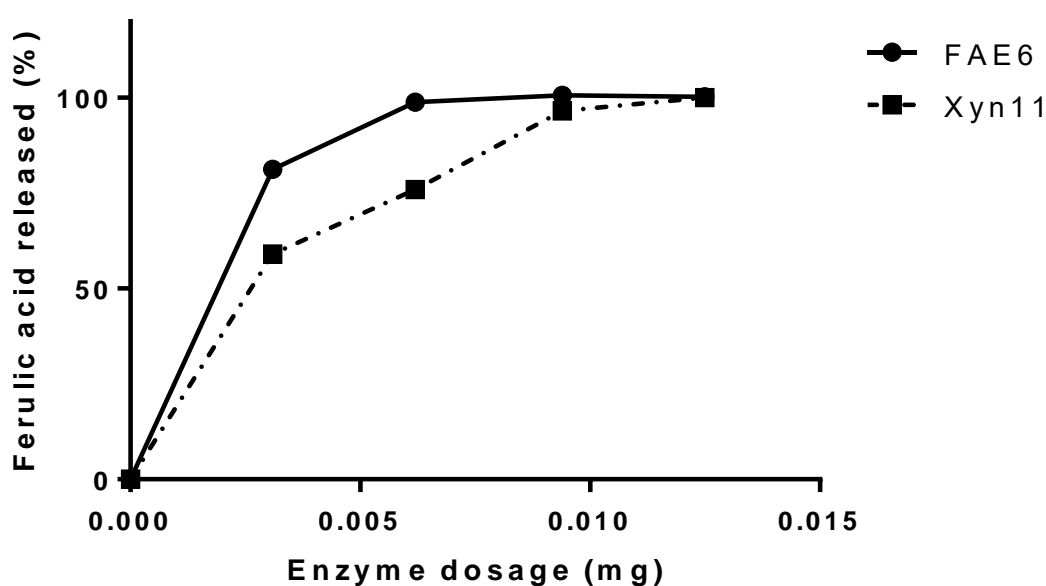
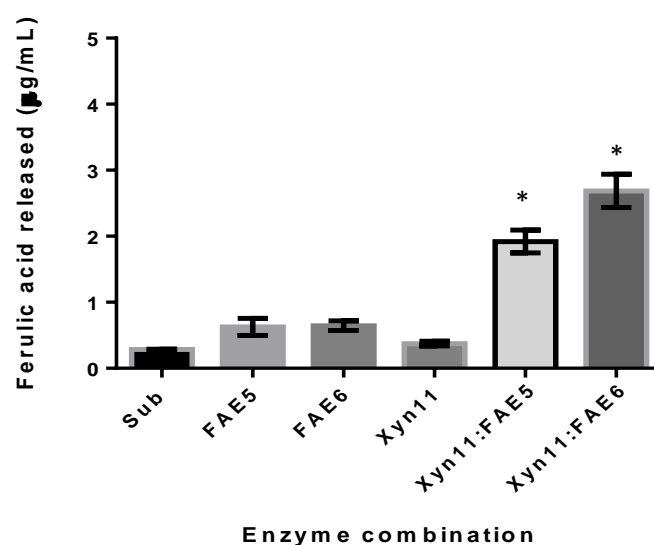


Figure 6.1: Release of ferulic acid from 0.5% (w/v) WAX at increasing enzyme doses of FAE6 or Xyn11. The amount of ferulic acid released was expressed as a percentage of the highest amount released. Solid line: release of ferulic acid at increasing FAE6 doses with a fixed amount Xyn11 (0.0125 mg); dashed line: increasing Xyn11 doses with a fixed amount FAE6 (0.0125 mg). Each data point represents the average \pm standard deviation of triplicate assays.

It has been reported that the synergistic effect of xylanases is influenced by a number of factors such as the type and degree of branching of the xylan backbone, physical properties of the substrate (solubility, particle size) and the enzymes' ability to withstand the heterogeneous nature of xylan (Wong et al., 2013). It has also been established that the two major families of xylanases, namely GH10 and GH11, show considerable differences in their mechanism of action in heteroxylan degradation. To better understand the synergistic effect of xylanases for

the release of FA, XT6 (GH10) and Xyn11 (GH11) were used to formulate xylanase-FAE enzyme cocktails. The optimised protein loading ratio of 66% xylanase to 33% FAE was used for all enzyme combination studies. Figure 6.2 shows the release of FA after enzymatic hydrolysis of 0.5% (w/v) WAX by single enzyme or a combination of the enzymes. It can be seen that there was no substantial release of FA by any single enzyme in any of the experiments. This was expected for xylanases, because previous substrate specificity (specific activity) data indicated that they could not act on the FAE substrate, EFA. When Xyn11 was added with FAE5 or FAE6, the enzymatic release of FA was substantially increased (Figure 6.2A). The amount of product released by the combination of Xyn11 and FAE5 or FAE6 was found to be 1.92 $\mu\text{g}/\text{mL}$ and 2.68 $\mu\text{g}/\text{mL}$, respectively. On the other hand, a significant change in the release of FA was observed when XT6 was combined with FAE5 or FAE6 (Figure 6.2B). It was found that co-incubation of XT6 with FAE5 or FAE6 resulted in the release of 16.96 $\mu\text{g}/\text{mL}$ and 5.05 $\mu\text{g}/\text{mL}$ of FA, respectively. It was apparent that the amounts of FA released by the synergistic action of XT6 with the FAEs were much higher compared to that when Xyn11 was used in the enzyme combinations. Similar observations have been reported where the synergistic action of a GH10 xylanase with FAE showed a much greater benefit in the release of FA, compared to when a GH11 xylanase was used (Wong et al., 2013).

A



B

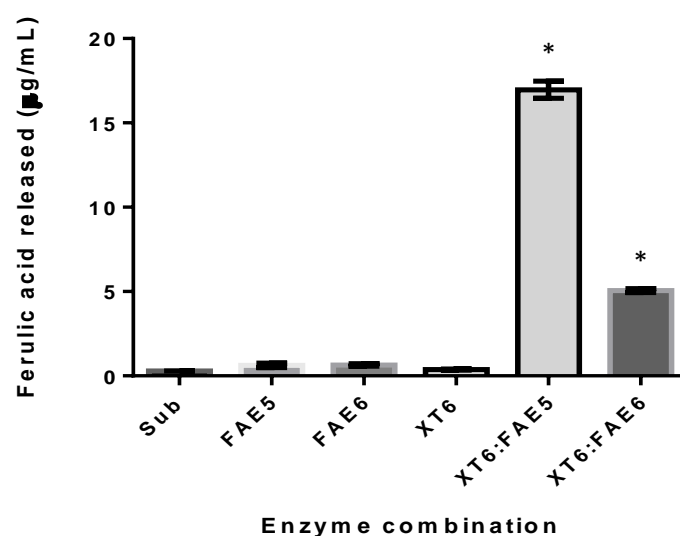


Figure 6.2: Release of ferulic acid during the degradation of 0.5% (w/v) WAX by individual enzymes or a combination of 66% xylanase: 33% FAE5 or FAE6. (A) Synergy studies for Xyn11 and FAEs. (B) Synergy studies for XT6 and FAEs. “Sub” represents substrate control. Each data point represents the average of triplicates \pm standard deviation. Statistical analysis was conducted using a t-test for improvement of ferulic acid release by the enzyme combinations compared to single enzyme (FAE5/6), key: * (p value < 0.05).

One possible explanation for the observed wide variation in FA release could be the differences in structural arrangement of the feruloylated XOS produced by these two different families of xylanases. The varying structural arrangement of the feruloylated XOS might affect the ability of FAE5 and FAE6 to cleave the ester-linkages between XOS and FA. It has been reported that for GH11 xylanases to attack the xylan main chain, three consecutive unsubstituted xylose monomers are required (Mathew et al., 2018; Linares-Pasten et al., 2018). Side-chain decorations on the xylan backbone are generally less well tolerated by GH11 xylanases. Therefore, it is likely that the enzymatic hydrolysis of WAX by Xyn11 resulted in a lower yield of feruloylated XOS, because of the inability of the GH11 xylanases to tolerate a substituted xylan backbone, resulting in the production of mostly unsubstituted XOS. Consequently, FAE5 and FAE6 would have a limited number of substrate molecules for the cleavage of ester-linkages, limiting the amount of FA released from WAX. In contrast, two consecutive unsubstituted xylose monomers are required for the GH10 xylanases to attack the xylan main chain (Mathew et al., 2018). Side-chain decorations of the xylan backbone are not a major hindrance for GH10 xylanases. It is possible that XT6 generated a high amount of feruloylated XOS because of the ability of GH10 xylanases to accommodate binding of xylan with side-chain decorations. Therefore, FAE5 and FAE6 would have a higher number of substrate molecules available for the potential cleavage of ester-linkages, resulting in a higher yield of released FA.

Significant differences were also observed in the amount of FA released by a combination of XT6-FAE5 and XT6-FAE6. The enzyme combination of XT6-FAE5 displayed a synergistic effect which was significantly greater than that of XT6-FAE6 (3.36-fold). This was not expected, as these two enzymes displayed relatively similar specific activities on the synthetic FAE substrate (shown in Chapter 4). There are several possible explanations for the differences observed in the synergistic effect of FAE5 and FAE6 with XT6. As mentioned earlier, GH10 xylanases are capable of accommodating binding of xylan with side-chain decorations, and they generally produce shorter XOS than GH11 xylanases. Therefore, it is likely that FAE5 is more efficient in cleaving ester-linkages from shorter feruloylated XOS compared to FAE6. Another factor which could have influenced the interaction of FAE5 and FAE6 with the feruloylated XOS might be the differences in molecular masses of these enzymes. Although the exact mechanisms behind this observation have yet to be resolved, it is likely that FAE5 and FAE6 might display varying preferences for feruloylated XOS. Further investigations will be required to understand precisely why FAE5 and FAE6 respond differently towards

feruloylated XOS generated from WAX. Overall, the data obtained demonstrated that purified recombinant FAE5 and FAE6 could release substantial amounts of FA from WAX only in the presence of Xyn11 or XT6. Furthermore, the GH10 xylanase (XT6) displayed a strong synergistic effect with FAEs compared to GH11 xylanase (Xyn11).

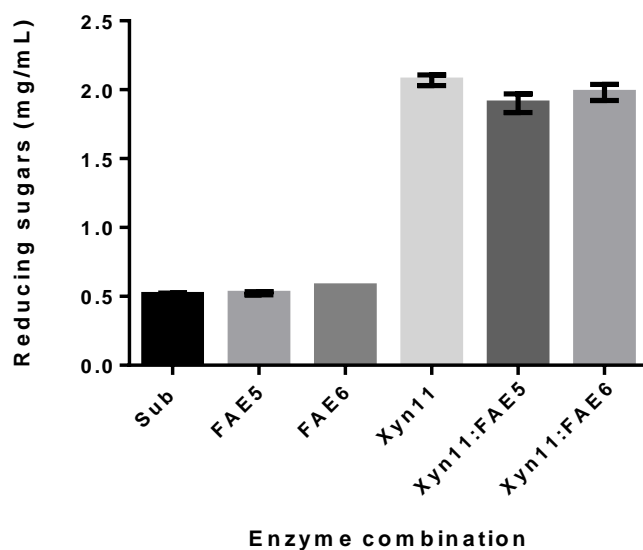
6.4.2. HPLC-MS/MS confirmation of FA released from WAX

The enzymatic release of FA from 0.5% (w/v) WAX - previously detected by the HPLC method - was confirmed by HPLC-MS/MS. The results obtained exhibited similar trends for all enzyme combinations. The extracted-ion chromatogram (XIC) and mass spectrum of FA released from WAX are shown in Figure 6.3 below. The HPLC-MS/MS data shows the enzymatic release of FA when the 66% Xyn11 and 33% FAE6 enzyme combination was used. The analysis was carried out with negative ionisation because FA can lose a proton to yield negative ions [M-H]⁻. The XIC and mass spectra obtained from the enzymatic hydrolysis samples were compared with the FA standard. The XIC displayed a peak with a retention time of 5.01 minutes (Figure 6.3A) and this corresponded to the retention time of the FA standard. The peak observed in the XIC had a specific ion *m/z* corresponding to that of the deprotonated FA ion (*m/z* = 193.06). From this ion, the fragmentation pattern was suggested considering the data obtained from MS/MS (Figure 6.3B). The MS/MS of the FA standard exhibited three major ions with *m/z*: 178.03, 149.06 and 134.06. It has been reported that in FA fragmentation, the first cleavage occurs by elimination of CH₃ to form *m/z* = 178, followed by the loss of CO₂ to form *m/z* = 134 ion, with the initial loss of CO₂ to form *m/z* = 149 ion shown to be thermodynamically unfavourable (Sinosaki et al., 2020). The fragmentation pattern of FA released from WAX in Figure 6.3B resulted in the formation of a fragment *m/z* = 134.06 which was consistent with data obtained for the standards. The fragmentation profile reported in this work confirmed that the compound released during the synergistic enzymatic hydrolysis of WAX was indeed FA.

6.4.3. Release of XOS from model substrates by enzymatic hydrolysis

In order to gain a deeper understanding of the synergistic interactions between xylanases and FAEs observed above, the production of XOS from model substrates was also studied. Based on their ability to release FA from feruloylated XOS, it was predicted that FAE5 and FAE6 would have a boosting effect on xylanase activity. To test this prediction, single enzymes and enzyme combinations were tested for their ability to generate XOS from oats spelt xylan (OSX) (Figure 6.4) and WAX (Figure 6.5). The XOS released from selected substrates were measured using the reducing sugar assay. The action of FAE5 and FAE6 on these substrates was assayed (without the addition of xylanases) and could not generate XOS – this was expected. The synergistic effects of FAE5 and FAE6 on the activities of Xyn11 and XT6 were investigated using the optimised protein loading ratio of 66% xylanase: 33% FAE. When using OSX as a substrate, the enzyme combinations did not increase the total amount of reducing sugars released compared to the reaction mixture containing only the single enzymes Xyn11 or XT6 (Figure 6.4). This was expected, because analysis of the liquor from alkaline hydrolysis indicated that OXS did not contain any feruloyl decorations. When enzymes were tested on WAX, both FAEs displayed synergism with Xyn11 by improving the release of reducing sugars (Figure 6.5A).

A



B

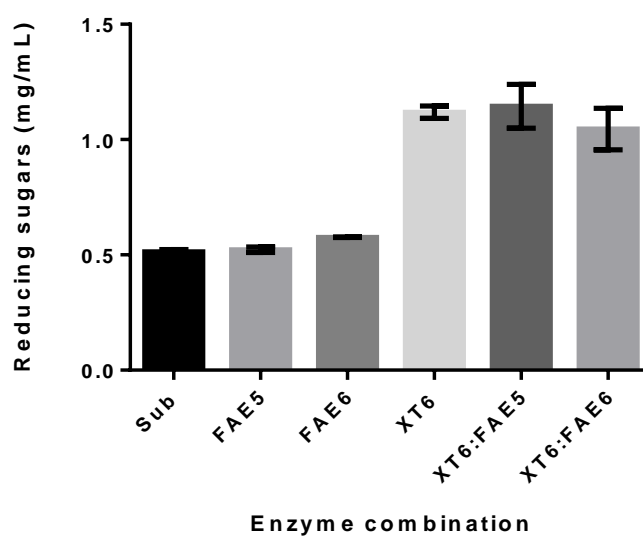


Figure 6.4: Release of reducing sugars during hydrolysis of 0.5% (w/v) oat-spelt xylan (OSX) by individual enzymes or a combination of 66% xylanase: 33% FAE5 or FAE6. (A) Synergy studies for Xyn11 and FAEs. (B) Synergy studies for XT6 and FAEs. “Sub” represents substrate control. Each data point represents the average of triplicates \pm standard deviation. Statistical analysis was conducted using a t-test for improvement of hydrolysis with respect to reducing sugar by the enzyme combinations compared to single enzyme (xylanase), key: * (p value < 0.05).

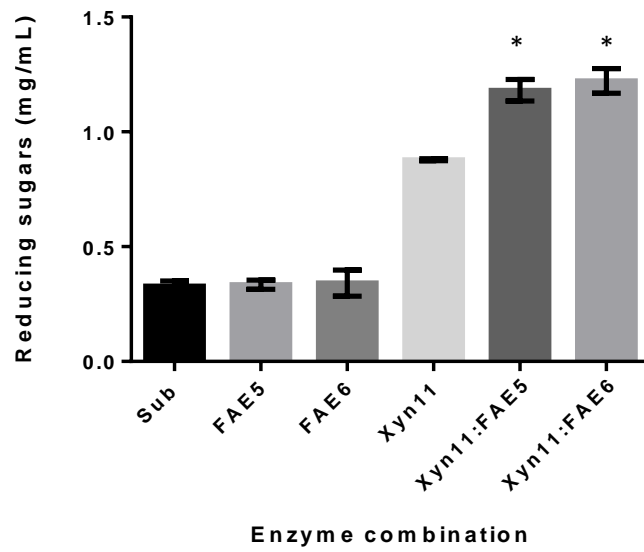
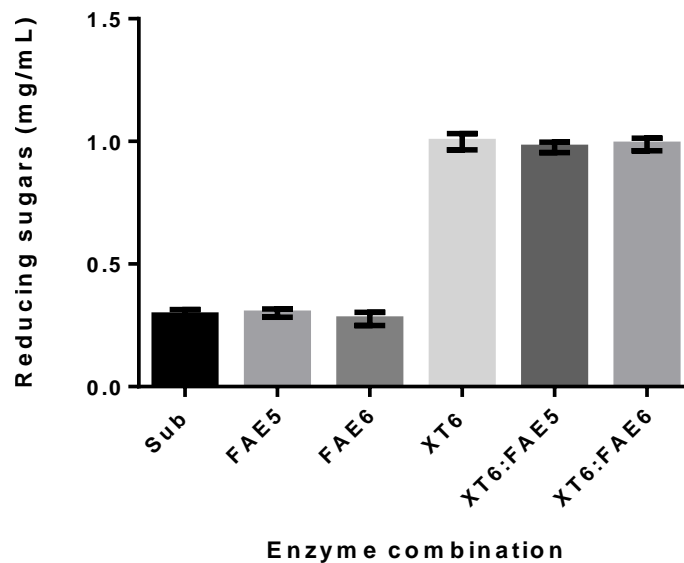
A**B**

Figure 6.5: Release of reducing sugars during hydrolysis of 0.5% (w/v) wheat arabinoxylan (WAX) by individual enzymes or a combination of 66% xylanase: 33% FAE5 or FAE6. (A) Synergy studies for Xyn11 and FAEs. (B) Synergy studies for XT6 and FAEs. “Sub” represents substrate control. Each data point represents the average of triplicates \pm standard deviation. Statistical analysis was conducted using a t-test for improvement of hydrolysis with respect to reducing sugar by the enzyme combinations compared to single enzyme (xylanase), key: * (p value < 0.05).

The reaction mixture with Xyn11 alone resulted in 0.89 mg/mL of reducing sugars, while co-incubation with FAE5 or FAE6 led to 1.18 mg/mL (25.61% increase) and 1.22 mg/mL reducing sugars (a 28.06% increase), respectively. On the other hand, co-incubation of XT6 with FAE5 or FAE6 did not result in an increased amount of reducing sugars compared to the reaction mixture containing only XT6 (Figure 6.5B), indicating that there was no synergy in the production of reducing sugars. This is in contrast with the pattern observed for Xyn11 (Figure 6.5A), where a significant synergistic effect of FAE5 and FAE6 with Xyn11 was observed. A possible explanation for this could lie in differences in the manner in which Xyn11 and XT6 bind to the substrate. As mentioned earlier, GH11 xylanases are known to be hampered by the presence of side chain decorations along the xylan backbone. In contrast, xylanases from family GH10 are able to tolerate binding of xylan backbone substituted with various side chains. As a result, GH10 xylanases generally produce shorter XOS than do members of the GH11 family (Falck et al., 2014; Gong et al., 2016). This would suggest that the presence of FAE5 or FAE6 would not improve the activity of XT6 in the release of XOS from WAX because it is unlikely that the action of the enzyme is influenced by the presence of FA. On the other hand, the presence of FA is more likely to impede the binding of Xyn11 to the substrate, resulting in generation of longer feruloylated XOS. Therefore, the addition of FAE5 or FAE6 would lead to cleavage of ester-linkages and removal of FA. This in turn would provide more binding sites for Xyn11 on these de-branched long chain XOS, thus producing a higher relative yield of short XOS compared to the reaction mixture with only Xyn11. Recent studies have reported the above-mentioned mechanism as a mode of synergistic interactions between xylanase and FAEs (Oliveira et al., 2019; Wang et al., 2020). Overall, the purified recombinant FAE5 and FAE6 enzymes exhibit strong synergistic interactions with Xyn11 and XT6 in the co-production of FA and XOS from WAX. The comparative study of the enzymes showed that XT6 acted synergistically with FAE5 and FAE6 only for the release of high amounts of FA, whereas co-incubation with Xyn11 resulted in low yield of FA but increased amount of XOS.

6.4.4. Determination of hydrolysate product profiles

Further analysis of the reaction products was carried out in an attempt to evaluate the types of XOS generated by single enzymes and their combinations. The initial analysis of reaction products from synergy assays was performed using a TLC method. The nature and relative abundance of XOS generated from WAX by Xyn11 and XT6 are shown in Figures 6.6A and 6.6B, respectively.

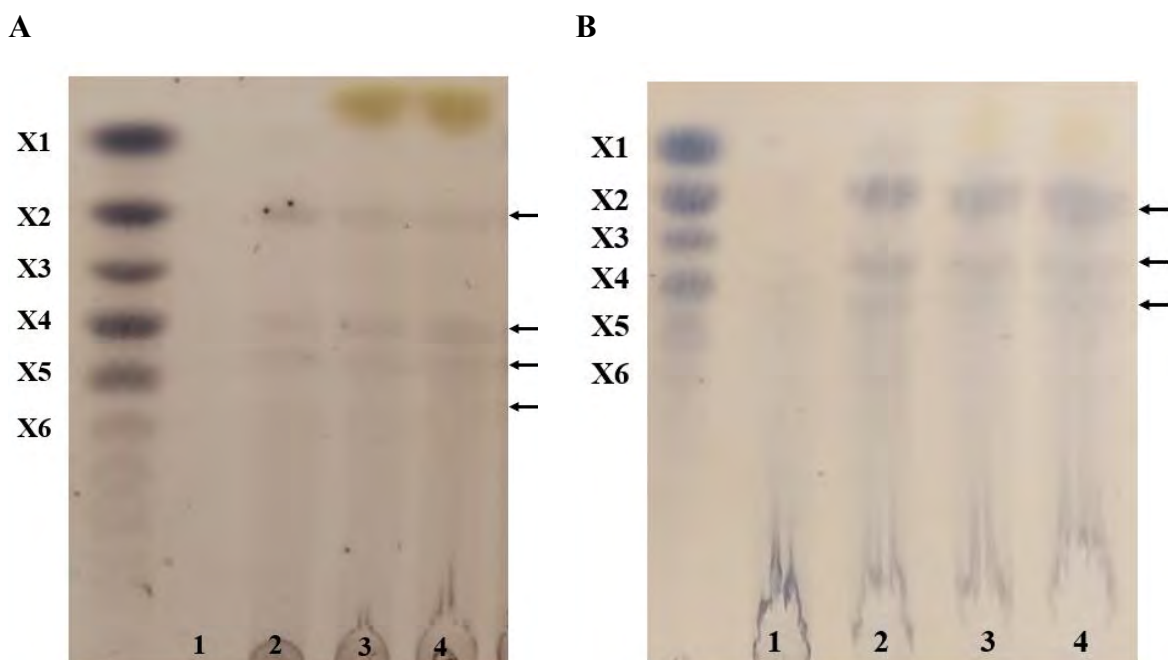


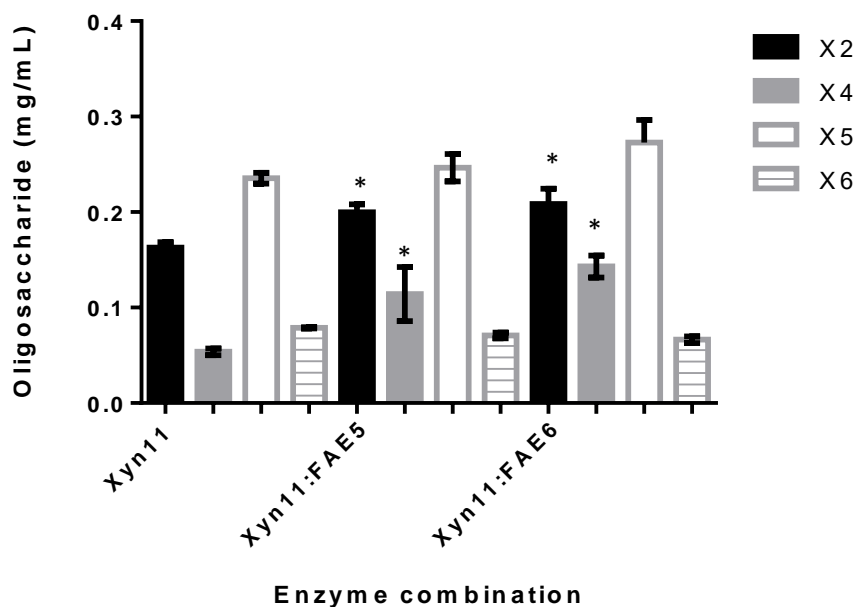
Figure 6.6: Thin-layer chromatography analysis of hydrolysis of 0.5% (w/v) WAX by (2) xylanase alone, (3) a combination of 66% xylanase: 33% FAE5, and (4) a combination of 66% xylanase: 33% FAE6. Substrate without enzyme was used as a control (1). **(A)** Synergy studies for Xyn11 and FAEs. **(B)** Synergy studies for XT6 and FAEs. A mixture of XOS (X1-X6) was used as a standard. Arrows indicate observed bands, albeit feint in some instances.

The hydrolytic product profiles demonstrated that Xyn11 and XT6 yielded XOS with a degree of polymerisation of 2 and higher, indicating that these enzymes are true xylanases with no xylosidase side activity. It is important to note that the dark-yellow coloured spots on the plates represent glycerol which was used as a stabiliser during the storage of the purified FAE5 and FAE6. As shown in Figure 6.6A, the hydrolytic products produced by Xyn11 were primarily xylobiose, xylotetraose, xylopentaose and xylohexaose. There were no clear differences in migration of XOS between the single enzyme (lane 3) and the enzyme combinations (lane 3 and 4). There were also no clear differences in the relative abundance of XOS produced by Xyn11 alone and the enzyme combinations. On the other hand, the major hydrolytic products generated by XT6 were xylobiose, xylotriose and xylotetraose. Among these XOS, xylobiose appeared to be the dominant product, indicating that the hydrolytic products produced by XT6 had a lower degree of polymerisation than those obtained using Xyn11. These findings are consistent with those of previous reports in which the hydrolytic products released by GH10

xylanases were shorter than those produced by GH11 xylanases (Biely et al., 2016; Linares-Pasten et al., 2018). These results indicate that the differences in synergistic action of Xyn11 and XT6 with FAEs are primarily associated with (and due to) the different hydrolysate product profiles that they generate.

In a further approach, the XOS generated by synergistic enzymatic hydrolysis were quantified using HPLC-RID. This was performed in order to further detect differences between the hydrolytic products of Xyn11 and XT6 (See Figure 6.7). The quantities of hydrolysis products formed by the action of Xyn11 alone - and in combination with FAE5 or FAE6 - are shown in Figure 6.7A. It was clear that Xyn11 and its enzyme combinations generated high quantities of xylopentaose. The combined action of Xyn11 and FAE5 or FAE6 showed an improvement in xylobiose production compared to the single enzyme reaction mixture. A similar pattern was also observed for generation of xyloetraose. These results are in agreement with those reported in the reducing sugar assay (Figure 6.5) where enzyme combinations enhanced the amount of reducing sugars released. On the other hand, the results presented in Figure 6.7B showed that there was no improvement in the release of XOS when XT6 was added alone compared to co-incubation with FAE5 or FAE6. This is consistent with the results obtained using the reducing sugar assay. Furthermore, it was clear that xylobiose and xylotriose were the dominant end products (more pronounced in the reaction mixture with XT6 alone), confirming the observations made in the TLC analysis. Based on all of the above results, it can be concluded that FAE5 and FAE6 exhibited strong synergistic relationships with Xyn11 and XT6 during hydrolysis of WAX. It was shown that FAEs work better with XT6 (GH10 xylanase) for the release of FA, while synergism with Xyn11 (GH11 xylanase) appeared to enhance the production of XOS. The nature of synergistic interactions between these enzymes was found to be dependent on the mode of hydrolysis (action) of the xylanases.

A



B

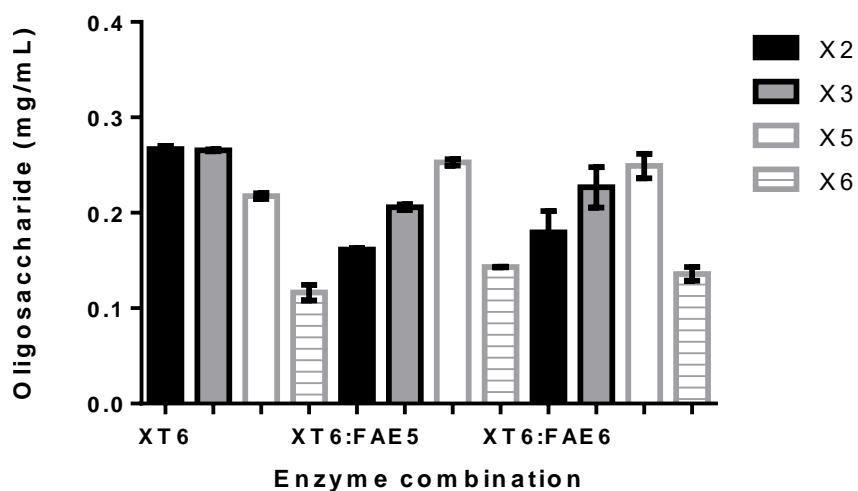


Figure 6.7: Xylo-oligosaccharide content measured from the hydrolysis of 0.5% (w/v) WAX after incubation with Xyn11 alone or a combination of 66% Xyn11: 33% FAE5 or FAE6. (A) Synergy studies for Xyn11 and FAEs. (B) Synergy studies for XT6 and FAEs. Each data point represents the average of triplicates \pm standard deviation. Statistical analysis was conducted using a t-test for improvement of hydrolysis with respect to xylo-oligosaccharides (XOS) by the enzyme combinations compared to single enzyme (xylanase), key: * (p value < 0.05).

6.4.5 Evaluation of synergism between FAEs and xylanases during the hydrolysis of agricultural residues

To determine if the xylanase-FAE synergism observed during the hydrolysis of WAX (a model substrate) could also be observed on complex substrates, different agricultural residues were hydrolysed using the same combinations of xylanases and FAEs as were performed with WAX. There are major differences between the structures of model substrates and those of agricultural residues. The structure and composition of agricultural residues is known to be complex. This complex structural arrangement of agricultural residues makes them recalcitrant to enzymatic hydrolysis. Therefore, a pre-treatment is a crucial step in the process of bioconversion of these complex substrates. This is because pre-treatment is known to disrupt the physical and chemical barriers that make native biomass recalcitrant and makes these complex substrates more amenable to enzymatic hydrolysis. In this study, xylanase-FAE synergism was evaluated during the enzymatic hydrolysis of untreated, hydrothermal pre-treated and dilute acid pre-treated agricultural residues, namely, corn cobs (CC), rice straw (RS) and sugarcane bagasse (SCB).

6.4.6. Release of XOS from agricultural residues by enzymatic hydrolysis

The enzymes were tested for their ability to release XOS (measured as reducing sugars) from untreated and pre-treated agricultural residues. The protein loadings for all reaction mixtures were kept at a total protein loading of 8 mg per g of substrate, and the enzyme mixture consisting of xylanase and FAE in a 66:33% protein ratio was used for all combination experiments. Unfortunately, incubations using XT6 (GH10 xylanase) did not generate any XOS from the substrates tested. The limitation of xylanases from GH10 family on insoluble substrates has been reported previously; studies show that larger xylanases have a slow penetration into the cell wall matrix, which makes them less efficient in hydrolysing insoluble xylan (Falck et al., 2014; Nordberg Karlsson et al., 2018). On the other hand, xylanases from GH family 11 are known to have a smaller size compared to GH10 xylanases, and as a result, can more easily penetrate the cell wall matrix which makes them more efficient against insoluble substrates. The synergistic enzymatic hydrolysis of untreated and pre-treated agricultural residues was then performed using Xyn11 and FAE5 or FAE6.

Figure 6.8 shows the production of reducing sugars after enzymatic hydrolysis of untreated (A), hydrothermally pre-treated (B) and dilute acid pre-treated CC (C) by single enzymes or combinations of these enzymes. The trend in the production of reducing sugars was similar in all substrates, with the Xyn11 to FAE5/6 combinations releasing higher reducing sugars than

those from the reaction mixture containing individual enzymes. The hydrolysis of untreated CC with Xyn11 alone and a combination of Xyn11 and FAE5 or FAE6 produced reducing sugars at concentrations of 0.94 mg/mL, 1.17 mg/mL, and 1.22 mg/mL, respectively (Figure 6.8A). It was clear that the hydrolysis of pre-treated CC with enzyme combinations resulted in the release of more reducing sugars compared to the hydrolysis of untreated CC. The hydrolysis of hydrothermally pre-treated CC with a combination of Xyn11 and FAE5 or FAE6 released reducing sugars at concentrations of 1.51 mg/mL, and 1.63 mg/mL, respectively (Figure 6.8B), while the hydrolysis of dilute acid pre-treated CC with the same enzyme combination resulted in reducing sugars of 1.59 mg/mL, and 1.66 mg/mL (Figure 6.8C). A dramatic decrease in reducing sugars when Xyn11 was used alone on dilute acid pre-treated CC was also observed. One likely explanation for this observation could be that the structural modifications of CC caused by dilute acid pre-treatment method may have resulted in the accumulation of highly feruloylated arabinoxylan. High levels of side-chain decoration along the arabinoxylan main chain are more likely to impede binding of Xyn11 to the substrate. As mentioned previously, side-chain decorations at the xylan backbone are generally less well tolerated by GH11 xylanases. It has been shown the structures that remain after pre-treatment are heavily affected by the method of pre-treatment. Some studies have been conducted on dilute acid pre-treated corn fibre and dilute ammonia pre-treated corn stover and have shown that pre-treatment leads to the generation of highly substituted xylan oligomers, many of which also contain acetyl and feruloyl esters (Appeldoorn et al., 2013; Jonathan et al., 2017). Overall, the findings indicated that FAE5 and FAE6 played an important role in the synergistic hydrolysis of arabinoxylan contained in CC samples. The effect of hydrothermal and dilute acid pre-treatment methods was beneficial as the synergistic enzyme cocktails produced more reducing sugars from pre-treated CC samples.

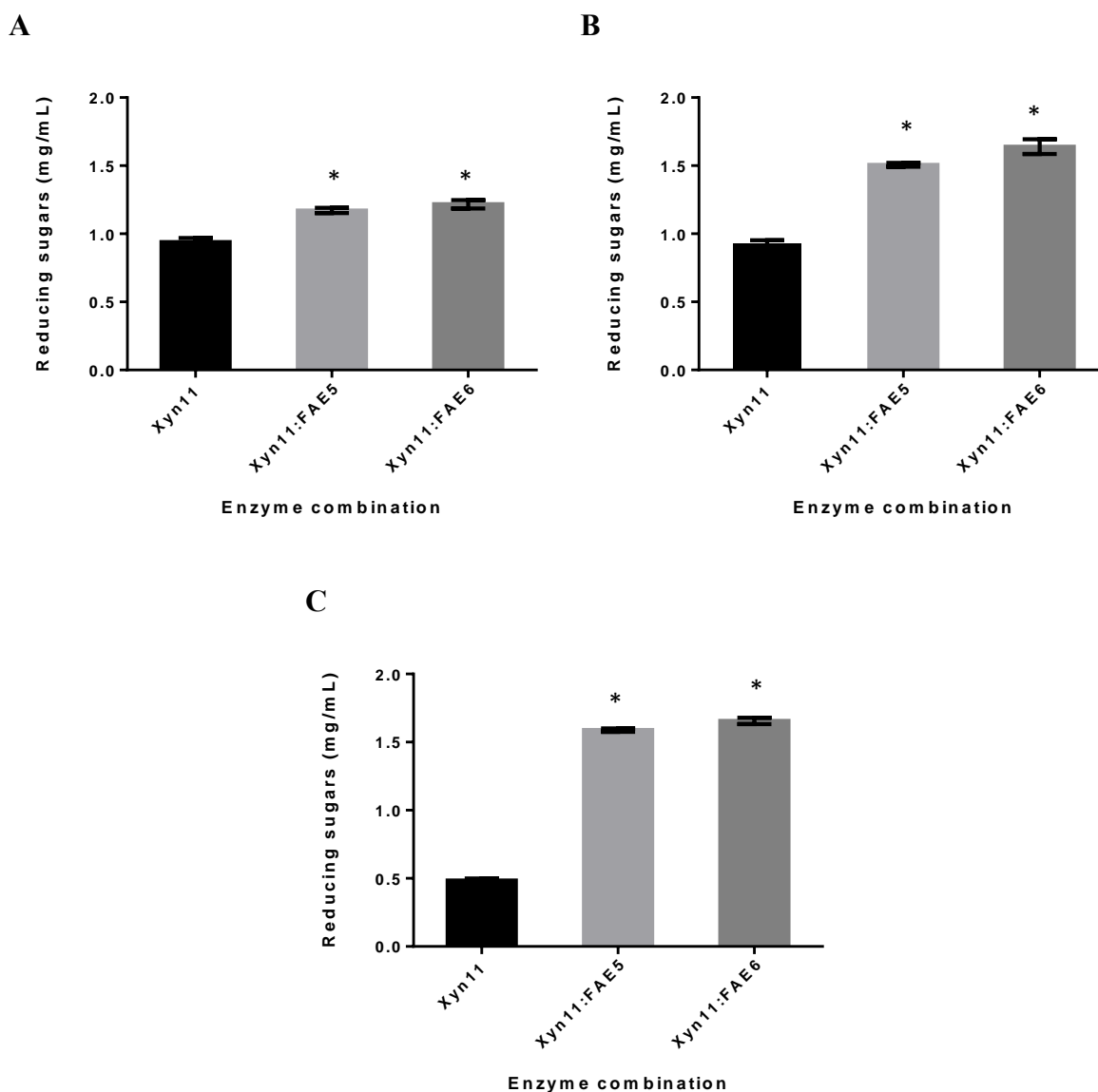


Figure 6.8: Release of reducing sugars during hydrolysis of 1% (w/v) untreated (A), hydrothermally pre-treated (B) and acid pre-treated corn cob (C) by individual enzymes or a combination of 66% Xyn11: 33% FAE5 or FAE6. Each data point represents the average of triplicates \pm standard deviation. Statistical analysis was conducted using a t-test for improvement of hydrolysis with respect to reducing sugar by the enzyme combinations compared to single enzyme (Xyn11), key: * (p value < 0.05).

The xylanase-FAE synergism was further evaluated during the enzymatic hydrolysis of two further complex substrates. The results for the release of reducing sugars from RS and SCB are presented in Figures 6.9 and 6.10, respectively. Comparison of the quantities of the reducing

sugars obtained after enzymatic hydrolysis of RS clearly showed that combinations of Xyn11 and FAE5 or FAE6 resulted in higher production compared to single enzyme incubations (Figure 6.9).

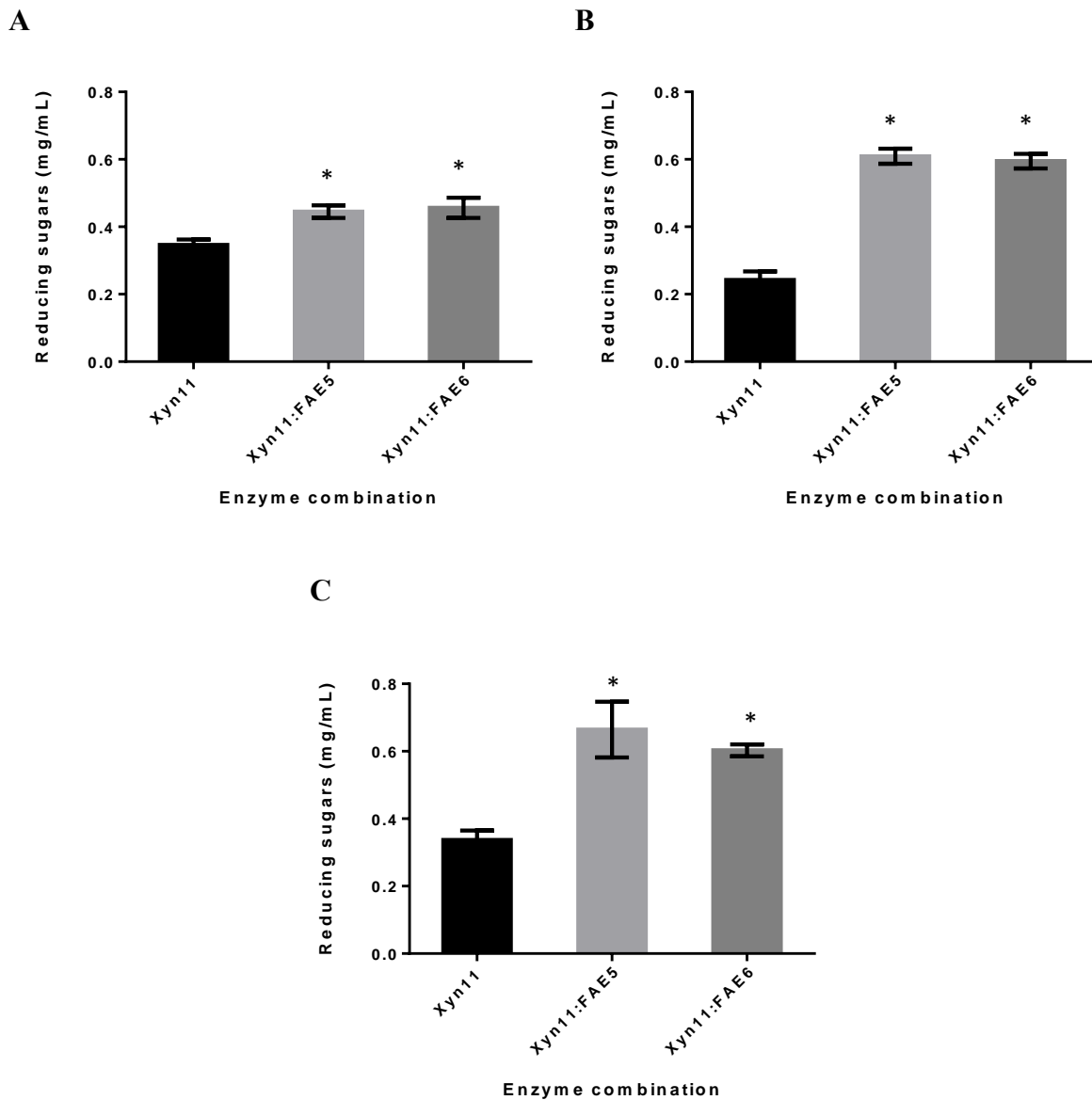


Figure 6.9: Release of reducing sugars during hydrolysis of 1% (w/v) untreated (A), hydrothermally pre-treated (B) and acid pre-treated rice straw (C) by individual enzymes or a combination of 66% Xyn11: 33% FAE5 or FAE6. Each data point represents the average of triplicates \pm standard deviation. Statistical analysis was conducted using a t-test for improvement of hydrolysis with respect to reducing sugar by the enzyme combinations compared to single enzyme (Xyn11), key: * (p value < 0.05).

Enzyme combinations appeared to release high quantities of reducing sugars from pre-treated RS compared to untreated RS. However, this increase was not as pronounced as the one observed for the hydrolysis of pre-treated CC. Furthermore, Xyn11 alone appeared to release small quantities of reducing sugars from hydrothermally pre-treated RS (Figure 6.9B) compared to untreated RS. This was similar to the pattern observed for the hydrolysis of dilute acid pre-treated CC.

The synergistic effect of Xyn11: FAE5/6 was tested similarly on untreated and pre-treated SCB (Figure 6.10). Again, enzyme combinations substantially facilitated an increase in reducing sugars release compared to when Xyn11 was used alone. Surprisingly, the data indicated that reducing sugars released from pre-treated SCB were less compared to untreated SCB. The quantities of reducing sugars released from untreated SCB by Xyn11: FAE5 and Xyn11: FAE6 were 0.72 mg/mL and 0.70 mg/mL, respectively. The same enzyme combinations released significantly lower quantities of reducing sugars from pre-treated SCB (less than 0.51 mg/mL). This was quite unexpected, and it was contrary to the observations made on CC and RS samples where hydrothermal and dilute acid pre-treatments appeared to significantly improve the enzymatic release of reducing sugars. This might be attributed to the differences in structure and chemical composition among these complex substrates. It has been shown that SCB generally contains considerably higher lignin content than RS and CC (Sahare et al., 2012; Sakdaronnarong et al., 2014). Therefore, it is possible that the impact of pre-treatment is influenced by the chemical composition of complex substrates. These results showed that production of high quantities of reducing sugars from untreated and pre-treated agricultural residues (complex substrates) could be achieved by Xyn11-FAE5/6 synergism.

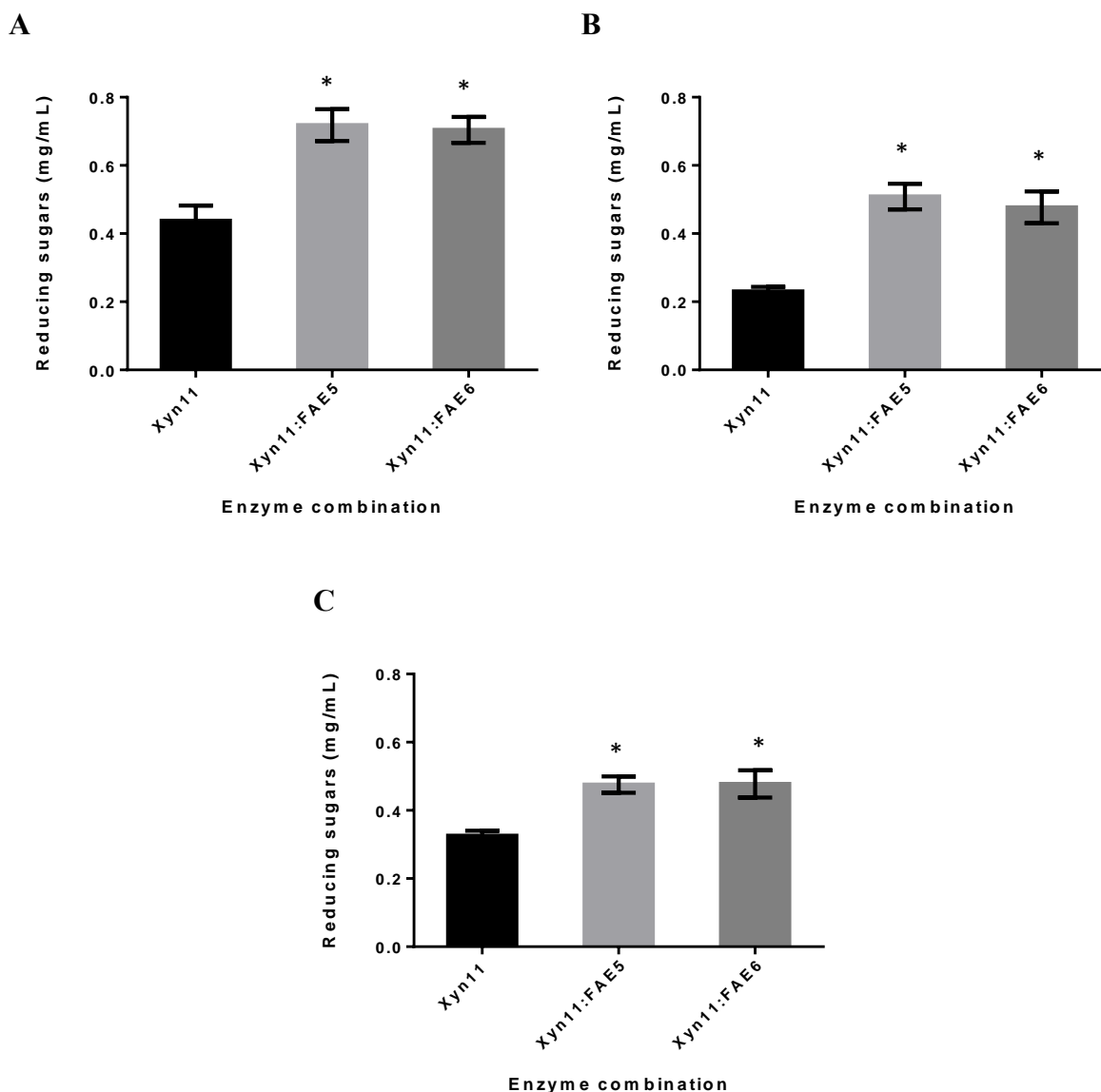


Figure 6.10: Release of reducing sugars during hydrolysis of 1% (w/v) untreated (A), hydrothermally pre-treated (B) and acid pre-treated sugarcane bagasse (C) by individual enzymes or a combination of 66% Xyn11: 33% FAE5 or FAE6. Each data point represents the average of triplicates \pm standard deviation. Statistical analysis was conducted using a t-test for improvement of hydrolysis with respect to reducing sugar by the enzyme combinations compared to single enzyme (Xyn11), key: * (p value < 0.05).

6.4.7. Determination of hydrolysate product profiles

In an attempt to further clarify the mechanisms behind the observed synergistic interactions between Xyn11 and FAE5 or FAE6 on complex substrates, the hydrolysis product profiles

generated by individual enzymes and enzyme combinations were also determined. The types and relative abundances of XOS in the hydrolysates of untreated and pre-treated CC hydrolysed by Xyn11 alone and combinations with FAEs are shown in Figure 6.11.

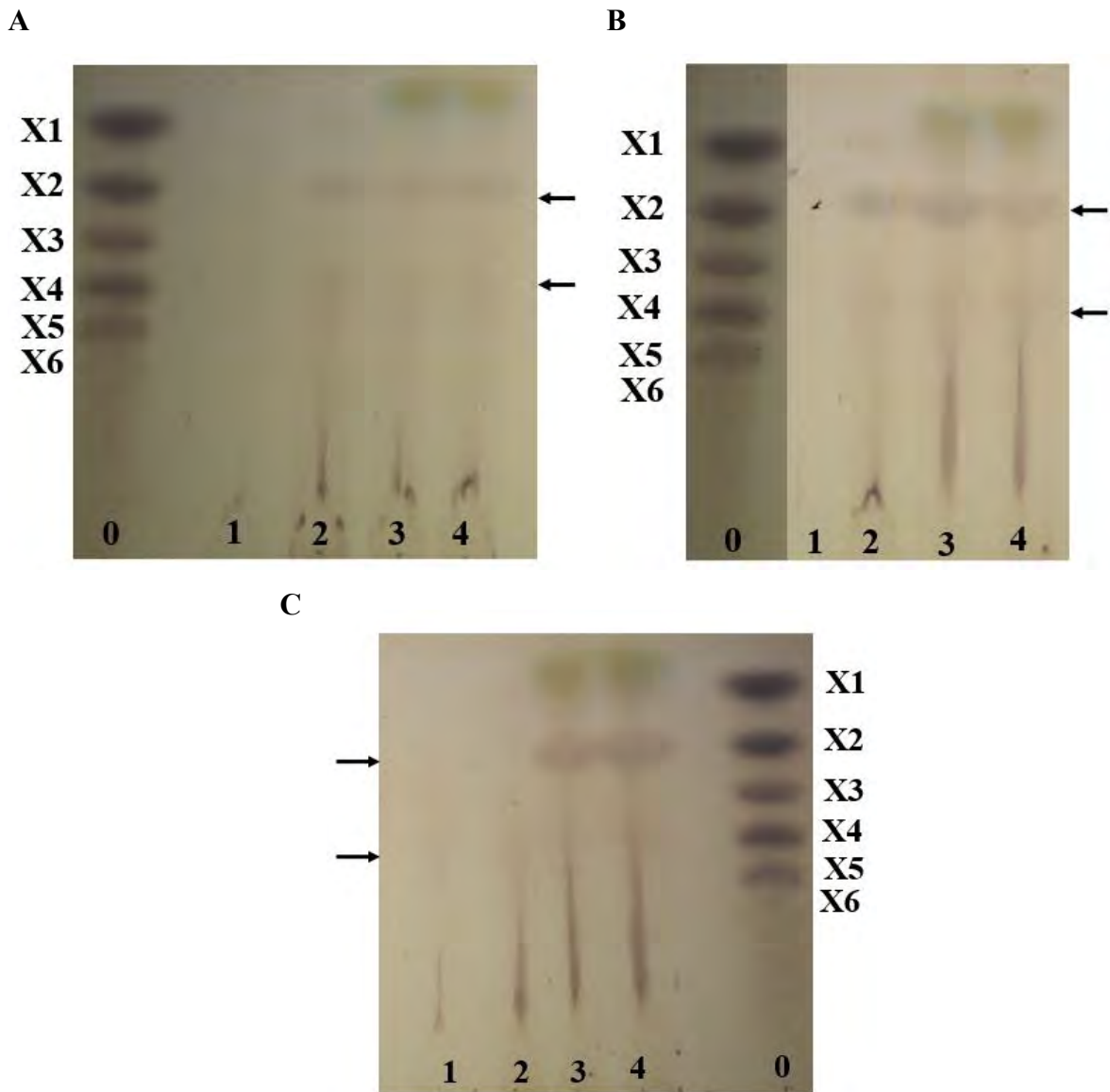


Figure 6.11: Thin-layer chromatography analysis of hydrolysis of 1% (w/v) untreated (A), hydrothermal pre-treated (B) and acid pre-treated corn cob (C) by (2) Xyn11 alone, (3) a combination of 66% Xyn11: 33% FAE5, and (4) a combination of 66% Xyn11: 33% FAE6. Substrate without enzyme was used as a control (1). A mixture of xylo-oligosaccharides (X1-X6) was used as a standard (0). Arrows indicate the observed bands, albeit feint in some instances.

As mentioned previously, the dark-yellow coloured spots on the plates represent glycerol which was used as a stabiliser during storage of the purified FAE5 and FAE6. The major hydrolysis products generated from CC were xylobiose, which was a dominant product, and small quantities of xylotetraose. The enzyme combinations (lane 3 and 4) appeared to generate more xylobiose when compared to the reaction mixture containing only Xyn11 (lane 2), this pattern was more pronounced for the hydrolysis of hydrothermal and dilute acid pre-treated CC as shown in Figures 6.11B and 6.11C, respectively. These results also suggested that the improvement in the release of reducing sugars observed in Figure 6.8 may result from the generation of high quantities of xylobiose by the enzyme combinations.

Furthermore, the product profiles generated by Xyn11 alone and by the enzyme combinations using RS and SCB were also determined, and the results are presented in Figures 6.12 and 6.13. The hydrolytic products generated from untreated and pre-treated RS appeared to consist of xylobiose, xylohexaose and trace amounts of xylopentaose (Figure 6.12). It was clear that the combined action of Xyn11 and FAE5 or FAE6 resulted in hydrolysis products with an increased amount of xylobiose compared to when Xyn11 was employed alone. Furthermore, the generation of xylobiose by the enzyme combinations was more pronounced for the pre-treated RS (Figure 6.12B and 6.12C), this was similar to the results obtained from enzymatic hydrolysis of CC (Figure 6.11). The hydrolysis product patterns obtained from SCB (Figure 6.13A-C) were similar to those of RS and CC, where xylobiose was a dominant product for enzyme combinations. Unlike RS and CC, the hydrolysis of pre-treated SCB did not lead to an improvement in relative abundance of XOS; this is consistent with the results observed during the quantification of reducing sugars released from SCB (Figure 6.10).

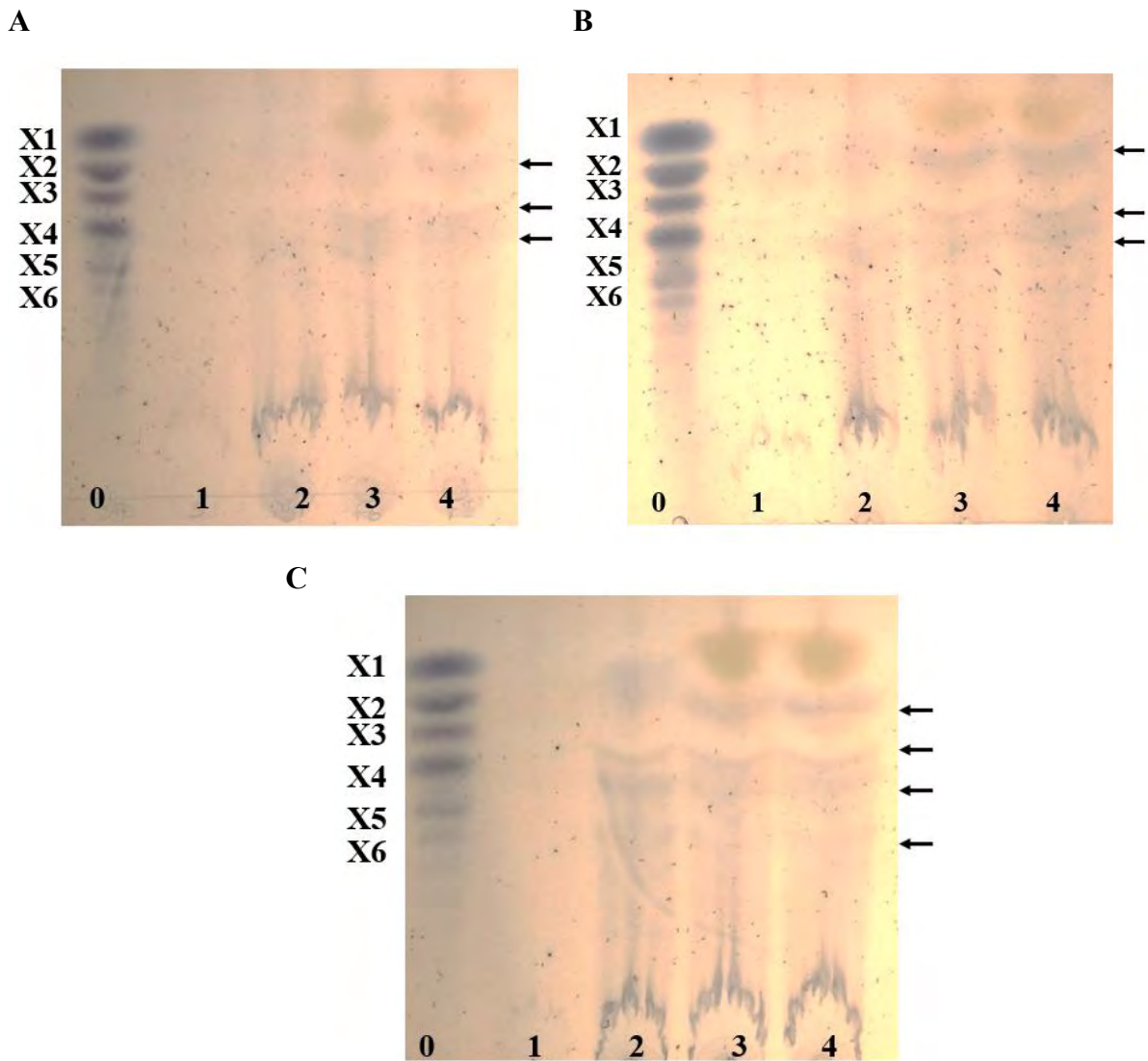


Figure 6.12: Thin-layer chromatography analysis of hydrolysis of 1% (w/v) untreated (A), hydrothermal pre-treated (B) and acid pre-treated rice straw (C) by (2) Xyn11 alone, (3) a combination of 66% Xyn11: 33% FAE5, and (4) a combination of 66% Xyn11: 33% FAE6. Substrate without enzyme was used as a control (1). A mixture of xylo-oligosaccharides (X1-X6) was used as a standard (0). Arrows indicated the observed bands, albeit feint in some instances.

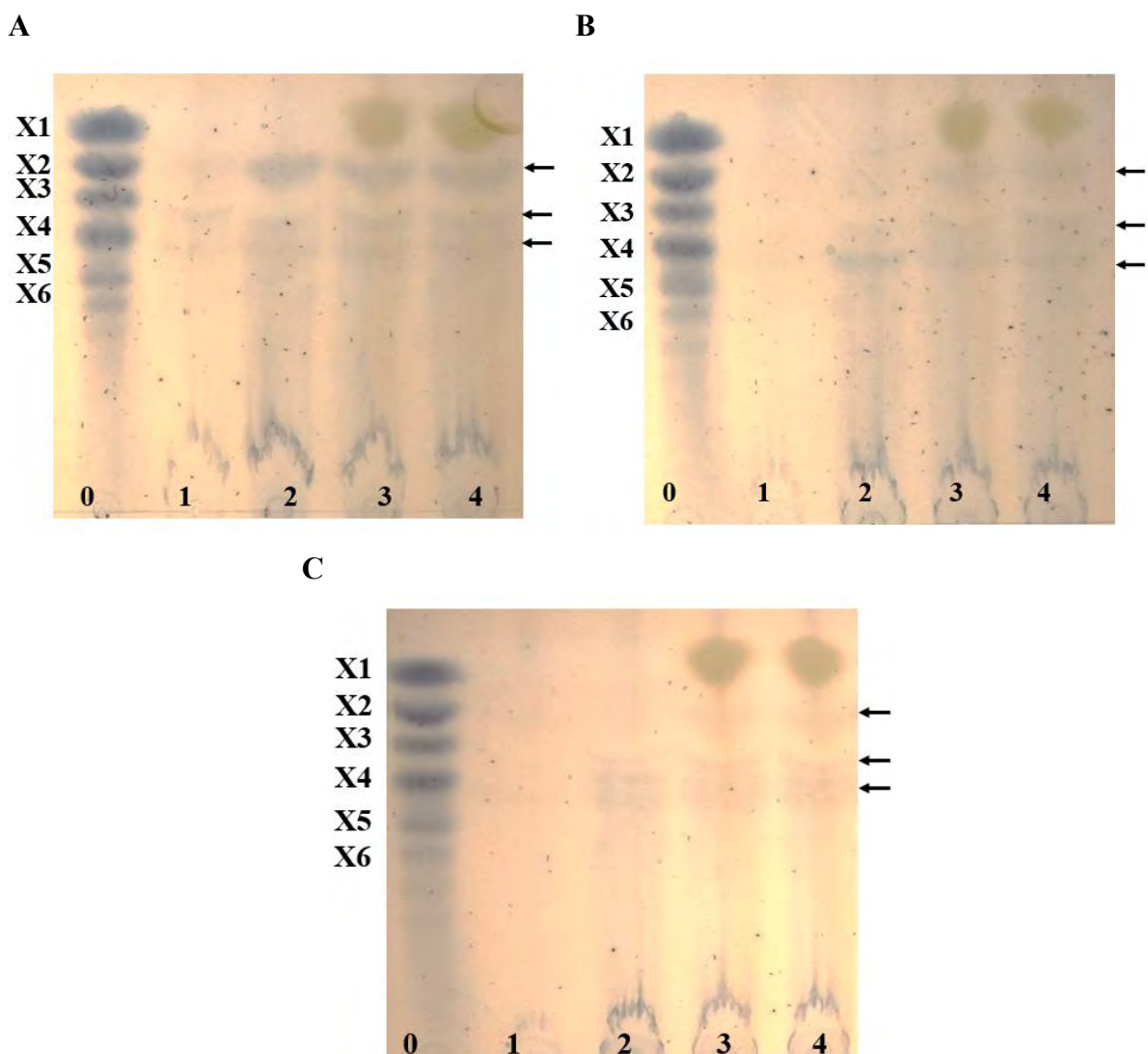


Figure 6.13: Thin-layer chromatography analysis of hydrolysis of 1% (w/v) untreated (A), hydrothermal pre-treated (B) and acid pre-treated sugarcane bagasse (C) by (2) Xyn11 alone, (3) a combination of 66% Xyn11: 33% FAE5, and (4) a combination of 66% Xyn11: 33% FAE6. Substrate without enzyme was used as a control (1). A mixture of xylo-oligosaccharides (X1-X6) was used as a standard (0). Arrows indicate the observed bands, albeit feint in some instances.

Overall, these results indicated that the Xyn11-FAE5/6 synergism observed in the release of reducing sugars from untreated and pre-treated agricultural residues is primarily associated with the generation of high quantities of xylobiose. One likely explanation for this observation could be that Xyn11 may cleave the xylan backbone found in these agricultural residues and produce longer feruloylated XOS. The removal of FA by FAE5 or FAE6 from feruloylated XOS is more likely to make them more accessible for further hydrolysis by Xyn11, yielding shorter XOS (xylobiose).

In addition, the amounts of XOS released from untreated and pre-treated substrates were also determined using HPLC-RID. This was to confirm the findings obtained from TLC analysis. It should be noted that the HPLC-RID system used in this study could not quantify XOS concentrations of less than 0.05 mg/mL. Unfortunately, it was not possible to compare XOS generated from RS and SCB due to the fact that most of these XOS could not be quantified. Therefore, only XOS generated from untreated and pre-treated CC were quantified, and the data is presented in Figure 6.14. These results supported the observations made during TLC analysis where Xyn11-FAE5/6 synergism led to a significant increase in the production of xylobiose. The highest concentrations of xylobiose were generated from hydrothermally pre-treated CC (0.28 mg/mL for Xyn11: FAE5 and 0.40 mg/mL for Xyn11: FAE6) and acid-treated CC (0.34 mg/mL for Xyn11: FAE5 and 0.43 mg/mL for Xyn11: FAE6). Again, the data indicated that the pre-treatment step substantially enhanced the enzymatic hydrolysis of CC. It can be speculated that hydrothermal and dilute acid pre-treatment methods improved the enzymatic release of XOS by increasing accessibility of arabinoxylan to the enzymes. Arabinoxylan found in complex substrates is usually embedded in the lignocellulosic matrix and therefore inaccessible to enzymatic hydrolysis. Based on all of the above results, it can be concluded that the Xyn11-FAE5/6 synergism observed in the release of XOS during hydrolysis of model substrates was also observed during the enzymatic hydrolysis of untreated and pre-treated complex substrates.

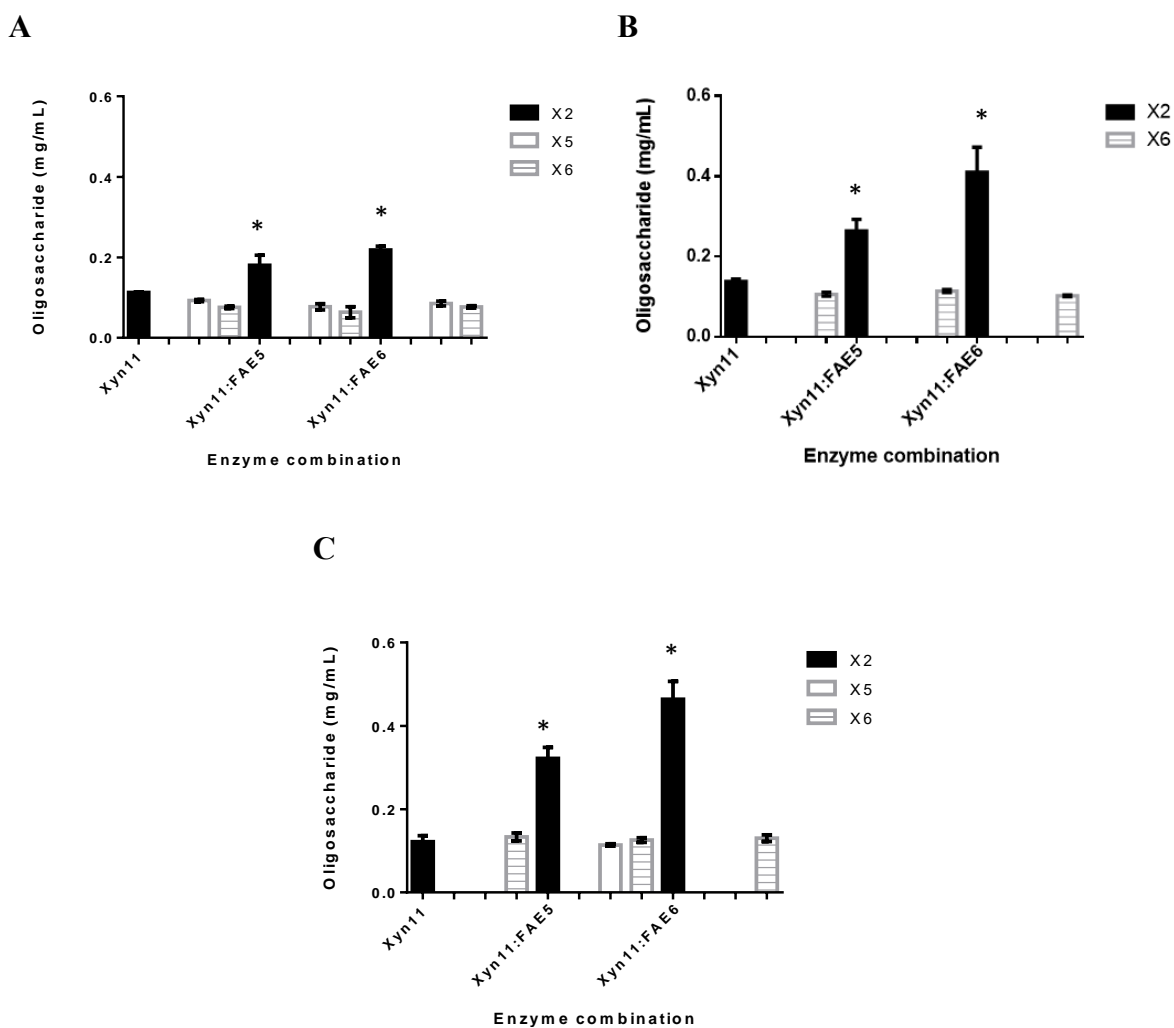


Figure 6.14: Xylo-oligosaccharide content measured from the hydrolysis of 1% (w/v) untreated (A), hydrothermal pre-treated (B) and acid pre-treated corn cob (C) after incubation with Xyn11 alone or a combination of 66% Xyn11: 33% FAE5 or FAE6. Each data point represents the average of triplicates \pm standard deviation. Statistical analysis was conducted using a t-test for the improvement of hydrolysis with respect to xylo-oligosaccharide (XOS) generation by the enzyme combinations, compared to the single enzyme (Xyn11), key: * (p value $<$ 0.05).

6.4.8. Release of hydroxycinnamic acids from agricultural residues by enzymatic hydrolysis

The findings from model substrate studies indicated that FAE5 and FAE6 released FA from the feruloylated XOS generated by the xylanases. The cleavage of FA from feruloylated XOS was also shown to be the major mechanism behind the improvements seen in the production of reducing sugars. It has been already established that the production of reducing sugars from untreated and pre-treated agricultural residues is significantly enhanced by the synergistic action of Xyn11 and FAE5 or FAE6. The improvements observed in the release of reducing sugars is more likely to be as a result of cleavage of ester-linkages between hydroxycinnamic acids and xylan found in these substrates. In this part of the study, the synergistic action of Xyn11 and FAE5 or FAE6 was evaluated for the release of hydroxycinnamic acids from untreated and pre-treated agricultural residues. The data presented below shows the release of hydroxycinnamic acids (FA and *p*-CA) from CC and RS. The enzymatic hydrolysis of pre-treated SCB did not show a significant increase in the amount of hydroxycinnamic acids released compared to the control reaction containing only the substrate. This may be due to the fact that Xyn11 generated very low quantities of XOS from pre-treated SCB (see Figure 6.10), and this meant that there would be fewer short chain feruloylated XOS available for FAE5 and FAE6 to cleave ester bonds and release hydroxycinnamic acids from.

The release of hydroxycinnamic acids from untreated, hydrothermal pre-treated and dilute acid pre-treated CC is shown in Figure 6.15. In the case of untreated CC, the results indicated that the amounts of FA and *p*-CA released were enhanced after the enzymatic hydrolysis with enzyme combinations compared to when single enzymes (FAE5 or FAE6) were used (Figure 6.15A). This significant increase in the release of FA and *p*-CA by enzyme combinations is an indication of the cleavage of ester bonds between hydroxycinnamic acids and short chain XOS generated by Xyn11. With respect to pre-treated CC substrates, the amount of hydroxycinnamic acids released (without enzymatic hydrolysis) was obviously enhanced (Figure 6.15B and C). This could be attributed to the disruption of the complex architecture of lignocellulose during the pre-treatment step. Hydroxycinnamic acids, most especially FA, are well known for their ability to cross-link cell wall polymers by ester-linking to the arabinosyl residue of arabinoxylan and ether-linking with lignin (Oliveira et al., 2019). Although pre-treated CC samples showed increased amounts of readily soluble FA and *p*-CA in the substrate controls, the enzyme combinations were still able to release considerable higher quantities compared to the reaction mixtures with single enzymes. It was clear that only Xyn11: FAE6

could significantly improve the release of FA from both pre-treated samples while both Xyn11: FAE5 and Xyn11: FAE6 could release comparable quantities of *p*-CA (Figures 6.15B and C).

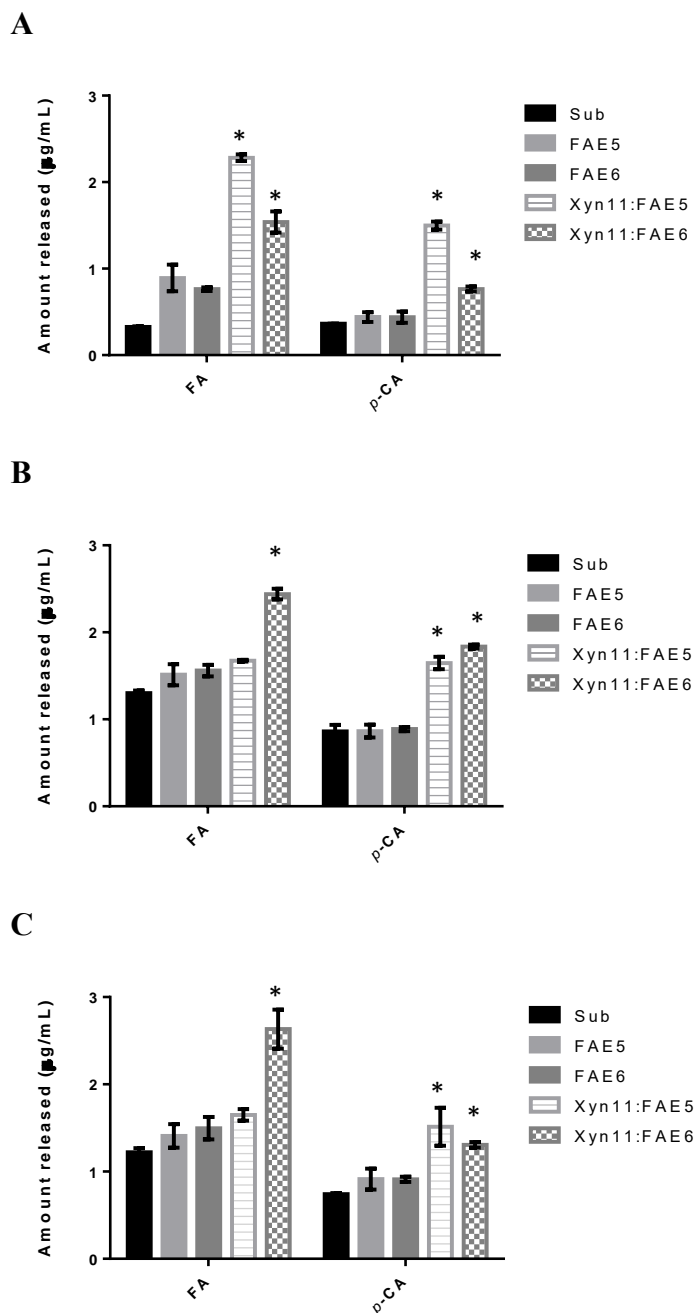


Figure 6.15: Release of *p*-coumaric (*p*-CA) and ferulic acid (FA) during the degradation of 1% (w/v) untreated (A), hydrothermal pre-treated (B) and dilute acid pre-treated corn cob (C) by individual enzymes or a combination of 66% Xyn11: 33% FAE5 or FAE6. “Sub” represents the substrate control. Each data point represents the average of triplicates \pm standard deviation. Statistical analysis was conducted using a t-test for improvement of *p*-coumaric or ferulic acid release by the enzyme combinations compared to the single enzymes (FAE5/6), key: * (p value $<$ 0.05).

A similar pattern was observed for the hydrolysis of RS where higher concentrations of FA and *p*-CA were released by the enzyme combinations, see Figure 6.16 below.

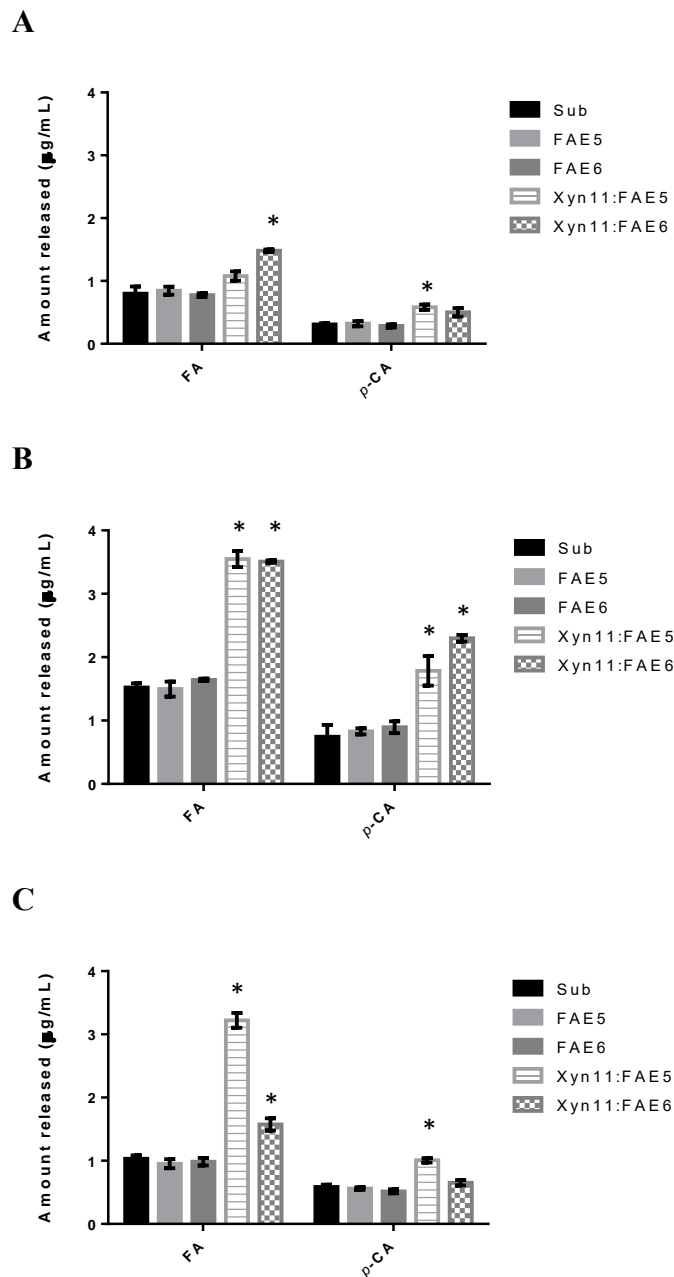


Figure 6.16: Release of *p*-coumaric (*p*-CA) and ferulic acid (FA) during the degradation of 1% (w/v) untreated (A), hydrothermal pre-treated (B) and dilute acid pre-treated rice straw (C) by individual enzymes or a combination of 66% Xyn11: 33% FAE5 or FAE6. “Sub” represents the substrate control. Each data point represents the average of triplicates \pm standard deviation. Statistical analysis was conducted using a t-test for improvement of *p*-coumaric or ferulic acid release by the enzyme combinations compared to single enzyme (FAE5/6), key: * (p value < 0.05).

Only a combination of Xyn11: FAE6 released more FA from untreated RS (Figure 6.16A). The results showed that pre-treatment of RS resulted in an improvement in the enzymatic release of FA and *p*-CA (Figures 6.16B and C). For hydrothermal pre-treated RS (Figure 6.16B), the combination of Xyn11 and FAE5 or FAE6 significantly improved the release of FA from 1.59 $\mu\text{g/mL}$ and 1.64 $\mu\text{g/mL}$ (single enzyme) to 3.55 $\mu\text{g/mL}$ and 3.51 $\mu\text{g/mL}$, respectively. In the case of *p*-CA release, Xyn11: FAE5 and Xyn11: FAE6 resulted in 2.12-fold and 2.96-fold improvement, respectively. For dilute acid pre-treated RS, a more pronounced improvement was observed for the release of FA where Xyn11: FAE5 and Xyn11: FAE6 exhibited 3.35-fold and 1.55-fold increment, respectively. These results clearly indicated that FAE5 and FAE6 acted synergistically with Xyn11 in the production of FA and *p*-CA from untreated and pre-treated CC and RS substrates.

Even though FAE-Xyn11 synergism resulted in improvements in the release of hydroxycinnamic acids from complex substrates, the yields obtained were much less (not more than 10%) when compared to release efficiencies (more than 60%) reported by some studies in the literature (Wu et al., 2012; Wu et al., 2017; Long et al., 2020). One likely explanation could be that Xyn11 generated fewer short chain XOS substituted with hydroxycinnamic acids (preferred substrates for FAE5 and FAE6). Once again, the data from the hydrolysis of model substrates indicated that the main factor by which xylanases contribute to enhancing FAE5 and FAE6 activity is by generating short chain feruloylated XOS with less steric hindrance. The data from the hydrolysis of model substrates also indicated that FAE5 and FAE6 released much higher quantities of FA from XOS produced by GH10 xylanase than those produced by the action of the GH11 xylanase. As mentioned previously, the GH10 xylanase could not hydrolyse untreated and pre-treated complex substrates and it was not possible to evaluate its synergistic action for the release of hydroxycinnamic acids from these substrates. This is also an indication that the choice of enzymes and substrates is a key factor in the formulation of efficient enzyme cocktails.

6.4.9. HPLC-MS/MS confirmation of FA and *p*-CA released from agricultural residues

An attempt was made to confirm the hydroxycinnamic acids released from the complex substrates with HPLC-MS/MS analysis. The analysis was performed on the untreated RS and CC substrates and the separation profiles and fragmentation patterns of the hydrolysis products were similar for both substrates. The extracted ion chromatogram and mass spectra of FA/*p*-CA shown below were obtained during the enzymatic hydrolysis of untreated RS by a combination of Xyn11 and FAE6 (see Figures 6.17 and 6.18). The analysis was carried out with negative ionisation because FA and *p*-CA are able to lose a proton to yield negative ions $[M-H]^-$. Surprisingly, spectra acquired from FA (Figure 6.17B) and *p*-CA (Figure 6.18B) showed major ions at $m/z = 195.05$ and $m/z = 165.06$ corresponding to the protonated $[M+H]^+$ masses of FA and *p*-CA, respectively. This was quite unexpected, since negative ionisation of FA and *p*-CA is supposed to yield negative ions at $m/z = 193$ and $m/z = 163$, respectively. The fragmentation patterns of both compounds resulted in the formation of a fragment $m/z = 131.07$, corresponding to a phenolic derivative of cinnamic acid. This fragment is likely to represent the loss of $[OH]$ ions from *p*-CA and loss of $[OH]$ and $[OCH_3]$ ions from FA. Based on this HPLC-MS/MS analysis and chromatograms obtained from the HPLC analysis, it can be concluded that hydroxycinnamic acids were generated from complex substrates during the synergistic cooperation of FAEs and xylanase.

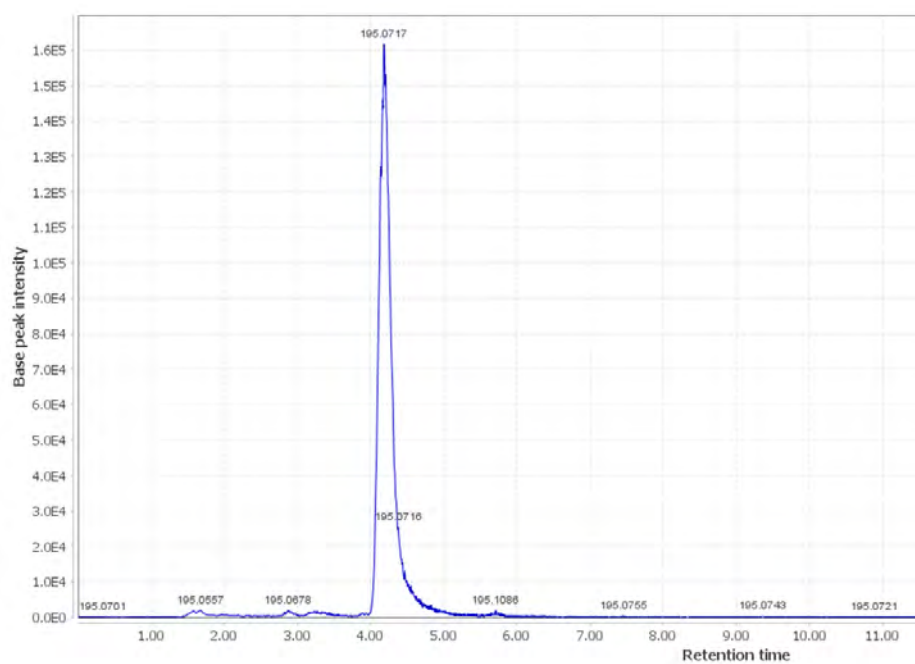
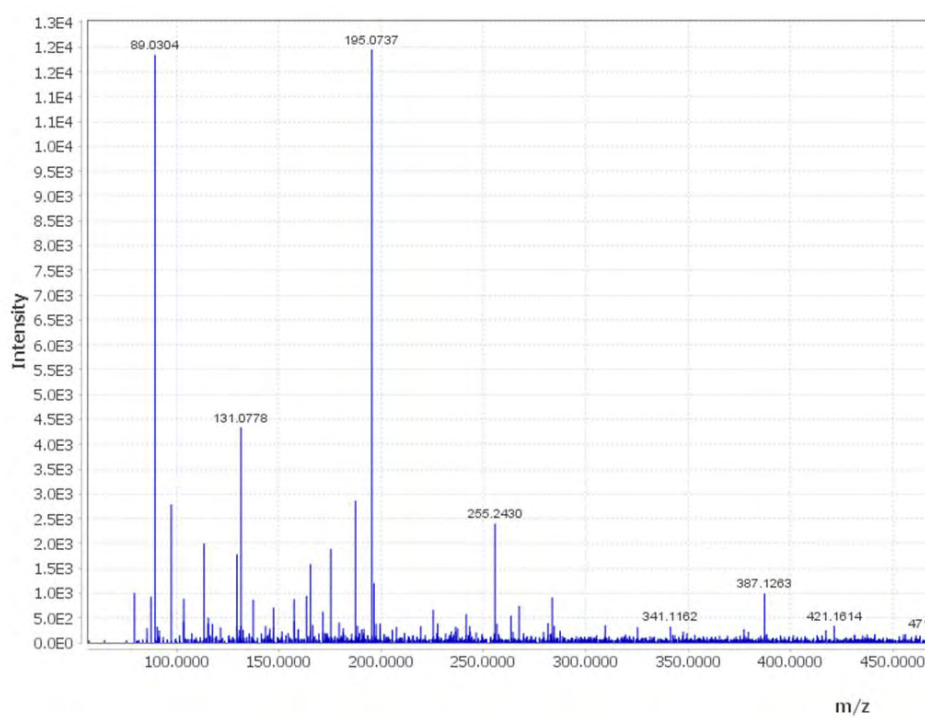
A**B**

Figure 6.17: HPLC-MS/MS analysis of ferulic acid released during hydrolysis of 1% (w/v) untreated rice straw by a combination of 66% Xyn11: 33% FAE6. (A) Extracted-ion chromatogram (XIC) for released ferulic acid. (B) Mass spectrum of ferulic acid corresponding to the peak observed on XIC.

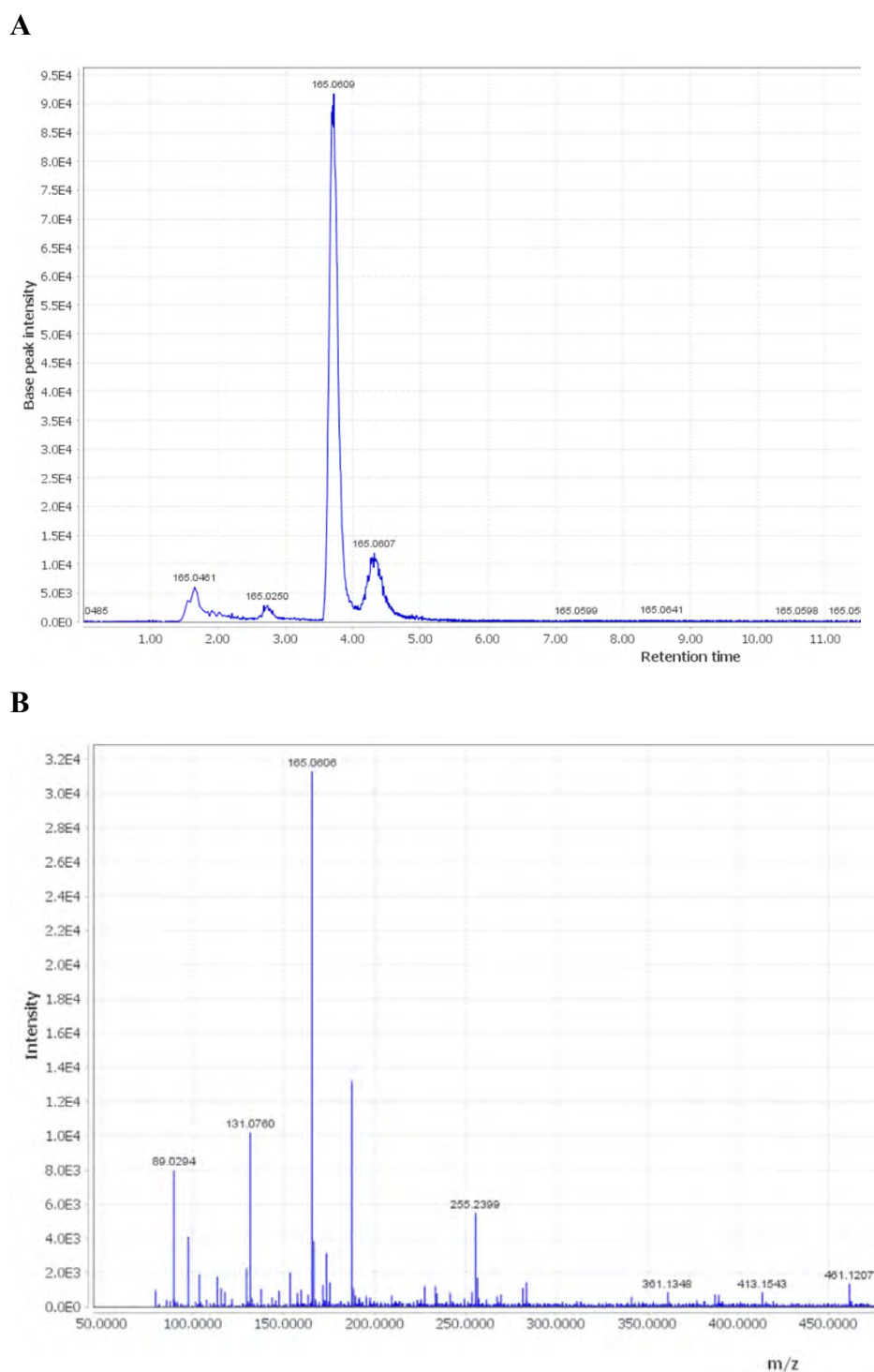


Figure 6.18: HPLC-MS/MS analysis of *p*-coumaric acid released during hydrolysis of 1% (w/v) untreated rice straw by a combination of 66% Xyn11: 33% FAE6. (A) Extracted-ion chromatogram (XIC) for released *p*-coumaric acid. (B) Mass spectrum of *p*-coumaric acid corresponding to the peak observed on XIC.

6.5. Conclusion

This study, for the first time, evaluated the synergistic interactions between two novel metagenome-derived FAEs and commercial xylanases for the co-production of XOS and hydroxycinnamic acids from various substrates. This was performed by first establishing the optimal protein loading ratios of FAE to xylanase through the quantification of FA and XOS release during the degradation of model substrates. The optimised enzyme combination consisted of 66% xylanase to 33% FAE (protein loading). A comparative study was conducted to determine the effect of adding two different families of xylanases to FAEs. The findings indicated that the FAEs, especially FAE5, liberated FA from WAX more efficiently when a GH10 xylanase was added rather than in the presence of a GH11 xylanase. On the other hand, both FAE5 and FAE6 enzymes were capable of significantly improving the performance of a GH11 xylanase for the production of reducing sugars. This would suggest that a GH10 xylanase is more useful than the GH11 xylanase for the release of FA, while the opposite is required for the optimal release of XOS. These findings make it evident that the synergistic interactions of xylanases with FAE5 or FAE6 are dependent on the mode of action of xylanases. The optimised enzyme combinations were also tested on untreated, hydrothermal pre-treated and dilute acid pre-treated agricultural residues. Again, the synergistic cooperation of a GH11 xylanase and FAEs could significantly promote the production of reducing sugars. Hydrothermal and dilute acid pre-treatment, especially of CC and RS, substantially enhanced the production of reducing sugars by the enzyme combinations. This study demonstrated that the efficient production of hydroxycinnamic acids and XOS from various substrates can be achieved through the synergistic action of FAE5 or FAE6 and xylanases.

Chapter 7: General discussion, conclusions, and future recommendations

7.1. General discussion and conclusions

Agricultural residues represent an enormous underutilised bioresource, which has great potential for use as a low-cost feedstock for the production of renewable energy and VAPs. Globally, agricultural residues such as CC, RS and SCB are produced in million tonnes per annum. RS is generated in large quantities worldwide, and it has been estimated that about 731-900 million tons of RS are produced each year (Tye et al., 2016). SCB is the major by-product of the sugar cane industry, and its production is estimated at a global yield of up to 540 million metric tons per year (Bezerra and Ragauskas, 2016). It has also been reported that corn production has reached a global yield of over 800 million tons (Ranum et al., 2014). This makes CC, a by-product of corn, one of the most abundant and attractive agricultural residues.

Given that agricultural residues are abundant and cheap, their exploitation has attracted considerable attention, and extensive research has focused on developing environmentally friendly methods of utilising these residues. In the context of sustainable processing, the application of enzymes has long been considered the most viable strategy for the production of VAPs. However, the efficient enzymatic hydrolysis of these materials presents a significant challenge, primarily due to their structural complexity and heterogeneity. To obtain high product yields, several enzymes working synergistically are required to facilitate efficient enzymatic hydrolysis. This has led to extensive research in the discovery of enzymes with new properties, and formulation of synergistic enzyme cocktails for the efficient conversion of agricultural residues into VAPs. This study evaluated the synergistic interactions between two novel metagenome-derived FAEs and commercially available xylanases for the production of hydroxycinnamic acids and XOS (i.e. industrially relevant chemicals) from untreated and pre-treated agricultural residues.

The metagenomic approach has been used to identify novel FAEs from hindgut prokaryotic symbionts of a termite (*T. trinervoides*) and six novel FAE genes have been discovered (Rashamuse et al., 2014). The functional screening and biochemical characterisation of recombinant FAEs (expressed in an *E. coli* expression system) were also investigated, but the application of these enzymes in lignocellulosic biomass degradation has not yet been explored. In this study, the potential application of two of these newly discovered FAEs in the enzymatic hydrolysis of lignocellulosic biomass was investigated. Firstly, it was important to produce

FAE5 and FAE6 in sufficient yields for use in subsequent application studies. The recombinant FAE5 and FAE6 enzymes were successfully overexpressed in an *E. coli* expression system in a soluble form and purified using His-tag affinity chromatography. SDS-PAGE analysis of recombinant FAE5 and FAE6 indicated that proteins were pure with molecular weights of about 30 kDa and 60 kDa, respectively. Reports on most well characterised FAEs show that the molecular weights of these proteins generally range from 25 to 70 kDa (Nieter et al., 2016; Wong et al., 2019; Antonopoulou et al., 2019). The molecular weights of the expressed recombinant FAEs are well within this range. In addition, the recombinant FAEs were purified to homogeneity and both enzymes appeared to be in their active form. The specific activities of purified FAE5 and FAE6 (28.36 and 27.34 U/mg protein, respectively) were comparable to those of the previous study investigating the specific activities of the same enzymes (Rashamuse et al., 2014). Based on the purity and yields obtained, the recombinant FAEs were deemed suitable for use in activity assays and in the formulation of synergistic enzyme cocktails for the efficient hydrolysis of lignocellulosic biomass.

FAEs are part of the enzyme complex that acts collectively to efficiently hydrolyse heteroxylan to industrially relevant compounds such as XOS and hydroxycinnamic acids (Malgas et al., 2019). The biochemical properties of these enzymes have a significant impact on the bioconversion of heteroxylan. As such, it is important to understand the factors that influence the activities of an individual enzyme. Information regarding the conditions required for optimal enzyme activity is key in developing synergistic enzyme cocktails. The recombinant FAEs were partially characterised along, with two selected commercially available xylanases (XT6 and Xyn11). Based on physico-chemical properties, the findings indicated that the optimal operating conditions for recombinant FAEs were pH 7.0 and a temperature of 40°C. The majority of known FAEs reported in literature show optimal activity in a temperature range of 30 - 60°C (Oliveira et al. 2019). Xyn11 and XT6 both exhibited activity at a broad pH optimum range, retaining high levels of their activities between pH 6.0 and 9.0. The temperature optima for Xyn11 and XT6 were much higher compared to the FAEs, but the enzymes still maintained appreciable levels of activities around 40°C. In addition, the enzymes showed tolerance against the major products that are usually generated from the enzymatic hydrolysis of heteroxylan. The data obtained thus provided a better understanding of the factors that influenced the activities of selected enzymes and allowed the selection of appropriate operating conditions for the synergistic enzymatic hydrolysis of heteroxylan contained in complex substrates.

Prior to enzymatic hydrolysis, pre-treatment of lignocellulosic biomass is required for efficient bioconversion. Pre-treatment is known to enhance the susceptibility of lignocellulosic biomass to enzymatic hydrolysis, by removing the hindrance caused by strong associations between plant cell wall components (Kumari and Singh, 2018). In this study, three complex substrates (CC, RS and SCB) were subjected to two pre-treatment strategies - hydrothermal and dilute sulfuric acid pre-treatment. Because most severe pre-treatment conditions are known to easily solubilise the hemicellulosic fraction of lignocellulosic biomass (Nitsos et al., 2013; Jiang et al., 2018), an extremely low thermo-chemical pre-treatment severity was employed. This was done to ensure that the hemicellulose contents were preserved in the solid fraction while retaining the capacity of pre-treatment to enhance the subsequent enzymatic hydrolysis of the biomass. The data obtained from composition analysis of untreated and pre-treated samples indicated that the majority of xylan content was maintained in pre-treated samples. However, the xylan content of CC was surprisingly lower than the values reported in other studies (28%) (Da Silva et al., 2015). The variation in chemical composition may be attributed to a plant's genotype, the time taken for the crop to mature, climatic effects, or other causes. The data also showed that the hydroxycinnamic content in pre-treated samples was not significantly different compared to that in the untreated samples. Furthermore, the FTIR spectra of the untreated samples and pre-treated samples were compared. The findings revealed that the intensities of bands (1730 and 1240 cm^{-1}) which are mainly attributed to the hemicellulose component were relatively similar in all samples, indicating that the hemicellulosic fraction was retained in the pre-treated solids. The efficiency of the pre-treatments was then evaluated by studying changes in the microscopic surfaces of untreated and pre-treated samples through SEM analysis. Changes in the surface morphology due to pre-treatment were observed and these are associated with increased surface area of pre-treated samples. The presence of such structural changes was an indication that the pre-treatments were more likely to enhance the enzyme hydrolysis of the pre-treated samples.

A pre-treatment step is necessary for achieving the highly efficient bioconversion of lignocellulosic biomass into VAPs. However, a side effect of pre-treatment is the formation of lignocellulose-derived by-products which could potentially affect enzymes. Therefore, it was important to evaluate the inhibitory effects of individual known pre-treatment by-products on the activities of FAE5 and FAE6, because these enzymes have never been applied to the enzymatic hydrolysis of pre-treated substrates. This study revealed that FAEs were not significantly affected by the presence of sugar degradation products (furfural and HMF). On

the other hand, lignin and its degradation products appeared to inhibit the enzymes in a concentration dependent manner. There is very little information available on the inhibition of FAEs by pre-treatment by-products. Information on the inhibitory effects of lignin degradation products is mostly available for cellulases, xylanases and mannanolytic enzymes (de Souza Moreira et al., 2013; Mhlongo et al., 2015; Malgas et al., 2016, Mathibe et al., 2020). In order to gain a better understanding of the interactions between lignin degradation products and FAEs, the mode of inhibition was assessed by determining the enzymatic inhibition parameters. The data showed that the mode of inhibition displayed by lignin and vanillin was mixed in nature. Mixed inhibition is reported to occur when an inhibitor binds to both the free enzyme and the enzyme-substrate complex, but with greater affinity for one state. In this case, it appears as if both inhibitors may favour the free enzyme because the K_M values of FAEs increased with concentration of inhibitors. It is likely that the manner of inhibition reflects non-productive binding of FAE5 and FAE6 on to these compounds. The non-productive binding of enzymes onto lignin has been reported as the main mechanism behind interactions between enzymes and lignin (dos Santos et al., 2019). This implies that the inhibitory effect of these compounds may be limited by a lignin-blocking agent such as BSA. Following the evaluation of inhibitory properties of individual pre-treatment by-products, the effects of wash liquors from pre-treated agricultural residues were also determined. The results indicated that the selected enzymes were not significantly affected by wash liquors generated from all three pre-treated agricultural residues. This was expected, because the low thermo-chemical pre-treatment severity used in this study was unlikely to generate high concentrations of pre-treatment by-products. In addition, all the pre-treated samples were subsequently washed with water which may have removed the majority of water-soluble inhibitors. Overall, the obtained data provided a better understanding of the interactions between FAEs and the pre-treatment by-products this may potentially contribute towards the development of improved strategies to limit the inhibitory effects of lignin and its degradation products.

In order to study the synergistic interactions between recombinant FAEs and xylanases on untreated and pre-treated complex substrates, the enzymes were first tested for their ability to release FA and XOS from model substrates. WAX is a well-known model substrate and several studies have reported that the xylanases can cooperate with FAEs to enhance the quantities of FA and XOS released from this substrate (Dilokpimol et al., 2017; Makela et al., 2018; Wang et al., 2020). The present study demonstrated that recombinant FAE5 and FAE6 could release FA from WAX only in the presence of a xylanase. This would suggest that the main mechanism

by which xylanase contributes to FA production is by generating short chain feruloylated XOS, which are preferred substrates for the recombinant FAEs. An enzyme combination of 66% xylanase and 33% FAE produced the highest amount of FA and it was selected as the optimum protein loading ratio for subsequent synergy studies.

Following optimisation of the FAE-xylanase enzyme cocktail, a comparative study was conducted in order to determine the effect of adding two different families of xylanases to the recombinant FAEs. Various studies have shown that GH10 and GH11 xylanases differ considerably in their catalytic mechanisms on heteroxylan (Paës et al., 2012; Biely et al., 2016; Gong et al., 2016). Therefore, adding these two different families of xylanases may provide a better interpretation of the synergistic interactions between recombinant FAEs and xylanases. The results indicated that the GH10 xylanase performed better with both FAE5 and FAE6 in releasing FA, compared to the GH11 xylanase. FAE5 and FAE6 released FA 9.03-fold and 2.31-fold more efficiently in the presence of GH10 xylanase, than when GH11 xylanase was added. Wong and co-workers (2013) have also evaluated the effect of adding two different families of xylanases to RuFae2 and demonstrated that RuFae2 worked more effectively with a GH10 xylanase in generating FA from WAX. The advantage of using GH10 xylanase in the release of FA could be attributed to its ability to tolerate side decorations on the xylan main chain, producing short feruloylated XOS, which are preferred substrates for FAEs. The amount of XOS released from WAX by enzyme combinations was also measured. The data indicated that both FAE5 and FAE6 substantially improved the release of XOS by the GH11 xylanase, but did not significantly affect the activity of the GH10 xylanase. This was expected because GH11 xylanases are known to prefer less decorated regions of the xylan main chain, therefore, removal of FA by FAEs may have improved the accessibility of GH11 xylanase to XOS for further hydrolysis. This study demonstrated that recombinant FAE5 and FAE6 could act synergistically with xylanases in the co-production of FA and XOS from WAX. The findings also highlighted the importance of considering different xylanase families when evaluating synergism between FAEs and xylanases.

The conversion of xylan, the most abundant type of hemicellulose, into VAPs by enzymatic means has emerged as the most prominent technology for the use of a variety of underutilised agricultural residues (Samanta et al., 2015; Poletto et al., 2020). As mentioned previously, the efficient enzymatic hydrolysis of heteroxylan in complex substrates requires the synergistic action of xylanolytic enzymes. In the present study, FAE-xylanase enzyme cocktails developed during the hydrolysis of model substrates were tested for their ability to release XOS and

hydroxycinnamic acids from untreated and pre-treated agricultural residues (CC, RS and SCB). Only GH11 xylanase (Xyn11) was used on agricultural residues because GH10 xylanase displayed extremely poor catalytic activity towards these substrates. It has been reported that GH10 xylanases have higher molecular weights, which limit their ability to penetrate the cell wall matrix, making them less efficient in degrading insoluble xylan (Falck et al., 2014). From the reducing sugar data obtained, two observations about these enzyme cocktails were made: Firstly, enzyme combinations of Xyn11 and FAE5 or FAE6 substantially facilitated an increase in the release of reducing sugars from all the substrates, compared to when Xyn11 was used alone. Secondly, both the hydrothermal and dilute acid pre-treatment strategies enhanced the enzymatic hydrolysis of CC and RS, but not SCB. It can be speculated that the variation in enzymatic hydrolysis of pre-treated substrates may be due to compositional and structural differences. It has been reported that CC contains a high percentage of cellulose (35-45.6%), hemicellulose (36.9-40%) and low lignin content (5-20%) (Boonchuay et al., 2014; Brar et al., 2016). On the other hand, SCB is generally known for containing significantly high lignin content (29.1%) (Sakdaronnarong et al., 2014). Lignin is a crucial barrier of glycosyl hydrolase accessibility toward polysaccharides in lignocellulosic biomass. Therefore, it is possible that pre-treatments were more effective on those substrates which contained less lignin. Furthermore, the mechanism of synergism was examined by analysing the hydrolysis products of Xyn11 and associated enzyme combinations. The data revealed that enzyme combinations of Xyn11 with FAE5 or FAE6 released XOS with a low DP (DP 4-6 and mainly xylobiose) from untreated and pre-treated samples. The high yield of xylobiose produced by the enzyme combinations is an indication that cleavage of hydroxycinnamic acids by FAEs allows further hydrolysis of longer XOS by Xyn11. The capacity of the FAE-xylanase enzyme cocktail to specifically generate XOS with a low DP from agricultural residues is very attractive for several biotechnological applications, because low DP XOS are known for their prebiotic properties (Singh et al., 2018; Amorim et al., 2019).

The release of hydroxycinnamic acids from untreated and pre-treated agricultural residues by the cooperative action of Xyn11 and FAE5 or FAE6 was also investigated. The data indicated that only small fraction of FA and *p*-CA could be recovered from the substrates by enzymatic hydrolysis. There are a number of likely explanations for this low efficiency of the FAE-xylanase cocktail for the release of FA and *p*-CA. Firstly, the results from the enzymatic hydrolysis of model substrates clearly demonstrated that FAE5 and FAE6 can only cleave ester linkages from XOS generated by xylanases but not from the xylan polymer. The inability of

Xyn11 to act on a substituted xylan main chain would result in XOS with a small number of ester linkages for FAEs to cleave. This, in turn, would lead to the production of low yields of hydroxycinnamic acids. Secondly, hydroxycinnamic acids, particularly FA, are usually found esterified to polysaccharides and also in ether-linkages with lignin or dimerized with other hydroxycinnamic acids (Oliveira et al., 2019). FAEs are known for specifically catalysing the hydrolysis ester bonds between FA and polysaccharides, but not the ether-linkages. The presence of ether-linkages is likely to be an additional restriction to the release of hydroxycinnamic acids. Even though the quantities of FA and *p*-CA released from untreated and pre-treated residues were relatively small, the action of FAEs was still able to substantially enhance the activity of Xyn11 for the production of XOS.

In conclusion, the findings from this study demonstrated that the co-production of hydroxycinnamic acids and XOS from various xylan-rich substrates can be achieved, based on the synergistic associations that exist between novel termite metagenome-derived FAEs and commercially available xylanases. This work paves the way towards the development of synergistic enzyme cocktails, with higher performance, for the efficient production of VAPs from lignocellulosic materials.

7.2. Future recommendations

In this study, an enzyme cocktail composed of recombinant FAEs and xylanases, was developed, and the synergistic mechanism by which these enzymes promote the hydrolysis of heteroxylan, was elucidated. Information generated in the present study lays the foundation for future studies for a better understanding of the cooperative manner between these enzymes. Some future recommendations for addressing some of the challenges encountered in this study are suggested below:

7.2.1. It was demonstrated that lignin and its degradation products have potential inhibitory effects on the activities of the recombinant FAEs. The precise mechanisms of inhibition of these compounds on the two FAE enzymes are still unclear. In addition to kinetic parameters, bioinformatic modelling and circular dichroism (CD) spectroscopy could be used to assess the influence of lignin and its degradation products on the two-dimensional structure of FAEs and provide useful insights into the mode of inhibition. This information would be useful for the development of strategies for minimising the effects of these compounds on enzymes during the degradation of pre-treated complex substrates.

7.2.2. This study noted that both recombinant FAEs could only release FA from feruloylated XOS generated by xylanases. Understanding the preferred substrate size for FAEs would be beneficial in better understanding the influence of substrate characteristics on these enzymes. This could be conducted by generating feruloylated XOS of varying DP using xylanases, and purifying them using methods such as column chromatography. Characterisation of purified XOS and FAE end reaction products could be performed using HPLC-MS analysis and nuclear magnetic resonance (NMR) spectroscopy.

7.2.3. This study also demonstrated that FAE-xylanase enzyme cocktails could be applied for the hydrolysis of arabinoxylan in complex substrates. There is still room for improving the yields of products generated from these substrates. High product yields can be increased by following a bioconversion process that involves extraction of arabinoxylan, followed by synergistic enzymatic hydrolysis. This approach is likely to generate high quantities of hydroxycinnamic acids and XOS. This could then allow for the assessment of potential antioxidant properties of hydroxycinnamic acids and prebiotic properties of XOS.

References

- Aachary, A. A. and Prapulla, S. G. (2010). Xylooligosaccharides (XOS) as an emerging prebiotic: Microbial synthesis, utilization, structural characterization, bioactive properties, and applications. *Compr. Rev. Food Sci. Food Saf.* 10, 2-16.
- Abbott, J.C., Barakate, A., Pincon, G., Legrand, M., Lapierre, C., Mila, I., Schuch, W. and Halpin, C. (2002). Simultaneous suppression of multiple genes by single transgenes. Down-regulation of three unrelated lignin biosynthetic genes in tobacco. *Plant Physiol.* 128, 844-853.
- Aboagye, D., Banadda, N., Kambugu, R., Seay, J., Kiggundu, N., Zziwa, A. and Kabenge, I. (2017). Glucose recovery from different corn stover fractions using dilute acid and alkaline pretreatment techniques. *J. Ecol. Environ.* 41, 26.
- Aguilar-Hernandez, I., Afseth, N. K., Lopez-Luke, T., Contreras-Torres, F., Wold, J. P. and Ornelas-Soto, N. (2017). Surface enhanced Raman spectroscopy of phenolic antioxidants: a systematic evaluation of ferulic acid, *p*-coumaric acid, caffeic acid and sinapic acid. *Vib spectrosc.* 89, 112-122.

Altschul, S. F., Madden, T. S., Schaffer, A. A., Zhang, J., Zhang, Z., Miller, W. and Lipman, D. J. (1997). Gapped BLAST and PSI-BLAST: a new generation of protein database search programs. *Nucleic Acids Res.* 25, 3389-3402.

Amin, F. R., Khalid, H., Zhang, H., Rahman, S., Zhang, R., Liu, G. and Chen, C. (2017). Pretreatment methods of lignocellulosic biomass for anaerobic digestion. *AMB Expr.* 7, 72.

Amiri, H. and Karimi, K. (2015). Improvement of acetone, butanol, and ethanol production from woody biomass by using organosolv pretreatment. *Bioprocess Biosyst. Eng.* 38, 1959-1972.

Amorim, C., Silvério, S. C., Prather, K. L. J. and Rodrigues, L. R. (2019). From lignocellulosic residues to market: production and commercial potential of xylooligosaccharides, *Biotechnol. Adv.* 37, 107397.

An, S., Li, W., Liu, Q., Xia, Y., Zhang, T., Huang, F., Lin, Q. and Chen, L. (2018). Combined dilute hydrochloric acid and alkaline wet oxidation pretreatment to improve sugar recovery of corn stover. *Bioresour. Technol.* 271, 283-288.

Anand, A., Kumar, V. and Satyanarayana, T. (2013). Characteristics of thermostable endoxylanase and β -xylosidase of the extremely thermophilic bacterium *Geobacillus thermodenitrificans* TSAA1 and its applicability in generating xylooligosaccharides and xylose from agro-residues. *Extremophiles* 17, 357-366.

Andersen, K. R., Leksa, N. C. and Schwartz, T. U. (2013). Optimized *E. coli* expression strain LOBSTR eliminates common contaminants from His-tag purification. *Proteins* 81, 1857-1861.

Andlar, M., Rezić, T., Mardetko, N., Kracher, D., Ludwig, R. and Šantek, B. (2018). Lignocellulose degradation: an overview of fungi and fungal enzymes involved in lignocellulose degradation. *Eng. Life Sci.* 11, 768-778.

Andrić, P., Meyer, A. S., Jensen, P. A. and Dam-Johansen, K. (2010). Reactor design for minimizing product inhibition during enzymatic lignocellulose hydrolysis II. Quantification of inhibition and suitability of membrane reactors. *Biotechnol. Adv.* 28, 407-425.

Antonopoulou, I., Iancu, L., Jutten, P., Piechot, A., Rova, U. and Christakopoulos, P. (2019). Screening of novel feruloyl esterases from *Talaromyces wortmannii* for the development of efficient and sustainable syntheses of feruloyl derivatives. *Enzyme. Microb. Technol.* 120, 124-135.

- Appeldoorn, M. M., de Waard, P., Kabel, M. A., Gruppen, H. and Schols, H. A. (2013). Enzyme resistant feruloylated xylooligomer analogues from thermochemically treated corn fiber contain large side chains, ethyl glycosides and novel sites of acetylation. *Carbohydr Res.* 381, 33-42.
- Arevalo-Gallegos, A. Ahmad, Z., Asgher, M., Parra-Saldivar, R. and Iqbal, H. M. (2017). Lignocellulose: a sustainable material to produce value-added products with a zero waste approach-A review. *Int. J. Biol. Macromol.* 99, 308-318.
- Azeri, C., Tamer, A. U. and Oskay, M. (2010). Thermoactive cellulase-free xylanase production from alkaliphilic *Bacillus* strains using various agro-residues and their potential in biobleaching of kraft pulp. *Afr. J. Biotechnol.* 9(1), 63-72.
- Barakat, A., Mayer, C., Solhy, A., Arancon, R. A. D., De Vries, H., Luque, R., Barakat, A., Mayer, C., Solhy, A., Arancon, R. A. D. and De Vries, H. (2014). Mechanical pretreatments of lignocellulosic biomass: towards facile and environmentally sound technologies for biofuels production. *RSC Adv.* 4, 48109-48127.
- Behera, S., Arora, R., Nandhagopal, N. and Kumar, S. (2014). Importance of chemical pretreatment for bioconversion of lignocellulosic biomass. *Renew. Sustain. Energy Rev.* 36, 91-106.
- Belorkar, S. A. and Gupta, A. K. (2016). Oligosaccharides: a boon from nature's desk. *AMB Express* 6 (1), 82.
- Benoit, I., Danchin, E. G., Bleichrodt, R. J. and de Vries, R. P. (2008). Biotechnological applications and potential of fungal feruloyl esterases based on prevalence, classification and biochemical diversity. *Biotechnol. Lett.* 30 (3), 387-396.
- Bezerra, T. L. and Ragauskas, A. J. (2016). A review of sugarcane bagasse for second-generation bioethanol and biopower production. *Biofuels Bioprod. Bioref.* 10, 634-647.
- Bhardwaj, N., Kumar, B. and Verma, P. (2019). A detailed overview of xylanases: an emerging biomolecule for current and future prospective Bioresour. *Bioprocess.* 6, 40.
- Bhatia, L., Sharma, A., Bachheti, R. K. and Chandel, A. K. (2019). Lignocellulose derived functional oligosaccharides: production, properties, and health benefits. *Prep. Biochem. Biotechnol.* 49, 744-758.

Biely, P. (2012). Microbial carbohydrate esterases deacetylating plant polysaccharides. *Biotechnol. Adv.* 30, 1575-1588.

Biely, P., Singh, S. and Puchart, V. (2016). Towards enzymatic breakdown of complex plant xylan structures: state of the art. *Biotechnol Adv.* 34, 1260-1274.

Block, H., Maertens, B., Spriestersbach, A., Brinker, N., Kubicek, J., Fabis, R., Labahn, J. and Schafer, F. (2009). Immobilized-metal affinity chromatography (IMAC): a review. *Methods Enzymol.* 463, 439-473.

Boerjan, W., Ralph, J. and Baucher, M. (2003). Lignin biosynthesis. *Annu Rev Plant Biol.* 166, 63-71.

Bonfiglio, F., Cagno, M., Rey, F., Torres, M., Böthig, S., Menéndez P. and Mussatto, S. I. (2019). Pretreatment of switchgrass by steam explosion in a semi-continuous pre-pilot reactor. *Biomass Bioenerg.* 121, 41-47.

Boonchuay, P., Techapun, C., Seesuriyachan P. and Chaiyaso, T. (2014). Production of xylooligosaccharides from corncob using a crude thermostable endo-xylanase from *Streptomyces thermovulgaris* TISTR1948 and prebiotic properties. *Food Sci. Biotechnol.* 23, 1515-1523.

Boukari, I., O'Donohue, M., Rémond, C. and Chabbert, B. (2011). Probing a family GH11 endo- β -1,4-xylanase inhibition mechanism by phenolic compounds: role of functional phenolic groups. *J. Mol. Catal., B Enzym.* 72, 130-138.

Brachet, M., Arroyo, J., Cazals, A., Bannelier, C. and Fortun-Lamothe, L. (2015). Hydration capacity: a new criterion for feed formulation. *Anim. Feed Sci. Technol.* 209, 174-185.

Bradford, M. M. (1976). A rapid and sensitive method for the quantitation of microgram quantities of protein utilizing the principle of protein-dye binding. *Anal. Biochem.* 72, 248-254.

Bragatto, J., Segato, F. and Squina, F. M. (2013). Production of xylooligosaccharides (XOS) from delignified sugarcane bagasse by peroxide-HAc process using recombinant xylanase from *Bacillus subtilis*. *Ind. Crops Products* 51, 123-129.

- Brar, K. K., Kaur S. and Chadha, B. S. (2016). A novel staggered hybrid SSF approach for efficient conversion of cellulose/hemicellulosic fractions of corncob into ethanol. *Renew. Energy* 98, 16-22.
- Britton, H. T. S. and Robinson, R. A. (1931). Universal buffer solutions and the dissociation constant of veronal. *J. Chem. Soc.* 1, 1456-1462.
- Brown, M. E. and Chang, M. C. Y. (2014). Exploring bacterial lignin degradation. *Curr. Opin. Chem. Biol.* 19, 1-7.
- Bruno, E. L. B., Diego, R. S. L., Oscar, F. H. A., Leandro, V. A. G. and Sérgio, F. D. A. (2016). Optimization of sugarcane bagasse autohydrolysis for methane production from hemicellulose hydrolyzates in a biorefinery concept. *Bioresour Technol*, 200,137-146.
- Cao, L. C., Chen, R., Xie, W. and Liu, Y. H. (2015). Enhancing the thermostability of feruloyl esterase EstF27 by directed evolution and the underlying structural basis. *J. Agric. Food Chem.* 63 (37), 8225-8233.
- Cao, S., Pu, Y., Studer, M., Wyman, C. and Ragauskas, A. J. (2012). Chemical transformations of *Populus trichocarpa* during dilute acid pretreatment. *RSC Adv.* 2, 10925-10936.
- Carvalho, A. F. A., Marcondes, W. F., de Oliva Neto, P., Pastore, G. M., Saddler, J. N. and Arantes, V. (2018). The potential of tailoring the conditions of steam explosion to produce xylo-oligosaccharides from sugarcane bagasse. *Bioresour. Technol.* 250, 221-229.
- Chandel, A. K., Garlapati, V. K., Singh, A. K., Antunes, F. A. F. and da Silva, S. S. (2018). The path forward for lignocellulose biorefineries: bottlenecks, solutions, and perspective on commercialization. *Bioresour. Technol.* 264, 370-381.
- Chandra, C. S. J., George, N. and Narayanankutty, S. K. (2016). Isolation and characterization of cellulose nanofibrils from arecanut husk fibre. *Carbohydr. Polym.* 142, 158-166.
- Chandra, R., Takeuchi, H. and Hasegawa, T. (2012). Methane production from lignocellulosic agricultural crop wastes: a review in context to second generation of biofuel production. *Renew Sustain Energy Rev*, 16, 1462-1476.
- Chen, H., Liu, J., Chang, X., Chen, D., Xue, Y., Liu, P., Lin, H. and Han, S. (2017). A review on the pretreatment of lignocellulose for high-value chemicals. *Fuel Process. Technol.* 160, 196-206.

- Chen, W. -H., Lin, Y. -Y., Liu, H. -C., Chen, T.-C., Hung, C. -H., Chen, C. -H. and Ong, H. C. (2019). A comprehensive analysis of food waste derived liquefaction bio-oil properties for industrial application. *Appl. Energy*, 237, 283-291.
- Cheung, R. C., Wong, J. H. and Ng, T. B. (2012). Immobilized metal ion affinity chromatography: a review on its applications. *Appl. Microbiol. Biotechnol.* 96, 1411-1420.
- Chio, C., Sain, M., Qin, W. (2019). Lignin utilization: a review of lignin depolymerization from various aspects. *Renew. Sustain. Energy Rev.* 107, 232-249.
- Collins, T., Gerday, C. and Feller, G. (2005). Xylanases, xylanase families and extremophilic xylanases. *FEMS Microbiol. Rev.* 29, 3-23.
- Cotana, F., Cavalaglio, G., Gelosia, M., Nicolini, A., Coccia, V. and Petrozzi, A. (2014). Production of bioethanol in a second-generation prototype from pine wood chips. *Energy Proc.* 45, 42-51.
- Crepin, V. F., Faulds, C. B. and Connerton, I. F. (2004). Functional classification of the microbial feruloyl esterases. *Appl. Microbiol. Biotechnol.* 63 (6), 647-652.
- da Silva, J. C., De Oliveira, R. C., Neto, A. D. S., Pimentel, V. C. and Santos, A. D. A. D. (2015). Extraction, addition and characterization of hemicelluloses from corn cobs to development of paper properties. *Procedia Mater. Sci.* 8, 793-801.
- da Silva, A. S., Inoue, H., Endo, T., Yano, S. and Bon, E. P. S. (2010). Milling pretreatment of sugarcane bagasse and straw for enzymatic hydrolysis and ethanol fermentation. *Bioresour. Technol.* 101, 7402-7409.
- da Silva, P. O., de Alencar Guimarães, N. C., Serpa, J. D. M., Masui, D. C., Marchetti, C. R., Verbisck, N. V., Zanoelo, F. F., Ruller, R. and Giannesi, G. C. (2019). Application of an endo-xylanase from *Aspergillus japonicus* in the fruit juice clarification and fruit peel waste hydrolysis. *Biocatal. Agric. Biotechnol.* 21, 101312.
- Dahadha, S., Amin, Z., Bazyar Lakeh, A. A. and Elbeshbishy, E. (2017). Evaluation of different pretreatment processes of lignocellulosic biomass for enhanced biomethane production. *Energy Fuels.* 31, 10335-10347.
- Daly, R. and Hearn, M. T. (2005). Expression of heterologous proteins in *Pichia pastoris*: a useful experimental tool in protein engineering and production. *J. Mol. Recognit.* 18, 119-138.

- Damasio, A. R. L., Braga, C. M. P., Brenelli, L. B., Citadini, A. P., Mandelli, F., Cota, J., de Almeida, R. F., Salvador, V. H., Paixao, D. A. A., Segato, F., Mercadante, A. Z., de Oliveira Neto, M., do Santos, W. D. and Squina, F. M. (2013). Biomass-to-bio-products application of feruloyl esterase from *Aspergillus clavatus*. *Appl. Microbiol. Biotechnol.* 97(15), 6759-6767.
- Daza Serna, L. V., Orrego Alzate, C. E. and Alzate, C. A. C. (2016). Supercritical fluids as a green technology for the pretreatment of lignocellulosic biomass. *Bioresour. Technol.* 199, 113-120.
- De Souza Moreira, L. R., De Carvalho Campos, M., De Siqueira, P. H. V. M., Silva, L. P., Ricart, C. A. O., Martins, P. A., Queiroz, R. M. L. and Filho, E. X. F. (2013). Two β -xylanases from *Aspergillus terreus*: characterization and influence of phenolic compounds on xylanase activity. *Fungal Genet. Biol.* 60, 46-52.
- Dilokpimol, A., Mäkelä, M. R., Aguilar-Pontes, M. V., Benoit-Gelber, I., Hilden, K. S. and de Vries, R. P. (2016). Diversity of fungal feruloyl esterases: updated phylogenetic classification, properties, and industrial applications. *Biotechnol. Biofuels* 9, 231.
- Dilokpimol, A., Makela, M. R., Mansouri, S., Belova, O., Waterstraat, M., Bunzel, M., de Vries, R. P. and Hilden, K.S., (2017). Expanding the feruloyl esterase gene family of *Aspergillus niger* by characterization of a feruloyl esterase. *FaeC. N. Biotechnol.* 37, 200-209.
- Dong, M., Wang, S., Xu, F., Wang, J., Yang, N., Li, Q., Chen, J. and Li, W. (2019). Pretreatment of sweet sorghum straw and its enzymatic digestion: insight into the structural changes and visualization of hydrolysis process. *Biotechnol Biofuels* 12, 276.
- Donohoe, B. S., Vinzant, T. B., Elander, R. T., Pallapolu, V.R., Lee, Y. Y., Garlock, R. J., Balan, V., Dale, B. E., Kim, Y., Mosier, N. S., Ladisch, M. R., Falls, M., Holtzapple, M. T., Sierra-Ramirez, R., Shi, J., Ebrik, M. A., Redmond, T., Yang, B., Wyman, C. E., Hames, B., Thomas, S., Warner, R. E., (2011). Surface and ultrastructural characterization of raw and pretreated switchgrass. *Bioresour. Technol.* 102, 11097-11104.
- dos Santos, A. C., Ximenes, E., Kim, Y. and Ladisch, M. R. (2019). Lignin-enzyme interactions in the hydrolysis of lignocellulosic biomass. *Trends Biotechnol.* 37, 518-531.
- Driss, D., Bhiri, F., Elleuch, L., Bouly, N., Stals, I., Miled, N., Blibech, M., Ghorbel, R. and Chaabouni, S. E. (2012). Purification and properties of an extracellular acidophilic endo-1, 4-

b-Xylanase, naturally deleted in the “thumb”, from *Penicillium occitanis* Pol6. Proc. Biochem. 46, 1299-1306.

Durazzo, A., Lucarini, M., Souto, E. B., Cicala, C. Caiazzo, E. Izzo, A. A., Novellino, E. and Santini, A. (2019). Polyphenols: A concise overview on the chemistry, occurrence, and human health. *Phytother. Res.* 33, 2221-2243.

Ebringerova, A., Hromadkova, Z., Heinze, T. (2005). Hemicellulose. In: Heinze, T. (Ed.) *Adv. Polym. Sci.* 186 (Polysaccharides I: Structure, Characterization and Use. Springer- Verlag, Berlin Heidelberg, Germany 1-67.

Ezeilo, U. R., Zakaria, I. I., Huyop, F. and Wahab, R. A. (2017). Enzymatic breakdown of lignocellulosic biomass: the role of glycosyl hydrolases and lytic polysaccharide monooxygenases. *Biotechnol. Biotechnol. Equip.* 31, 647-662.

Falck, P., Aronsson, A., Grey, C., Stalbrand, H., Nordberg Karlsson, E. and Adlercreutz, P. (2014). Production of arabinoxylan-oligosaccharide mixtures of varying composition from rye bran by a combination of process conditions and type of xylanase. *Bioresour. Technol.* 174, 118-125.

Faulds, C. B. (2010). What can feruloyl esterases do for us? *Phytochem. Rev.* 9, 121-132.

Ferreira, P. S., Victorelli, F. D., Fonseca-Santos, B. and Chorilli, M. (2018). A review of analytical methods for *p*-coumaric acid in plant-based products, beverages, and biological matrices. *Crit. Rev. Anal. Chem.* 49(1), 21-31.

Florencio, C., Badino, A. C. and Farinas, C. S. (2016). Soybean protein as a cost-effective lignin-blocking additive for the saccharification of sugarcane bagasse. *Bioresour. Technol.* 221, 172-180.

Froger, A. and Hall, J. E. (2007). Transformation of plasmid DNA into *E. coli* using the heat shock method. *J. Vis. Exp.* 6, 253.

Furuya, T., Kuroiwa, M. and Kino, K., (2017). Biotechnological production of vanillin using immobilized enzymes. *J. Biotechnol.* 243, 25-28.

Gabhane, J., Prince William, S. P. M., Vaidya, A. N., Das, S. and Wate, S. R. (2015). Solar assisted alkali pretreatment of garden biomass: effects on lignocellulose degradation, enzymatic hydrolysis, crystallinity and ultra-structural changes in lignocellulose. *Waste Manag.* 40, 92-99.

- Gasteiger, E., Hoogland, C., Gattiker, A., Duvaud, S., Wilkins, M. R., Appel, R. D. and Bairoch, A. (2005). Protein identification and analysis tools on the ExPASy server; (In) John M. Walker (ed): The proteomics protocols handbook, Humana Press 571-607.
- Gatenholm P. and Tenkanen M. (2003). Hemicelluloses: science and technology. In: Gatenholm P, Tenkanen M, editors. ACS Symposium Series. American Chemical Society 2-22.
- Giummarella, N., Pu, Y., Ragauskas, A. J. and Lawoko, M. (2019). A critical review on the analysis of lignin carbohydrate bonds in plants. *Green Chem.* 21, 1573–1595.
- Goldstone, D. C., Villas-Bôas, S. G., Till, M., Kelly, W. J., Attwood, G. T. and Arcus, V. L. (2010). Structural and functional characterization of a promiscuous feruloyl esterase (Est1E) from the rumen bacterium *Butyrivibrio proteoclasticus*. *Proteins* 78, 1457-1469.
- Gong, W., Zhang, H., Tian, L., Liu, S., Wu, X., Li, F. and Wang, L. (2016). Determination of the modes of action and synergies of xylanases by analysis of xylooligosaccharide profiles over time using fluorescence-assisted carbohydrate electrophoresis. *Electrophoresis* 37, 1640-1650.
- Gopalan, N., Rodríguez-Duran, L., Saucedo-Castaneda, G. and Nampoothiri, K. M. (2015). Review on technological and scientific aspects of feruloyl esterases: a versatile enzyme for biorefining of biomass. *Biores. Technol.* 193, 534-544.
- Guerriero, G., Hausman, J. F., Strauss, J., Ertan, H. and Siddiqui, K. S. (2016). Lignocellulosic biomass: biosynthesis, degradation, and industrial utilization. *Eng. Life Sci.* 16, 1-16.
- Hegazy, U. M., El-Khonezy, M.I., Shokeer, A., Abdel-Ghany, S. S., Bassuny, R. I., Barakat, A. Z., Salama, W. H., Azouz, R. A. M. and Fahmy, A. S. (2019). Revealing of a novel xylose-binding site of *Geobacillus stearothermophilus* xylanase by directed evolution. *J. Biochem.* 165(2), 177-84.
- Hermoso, J. A., Sanz-Aparicio, J., Molina, R., Juge, N., Gonzalez, R. and Faulds, C. B. (2004). The crystal structure of feruloyl esterase A from *Aspergillus niger* suggests evolutive functional convergence in feruloyl esterase family. *J. Mol. Biol.* 338, 495-506.
- Hu, F. and Ragauskas, A. (2012). Pretreatment and lignocellulosic chemistry. *Bioenerg. Res.* 5, 1043-1066.
- Huang, Y. -F., Chiueh, P. -T. and Lo, S. -L. (2016). A review on microwave pyrolysis of lignocellulosic biomass. *Sustain. Environ. Res.* 26, 103-109.

- Hunt, C. J., Tanksale, A. and Haritos, V. S. (2016). Biochemical characterization of a halotolerant feruloyl esterase from *Actinomyces spp.*: refolding and activity following thermal deactivation. *Appl. Microbiol. Biotechnol.* 100 (4), 1777-1787.
- Isikgor, F. H. and Becer, C. R. (2015). Lignocellulosic biomass: a sustainable platform for the production of bio-based chemicals and polymers. *Polym. Chem.* 6, 4497-4559.
- Ivo, A. N., Chao, L., Bing, W., Liang, X., Zili, Y. and Jing, L. (2016). Physico-chemical pretreatments for improved methane potential of *Miscanthus lutarioriparius*. *Fuel* 166, 29-35.
- Jalak, J., Kurašin, M., Teugjas, H. and Väljamä, P. (2012). Endo-exo synergism in cellulose hydrolysis revisited. *J. Biol. Chem.* 287, 28802-28815.
- Jhamb, K. and Sahoo, D. K. (2012). Production of soluble recombinant proteins in *Escherichia coli*: effects of process conditions and chaperone co-expression on cell growth and production of xylanase. *Bioresour. Technol.* 123, 135-143.
- Ji, W., Shen, Z. and Wen, Y. (2015). Hydrolysis of wheat straw by dilute sulfuric acid in a continuous mode. *Chem. Eng. J.* 260, 20-27.
- Jiang, K. K., Li, L. L., Long, L. K. and Ding, S. J. (2018). Comprehensive evaluation of combining hydrothermal pretreatment (autohydrolysis) with enzymatic hydrolysis for efficient release of monosaccharides and ferulic acid from corn bran. *Ind. Crop Prod.* 113, 348-357.
- Jommuengbout, P., Pinitglang, S., Kyu, K. L. and Ratanakhanokchai, K. (2009). Substrate-binding site of Family 11 xylanase from *Bacillus firmus* K-1 by molecular docking. *Biosci. Biotech. Bioch.* 73, 833-839.
- Jonathan, M. C., DeMartini, J. Van Stigt Thans, S., Hommes, R. and Kabel, M. A. (2017). Characterisation of non-degraded oligosaccharides in enzymatically hydrolysed and fermented, dilute ammonia-pretreated corn stover for ethanol production. *Biotechnol. Biofuels* 10, 112.
- Jönsson, L. J. and Martín, C. (2016). Pretreatment of lignocellulose: formation of inhibitory by-products and strategies for minimizing their effects. *Bioresour. Technol.* 199, 103-112.
- Juturu, V. and Wu, J. C. (2012). Microbial xylanases: engineering, production and industrial applications. *Biotechnol. Adv.* 30, 1219-1227.

- Juturu, V. and Wu, J. C. (2018). Heterologous protein expression in *Pichia pastoris*: Latest research progress and applications. *Chembiochem*. 19, 7-21.
- Kapoor, M. Soam, S., Agrawal, R., Gupta, R. P., Tuli, D. K. and Kumar, R. (2017). Pilot scale dilute acid pretreatment of rice straw and fermentable sugar recovery at high solid loadings. *Bioresour. Technol.* 224, 688-693.
- Karimi, K. and Taherzadeh, M. J. (2016). A critical review of analytical methods in pretreatment of lignocelluloses: composition, imaging, and crystallinity. *Bioresour. Technol.* 200, 1008-1018.
- Karlsson, E. N., Schmitz, E., Linares-Pastén, J. A. and Patrick, A. (2018). Endo-xylanases as tools for production of substituted xylooligosaccharides with prebiotic properties *Appl. Microbiol. Biotechnol.* 102, 9081-9088.
- Kaur, J., Kumar, A. and Kaur, J. (2018). Strategies for optimization of heterologous protein expression in *E. coli*: Roadblocks and reinforcements. *Int. J. Biol. Macromol.* 106, 803-822.
- Kelainy, E. G., Ibrahim Laila, I. M. and Ibrahim, S. R. (2019). The effect of ferulic acid against lead-induced oxidative stress and DNA damage in kidney and testes of rats. *Environ. Sci. Pollut. Res.* 26, 31675-31684.
- Kellock, M., Maaheimo, H., Marjamaa, K., Rahikainen, J., Zhang, H., Holopainen-Mantila, U., Ralph, J., Tamminen, T., Felby, C. and Kruus, K. (2019). Effect of hydrothermal pretreatment severity on lignin inhibition in enzymatic hydrolysis. *Bioresour. Technol.* 280, 303-312.
- Khandeparker, R., Parab, P. and Amberkar, U. (2017). Recombinant xylanase from *Bacillus tequilensis* BT21: Biochemical characterisation and its application in the production of xylobiose from agricultural residues. *Food Technol. Biotechnol.* 55, 164-172.
- Khoddami, A., Wilkes, A. M., and Roberts, H. T. (2013). Techniques for analysis of plant phenolic compounds. *Molecules* 18, 2328-2375.
- Khucharoenphaisan, K. and K. Sinma, (2011). Effect of signal sequence on the β -xylanase from *Thermomyces lanuginosus* SKR expression in *Escherichia coli*. *Biotechnol.* 10, 209-214
- Kim, D. (2018). Physico-chemical conversion of lignocellulose: inhibitor effects and detoxification strategies: a mini review. *Molecules* 23 (2), 309.

- Kim, J. S., Lee, Y. Y. and Kim, T. H. (2016). A review on alkaline pretreatment technology for bioconversion of lignocellulosic biomass. *Bioresource Technol.* 199, 42-48.
- Kim, Y., Ximenes, E., Mosier, N. S. and Ladisch, M. R. (2011). Soluble inhibitors/deactivators of cellulase enzymes from lignocellulosic biomass. *Enzyme Microb. Tech.* 48, 408-415.
- Kmezik, C., Bonzom, C., Olsson, L., Mazurkewich, S. and Larsbrink, J. (2020). Multimodular fused acetyl-feruloyl esterase from soil and gut bacteroidetes improve xylanase depolymerization of recalcitrant biomass. *Biotechnol. Biofuels* 13(1), 60.
- Kubicek, C. P. and Kubicek, E. M. (2016). Enzymatic deconstruction of plant biomass by fungal enzymes. *Curr. Opin. Chem. Biol.* 35, 51-57.
- Kucharska, K., Rybarczyk, P., Hołowacz, I., Łukajtis, R., Glinka, M. and Kamiński, M. (2018). Pretreatment of lignocellulosic materials as substrates for fermentation processes. *Molecules* 23 (11), 2937.
- Kumar, A. K. and Sharma, S. (2017). Recent updates on different methods of pretreatment of lignocellulosic feedstocks: a review. *Bioresour. Bioprocess.* 4, 7.
- Kumar, B., Bhardwaj, N., Agrawal, K., Chaturvedi, V. and Verma, P. (2020). Current perspective on pretreatment technologies using lignocellulosic biomass: an emerging biorefinery concept. *Fuel Process. Technol.* 199, 106244.
- Kumar, N. and Pruthi, V. (2014). Potential applications of ferulic acid from natural sources. *Appl. Biotechnol. Rep.* 4, 86-93.
- Kumar, V. and Shukla, P. (2018). Extracellular xylanase production from *T. lanuginosus* VAPS24 at pilot scale and thermostability enhancement by immobilization. *Process Biochem.* 71, 53-60.
- Kumari, D. and Singh, R. (2018). Pretreatment of lignocellulosic wastes for biofuel production: a critical review *Renew. Sust. Energ. Rev.* 90, 877-891.
- Laemmli, U. K. (1970). Cleavage of structural proteins during the assembly of the head of bacteriophage T4. *Nature* 227, 680-685.
- Lagaert, S., Pollet, A., Courtin, C. M. and Volckaert, G. (2014). β -Xylosidases and α -L-arabinofuranosidases: Accessory enzymes for arabinoxylan degradation. *Biotechnol. Adv.* 32, 316-32.

- Li, X., Guo, J., Hu, Y., Yang, Y., Jiang, J., Nan, F., Wu, S. and Xin, Z. (2018). Identification of a novel feruloyl esterase by functional screening of a soil metagenomic library. *Appl. Biochem. Biotechnol.* 187, 1-14.
- Linares-Pastén, J. A., Aronsson, A. and Nordberg Karlsson, E. (2018). Structural considerations on the use of endo-xylanases for the production of prebiotic xylooligosaccharides from biomass. *Curr. Protein Pept. Sci.* 19, 48-67.
- Liu, L. Y., Zhao, M. L., Liu, X. X., Zhong, K., Tong, L. T., Zhou, X. R. and Zhou, S. (2016). Effect of steam explosion-assisted extraction on phenolic acid profiles and antioxidant properties of wheat bran. *J. Sci. Food Agric.* 96 (10), 3484-3491.
- Liu, Q., Li, W., Ma, Q., An, S., Li, M., Jameel, H. and Chang, H.-M. (2016). Pretreatment of corn stover for sugar production using a two-stage dilute acid followed by wet-milling pretreatment process. *Bioresour. Technol.* 211, 435-442.
- Liu, X., Hilgsmann, S., Gourdon, R. and Bayard, R. (2017). Anaerobic digestion of lignocellulosic biomasses pretreated with *Ceriporiopsis subvermispora*. *J. Environ. Manage.* 193, 154-162.
- Lombard, V., Golaconda Ramulu, H., Drula, E., Coutinho, P.M. and Henrissat, B. (2014). The carbohydrate-active enzymes database (CAZy) in 2013. *Nucleic Acids Res.* 42, D490–D495.
- Long, L., Wu, L., Lin, Q. and Ding, S. (2020). Highly efficient extraction of ferulic acid from cereal brans by a new Type A feruloyl esterase from *Eupenicillium parvum* in combination with dilute phosphoric acid pretreatment. *Appl Biochem Biotechnol.* 190, 1561-1578.
- Long, L., Zhao, H., Ding, D., Xu, M. and Ding, S. (2018). Heterologous expression of two *Aspergillus niger* feruloyl esterases in *Trichoderma reesei* for the production of ferulic acid from wheat bran. *Bioprocess Biosyst. Eng.* 41 (5), 593-601.
- Lopes, A. M., Ferreira Filho, E. X. and Moreira, L. R. S. (2018). An update on enzymatic cocktails for lignocellulose breakdown. *J. Appl. Microbiol.* 125, 632-645.
- Mahmoud, A. M., Hussein, O. E., Hozayen, W. G., Bin-Jumah, M. and Abd El-Twab, S. M. (2020). Ferulic acid prevents oxidative stress, inflammation, and liver injury via upregulation of Nrf2/HO-1 signalling in methotrexate-induced rats. *Environ. Sci. Pollut. Res.* 27, 7910-7921.

- Mäkelä, M. R., Dilokpimol, A., Koskela, S. M., Kuuskeri, J., de Vries, R. P. and Hildén, K. (2018). Characterization of a feruloyl esterase from *Aspergillus terreus* facilitates the division of fungal enzymes from Carbohydrate Esterase family 1 of the carbohydrate-active enzymes (CAZy) database. *Microbial Biotechnol.* 11 (5), 869-880.
- Makino, T., Skretas, G. and Georgiou, G. (2011). Strain engineering for improved expression of recombinant proteins in bacteria. *Microb. Cell Fact.* 10, 32.
- Malgas, S., Mafa, M. S., Mkabayi, L. and Pletschke B. (2019). A mini review of xylanolytic enzymes with regards to their synergistic interactions during hetero-xylan degradation. *World J. Microbiol. Biotechnol.* 35(12), 187.
- Malgas, S., Van Dyk, J. S., Abboo, S. and Pletschke, B. I. (2016). The inhibitory effects of various substrate pre-treatment by-products and wash liquors on mannanolytic enzymes. *J. Mol. Catal. B: Enzym.* 123, 132-140.
- Malhotra, G. and Chapadgaonkar, S. S. (2018). Production and applications of xylanases-an overview. *BioTechnologia* 99, 59-72.
- Mangan, D., Cornaggia, C., Liadova, A., McCormack, N., Ivory, R., McKie, V. A., Ormerod, A. and McCleary, B. V. (2017). Novel substrates for the automated and manual assay of endo-1,4- β -xylanase. *Carbohydr. Res.* 445, 14-22.
- Maret, W. (2013). Inhibitory zinc sites in enzymes. *Biometals* 26, 197-204.
- Maslen, S. L., Goubet, F., Adam, A. Dupree, P. and Stephens, E. (2007). Structure elucidation of arabinoxylan isomers by normal phase HPLC–MALDI-TOF/TOF-MS/MS. *Carbohydr. Res.* 342, 724-735.
- Mathew, S., Aronsson, A., Nordberg Karlsson, E. and Adlercreutz, P. (2018). Xylo- and arabinoxylooligosaccharides from wheat bran by endoxylanases, utilisation by probiotic bacteria, and structural studies of the enzymes. *Appl. Microbiol. Biotechnol.* 102, 3105-3120.
- Mathibe, B. N., Malgas, S., Radosavljevic, L., Kumar, V., Shukla, P. and Pletschke, B. I. (2020). Lignocellulosic pretreatment-mediated phenolic by-products generation and their effect on the inhibition of an endo-1,4- β -xylanase from *Thermomyces lanuginosus* VAPS-24. *3 Biotech.* 10, 349.

- Maulana Hidayatullah, I., Setiadi, T., Tri Ari Penia Kresnowati, M. and Boopathy, M. (2020). Xylanase inhibition by the derivatives of lignocellulosic material. *Bioresour. Technol.* 300, 122740.
- Mendis, M. and Simsek, S. (2015). Production of structurally diverse wheat arabinoxylan hydrolyzates using combinations of xylanase and arabinofuranosidase. *Carbohydr. Polym.* 132, 452-459.
- Mhillaj, E., Catino, S., Miceli, F. M., Santangelo, R., Trabace, L., Cuomo, V. and Mancuso, C. (2018). Ferulic acid improves cognitive skills through the activation of the Heme oxygenase system in the rat. *Mol. Neurobiol.* 55, 905-916.
- Mhlongo, S. I., den Haan, R., Viljoen-Bloom, M. and van Zyl, W. H. (2015). Lignocellulosic hydrolysate inhibitors selectively inhibit/deactivate cellulase performance. *Enzyme Microb. Technol.* 81, 16-22.
- Michelin, M., Ximenes, E., de Lourdes Teixeira de Moraes Polizeli, M. and Ladisch, M. R. (2016). Effect of phenolic compounds from pretreated sugarcane bagasse on cellulolytic and hemicellulolytic activities. *Bioresour. Technol.* 199, 275-278.
- Miller, G.L. (1959). Use of dinitrosalicylic acid reagent for the determination of reducing sugars. *Anal. Chem.* 31, 426-428.
- Mkabayi, L., Malgas, S., Wilhelmi, B. S. and Pletschke, B. I. (2020). Evaluating feruloyl esterase—xylanase synergism for hydroxycinnamic acid and xylo-oligosaccharide production from untreated, hydrothermally pre-treated and dilute-acid pre-treated corn cobs. *Agronomy* 10, 688.
- Mohamad, N., Mustapa Kamal, S., and Mokhtar, M. (2015). Xylitol biological production: A review of recent studies. *Food Rev. Int.* 31(1), 74-89.
- Monclaro, A. V., Recalde, G. L., da Silva, F. G., de Freitas, S. M., Ferreira Filho, E. X. (2019). Xylanase from *Aspergillus tamarii* shows different kinetic parameters and substrate specificity in the presence of ferulic acid. *Enzyme Microb. Technol.* 120, 16-22.
- Mota, T. R., Oliveira, D. M., Rogério Marchiosi, O., Ferrarese-Filho and Santos, W. D. (2018). Plant cell wall composition and enzymatic deconstruction. *AIMS Bioeng.* 5, 63-77.
- Motta, F. L., Andrade, C. C. P. and Santana, M. H. A. (2013). A review of xylanase production by the fermentation of xylan: classification, characterization and applications. *Sustainable*

degradation of lignocellulosic biomass-techniques, applications and commercialization. InTechOpen, New York, 251-275.

Naidu, D. S., Hlangothi, S. P. and John, M. J. (2018). Bio-based products from xylan: A review. Carbohydr. Polym. 179, 28-41.

Nieter, A., Kelle, S., Linke, D. and Berger, R. G., (2016). Feruloyl esterases from *Schizophyllum commune* to treat food industry side-streams. Bioresour. Technol. 220, 38-46.

Nitsos, C. K., Matis, K. A. and Triantafyllidis, K. S. (2013). Optimization of hydrothermal pretreatment of lignocellulosic biomass in the bioethanol production process. Chem.Sus. Chem. 6, 110-122.

Nordberg Karlsson, E., Schmitz, E., Linares-Pasten, J. A. and Adlercreutz, P. (2018). Endo-xylanases as tools for production of substituted xylooligosaccharides with prebiotic properties. Appl. Microbiol. Biotechnol. 102, 9081-9088.

Oliveira, D. M., Mota, T. R., Oliva, B., Segato, F., Marchiosi, R., Ferrarese, O., Faulds, C. B. and dos Santos, W. D. (2019). Feruloyl esterases: Biocatalysts to overcome biomass recalcitrance and for the production of bioactive compounds. Bioresour. Technol. 278, 408-423.

Oliveira, D. M., Salvador, V. H., Mota, T. R., Finger-Teixeira, A., Almeida, R. F., Paixao, D. A. A., de Souza, A. P., Buckeridge, M. S., Marchiosi, R., Ferrarese-Filho, O., Squina, F. M., dos Santos, W. D., (2016). Feruloyl esterase from *Aspergillus clavatus* improves xylan hydrolysis of sugarcane bagasse. AIMS Bioeng. 4, 1-11.

Paes, G., Berrin, J. G. and Beaugrand, J. (2012). GH11 xylanases: structure/function/ properties relationships and applications. Biotechnol Adv. 30(3), 564-592.

Paiva, L., Goldbeck, R., Santos, W. D. and Squina, F. (2013). Ferulic acid and derivatives: molecules with potential application in the pharmaceutical field. Braz. J. Pharm. Sci. 49, 395-411.

Pei, K., Ou, J., Huang, J. and Ou, S. (2016). *p*-Coumaric acid and its conjugates: Dietary sources, pharmacokinetic properties and biological activities. J. Sci. Food Agric. 96, 2952-2962.

- Peng, P. and She, D. (2014). Isolation, structural characterization, and potential applications of hemicelluloses from bamboo: A review. *Carbohydr. Polym.* 112, 701-20.
- Poletto, P., Pereira, G. N., Monteiro, C. R. M., Pereira, M. A. F., Bordignon, S. E. and de Oliveira, D. (2020). Xylooligosaccharides: transforming the lignocellulosic biomasses into valuable 5-carbon sugar prebiotics. *Process. Biochem.* 91, 352-363.
- Rabemanolontsoa, H. and Saka, S. (2016). Various pretreatments of lignocellulosics. *Bioresour. Technol.* 199, 83-91.
- Ragauskas, A. J., Beckham, G. T., Biddy, M. J., Chandra, R., Chen, F., Davis, M. F., Davison, B. H., Dixon, R. A., Gilna, P., Keller, M., Langan, P., Naskar, A. K., Saddler J. N., Tschaplinski, T. J., Tuskan, G. A., Wyman, C. E. (2014). Lignin valorization: improving lignin processing in the biorefinery. *Science* 344, 1246843.
- Ranum, P., Pena-Rosas, J. P. and Garcia-Casal, M. N. (2014). Global maize production, utilization, and consumption. *Ann. N.Y. Acad. Sci.* 1312, 105-112.
- Rashamuse, K., Ronneburg, T., Sanyika, W., Mathiba, K., Mmutlane, E. and Brady, D. (2014). Metagenomic mining of feruloyl esterases from termite enteric flora. *Appl. Microbiol. Biotechnol.* 98, 727-737.
- Rastogi, M. and Shrivastava, S. (2017). Recent advances in second generation bioethanol production: An insight to pretreatment, saccharification and fermentation processes. *Renew. Sust. Energ. Rev.* 80, 330-340.
- Revanappa, S. B., Nandini, C. D. and Salimath, P. V. (2015). Structural variations of arabinoxylans extracted from different wheat (*Triticum aestivum*) cultivars in relation to chapati-quality. *Food Hydrocoll.* 43, 736-42.
- Robak, K., and Balcerek, M. (2018). Review of second generation bioethanol production from residual biomass. *Food Technol. Biotech.* 56, 174–187.
- Rocha, G. J. D. M., Nascimento, V. M., Gonçalves, A. R., Silva, V. F. N. and Martín, C. (2015). Influence of mixed sugarcane bagasse samples evaluated by elemental and physical–chemical composition. *Ind. Crops Prod.* 64, 52-58.
- Rouches, E., Herpoël-Gimbert, I., Steyer, J. and Carrere, H. (2016). Improvement of anaerobic degradation by white-rot fungi pretreatment of lignocellulosic biomass: a review. *Renew. Sustain. Energy Rev.* 59, 179-198.

- Saha, B. C. (2003). Hemicellulose bioconversion. *J. Ind. Microbiol. Biotechnol.* 30:279-91.
- Sahare, P., Singh, R., Laxman, R.S. and Rao M. (2012). Effect of alkali pretreatment on the structural properties and enzymatic hydrolysis of corn cob. *Appl. Biochem. Biotechnol.* 168, 1806-1819.
- Sahoo, D., Ummalya, S. B., Okram, A. K., Pandey, A., Sankar, M. and Sukumaran, R. K. (2018). Effect of dilute acid pretreatment of wild rice grass (*Zizania latifolia*) from Loktak Lake for enzymatic hydrolysis. *Bioresour. Technol.* 253, 252-255.
- Sakdaronnarong, C., Srimarut, N., Lucknakhul, N., Na-songkla, B. and Jonglertjunya, W. (2014). Two-step acid and alkaline ethanolysis/alkaline peroxide fractionation of sugarcane bagasse and rice straw for production of polylactic acid precursor. *Biochem. Eng. J.* 85, 49-62.
- Samanta, A. K., Jayapal, N., Jayaram, C., Roy, S., Kolte, A. P., Senani, S. and Sridhar, M. (2015). Xylooligosaccharides as prebiotics from agricultural by-products: production and applications. *Bioact. Carbohydr. Diet. Fibre.* 5, 62-71.
- Sanchez, A., Hernandez-Sanchez, P. and Puente, R. (2019). Hydration of lignocellulosic biomass. Modelling and experimental validation. *Ind. Crops Prod.* 131, 70-77.
- Saville, B. A. and Saville, S. (2018). Xylooligosaccharides and arabinoxylanoligosaccharides and their application as prebiotics, *Appl. Food Biotechnol.* 5, 121-130.
- Scheller, H. V and Ulvskov, P. (2010). Hemicelluloses. *Annu. Rev. Plant Biol.* 61, 263-289.
- Şenol, H., Açıke, U. and Oda, V. (2019). Anaerobic digestion of sugar beet pulp after acid thermal and alkali thermal pretreatments. *Biomass Conv. Bioref.* 25, 1-11.
- Shahabazuddin, M., Chandra, T. S., Meena, S., Sukumaran, R. K., Shetty, N. P. and Mudliar, S. N. (2018). Thermal assisted alkaline pretreatment of rice husk for enhanced biomass deconstruction and enzymatic saccharification: physico-chemical and structural characterization. *Bioresour. Technol.* 263, 199-206.
- Sharma, H. K., Xu, C., and Qin, W. (2019). Biological pretreatment of lignocellulosic biomass for biofuels and bioproducts: an overview. *Waste Biomass Valorization* 10, 235-251.
- Shigeto, J., Ueda, Y., Sasaki, S., Fujita, K. and Tsutsumi, Y. (2017). Enzymatic activities for lignin monomer intermediates highlight the biosynthetic pathway of syringyl monomers in *Robinia pseudoacacia*. *J. Pl. Res.* 130, 203-210.

Shirai, A., Matsuki, H. and Watanabe, T. (2017). Inactivation of foodborne pathogenic and spoilage micro-organisms using ultraviolet-A light in combination with ferulic acid. *Lett. Appl. Microbiol.* 64, 96-102.

Shrivastava, S., Shukla, P., Deepalakshmi, P. D. and Mukhopadhyay, K. (2013). Characterization, cloning and functional expression of novel xylanase from *Thermomyces lanuginosus* SS-8 isolated from self-heating plant wreckage material. *World J. Microbiol. Biotechnol.* 29, 2407-2415.

Sievers, F., Wilm, A., Dineen, D., Gibson, T. J., Karplus, K., Li, W., Lopez, R., McWilliam, H., Remmert, M., Söding, J., Thompson, J. D. and Higgins, D. G. (2011). Fast, scalable generation of high-quality protein multiple sequence alignments using Clustal Omega. *Mol. Syst. Biol.* 7, 539.

Silva, L. A. O., Terrasan, C. R. F. and Carmona, E. C. (2015). Purification and characterization of xylanases from *Trichoderma inhamatum*. *Electron. J. Biotechnol.* 18, 307-313.

Singh, J. K., Vyas, P., Dubey, A. Upadhyaya, C. P., Kothari, R., Tyagi, V. V. and Kumar, A. (2018). Assessment of different pretreatment technologies for efficient bioconversion of lignocellulose to ethanol. *Front. Biosci. Sch.* 10, 10-2741.

Singh, R. D., Banerjee, J., Sasmal, S., Muir, J. and Arora, A. (2018). High xylan recovery using two stage alkali pre-treatment process from high lignin biomass and its valorisation to xylooligosaccharides of low degree of polymerisation. *Bioresour. Technol.* 256, 110-117.

Sinosaki, N. B. M., Tonin, A. P. P., Ribeiro, M. A. S., Polisele, C. B., Roberto, S. B., da Silveira, R., Visentainer, J. V., Santos, O. O. and Meurer, E. C. (2020). Structural study of phenolic acids by triple quadrupole mass spectrometry with electrospray ionization in negative mode and H/D isotopic exchange. *J. Braz. Chem. Soc.* 31, 402-408.

Siqueira, G., Arantes, V., Saddler, J. N., Ferraz, A. and Milagres, A. M. F. (2017). Limitation of cellulose accessibility and unproductive binding of cellulases by pretreated sugarcane bagasse lignin. *Biotechnol. Biofuels* 10, 1-12.

Sluiter, A., Hames, B., Ruiz, R., Scarlata, C., Sluiter, J., Templeton, D. and Crocker, D. (2008). Determination of structural carbohydrates and lignin in biomass. Laboratory Analytical Procedure, NREL/TP-510-42618.

- Sluiter, J. B., Ruiz, R. O., Scarlata, C. J., Sluiter, A. D. and Templon, D. W. (2010). Compositional analysis of lignocellulosic feedstocks 1: Review and description of methods. *J. Agric. Food Chem.* 58, 9043-9053.
- Soares Rodrigues, C. I., Jackson, J. J. and Montross, M. D. (2016). A molar basis comparison of calcium hydroxide, sodium hydroxide, and potassium hydroxide on the pretreatment of switchgrass and miscanthus under high solids conditions. *Ind. Crops Prod.* 92, 165-173.
- Solarte-Toro, J. C., Romero-García, J. M., Martínez-Patiño, J. C., Ruiz-Ramos, E., Castro-Galiano, E. and Cardona-Alzate, C. A. (2019). Acid pretreatment of lignocellulosic biomass for energy vectors production: a review focused on operational conditions and techno-economic assessment for bioethanol production. *Renew. Sust. Energ. Rev.* 107, 587-601.
- Srivastava, N., Srivastava, M., Mishra, P. K., Gupta, V. K., Molina, G., Rodriguez-Couto, S., Manikanta, A. and Ramteke, P. W. (2018). Applications of fungal cellulases in biofuel production: advances and limitations. *Renew. Sustain. Energy Rev.* 82(3), 2379-2386.
- Stoklosa, R. J., Latona, R. J., Bonnaille L. M. and Yadav, M. P. (2019). Evaluation of arabinoxylan isolated from sorghum bran, biomass, and bagasse for film formation. *Carbohydr. Polym.* 213, 382-392.
- Studier, F. W. (2014). Stable expression clones and auto-induction for protein production in *E. coli*. *Methods Mol. Biol.* 1091, 17-32.
- Surendran, A., Siddiqui, Y., Ali, N. S. and Manickam, S. (2018). Inhibition and kinetic studies of cellulose- and hemicellulose-degrading enzymes of *Ganoderma boninense* by naturally occurring phenolic compounds. *J. Appl. Microbiol.* 124, 1544-1555.
- Suzuki, K., Hori, A., Kawamoto, K., Thangudu, R., Ishida, T., Igarashi, K., Samejima, M., Yamada, C., Arakawa, T., Wakagi, T., Koseki, T. and Fushinobu, S. (2014). Crystal structure of a feruloyl esterase belonging to the tannase family: a disulfide bond near a catalytic triad. *Proteins* 82(10), 2857-2867.
- Tao, X., Li, J., Zhang, P., Nabi, M., Jin, S., Li, F., Wang, S. and Ye, J. (2017). Reinforced acid-pretreatment of *Triarrhena lutarioriparia* to accelerate its enzymatic hydrolysis. *Int. J. Hydrog. Energy* 42, 18301-18308.

- Teplitsky, A., Shulami, S., Moryles, S., Shoham, Y. and Shoham, G. (2000). Crystallization and preliminary X-ray analysis of an intracellular xylanase from *Bacillus stearothermophilus* T-6. *Acta. Crystallogr. D. Biol. Crystallogr.* 56, 181-184.
- Terrett, O. M. and Dupree, P. (2019). Covalent interactions between lignin and hemicelluloses in plant secondary cell walls. *Curr. Opin. Biotechnol.* 56, 97-104.
- Tian, Y., Jiang, Y. and Ou, S. (2013). Interaction of cellulase with three phenolic acids. *Food Chem.* 138, 1022-1027.
- Topakas, E., Vafiadi, C. and Christakopoulos, P. (2007). Microbial production, characterization and applications of feruloyl esterases. *Process Biochem.* 42, 497-509.
- Torronen, A. and Rouvinen, J. (1997). Structural and functional properties of low molecular weight endo-1,4-b-xylanases. *J. Biotechnol.* 57, 137-149.
- Tye, Y. Y., Lee, K. T., Abdullah, W. N. W. and Leh, C. P. (2016). The world availability of non-wood lignocellulosic biomass for the production of cellulosic ethanol and potential pretreatments for the enhancement of enzymatic saccharification. *Renew. Sustain. Energy. Rev.* 60, 155-172.
- Udatha, D. B., Kouskoumvekaki, I., Olsson, L. and Panagiotou, G. (2011). The interplay of descriptor-based computational analysis with pharmacophore modeling builds the basis for a novel classification scheme for feruloyl esterases. *Biotechnol. Adv.* 29, (1), 94-110.
- Uraji, M., Arima, J., Inoue, Y., Harazono, K. and Hatanaka, T. (2014). Application of two newly identified and characterized feruloyl esterases from *Streptomyces* sp. in the enzymatic production of ferulic acid from agricultural biomass. *PLoS ONE* 9 (8), e104584.
- Uraji, M., Tamura, H., Mizohata, E., Arima, J., Wan, K., Ogawa, K., Inoue, T. and Hatanaka, T., (2018). Loop of *streptomyces* feruloyl esterase plays an important role in the enzyme's catalyzing the release of ferulic acid from biomass. *Appl. Environ. Microbiol.* 84 (3), e02300-17.
- Van Dyk, J. S., Pletschke, B. I. (2012). A review of lignocellulose bioconversion using enzymatic hydrolysis and synergistic cooperation between enzymes – factors affecting enzymes, conversion and synergy. *Biotechnol. Adv.* 30, 1458-1480.

- Varnai, A., Tang, C., Bengtsson, O., Atterton, A., Mathiesen, G. and Eijssink, V. G. (2014). Expression of endoglucanases in *Pichia pastoris* under control of the GAP promoter. *Microb. Cell Fact.* 13, 57.
- Visser, E. M., Falkoski, D. L., de Almeida, M. N., Maitan-Alfenas, G. P. and Guimarães, V. M. (2013). Production and application of an enzyme blend from *Chrysosporthe cubensis* and *Penicillium pinophilum* with potential for hydrolysis of sugarcane bagasse. *Bioresour. Technol.* 144, 587-594.
- Walia, A., Mehta, P., Chauhan, A. and Shirkot, C. K. (2013). Optimization of cellulase-free xylanase production by alkalophilic *Cellulosimicrobium* sp. CKMX1 in solid-state fermentation of apple pomace using central composite design and response surface methodology. *Ann. Microbiol.* 63, 187-198.
- Wan, C. and Li, Y. (2012). Fungal pretreatment of lignocellulosic biomass. *Biotechnol. Adv.* 30(6), 1447-1457.
- Wan, Q., Zhang, Q., Hamilton-Brehm, S., Weiss, K., Mustyakimov, M., Coates, L., Langan, P., Graham, D. and Kovalevsky, A. (2014). X-ray crystallographic studies of family 11 xylanase Michaelis and product complexes: implications for the catalytic mechanism. *Acta Crystallogr. Sect. D: Biol. Crystallogr.* 70, 11-23.
- Wang, L., Li, Z., Zhu, M., Meng, L., Wang, H. and Ng, T. B. (2016). An acidic feruloyl esterase from the mushroom *Lactarius hatsudake*: a potential animal feed supplement. *Int. J. Biol. Macromol.* 93 (Pt A), 290-295.
- Wang, L., Ma, Z., Du, F., Wang, H. and Ng, T. B. (2014). Feruloyl esterase from the edible mushroom *Panus giganteus*: a potential dietary supplement. *J. Agric. Food Chem.* 62 (31), 7822-7827.
- Wang, R., Yang, J., Jang, J. M., Liu, J., Zhang, Y., Liu, L. and Yuan, H. (2020). Efficient ferulic acid and xylo-oligosaccharides production by a novel multi-modular bifunctional xylanase/feruloyl esterase using agricultural residues as substrates. *Bioresour. Technol.* 297, 122487.
- Wefers, D., Cavalcante, J. J. V., Schendel, R. R., Deveryshetty, J., Wang, K., Wawarzak, Z., Mackie, R. I., Koropatkin, N. M., Cann, I. 2017. Biochemical and structural analyses of two

cryptic esterases in *Bacteroides intestinalis* and their synergistic activities with cognate xylanases. *J Mol Biol.* 429, 2509-2527.

Wei, Y., Li, X., Yu, L., Zou, D. and Yuan, H. (2015). Mesophilic anaerobic co-digestion of cattle manure and corn stover with biological and chemical pretreatment. *Bioresource Technol.* 198, 431-436.

Weiss, N. D., Felby, C. and Thygesen, L. G. (2018). Water retention value predicts biomass recalcitrance for pretreated lignocellulosic materials across feedstocks and pretreatment methods. *Cellulose* 25, 3423-3434.

Wen, H. C., Ben, L. P., Ching, T. Y. and Wen, S. H. (2011). Pretreatment efficiency and structural characterization of rice straw by an integrated process of dilute-acid and steam explosion for bioethanol production. *Bioresour Technol*, 102 (3), 2916-2924.

Wong, D. W. S., Chan, V. J. and Liao, H. (2019). Metagenomic discovery of feruloyl esterases from rumen microflora. *Appl. Microbiol. Biotechnol.* 103, 8449-8457.

Wong, D. W. S., Chan, V. J., Liao, H. and Zidwick, M. J. (2013). Cloning of a novel feruloyl esterase gene from rumen microbial metagenome and enzyme characterization in synergism with endoxylanases. *J. Ind. Microbiol. Biotechnol.* 40, 287-295.

Wu, H., Li, H., Xue, Y., Luo, G., Gan, L., Liu, J., Mao, L. and Long, M. (2017). High efficiency co-production of ferulic acid and xylooligosaccharides from wheat bran by recombinant xylanase and feruloyl esterase. *Biochem. Eng. J.* 120, 41-48.

Wu, M., Abokitse, K., Grosse, S., Leisch, H. and Lau, P.C. (2012). New feruloyl esterases to access phenolic acids from grass biomass. *Appl. Biochem. Biotechnol.* 168, 129-143.

Wu, S., Nan, F., Jiang, Zhang, Y., Qiao, B., Li, S. and Xin, Z. (2019). Molecular cloning, expression and characterization of a novel feruloyl esterase from a soil metagenomic library with phthalate-degrading activity. *Biotechnol. Lett.* 41, 995-1006.

Ximenes, E., Kim, Y., Mosier, N., Dien, B. and Ladisch, M. (2011). Deactivation of cellulases by phenols. *Enzyme Microb. Technol.* 48, 54-60.

Xiros, C., Moukouli, M., Topakas, E. and Christakopoulos, P. (2009). Factors affecting ferulic acid release from Brewer's spent grain by *Fusarium oxysporum* enzymatic system. *Bioresour. Technol.* 100, 5917-5921.

- Xu, F., Yu, J., Tesso, T., Dowell, F. and Wang, D. (2013). Qualitative and quantitative analysis of lignocellulosic biomass using infrared techniques: A mini-review. *Appl. Energy*, 104, 801-809.
- Yang, Y., Ma, W., Guo, J., Lin, Y. and Wang, C. (2013). Uniform magnetic core/shell microspheres functionalized with Ni²⁺-iminodiacetic acid for one step purification and immobilization of His-tagged enzymes. *ACS Appl. Mater. Interfaces* 5, 2626-2633.
- Yao, J. Chen, Q. L., Shen, A. X., Cao, W. and Liu, Y. H. (2013). A novel feruloyl esterase from a soil metagenomic library with tannase activity. *J. Mol. Catal. B Enzym.* 95, 55-61.
- Ying, W., Shi, Z., Yang, H., Xu, G., Zheng, Z. and Yang, J. (2018). Effect of alkaline lignin modification on cellulase–lignin interactions and enzymatic saccharification yield. *Biotechnol. Biofuels* 11 (1), 214.
- Yoo, C. G., Kim, H., Lu, F., Azarpira, A., Pan, X., Oh, K. K., Kim, J. S., Ralph, J. and Kim, T. H. (2016). Understanding the physicochemical characteristics and the improved enzymatic saccharification of corn stover pretreated with aqueous and gaseous ammonia. *BioEnergy Res.* 9 (1), 67-76.
- Yuan, Z., Wen, Y., and Li, G. (2018). Production of bioethanol and value-added compounds from wheat straw through combined alkaline/alkaline-peroxide pretreatment. *Bioresour. Technol.* 259, 228-236.
- Yuan, Z., Wen, Y., Kapu, N. S., Beatson, R. and Martinez, D. M. (2017). A biorefinery scheme to fractionate bamboo into high-grade dissolving pulp and ethanol. *Biotechnol. Biofuels* 10, 38.
- Zeng, Y., Yin, X., Wu, M. -C., Yu, T., Feng, F., Zhu, T. -D. and Pang, Q. -F. (2014). Expression of a novel feruloyl esterase from *Aspergillus oryzae* in *Pichia pastoris* with esterification activity. *J. Mol. Catal., B Enzym.* 110, 140-146.
- Zhang, H., Ning, Z., Khalid, I., Zhang, R., Liu, G. and Chen, C. (2018). Enhancement of methane production from Cotton Stalk using different pretreatment techniques. *Sci. Rep.* 8, 1-9.
- Zhang, J., Siika-Aho, M., Tenkanen, M. and Viikari, L. (2011). The role of acetyl xylan esterase in the solubilization of xylan and enzymatic hydrolysis of wheat straw and giant reed. *Biotechnol. Biofuels* 4, 60.

- Zhang, S. B., Wang, L., Liu, Y., Zhai, H. C., Cai, J. P. and Hu, Y. S. (2015). Expression of feruloyl esterase A from *Aspergillus terreus* and its application in biomass degradation. *Protein Expr. Purif.* 115, 153-157.
- Zhang, S. B., Zhai, H. C., Wang, L. and Yu, G. H. (2013). Expression, purification and characterization of a feruloyl esterase A from *Aspergillus flavus*. *Protein Expr. Purif.* 92 (1), 36-40.
- Zheng, Q., Zhou, T., Wang, Y., Cao, X., Wu, S., Zhao, M., Wang, H., Ming Xu, Zheng, B., Zheng, J. and Guan, X. (2018). Pretreatment of wheat straw leads to structural changes and improved enzymatic hydrolysis. *Sci. Rep.* 8, 1321.
- Zheng, Y., Lee, C., Yu, C., Cheng, Y.-S., Zhang, R., Jenkins, B. M. and Van der Gheynst, J. S. (2013). Dilute acid pretreatment and fermentation of sugar beet pulp to ethanol. *Appl. Energy* 105, 1-7.
- Zhou, M., Huang, Z. Q., Zhou, B., Luo, Y. L., Jia, G., Liu, G. M., Zhao, H. and Chen, X. L. (2015). Construction and expression of two-copy engineered yeast of feruloyl esterase. *Electron. J. Biotechnol.* 18, 338-342.
- Zubrowska-Sudol, M. and Walczak, J. (2014). Effects of mechanical disintegration of activated sludge on the activity of nitrifying and denitrifying bacteria and phosphorus accumulating organisms. *Water Res.* 61, 200-209.

Appendices

Appendix A: Reagents list and suppliers

Acetonitrile	Merck (Cat. No. 1.00030)
Acrylamide	Sigma (Cat. No. A8887)
Ammonium persulphate	Sigma Aldrich (Cat. No. A3678)
Bovine serum albumin (BSA)	Sigma (Cat. No. A7906)
Bradford reagent	Sigma (Cat. No. B6916)
Bromophenol blue	Sigma (Cat. No. B8026)
Coomassie Brilliant Blue R250	Merck (Cat. No. 1.12553)
<i>p</i> -Coumaric acid	Sigma (Cat. No. C9008)
3,5-Dinitrosalicylic acid	Sigma (Cat No. D0550)
Di-sodium hydrogen orthophosphate	Saarchem (Cat. No. 5822860)
Ethanol	Merck (Cat. No. 8.18700)
Ethyl ferulate	Sigma (Cat. No. 320617)
Ferulic acid	Sigma (Cat. No. 128708)
Formic acid	Merck (Cat. No. UN1779)
Glacial acetic acid	Merck (Cat. No. 1.00063)
D-Glucose	Saarchem (Cat. No. 2676020)
Glucose assay kit	Megazyme (Cat. No. K-GLUC)
Glycerol	Saarchem (Cat. No. 2676520)
Glycine	Merck (Cat. No. 1.04169)
Imidazole	Merck (Cat. No. 1.04716)
IPTG	Calbiochem (Cat. No. 420322)
Kanamycin (Monosulphate)	Melford (Cat. No. K0126)
Lysozyme	Sigma (Cat. No. 62971)

2-mercaptoethanol	Fluka (Cat. No. 63700)
Methanol	Merck (Cat. No. 8.22283)
N,N,N',N'-tetramethylethylene diamine	Sigma (Cat. No. T22500)
<i>p</i> -Nitrophenol	Sigma (Cat. No. 42,575-3)
<i>p</i> -Nitrophenol-acetate	Sigma (Cat. No. N8130)
PageRuler™ prestained protein ladder	Thermo Scientific (Cat. No. 26616)
Phloroglucinol	Sigma (Cat. No. P3502)
Phosphoric acid	Sigma (Cat. No. P6560)
Sodium carbonate	Merck (Cat. No. 1.06392.0500)
Sodium chloride	Saarchem (Cat. No. 5822320)
Sodium dodecyl sulphate (SDS)	BDH biochemicals (Cat. No. 301754)
Sodium hydroxide	Saarchem (Cat. No. 5823200)
Sodium metabisulfite	Sigma (Cat. No. 255556)
Sodium Potassium tartrate	Merck (Cat. No. 1.08087)
Sulphuric acid	Sigma (Cat. No. 30743)
Tris (hydroxymethyl) aminomethane	Merck (Cat. No. 1.08382)
<i>D</i> -Xylose	Sigma (Cat. No. X3877)
Xylose assay kit	Megazyme (Cat. No. K-XYLOSE)

Appendix B: Standard curves

B. 1. Protein standard curve

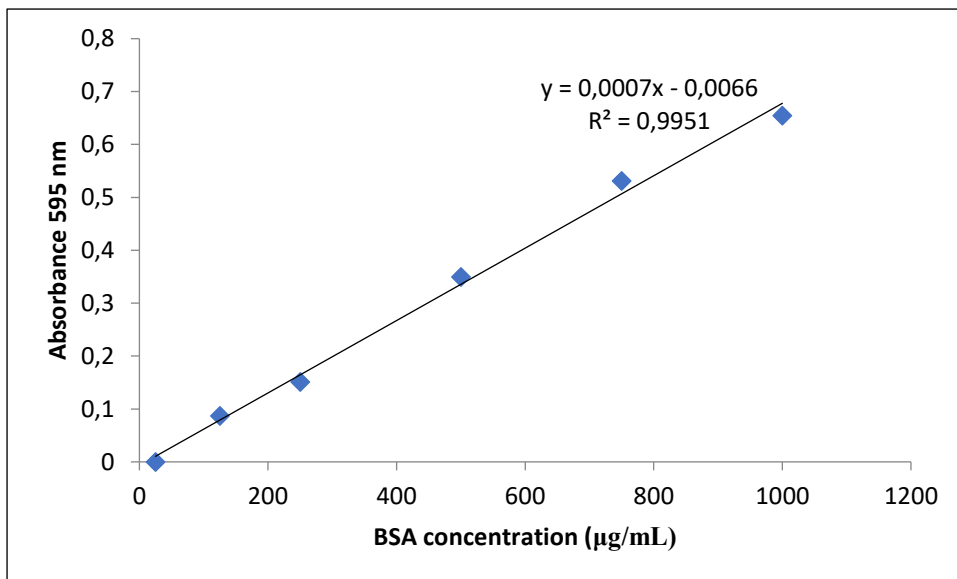


Figure B. 1.1: Protein standard curve generated using the Bradford protein assay using various concentrations of BSA. All the readings were performed in triplicate. Values are represented as means \pm SD.

B. 2. DNS assay

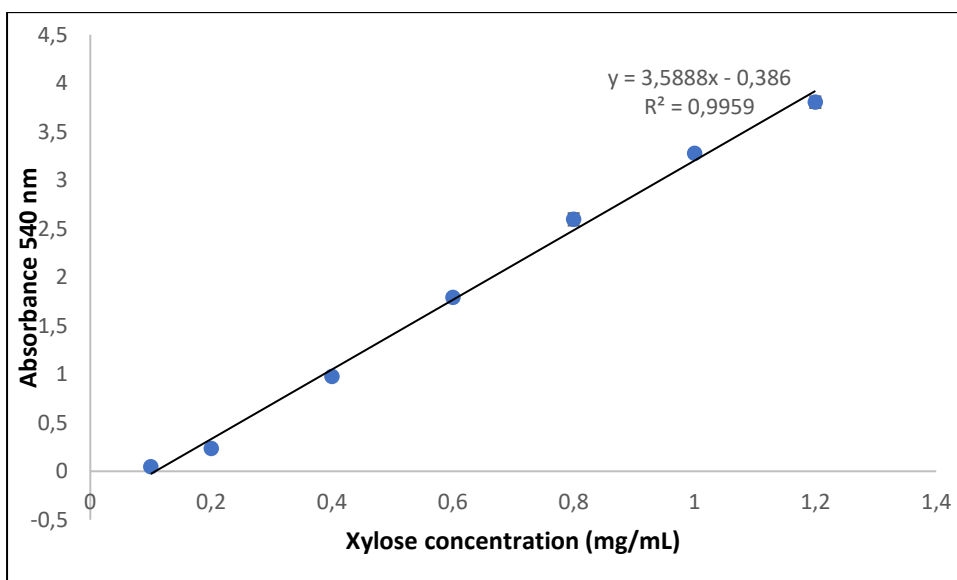


Figure B. 2.1: Xylose standard curve generated using the DNS assay. All the readings were performed in triplicate. Values are represented as means \pm SD.

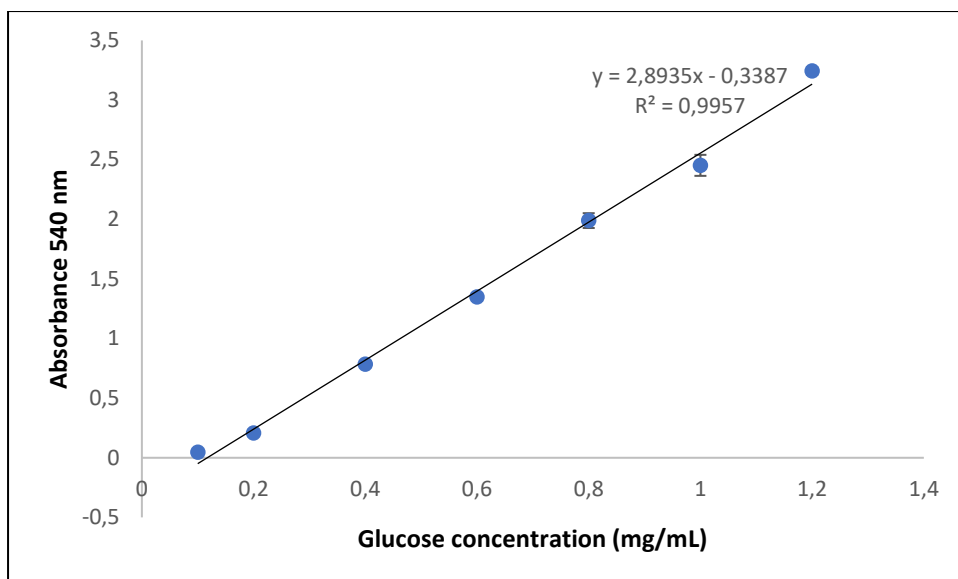


Figure B. 2.2: Glucose standard curve generated using the DNS assay. All the readings were performed in triplicate. Values are represented as means \pm SD.

B. 3. Enzyme activity curve

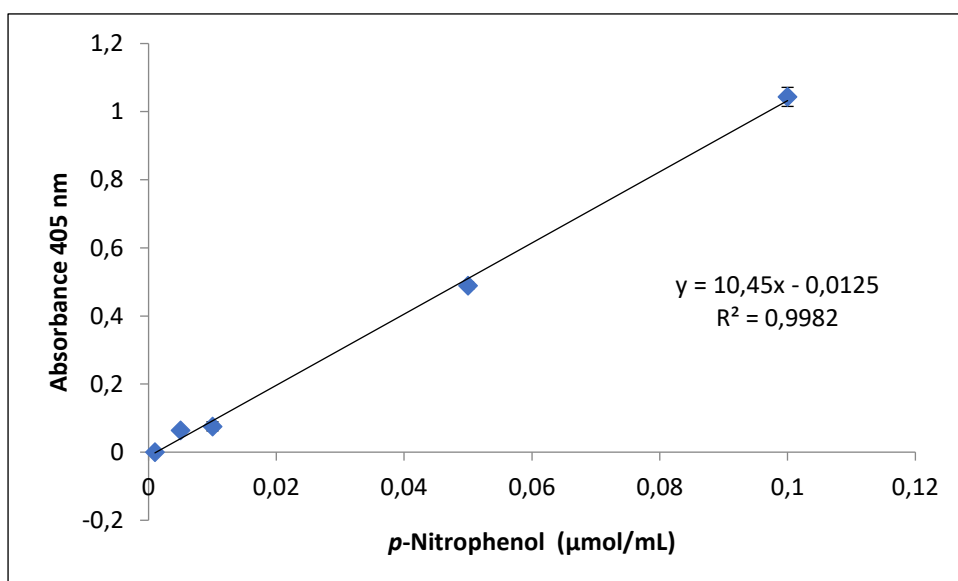


Figure B. 3.1: p-nitrophenol standard curve. All the readings were performed in triplicate. Values are represented as means \pm SD.

B. 4. Sugar assay kit

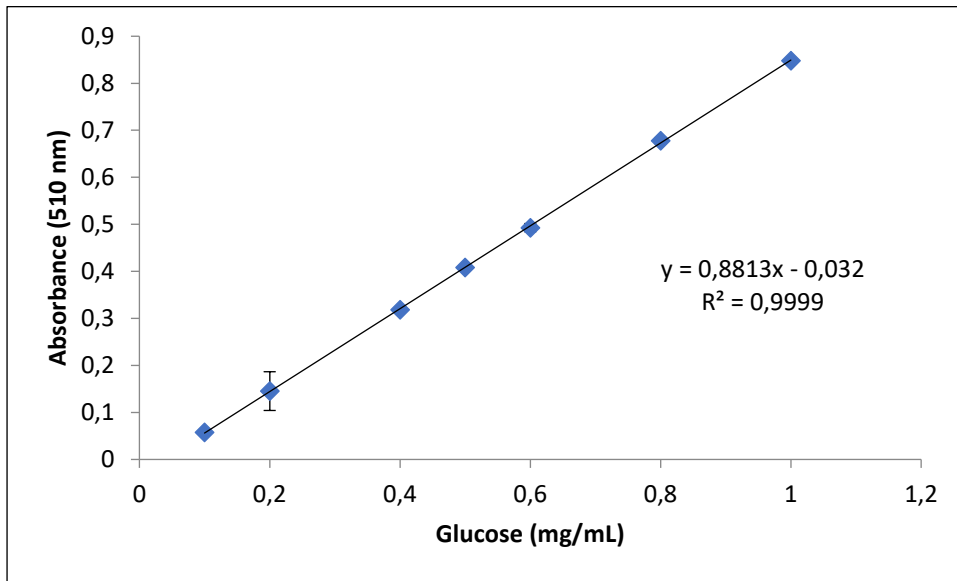


Figure B. 4.1: Glucose standard curve using Megazyme™ kit for glucose determination (K-GLUC). All the readings were performed in triplicate. Values are represented as means \pm SD.

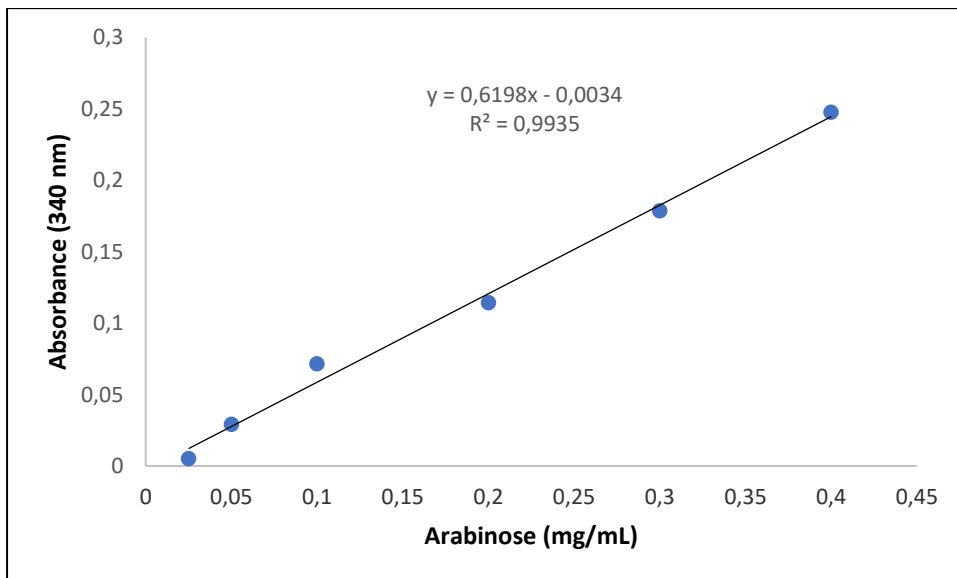


Figure B. 4.2: Arabinose standard curve using Megazyme™ kit for arabinose determination (K-ARGA). All the readings were performed in triplicate. Values are represented as means \pm SD.

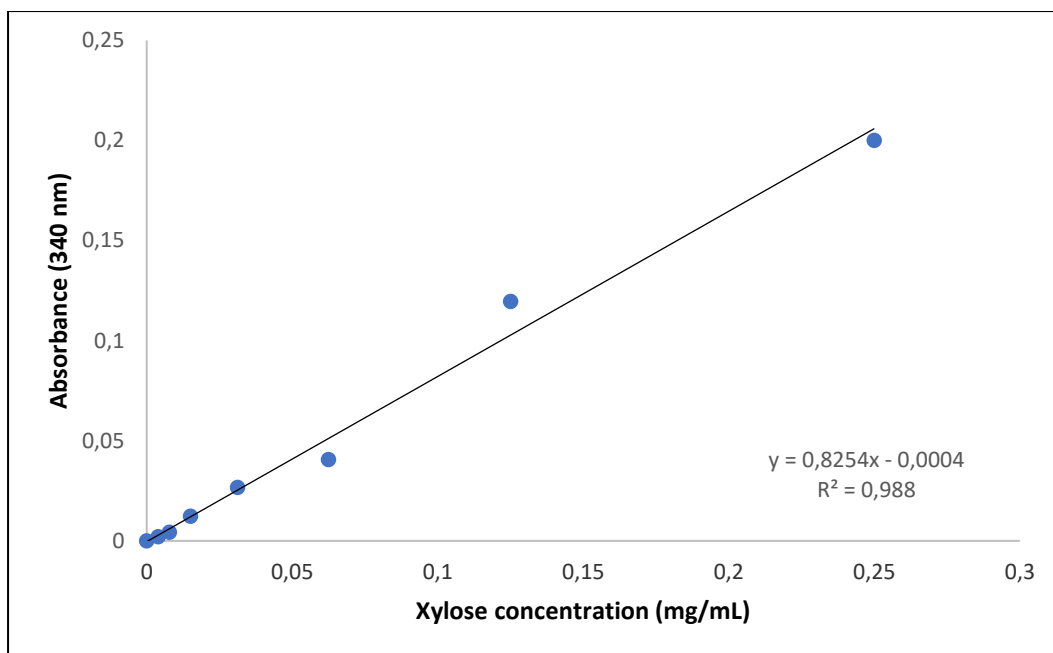


Figure B. 4.3: Xylose standard curve using Megazyme™ kit for xylose determination (K-XYLOSE). All the readings were performed in triplicate. Values are represented as means \pm SD.

B. 5. HPLC analysis

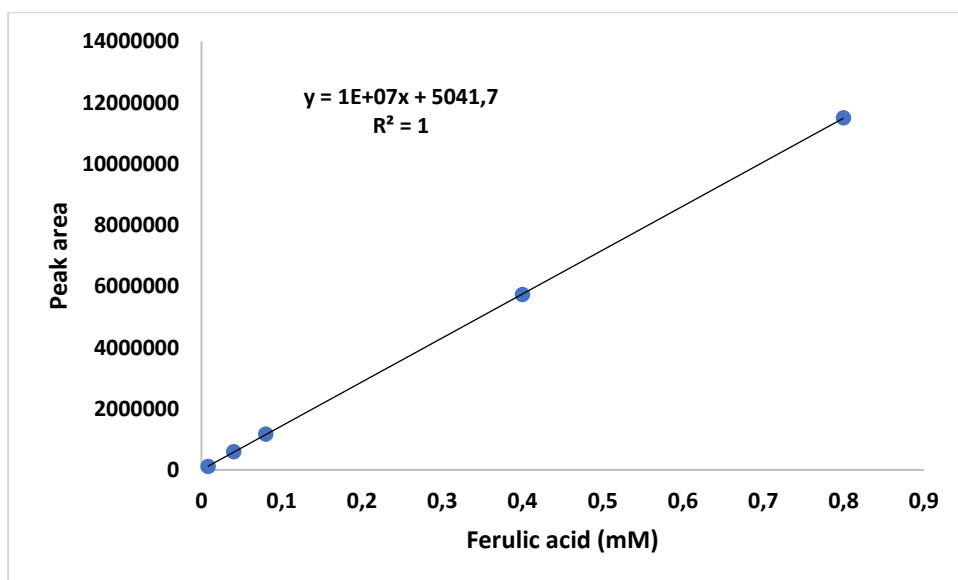


Figure B. 5.1: Ferulic acid standard curve generated using HPLC- UV analysis. All the readings were performed in triplicate. Values are represented as means \pm SD.

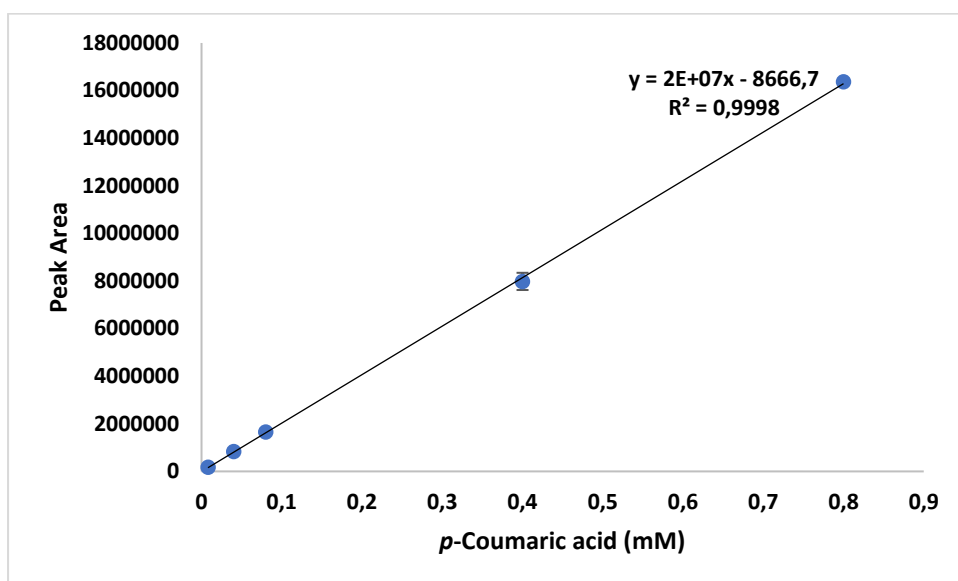


Figure B. 5.2: *p*-Coumaric acid standard curve generated using HPLC- UV analysis. All the readings were performed in triplicate. Values are represented as means \pm SD.

Appendix C: Chromatograms from HPLC-UV/RID analysis

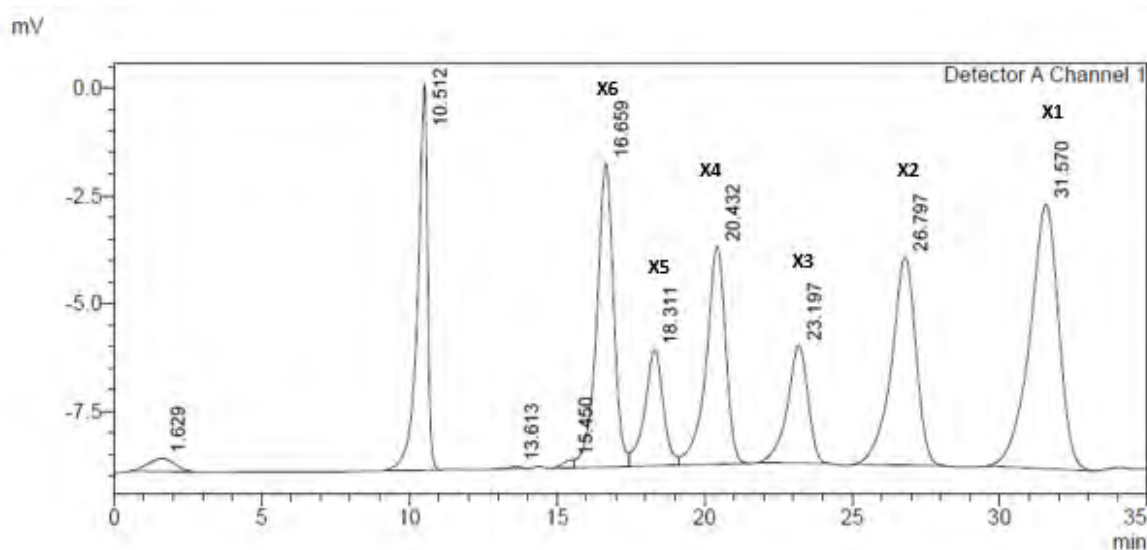


Figure C. 1.1: HPLC-RID chromatogram of separation of XOS standards (0.4 mg/mL, injected 20 μ L). X1 – Xylose; X2 – Xylobiose; X3 – Xylotriose; X4 – Xylotetraose; X5 – Xylopentaose; X6 – Xylohexaose. The chromatographic separation was carried out on a CarboSep CHO411 column.

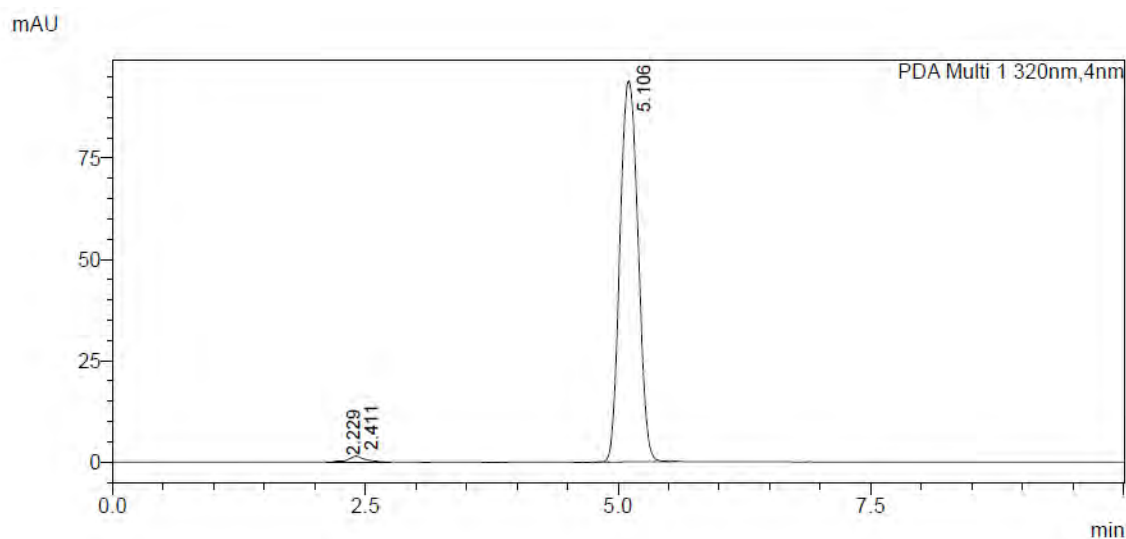


Figure C. 1.2: HPLC-UV chromatogram of ferulic acid standard (0.04 mM, injected 10 μ L). The chromatographic separation was carried on a Phenomenex® C18 5 μ m (150 \times 4.6 mm) LC column.

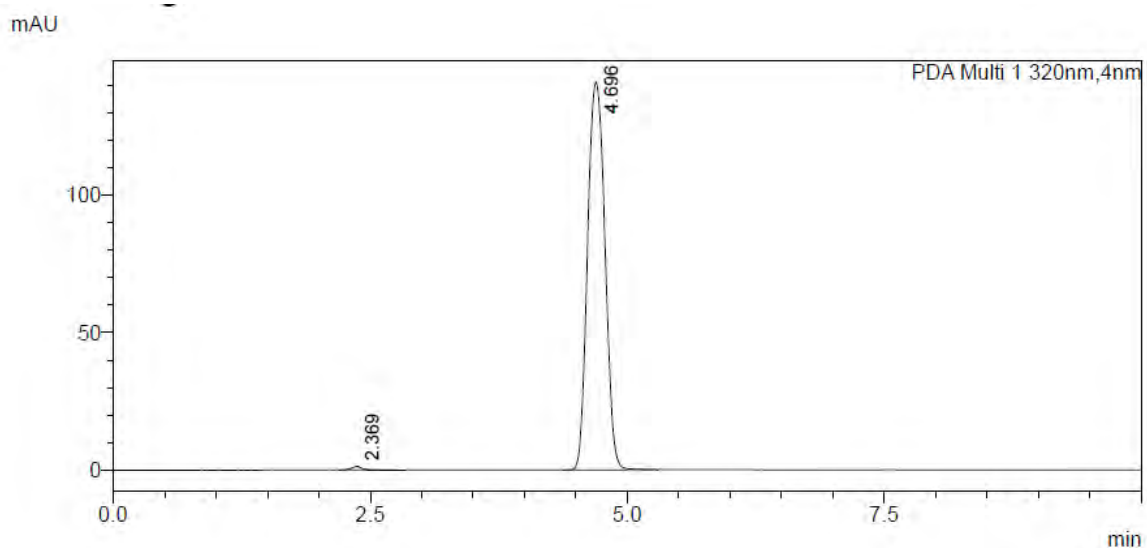


Figure C. 1.3: HPLC-UV chromatogram of *p*-coumaric acid standard (0.04 mM, injected 10 μ L). The chromatographic separation was carried out on Phenomenex® C18 5 μ m (150 \times 4.6 mm) LC column.